UAB
Universitat Autònoma de Barcelona

Exploring predictive biomarkers of response and overcoming resistance to PARP inhibitors and platinum-based chemotherapy in hereditary breast cancer

Andrea Herencia Ropero

ADVERTIMENT. L'accés als continguts d'aquesta tesi queda condicionat a l'acceptació de les condicions d'ús establertes per la següent llicència Creative Commons: https://creativecommons.org/licenses/?lang=ca

ADVERTENCIA. El acceso a los contenidos de esta tesis queda condicionado a la aceptación de las condiciones de uso establecidas por la siguiente licencia Creative Commons: https://creativecommons.org/licenses/?lang=es

WARNING. The access to the contents of this doctoral thesis it is limited to the acceptance of the use conditions set by the following Creative Commons license: https://creativecommons.org/licenses/?lang=en

Exploring predictive biomarkers of response and overcoming resistance to PARP inhibitors and platinum-based chemotherapy in hereditary breast cancer

DOCTORAL THESIS

Andrea Herencia Ropero

Experimental Therapeutics Group

Vall d'Hebron Institute of Oncology (VHIO)

Universitat Autònoma de Barcelona (UAB)

Barcelona, 2024

About the cover:

Butterflies on dandelions.

Dandelions represent the two mammary glands of a breast cancer patient, the main target population of this thesis. Butterflies' wings exhibit images of the different immunofluorescence-based biomarkers developed and studied in this work: RAD51, BRCA1 and γ-H2AX.

Butterflies are a tribute to my father, who passed away, but that is present in every single page of this thesis.

Cover design: lacienciaclara, by Clara Borràs

Exploring predictive biomarkers of response and overcoming resistance to PARP inhibitors and platinum-based chemotherapy in hereditary breast cancer

PhD program in Biochemistry, Molecular Biology and Biomedicine

Department of Biochemistry and Molecular Biology

Universitat Autònoma de Barcelona (UAB)

Thesis directors

Violeta Serra Elizalde Judith Balmaña Gelpí Alba Llop Guevara

Academic tutor

Laura Soucek

This thesis received the support of a fellowship from Generalitat de Catalunya (PERIS SLT017/20/000081).

A mi hermana, a mamá y a

papá, allá donde estés

INDEX

LIST OF TABLES ..... - 1 -

Introduction ..... - 3 -
Materials and methods ..... - 3 -
Results ..... - 3 -

LIST OF FIGURES ..... - 5 -

Introduction ..... - 7 -
Materials and methods ..... - 8 -
Results ..... - 8 -

ABBREVIATIONS ..... - 11 -

SUMMARY ..... - 21 -

RESUMEN ..... - 27 -

INTRODUCTION ..... - 33 -

Hallmarks of cancer ..... - 35 -
DNA damage response (DDR) ..... - 39 -
Alterations in HRR-related genes and homologous recombination repair deficiency (HRD) ..... - 49 -
Breast cancer (BC) ..... - 51 -
DNA damaging agents ..... - 59 -

HYPOTHESES AND OBJECTIVES ..... - 71 -

MATERIALS AND METHODS ..... - 77 -

1. Animal models and *in vivo* experiments ..... - 79 -
2. Patient-derived tumour cells (PDCs) and *ex vivo* experiments ..... - 84 -
3. DNA sequencing ..... - 85 -
4. RNA sequencing ..... - 88 -
5. *BRCA1* promoter hypermethylation quantitative assays ..... - 90 -
6. Protein quantification and biomarker analysis ..... - 91 -
7. Study and validation of functional HRD biomarkers in clinical samples ..... - 95 -
8. Statistical analysis ..... - 101 -

RESULTS ..... - 103 -

Results summary ..... - 105 -
PART 1 ..... - 107 -
First-generation PARP1/2 inhibitors antitumour activity in a panel of PDX models ..... - 107 -
Biomarkers of homologous recombination deficiency (HRD) and sensitivity to DNA-damaging agents ..... - 115 -
RAD51 as an HRD biomarker in ductal carcinoma *in situ* (DCIS) ..... - 127 -

PART 2 ..... - 131 -
The PARP1 selective inhibitor AZD5305 elicits more potent and durable antitumour activity than olaparib in patient-derived *BRCA/PALB2*-associated cancer models ..... - 131 -
Overcoming PARPi resistance by inhibiting alternative DNA damage repair pathways: POLθ and DNA-PK inhibitors ..... - 148 -
Dysregulation of the end resection pathway is associated with DNA-damaging agents in combination with PARPi in *BRCA1*-mutated tumours ..... - 158 -
PART 3 ..... - 165 -
Establishment of the BRCA1 cut-off to evaluate HRR functionality in combination with RAD51 by IF ..... - 167 -
Prevalence of HRD in non-invasive ductal carcinoma *in situ* (DCIS) ..... - 170 -
Prevalence of HRD and predictive value of the RAD51 assay in primary invasive breast cancer patients ..... - 171 -
Inter-laboratory analytical validation of the RAD51 test: RING trial ..... - 179 -

DISCUSSION ..... - 183 -

CONCLUSIONS ..... - 207 -

REFERENCES ..... - 213 -

ANNEXES ..... - 231 -

Annex I: Genes included in the panels (targeted sequencing) performed ..... - 233 -
Annex II: Supplementary tables ..... - 235 -
Annex III: Supplementary figures ..... - 257 -
Annex IV: Other publications ..... - 279 -

LIST OF TABLES

Introduction

Table 1. Clinically approved PARP inhibitors. .....- 62 -

Materials and methods

Table 2. Details of TaqMan® MGB probes used for the RT-qPCR.....- 90 -

Table 3. Details of antibodies used for IHC, WB and IF.....- 94 -

Results

Table 4. Homologous recombination deficiency (HRD) prevalence according to different HRD tests compared to the proportion of PARPi-sensitive tumours. ..- 115 -

Table 5. Test performance values for the indicated HRD biomarkers predicting PARPi response.....- 116 -

Table 6. Test performance values for the indicated HRD biomarkers predicting platinum response.....- 124 -

Table 7. Antitumour activity and durability of response of the POLθi plus AZD5305 combination vs. AZD5305 as single agent in combination-sensitive models. ...- 152 -

Table 8. Response rate (RR) observed upon treatment with the different DNA-damaging agents alone vs. in combination with PARPi assessed in this thesis.- 158 -

LIST OF FIGURES

Introduction

Figure 1. Hallmarks of Cancer. ..... - 36 -

Figure 2. Double-strand break (DSB) repair pathway choice. ..... - 41 -

Figure 3. Error-prone non-homologous end joining (NHEJ) and microhomology-mediated end joining (MMEJ) pathways lead to genome instability upon double-strand break (DSB) repair. ..... - 43 -

Figure 4. Molecular mechanisms of the DNA-damage repair (DDR) and further homologous recombination (HR)..... - 46 -

Figure 5. BRCA1 functional domains..... - 47 -

Figure 6. Paths to homologous recombination deficiency (HRD) in breast cancer. ..... - 50 -

Figure 7. Breast cancer (BC) incidence. ..... - 51 -

Figure 8. Breast cancer (BC) classification. ..... - 53 -

Figure 9. Early breast cancer (EBC) treatment overview. ..... - 56 -

Figure 10. Advanced breast cancer (ABC) treatment overview. ..... - 58 -

Figure 11. Cooperation of the Fanconi Anaemia (FA) and homologous recombination repair (HRR) proteins in a common inter-strand cross-links (ICL) repair pathway..... - 59 -

Figure 12. Mechanisms of action of PARP inhibitors. ..... - 61 -

Figure 13. Immunofluorescence-based assay to evaluate the homologous recombination repair (HRR) functionality. ..... - 65 -

Figure 14. Described mechanisms of resistance (MoR) to PARPi. ..... - 67 -

Figure 15. Chemical structure of compounds evaluated to overcome PARPi resistance[31,117,126] ..... - 70 -

Materials and methods

Figure 16. Outline of study arms of the neoadjuvant PETREMAC trial. - 96 -

Figure 17. Outline of study arms of the neoadjuvant GeparSixto trial. .. - 98 -

Figure 18. Schematic overview of the design of the training phase of the RING study. ..... - 100 -

Results

Figure 19. Disease characteristics of the PDX cohort. ..... - 108 -

Figure 20. Frequencies of homologous recombination repair (HRR)-related gene alterations in the PDX cohort. ..... - 109 -

Figure 21. Antitumour activity of PARPi in PDXs. ..... - 114 -

Figure 22. HRD tests scoring according to response to PARPi. ..... - 118 -

Figure 23. Antitumour activity of cisplatin in PDXs. ..... - 123 -

Figure 24. Homologous recombination repair functionality and PARPi sensitivity is concordant in PDXs, PDCs and patients. ..... - 126 -

Figure 25. Analysis of HRD tumour biomarkers by immunofluorescence (IF) in untreated patient-derived DCIS mouse-intraductal xenografts (MINDs).... - 129 -

Figure 26. Antitumour activity of AZD5305 and olaparib in PDXs. ..... - 134 -

Figure 27. Analysis of response to AZD5305 and olaparib in PDXs. .. - 136 -

Figure 28. Mechanisms of resistance to AZD5305 and olaparib in PDXs. ... - 138 -

Figure 29. Characterization of *BRCA1/2* genetic-based mechanisms of resistance to PARPi in PDXs. ..... - 139 -

Figure 30. Evaluation of the presence of BRCA1 hypomorphic protein as a mechanism of resistance to PARPi in the *BRCA1* exon 11-mutated PDX124 and PDX341. ..... - 141 -

Figure 31. Distribution of the resistance mechanisms detected in individual tumours that progressed to AZD5305 and olaparib in purple and green, respectively. ..... - 143 -

Figure 32. Biomarkers of DNA damage and replication stress in PDX models at baseline or treated with olaparib or AZD5305..... - 145 -

Figure 33. Antitumour activity of AZD5305 as single agent or in combination with other DNA-damaging agents..... - 146 -

Figure 34. Evaluation of POLθi antitumour activity as single agent or in combination with the PARP1 selective inhibitor AZD5305. ..... - 150 -

Figure 35. Evaluation of DNA-PKi antitumour activity as single agent or in combination with olaparib. ..... - 155 -

Figure 36. Evaluation of DNA-damaging agents antitumour activity as single alone or in combination with PARPi according to the affected gene domain in PARPi-resistant *BRCA1*-mutated PDX models. ..... - 161 -

Figure 37. Schematic overview of the patients' cohorts used to validate the RAD51 assay in different scenarios within the primary setting of breast cancer. ..... - 166 -

Figure 38. Establishment of BRCA1 nuclear foci cut-off in tumour samples. - 169 -

Figure 39. Analysis of homologous recombination deficiency (HRD) biomarkers by immunofluorescence (IF) in ductal carcinoma *in situ* (DCIS) clinical samples. ..... - 171 -

Figure 40. Prevalence of homologous recombination deficiency (HRD) by RAD51 in untreated primary invasive breast cancer patients. ..... - 172 -

Figure 41. Analysis of homologous recombination deficiency (HRD) biomarkers by immunofluorescence (IF) in untreated triple-negative breast cancer (TNBC) patients from the PETREMAC trial. ..... - 173 -

Figure 42. Analysis of homologous recombination deficiency (HRD) in TMA preparations biomarkers by immunofluorescence (IF) of untreated triple-negative breast cancer (TNBC) patients from de GeparSixto trial. ..... - 175 -

Figure 43. Association of the RAD51 score with clinical outcomes. .... - 178 -

Figure 44. RAD51 scores of individual observers per **A.** training phase and **B.** testing phase cases, sorted from largest to smallest RAD51. ..... - 180 -

ABBREVIATIONS

A

ABC: Advanced breast cancer

ABCB1: ATP binding cassette subfamily B member 1

ADC: Antibody-drug conjugate

ATM: Ataxia-telangiectasia mutated

ATRi: Ataxia-telangiectasia and Rad3-related protein inhibitors

AUC: Area under the curve

B

BARD1: BRCA1 associated RING domain 1

BC: Breast cancer

BER: Base excision repair

BID: Twice a day

BLM: Bloom syndrome protein

BRCA: BRCA1/2

BRCA1: Breast cancer growth suppressor protein 1

BRCA2: Breast cancer growth suppressor protein 2

BRCT: BRCA1 C-terminal

BRIP1: BRCA1 interacting helicase 1

BSA: Bovine serum albumin

bp: base pair

C

CC: Coiled-coil

CDK: Cyclin-dependent kinase

CHEK2: Checkpoint kinase 2

CI: Confidence intervals

CR: Complete response

CT: Chemotherapy

D

DDR: DNA-damage response

DCIS: Ductal carcinoma *in situ*

Del: Deletion

DFS: Disease-free survival

DNA-PKi: DNA-dependent protein kinase inhibitors

DSB: Double-strand break

E

EBC: Early breast cancer

EMA: European Medicines Agency

ER: Estrogen receptor

ET: Endocrine therapy

F

FA: Fanconi Anaemia

FDA: Food and drug administration

FFPE: Formalin-fixed paraffin embedded

G

GBG: German breast group

g*BRCA1/2*: Germline *BRCA1/2* mutation

GES: Gene expression signature

gsLOH: Gene-specific loss of heterozygosity

H

HBOC: Hereditary breast and ovarian cancer

HER2: Human epidermal growth factor receptor 2

HGSOC: High-grade serous ovarian cancer

HR: Homologous recombination

HR: Hazard ratio

HR: Hormone receptors

HRR: Homologous recombination repair

HRD: Homologous recombination deficiency

HRD-S: HRD-strict definition

HRD-W: HRD-wide definition

HRP: Homologous recombination proficiency

HUVH: Vall d'Hebron University Hospital

I

IBC: Invasive breast cancer

ICL: Inter-strand cross-links

IF: Immunofluorescence

IGR: Institute Gustave Roussy

IHC: Immunohistochemistry

IT: Immunotherapy

L

LIG: Ligase

LOH: Loss of heterozygosity

LST: Large scale transition

LUMC: Leiden University Medical Center

M

mBC: Metastatic breast cancer

MIND: Mouse-intraductal xenogratf

MMEJ: Microhomology-mediated end joining

MoR: Mechanisms of resistance

mRECIST: Modified RECIST

MRI: Magnetic resonance imaging (MRI)

MRN complex: MRE11-RAD51-NBS1 complex

MS-MLPA: Methylation-specific multiplex ligation-dependent probe amplification

N

n: Sample size

NA: Non-available

NAD: Nicotinamide adenine dinucleotide

NE: Non-evaluable

NER: Nucleotide excision repair

NGS: Next-generation sequencing

NKI: National Cancer Institute

NHEJ: Non-homologous end joining

NLS: Nuclear localisation signal

NMRI: Naval medical research institute

NPV: Negative predictive value

NSG: NOD scid gamma

O

OR: Olaparib-resistant

OR: Odd ratio

OS: Overall survival

OvC: Ovarian cancer

P

P: Progression

p: Phosphorylated

PaC: Pancreatic cancer

PALB2: Partner and localiser of BRCA2

PAR: Poly(ADP-ribosylation)

PARG: Poly(ADP-ribose) glycohydrolase

PARPi: Poly(ADP-ribose) polymerase inhibitors

pCBR: Preclinical benefit rate

PCR: Polymerase chain reaction

pCR: Pathological complete response

pCRR: Preclinical complete response rate

PD: Progressive disease

PDC: Patient-derived cell

PD-L1: Programmed death-ligand 1

PDX: Patient-derived xenograft

PgR: Progesterone receptor

PMC: Parma Medical Center

pPFS: Preclinical progression-free survival

PPV: Positive predictive value

p.o: Orally

POLθi: Polymerase theta inhibitors

pORR: Preclinical overall response rate

PR: Partial response

pTBR: Preclinical time to best response

pTTP: Preclinical time to progression

Q

Q: Quartile

QD: daily

R

RECIST: Response evaluation criteria in solid tumours

Rev: Reversion

Ref: Reference

RF: Replication fork

RIPA: Radioimmunoprecipiation assay buffer

RNA-seq: RNA-sequencing

ROC: Receiver operating characteristic

RPA: Replication protein A

RRBS: Reduced-representation bisulfite sequencing

RT: Radiotherapy

RT-qPCR: Reverse transcription-qualitative PCR

RTV: Relative tumour volume

S

SD: Stable disease

SEM: Standard error of the mean

SF: Splicing fraction

SHLD: Shieldin

SR: Saruparib-resistant

SSB: Single-strand break

ssDNA: Single-strand DNA

STING: Stimulator of interferon genes

T

TAI: Telomeric allelic imbalance

tBRCA: Tumour mutations in *BRCA*

TLS: Translesion synthesis

TMA: Tissue microarray

TNBC: Triple-negative breast cancer

tpm: Transcript per million

V

VAF: Variant allele frequency

VEGF: Vascular endothelial growth factor

VHIO: Vall d'Hebron Institute of Oncology

W

WB: Western blot

WEE1i: WEE1 inhibitors

WES: Whole-exome sequencing

WGS: Whole-genome sequencing

WHO: World Health Organization

WRN: Wener syndrome protein

WT: Wild-type

X

XRCC: X-ray repair cross complementing

53BP1: Tumour suppressor p53-binding protein 1

SUMMARY

Breast cancer (BC) is one of the most common cancers worldwide and the leading cause of cancer-related deaths among women from industrialised countries. Traditionally, conventional chemotherapy has been one of the few options to combat this aggressive disease, leading to low success and high mortality rates. In recent years, however, a more personalised medicine has been introduced. In particular, targeted therapies, which take advantage of the specific molecular characteristics of tumours to attack them, have accelerated the increase in BC survival. Approximately, 18% of BC exhibits a deficiency in the homologous recombination (HR) repair (HRR) pathway, an error-free mechanism for repairing DNA double-strand breaks (DSBs), due to somatic or germline alterations in key genes of the pathway such as *BRCA1*, *BRCA2* (*BRCA1/2*) or *PALB2*. Although it usually leads to tumour development, it is precisely due to this HR deficiency (HRD) that these tumours are exquisitely sensitive to DNA-damaging agents, like poly(ADP-ribose) polymerase inhibitors (PARPi) or platinum-based chemotherapy. Nowadays, PARPi are mostly recommended in a context of tumours with HRD, identified either by platinum-sensitivity or by the detection of *BRCA1/2* mutations. However, there is still room to improve selection of patients who may benefit from PARPi as i) a high proportion of *BRCA1/2*-mutated tumours exhibit primary or acquired resistance to therapy and ii) there are patients with alterations in other genes, such as *PALB2* or *BRCA1* promoter hypermethylation, that may benefit from these therapies. Accordingly, our laboratory has developed the RAD51 test, an immunofluorescence-based assay that evaluates the presence of nuclear foci of this key downstream effector of the HRR pathway.

In this thesis, we firstly assessed the predictive value of the different available HRD biomarkers of response to DNA-damaging agents including the detection of HRR-related gene mutations, genomic scars, and the RAD51 test in a panel of more than 100 cancer patient-derived xenografts (PDXs). We established that, by using a 10% cut-off, the RAD51 test showed a higher

positive predictive value compared to genetic and genomic HRD tests, suggesting a better ability to identify tumours that are sensitive to PARPi and to discriminate them from those that become PARPi-resistant after restoration of the HRR pathway functionality.

In addition, a post-hoc analysis of RAD51 was conducted in tumour samples from patients with early-stage triple negative breast cancer who participated in two clinical trials: PETREMAC and GeparSixto. The test demonstrated to be a robust biomarker to estimate the prevalence of functional HRD and was associated with clinical benefit when the first-generation PARPi olaparib or carboplatin are added to the neoadjuvant regimen.

Beyond identifying tumours that are sensitive to first-generation PARP1/2i and platinum salts, we aimed to find therapeutic options for those that did not respond. Specifically, we evaluated the antitumour activity of the new-generation PARP1 selective inhibitor AZD5305 (saruparib), which exhibits an enhanced ability to trap PARP1 on DNA while preventing the haematological adverse effects described when PARP2 is inhibited. We found that AZD5305 exhibited more profound and durable responses than olaparib *in vivo* in a panel of 13 HRR-altered PDXs.

We further showed that the combination of agents inducing replication stress, like carboplatin or an ATR inhibitor (ATRi), with AZD5305 overcome resistance to PARPi alone, with ATRi being the most potent therapeutic approach. Consistently, we also demonstrated that combinations of PARPi with other inhibitors targeting the DNA damage repair (DDR) are effective strategies to overcome PARPi resistance. For instance, inhibition of the microhomology-mediated end joining (MMEJ) polymerase theta (POLθi) or the non-homologous end joining (NHEJ) essential protein DNA-PK (DNA-PKi) together with PARPi showed durable responses in tumours that were resistant to the single agents.

In addition, we finally found that mutations in the RING domain of *BRCA1* predispose tumours to develop resistance to PARPi specifically through the dysregulation of the end resection pathway but, unexpectedly, they predict sensitivity to these combinations with PARPi.

In conclusion, our data suggest that RAD51 is an accurate and dynamic biomarker that predicts response to PARPi and platinum salts. Its performance has been validated in preclinical models and further confirmed in breast cancer samples from two clinical trials. Finally, combinations of PARPi with other DDR agents are effective strategies to overcome resistance to PARPi alone, particularly in tumours with mutations in the RING domain of the *BRCA1* gene.

RESUMEN

El cáncer de mama (CM) es uno de los cánceres más frecuentemente diagnosticados y la principal causa de muerte relacionada con cancer en mujeres de países industrializados. Tradicionalmente, la quimioterapia convencional ha sido una de las pocas opciones para combatir esta agresiva enfermedad, la cual ha llevado a una baja tasa de éxito de respuesta y a una elevada mortalidad. Sin embargo, en los últimos años, se ha ido introduciendo el concepto de medicina personalizada, en el que las terapias dirigidas, las cuales explotan las características moleculares específicas de los tumores para atacarlos, han acelerado el aumento en la supervivencia de pacientes con CM. Aproximadamente, el 18% de los tumores de mama muestran alteraciones somáticas o germinales en genes esenciales de la vía de recombinación homóloga (HRR, por sus siglas en inglés), un mecanismo de reparación del daño de doble cadena del ADN libre de errores, como *BRCA1*, *BRCA2* (*BRCA1/2*) o *PALB2*. Aunque, generalmente, conducen al desarrollo de tumores, es precisamente debido a estas deficiencias en la vía de HRR (HRD, por sus siglas en inglés) que estos tumores son extraordinariamente sensibles a agentes inductores de daño en el ADN, como los inhibidores de PARP (PARPi) o la quimioterapia basada en platino. Hoy en día, los PARPi están aprobados principalmente para su uso en un contexto de tumores con HRD, identificados por una previa sensibilidad al platino o por la detección de mutaciones en *BRCA1/2.* Sin embargo, se ha demostrado que, i) hay tumores con mutaciones en *BRCA1/2* que presentan o adquieren resistencia a estas terapias y que ii) tumores con alteraciones en otros genes, como con mutaciones en *PALB2 o* hipermetilación del promotor de *BRCA1*, también podrían beneficiarse. Por ello, nuestro laboratorio ha desarrollado el test de RAD51, un ensayo basado en inmunofluorescencia que evalúa la presencia de focos nucleares de uno de los últimos efectores de la vía de HRR, RAD51.

Uno de los objetivos principales de esta tesis consiste en buscar biomarcadores de respuesta a agentes inductores de daño en el ADN más

allá de la detección de mutaciones en genes de la vía de HRR o cicatrices genómicas, como con el test de RAD51, para mejorar la selección de pacientes que podrían beneficiarse de recibir PARP1/2i (PARPi de primera generación) y sales de platino. Para ello, empleamos un panel de más de 100 tumores derivados de pacientes (PDXs, de sus siglas en inglés), que recapitulan fielmente las características observadas en los tumores de los pacientes, para comparar los diferentes tests de HRD. Utilizando un punto de corte del 10%, el test de RAD51 mostró un valor predictivo positivo más alto en comparación con otras pruebas genéticas y genómicas de HRD, lo que sugiere una mejor capacidad para identificar tumores sensibles a PARPi y para diferenciarlos de aquellos que adquieren resistencia tras restaurar la funcionalidad de la vía de HRR.

Asimismo, un el test de RAD51 ha sido ampliamente evaluado en el contexto clínico en tumores triples negativos primarios de pacientes incluidas en dos ensayos clínicos: PETREMAC y GeparSixto. El test demostró ser un biomarcador robusto para estimar la prevalencia de HRD funcional y mostró asociación con beneficio clínico al añadir el PARPi de primera generación olaparib o carboplatino en neoadjuvancia.

Además de poder identificar tumores sensibles a PARPi de primera generación y/o a sales de platino, esta tesis tiene como objetivo encontrar opciones terapéuticas para aquellos tumores que no responden a dichos fármacos. De esta forma, evaluamos la actividad antitumoral del inhibidor selectivo de PARP1 de nueva generación AZD5305 (saruparib), el cual mostró una mayor capacidad para atrapar PARP1 en el ADN sin producir los efectos secundarios hematológicos observados al inhibir PARP2 con los PARPi de primera generación. El AZD5305 mostró respuestas más profundas y duraderas que olaparib *in vivo* en un panel de 13 PDXs con alteraciones en la HRR.

Además, observamos que la combinación de un agente inductor de estrés replicativo, como el carboplatino o un inhibidor de ATR (ATRi), al tratamiento con AZD5305 mejora la respuesta en tumores resistentes a PARPi en monoterapia. De acuerdo con lo anterior, observamos que las combinaciones de PARPi con otros compuestos, como aquellos que inhiben las vías alternativas de reparación de daño en el ADN de las cuales dependen estos tumores para sobrevivir, son estrategias efectivas para superar la resistencia a PARPi en monoterapia. Por ejemplo, la inhibición de la polimerasa theta (POLθi), esencial en la vía de unión de extremos mediada por microhomología (MMEJ), o de DNA-PK (DNA-PKi), una proteína esencial en la vía de unión de extremos no homólogos (NHEJ), en combinación con PARPi, mostró sensibilidad y respuestas duraderas en tumores que eran resistentes a PARPi en monoterapia.

Finalmente, encontramos que las mutaciones localizadas específicamente en el dominio RING del gen *BRCA1* predisponen a los tumores a desarrollar resistencia a PARPi mediante una desregulación de la vía de resección del ADN. Sin embargo, este mecanismo de resistencia conduce a estos tumores a una mayor susceptibilidad al tratamiento con combinaciones basadas en PARPi.

En conclusión, nuestros datos sugieren que, utilizando un punto de corte del 10%, el test de RAD51 es un biomarcador preciso y dinámico que predice la respuesta a PARPi y platinos. Este ensayo fue validado, por un lado, en modelos preclínicos y, por otro, en dos ensayos clínicos. Finalmente, nuestros resultados indican que las combinaciones de PARPi con otros agentes que dañan el ADN son estrategias efectivas para superar la resistencia a PARPi en monoterapia, particularmente en tumores con mutaciones en el dominio RING del gen *BRCA1*.

INTRODUCTION

Hallmarks of cancer

After many years of rapid progress, research has generated a rich and complex body of knowledge that has revealed cancer as a disease involving dynamic changes in the genome[1]. It is now well known that tumourigenesis is a multistep process that drives the progressive transformation of normal cells into a neoplastic state, as they acquire a series of traits that enable them to become tumourigenic and, ultimately, malignant. These hallmark traits have been called the Hallmarks of Cancer[1,2], which initially comprised the acquired abilities to sustain proliferative signalling, evade growth suppressors, resist cell death, enable replicative immortality, induce/access the vasculature, activate invasion and metastasis, reprogramme cellular metabolism and avoid immune destruction. However, it was further noted that these eight hallmarks failed to address the precise molecular and cellular mechanisms that allow evolving preneoplastic cells to acquire these aberrant phenotypic capabilities during tumour development. Thus, two additional enabling characteristics were incorporated as means by which cancer cells can adopt these functional traits: tumour-promoting inflammation and genome instability and mutation[2].

Recently, an updated review added two additional emerging hallmarks and two enabling characteristics: unlocking phenotypic plasticity and senescent cells, and nonmutational epigenetic reprogramming and polymorphic microbiomes, respectively, resulting in the current concept of Hallmarks of Cancer (**Figure 1**)[3].

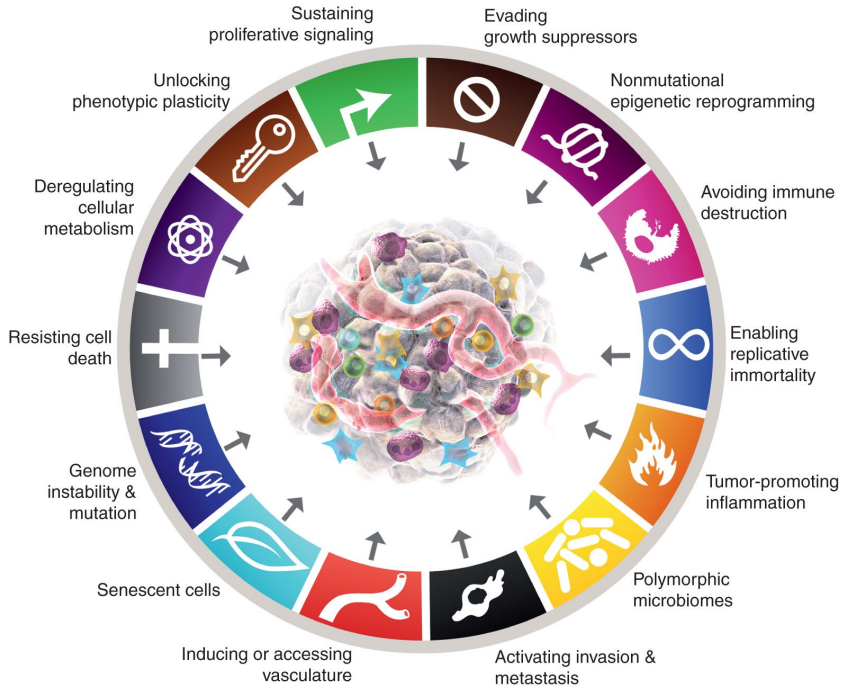


Figure 1. Hallmarks of Cancer.

The canonical and prospective "Hallmarks of Cancer." Taken from *Hanahan et al.,*[3].

Genome instability and mutation

Genomic instability is a characteristic of most cancers. The acquisition of the multiple hallmarks listed above depends in large part on a sequence of alterations in the genome of neoplastic cells. In short, certain mutant genotypes confer selective advantage on subclones of cells, enabling their proliferation and eventual dominance in a local tissue environment[2].

Although human cells have exceptional genome maintenance mechanisms to detect and repair defects in the DNA, cancer cells develop several strategies to increase mutation rates[4,5]. This mutability is achieved by one or more of the following: i) increased sensitivity to mutagenic agents, ii) breakdown of one or more components of the genome maintenance machinery and iii) compromise of the surveillance systems that monitor genome integrity and force genetically damaged cells into either senescence

or apoptosis[6,7]. Thus, defects in DNA damage response are selectively advantageous and therefore critical for tumour progression. The role of the tumour suppressor gene *TP53* in maintaining genome stability is central, leading to it being called the “guardian of the genome”[8,9].

DNA damage response (DDR)

In human cells, DNA is constantly exposed to damage from both normal cellular metabolism and external factors, resulting in tens of thousands of DNA lesions every day[7]. To combat DNA damage, cells have developed mechanisms, collectively termed DNA-damage response (DDR), to detect DNA lesions, signal their presence and promote their repair[7,10]. It is well known that these pathways share many components and operate in harmony to minimise genomic damage. Deficiencies in these mechanisms cause genomic instability and are associated with human diseases, including cancer and ageing[4,11].

Of note, the genome is particularly susceptible to DNA damage during replication, as single-strand lesions can be converted into two-ended double-strand breaks (DSBs) and lead to replication fork collapse. The emergence of DSBs, the most cytotoxic form of DNA damage, poses an immediate threat to genome stability by provoking chromosome rearrangements, thereby disrupting gene structure and function[12]. Two main pathways dominate the repair of DSBs: non-homologous end joining (NHEJ) and homologous recombination (HR). Recently, a third pathway previously thought to be a backup repair mechanism, namely alternative NHEJ or microhomology-mediated end joining (MMEJ), has been shown to play a more primary role depending on the context (**Figure 2**)[13,14].

Therefore, upon recognition of a DSB, cells orchestrate a rapid series of responses affecting many aspects of cellular physiology (e.g., transcription, chromatin remodelling, cell cycle arrest, senescence and apoptosis)[15], that ultimately recruit the DDR machinery. Specifically, the DSB “sensors” ATM (activated by the MRE11-RAD51-NBS1 (MRN) complex), ATR (activated by single-stranded DNA and replication protein A (RPA)) and DNA-PK (activated by Ku70-Ku80)[16] phosphorylate the Ser139 of the histone variant H2AX,

thereby forming γ-H2AX[17]. This event facilitates the recruitment of other factors such as the breast cancer growth suppressor protein 1 (BRCA1) and the tumour suppressor p53-binding protein 1 (53BP1, encoded by the *TP53BP1* gene; **Figure 2**).

At this point, the choice of the repair pathway depends on the phase of the cell cycle and the level of DNA end resection in the DSB, which is controlled by cyclin-dependent kinases (CDKs)[18]. Briefly, in G0/G1 phases, when end resection is suppressed by CDK-mediated phosphorylation and factors such as 53BP1, HR is suppressed and NHEJ is favoured (**Figure 2**). However, in the S/G2 phases, CtIP, the MRN complex, BRCA1 and its interacting protein BARD1 inhibit 53BP1 to allow end resection to occur. Thus, NHEJ is prevented and either MMEJ or HR can be invoked[12,14]. Thus, BRCA1 exhibits an antagonistic role with respect to 53BP1 with regards to the DSB repair pathway choice[19]. In line with this, if NHEJ has been ruled out as an option, the extent of resection will further determine the pathway choice between MMEJ and HR. In the first phase of end resection, known as “end clipping”, approximately 20 base pairs (bp) are processed, making the DNA ends available for MMEJ. In the second phase of end resection, called “extensive resection”, helicases and exonucleases generate long stretches of ssDNA, thereby committing the cells to HR (**Figure 2**)[18].

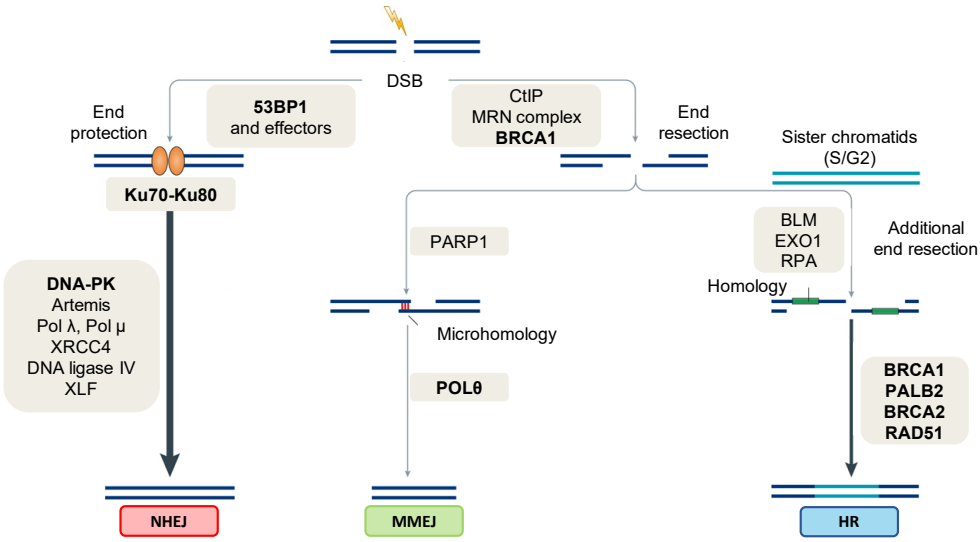


Figure 2. Double-strand break (DSB) repair pathway choice.
DSBs can be repaired by the classical NHEJ pathway, by MMEJ or by HR. The main factor affecting the pathway of choice is the requirements for DNA end resection. 53BP1 is a chromatin remodeller that favours NHEJ, in which ends are protected by Ku70-Ku80 complex as it does not require resection. By contrast, CtIP and the MRN complex are involved in extensive 5' to 3' resection to generate ssDNA to direct repair towards MMEJ or HR. PARP1 and POLθ are important to promote MMEJ. In contrast, BLM and EXO1 provide additional resection, being RPA then able to bind to ssDNA and promote HR, in which the RAD51-mediated strand exchange, mediated by BRCA1, PALB2 and BRCA2, is key. Proteins involved in each step are indicated in brown boxes, being the essential ones highlighted in bold. Abbreviations: DSB: double-strand break; NHEJ: non-homologous end joining; MMEJ: microhomology-mediated end joining; HR: homologous recombination. Adapted from *Chang et al.,*[20].

Non-homologous end joining (NHEJ)

NHEJ is an efficient but error-prone pathway in which non-homologous DNA ends are joined. Specifically, DSBs are repaired by the blunt end ligation independently of end resection, which leads to deletions or insertions as the DNA ends are modified before joining[18]. Briefly, the pathway is initiated by the binding of the Ku70-Ku80 heterodimer to the DSB ends to protect them from extensive end resection, as it presents high affinity for short single-stranded

DNA (ssDNA) overhangs (**Figure 3**). Importantly, NHEJ appears to be the dominant repair pathway used in mammalian cells and is active throughout the cell cycle, particularly in G0/G1. The high abundance of the Ku70-Ku80 complex in cells increases the likelihood that it is the first protein to bind to a broken DNA end and, therefore, that repair is carried out through NHEJ[13,21]. Although they are not “core” NHEJ factors, 53BP1 and its effectors RIF1, PTIP, REV7, DYNLL1, the Shieldin and the CST complexes (formed by SHLD1, SHLD2, SHDL3 and CTC1, STN1, TEN1, respectively)[22-26] assist the Ku70-Ku80 complex in its role of favouring NHEJ[27-29].

Following the heterodimer formation, the DNA-Ku complex initiates the recruitment of the DNA-dependent protein kinase catalytic subunit (DNA-PKcs) to form the DNA-PK complex (**Figure 3**). This facilitates the recruitment of end processing and ligation enzymes[13,30]. Additionally, DNA-PKcs autophosphorylation appears to be relevant in increasing the ability of DNA end-processing enzymes (such as Artemis) and ligases to access DNA ends. Eliminating the catalytic activity of DNA-PK therefore sensitises cells to DSB-inducing agents[30,31].

Artemis has been described to play a critical role in the end processing step of NHEJ. Once stimulated by autophosphorylated DNA-PKcs, this complex acquires endonuclease activity on both the 5’ and the 3’ DNA overhangs and removes ssDNA containing damaged nucleotides (typically ≤ 4 bp)[20]. The specialised DNA polymerases λ and μ then ensure compatibility of the ligated ends in a template-independent manner[32,33]. Other processing enzymes such as WRN (WeRNer) syndrome protein, MRE11 and the BLM (BLooM) helicase have also been described to be involved in NHEJ (**Figure 3**)[18]. The final step of NHEJ is the joining of DNA ends by the XRCC4-Ligase IV (LIG4)-XLF complex[34].

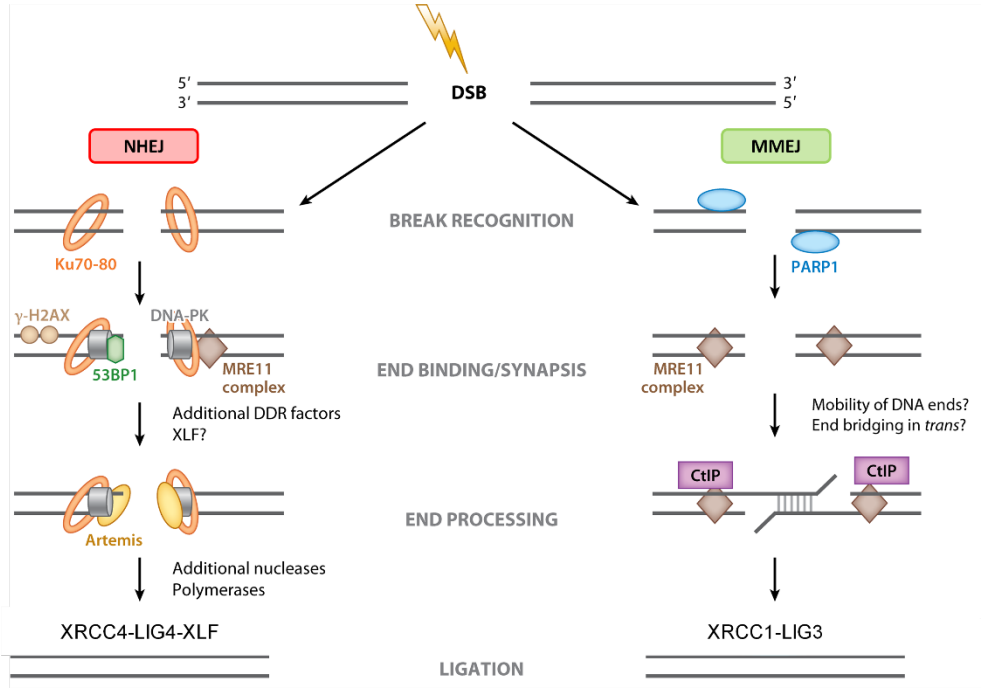


Figure 3. Error-prone non-homologous end joining (NHEJ) and microhomology-mediated end joining (MMEJ) pathways lead to genome instability upon double-strand break (DSB) repair.

Abbreviations: DSB: double-strand break; NHEJ: non-homologous end joining; MMEJ: microhomology-mediated end joining. Adapted from *Deriano et al.,*[13].

Microhomology-mediated end joining (MMEJ)

In the recent years, the notion of an alternative end joining pathway has become more evident, as it has been observed that yeast and mammalian cells deficient in NHEJ are still able to repair DSBs via end joining[13]. However, due to its error-prone nature and the fact that it was originally detected only in the absence of NHEJ, MMEJ was initially considered to be a backup repair pathway for NHEJ[35]. Notably, subsequent studies demonstrated that MMEJ may play also a more relevant role in repairing DSBs depending on the biological context, even in cells thar are competent for NHEJ[13,14].

When NHEJ is compromised due to the lack of one or more of its key components, the activity of MMEJ becomes relevant, which involves more

extensive resection of the DNA ends to reveal sequence homology (between 2 pb and 20 bp).

Therefore, upon DSB detection, end resection mediators such as the MRN complex together with BRCA1, stimulated by phosphorylated CtIP, displace 53BP1 and compete with Ku70-Ku80 for binding to DNA (**Figure 3**)[14,20]. This process appears to initiate MMEJ by processing DNA ends to generate ssDNA overhangs[36]. Alignment of microhomology sequences is next accomplished through PARP1 and the MRN complex and results in the generation of nonhomologous 3' tails that are then removed to complete the repair process[36]. Once the DNA sequences have been aligned and the 3' nonhomologous tails have been removed, the remaining gaps between the duplex DNA are filled by the highly error-prone, proof-reading deficient polymerase θ (POLθ), encoded by the *POLQ* gene (**Figure 3**)[37].

Finally, DSB repair is completed by ligation of the DNA ends through Ligase III (LIG3; **Figure 3**)[38]. Specifically, the MRN complex recruits LIG3 to the DSBs and forms a stable complex with the scaffold protein, X-ray repair cross-complementing protein 1 (XRCC1)[39]. As a consequence, the resulting structures, such as large deletions, microhomologies or occasional insertions of large DNA segments of unknown origin, are considered signatures of MMEJ[13].

Homologous recombination repair (HRR)

If the resection is even more extensive and leaves longer 3' ssDNA overhangs than in the case of MMEJ, the resected DSB ends can be repaired by the high-fidelity HRR pathway. This pathway predominates in the mid-S and G2 cell cycle phases, when an intact sister chromatid is available to serve as a template for repair. HRR appears to be the most important mechanism for protecting genome integrity in proliferating cells, as it is the only error-free DSB repair mechanism.

In short, as mentioned above, upon detection of DSBs by damage "sensors" (ATM, ATR and γ-H2AX, among others) end resection is initiated by the MRN complex, stimulated by phosphorylated CtIP (**Figure 4**)[12,16]. At this stage, BRCA1, together with BARD1 and CtIP, inhibits 53BP1 and its effectors[19]. This initial step (end clipping) is thought to displace Ku70-Ku80 from the DNA ends and provides an entry point for factors that perform long-range resection to direct repair towards HRR. Then, the second phase (extensive resection) is mediated by exonuclease 1 (EXO1), the endonuclease DNA2 and the BLM helicase[16].

The emergent ssDNA is rapidly coated with the abundant RPA complex, preventing it from pairing with other ssDNA. RPA is then displaced by the essential recombination "mediators" BRCA2, PALB2 and BRCA1-BARD1, which will further recruit the HRR "effector", the recombinase RAD51 (**Figure 4**).

The RAD51-ssDNA nucleoprotein filament mediates the homology search that defines HRR by invading duplex DNA molecules, forming a D-loop and facilitating base pairing with complementary molecules. Therefore, RAD51 filament assembly is stimulated by mediators along with RAD51 paralogs, namely RAD51B, RAD51C, RAD51D, XRCC2, XRCC3 and SWSAP1[40]. The invading strand is then extended by DNA polymerase using the invaded DNA molecule[12]. Finally, DNA ligases and endonucleases solve all DNA structures to complete the HR.

Importantly, the association of BRCA1 with proteins involved in both DNA end resection and RAD51 loading suggests that BRCA1 couples these two HRR steps[12,16].

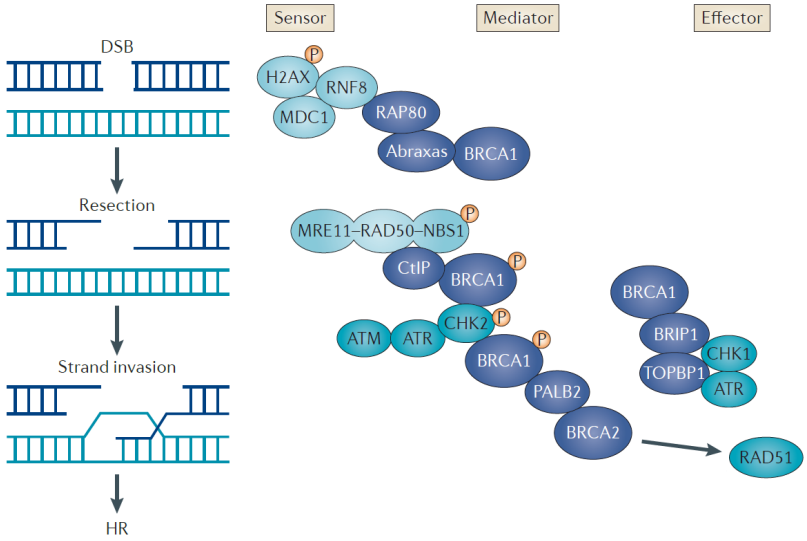


Figure 4. Molecular mechanisms of the DNA-damage repair (DDR) and further homologous recombination (HR).

In response to DSBs, sensors (light blue) detect the damage, and signalling mediators (dark blue) recruit or activate effectors that repair the damage and activate cell cycle checkpoints. Abbreviations: DSB: double-strand break; HR: homologous recombination. Adapted from *Roy et al.,*[16].

BRCA1 domains and binding proteins

BRCA1 is a 24-exon gene that encodes a multifaceted protein that links DNA damage sensing and DDR effectors. This versatility is due to the different functional and well-uncoupled domains that exert specific functions independently of each other[41].

BRCA1 has the zinc finger binding domain RING at its amino terminus, which is required for BRCA1 and BARD1 heterodimerization and therefore, for E3 ubiquitin ligase complex formation (**Figure 5**)[16,42]. The BRCA1/BARD1 complex has been implicated in maintaining genome stability and tumour suppression through its involvement in DNA damage signalling, DNA repair and transcriptional regulation[43].

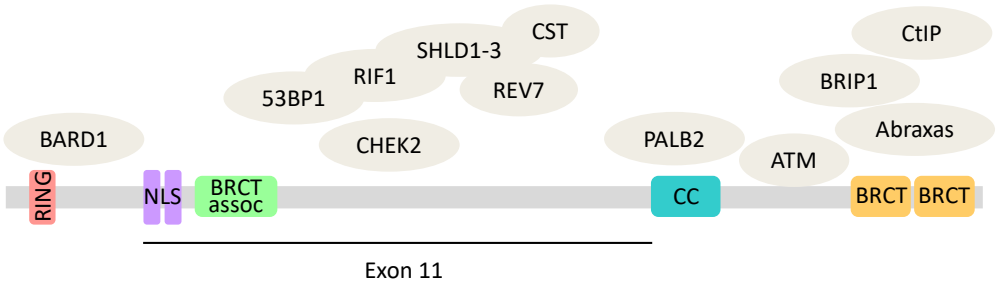


Figure 5. BRCA1 functional domains.

The BRCA1 amino N-terminus contains a RING domain that associates with BARD1 and NLS. The central region of BRCA1 contains a CHEK2 phosphorylation site and it interacts with 53BP1 and its effectors. The coiled-coil domain associates with partner and localizer of BRCA2 (PALB2). The C-terminal part of the protein contains approximately ten potential ATM phosphorylation sites and a BRCT domain that binds ATM-phosphorylated Abraxas, BRIP1 or CtIP. Abbreviations: NLS: nuclear localization sequence; CC: coiled-coil.

The central region of BRCA1, encoded by the exon 11, contains a CHEK2 (an HRR mediator) phosphorylation site and the nuclear localisation sequences (NLS). This part of the protein is also important for the interaction of BRCA1 with other DDR proteins to eventually recruit RAD51[16]. Recently, the *BRCA1* exon 11 coding region has been described to be required for counteracting 53BP1-RIF1-Shieldin activity, implying a role in the DNA end resection process[41]. In addition, BRCA1 contains a coiled-coil domain in the central part of the protein that mediates its association with PALB2 to form the BRCA1-PALB2-BRCA2-RAD51 complex, involved in the HRR pathway (**Figure 5**)[41,44-46].

Finally, the C-terminus sequence of *BRCA1* contains two tandem copies of the BRCA1 C-terminal (BRCT) domain, which mediates the interaction between BRCA1 and its associated proteins such as Abraxas, BRIP1 or CtIP, which aid in its recruitment to sites of DSBs, DNA repair during replication and end resection mediation, respectively (**Figure 5**)[16,47,48]. In addition, BRCA1 has been reported to interact with numerous cell cycle checkpoints, chromatin remodelling factors and components of the transcriptional machinery through its BRCT domain[49,50].

Alterations in HRR-related genes and homologous recombination repair deficiency (HRD)

Pathogenic alterations in any of the key genes involved in the HRR pathway, such as the tumour suppressors *BRCA1*, *BRCA2* or *PALB2*, give rise to a status of homologous recombination deficiency (HRD). This defect results in the repair of DSBs by the non-conservative, potentially mutagenic mechanisms NHEJ or MMEJ, and leads to genome instability that fosters cancer progression[51,52]. Patients with germline mutations in these genes are diagnosed of hereditary breast and ovarian cancer (HBOC) syndrome, which is associated, not only with an increased risk of breast cancer (BC) and ovarian cancer (OvC), but also pancreatic cancer (PaC) and prostate cancer when the remaining wild-type (WT) copy of the gene is lost[16]. In fact, the HBOC syndrome accounts for approximately 15% of all cases of BC, and patients have a lifetime risk of developing BC of 55-72% and of 11-44% for OvC, depending on the specific gene that is altered[53-55]. In addition, mutations in these genes or epigenetic alterations in *BRCA1* or *RAD51C* can emerge at the tumour level, displaying an HRD and "BRCAness" phenotype[56]. In total, it is well known that 18% of BC harbours HRD (**Figure 6**).

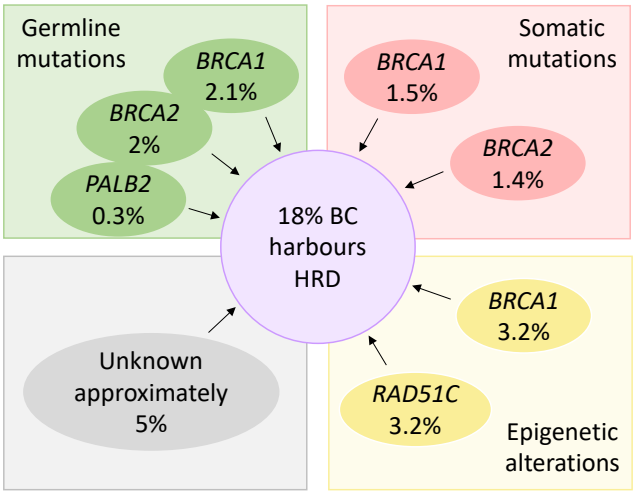


Figure 6. Paths to homologous recombination deficiency (HRD) in breast cancer (BC). Each individual mutation or epigenetic aberration occurs at low frequency. However, when these mutations are summed together, HRD is a common feature of BC. Abbreviations: HRD: homologous recombination deficiency; BC: breast cancer. Adapted from *Turner et al.,*[56].

Unrepaired DNA damage generally triggers cell cycle arrest or apoptosis. Therefore, for HRR-deficient tumours to develop, cell cycle checkpoints must be disrupted[57], which is the main reason why these cancers carry *TP53* mutations more frequently than cancers with HR proficiency (HRP)[58].

Interestingly, although HRD may be advantageous for tumour development, it also makes tumour cells exquisitely sensitive to DNA cross-linkers, such as platinum-based drugs, or other DNA-damaging agents, such as poly(ADP-ribose) polymerase (PARP) inhibitors (PARPi)[59,60]. Since they were discovered, the use of PARPi in the context of HRD has been widely exploited, particularly in the four cancer types described to be within the HRD spectrum: BC, OvC, PaC and prostate cancer. In this thesis, we focused essentially on BC patients.

Breast cancer (BC)

Epidemiology

Cancer ranks as the leading cause of death and as a major obstacle to increase life expectancy in every country in the world, with a mortality-to-incidence ratio of 15%[61-63]. Specifically, BC is the most commonly diagnosed cancer worldwide, with an estimated 2.3 million new cases (11.7% of all cancer) and affecting to one in eight women (**Figure 7**). However, death rates continue to decline, although not everywhere, due to access to high-quality prevention, early detection, and treatment services.



Figure 7. Breast cancer (BC) incidence.
About 1 in 8 women will develop BC during her life.

Most cases of BC (around 90%) are classified as sporadic and are attributed to lifestyle factors such as obesity, physical inactivity, alcohol consumption, low-fibre diet and smoking, and other unknown causes. In contrast, it is estimated that approximately 10-15% of BC patients have a genetic predisposition due to germline alterations in one of the 25 genes associated with the HBOC syndrome[64]. Within this group, the most common alterations are known to happen in the *BRCA1* and *BRCA2* (*BRCA*) genes. Genetic counselling, testing and management should be offered in cases where characteristics of the tumour, the patient's family or clinical history are suggestive of the HBOC syndrome and meet the respective national criteria.

BC subtypes

Current clinical management of BC begins with a deep histomorphological and molecular characterisation of the tumour, which provides pre-treatment information for diagnosis. As part of the evaluation, the size and the histological grade, as well as the lymphovascular invasion are the basic elements assessed[65]. In addition, BC is classified into four subtypes according to the expression of molecular biomarkers assessed by immunohistochemistry (IHC): estrogen receptor (ER), progesterone receptor (PgR), human epidermal growth factor receptor 2 (HER2) and a proliferation marker such as Ki-67 (**Figure 8**). BC subtypes have different incidence, prognosis and therapeutic implications[65-67]:

- Luminal A-like (60-70%): ER-positive (ER+) and/or PgR-positive (PgR+), HER2-negative (HER2-) and Ki-67-low (<14%).
- Luminal B-like (10-20%): ER+ and/or PgR+, HER2- and Ki-67-high or ER+ and/or PgR+, HER2-positive (HER2+).
- HER2-positive (13-15%): ER-negative (ER-), PgR-negative (PgR-) and HER2+ (*ERBB2*-amplified).
- Triple-negative (TN, 10-15%): ER-, PgR- and HER2-.

Molecular subtypes are essential for decision making and prediction of response, but they do not capture the wide heterogeneity of BC. In 2000, distinct subgroups of BC, based on gene expression profiling, were identified and defined by *Perou & Sorlie et al.*,[68]. Accordingly, in 2009, a 50-gene signature for BC classification, known as PAM50, divided tumours into five clinically relevant molecular subtypes: Luminal A, Luminal B, HER2-enriched, Basal-like and Claudin-low (**Figure 8**)[69]. Although these entities differ in incidence, prognosis, genomic drivers and response to treatment, still the PAM50 assay has not been broadly implemented in the clinic and its predictive value has only been reported in clinical trials[70].

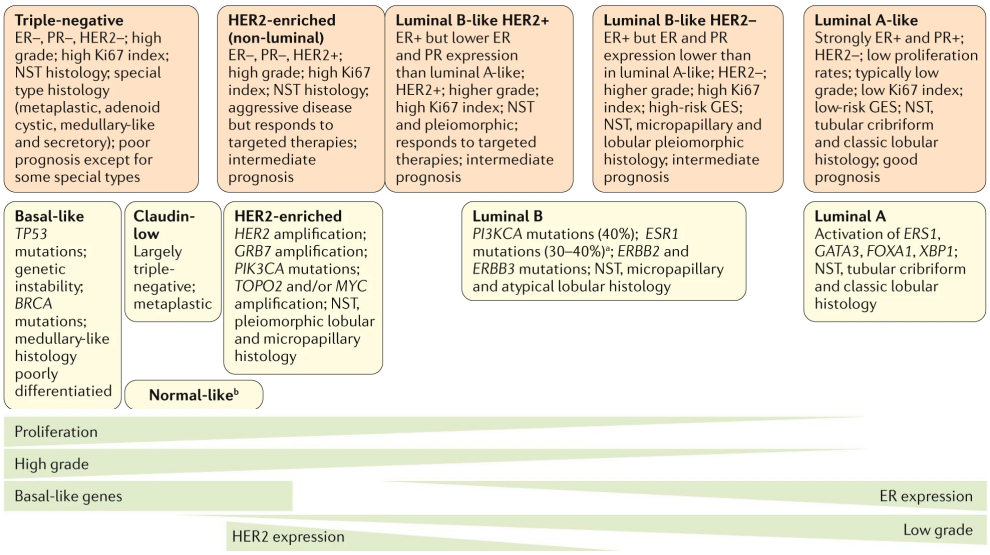


Figure 8. Breast cancer (BC) classification.

The molecular subtypes, labelled in orange, are typically used clinically and are based on histology and IHC expression of ER, PgR, HER2 and Ki-67. The intrinsic subtype of *Perou and Sorlie et al.,*[68], labelled in yellow, are based the PAM50 signature. The relative placement of the boxes aligns with the characteristics in green. Abbreviations: +: positive; -: negative; GES: gene expression signature; [a]ESR1: mutations induced by aromatase inhibitor targeted therapy; [b]Artefact, expression of normal breast components due to low tumour cellularity; NST: ductal carcinoma no special type. Adapted from *Harbeck et al.,*[71].

Clinical management

BC can also be classified into early non-metastatic disease and advanced BC, being the management and treatment, as well as prognosis, different in each case[65,71]. In addition, success rates vary also according to BC subtype and clinical stage[71].

Ductal carcinoma *in situ* (DCIS)

DCIS is a non-invasive lesion that respects the natural tissue barriers of the breast and is, therefore, not life-threatening. However, there is a subset of DCIS that eventually overrules the tissue barriers imposed by the healthy

breast tissue, leading to invasive BC (IBC), a potentially life-threatening disease[72].

All women diagnosed with DCIS undergo breast-conserving surgery followed by radiotherapy (RT) or mastectomy, with a subset also receiving endocrine therapy (ET)[65,73].

Early breast cancer (EBC)

Most early breast cancer (EBC, 70-80%) can be cured by multimodality treatment, which includes locoregional therapy (surgery or RT), systemic treatments (chemotherapy (CT), ET, molecular targeted therapies, immunotherapy (IT)) and supportive measures[65].

If EBC is suspected, a core biopsy should be taken, and the aforementioned biomarkers should be tested by IHC. If necessary, genetic testing is performed to confirm the diagnosis and characterise the cancer subtype.

As mentioned above, treatment therapy selection is essentially based on the tumour stage and biology. A general overview of the EBC management is given in **Figure 9**. In brief, operable tumours are typically removed by breast-conserving surgery. Prior to surgery, systemic treatment, known as neoadjuvant therapy, is often given to reduce tumour size, especially in those patients with larger tumours, clinical nodal involvement or HER2+/TNBC. Neoadjuvant treatment usually involves CT, which uses chemical drugs to kill or inhibit the growth and proliferation of tumour cells. After surgery, adjuvant therapy is administered, and RT is added if indicated. All patients with ER+/HER2- disease receive ET with or without CT depending on their risk of recurrence, which is based on gene expression signatures and lymph node involvement. Genetic testing is indicated in cases of stage III or high-risk stage II ER+ BC and, if a germline *BRCA1/2* (g*BRCA*) mutation is detected, patients are eligible to receive PARPi treatment (olaparib)[65]. In HER2+ EBC, treatment is determined by the tumour stage, with the addition of HER2-

targeted therapies improving overall survival by about one-third (trastuzumab, trastuzumab-pertuzumab (labelled as HP in **Figure 9**), or the antibody-drug conjugate (ADC) trastuzumab emtansine (labelled as T-DM1 in **Figure 9**)).

As it is known that approximately 15-20% of TNBC are associated with germline mutations in the *BRCA* genes, genetic testing is performed at diagnosis as the *BRCA* status helps to determine how conservative surgery will be[74]. Additional adjuvant CT with or without IT (anti-programmed death-ligand 1, PD-L1, pembrolizumab) is considered if a pathological complete response (pCR) is not achieved and there is residual disease after surgery. If a pathogenic g*BRCA* variant is found, patients are eligible to receive PARPi (**Figure 9**).

Overall, patients with EBC harbouring g*BRCA* pathogenic variants may opt for different locoregional management and contralateral surgical prophylaxis, as well as warrant more intensive risk-reducing measures for other malignancies, such as ovarian cancer, regardless of the hormone receptor status[65,74].

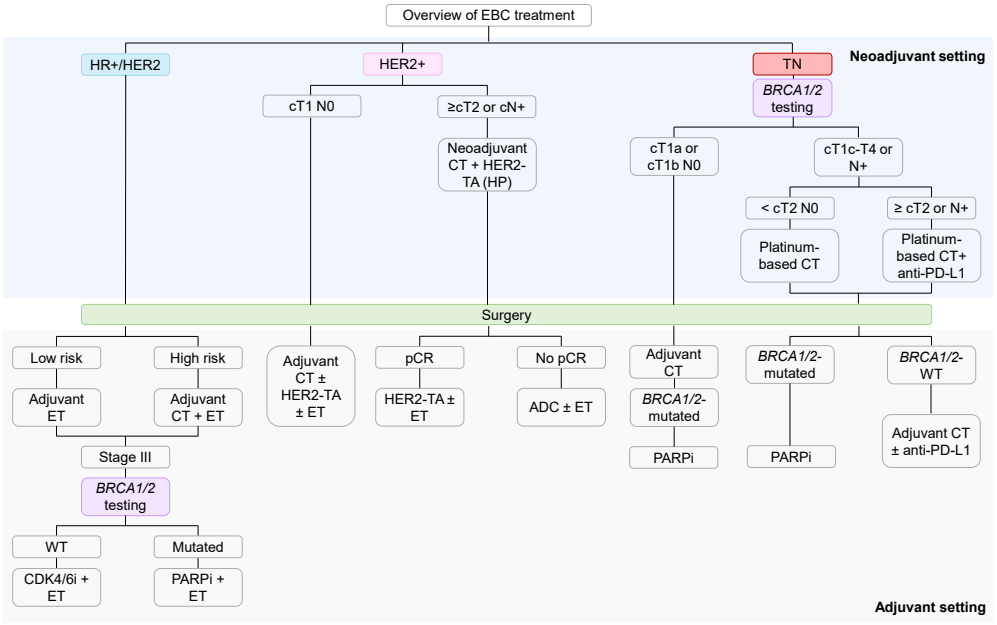


Figure 9. Early breast cancer (EBC) treatment overview.

Clinical management of HR+/HER2-, HER2+ and TN EBC. Abbreviations: EBC: early breast cancer; HR: hormone receptors; CT: chemotherapy; ET: endocrine therapy; WT: wild-type; CDK4/6i: CDK4/6 inhibitors (abemaciclib); PARPi: PARP inhibitors (olaparib); pCR: pathological complete response; HER2-TA: HER2-targeted therapy (trastuzumab); HP: trastuzumab-pertuzumab; ADC: antibody-drug conjugate (trastuzumab emtansine, T-DM1); TN: triple-negative BC. Adapted from *Loibl et al.*,[65].

Advanced breast cancer (ABC)

Advanced breast cancer (ABC) is a treatable but virtually incurable disease that includes unresectable locally advanced (not spread to distant organs) and metastatic BC (mBC). Common sites of spread are the bones, lungs and liver, having the patients a median overall survival of 2-3 years[75]. Therefore, patients with mBC receive treatments to relieve symptoms and prolong life.

Patients with newly diagnosed or recurrent mBC should undergo biopsy to confirm histology and (re-)assess IHC biomarkers. In ER+ mBC, the first-line treatment consists of CDK4/6 inhibitors (CDK4/6i), and in case of progression, tumour mutation testing is essential to recommend the

appropriate targeted therapy (**Figure 10**). If a g*BRCA* alteration is found, PARPi are administered as second-line treatment[75]. In HER2+ mBC, the standard of care is HER2-directed therapies (**Figure 10**).

In mTNBC, determination of PD-L1 and *BRCA* status is critical to optimise management. In PD-L1-positive (≥1%) mTNBC, IT with pembrolizumab or atezolizumab is recommended in combination with CT (**Figure 10**). In patients with *gBRCA* mutations, platinum-based CT or PARPi are the preferred option due to the significant improvements in progression-free survival (PFS) compared with conventional CT[76,77]. In PD-L1-negative and *BRCA*-WT mTNBC, the treatment of choice is CT with or without a vascular endothelial growth factor inhibitor (anti-VEGF, bevacizumab)[75]. Upon progression to first-line treatment, an anti-Trop2 antibody and topoisomerase inhibitor drug conjugate (ADC) is recommended (**Figure 10**).

Overall, HER2- mBC patients should be considered for treatment with a PARPi (olaparib or talazoparib) and, therefore, they should be offered genetic testing. If germline pathogenic variants in *BRCA1* or *BRCA2* are detected, PARPi treatment is indicated as an alternative to CT, regardless of the hormone receptor status[75].

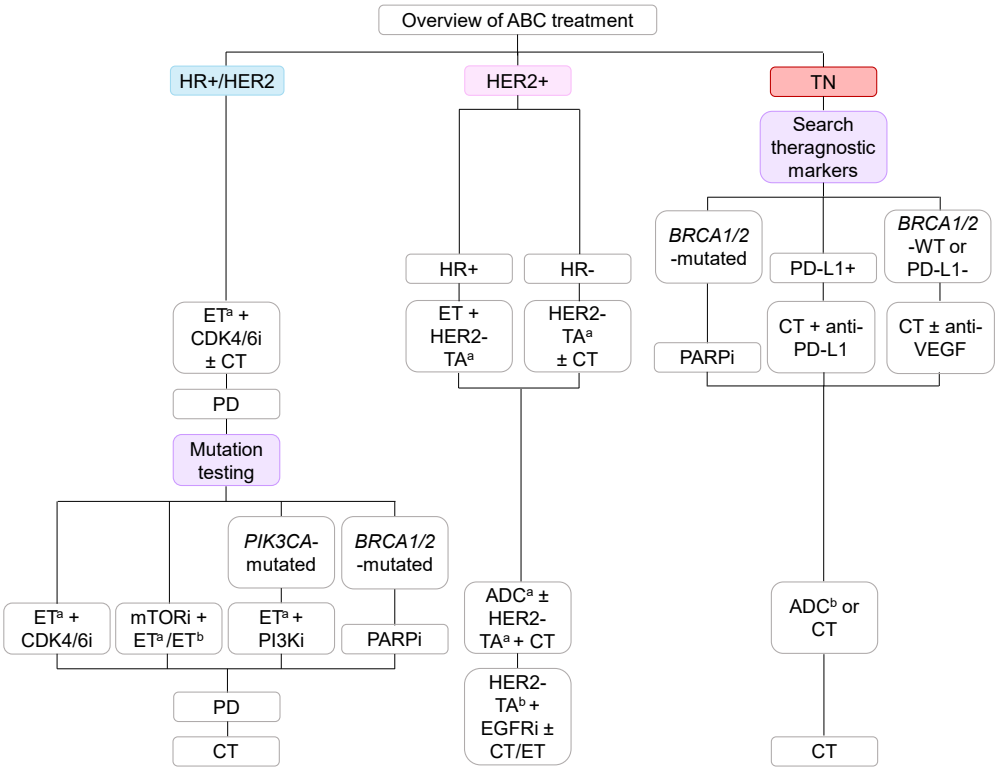


Figure 10. Advanced breast cancer (ABC) treatment overview.

Clinical management of HR+/HER2-, HER2+ and TN ABC. Abbreviations: ABC: advanced breast cancer; HR: hormone receptors; ET: endocrine therapy (ET[a]: fulvestrant; ET[b]: exemestane); CDK4/6i: CDK4/6 inhibitors (palbociclib; ribociclib); CT: chemotherapy; mTORi: mTOR pathway inhibitor (everolimus); PD: progressive disease; PI3Ki: PI3K inhibitors (alpelisib); PARPi: PARP inhibitors (olaparib; talazoparib); HER2-TA: HER2-targeted therapy (HER2-TA[a]: trastuzumab-pertuzumab; HER2-TA[b]: trastuzumab emtansine, T-DM1); ADC: antibody-drug conjugate (ADC[a]: trastuzumab deruxtecan; ADC[b]: sacituzumab govitecan); EGFRi: EGFR inhibitors (lapatinib); TN: triple-negative; WT: wild-type. Adapted from *Gennari et al.*,[75].

DNA damaging agents

Approximately 60% of BC arising in *gBRCA* mutation carriers are TNBC, being these tumours exquisitely sensitive to DNA-damaging agents, such as platinum salts and PARPi, due to their HRD status[78].

Platinum-based chemotherapy (CT)

Platinum-based chemotherapy (CT), such as carboplatin or cisplatin, are compounds used to treat various types of cancer and, as previously mentioned, are part of the standard of care for TNBC.

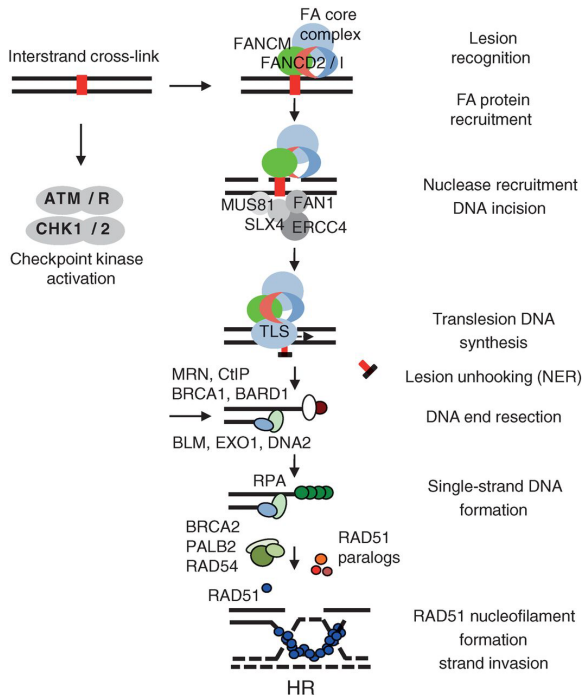


Figure 11. Cooperation of the Fanconi Anaemia (FA) and homologous recombination repair (HRR) proteins in a common inter-strand cross-links (ICL) repair pathway.
Stalling of replication forks (RF) on DNA ICL induces lesion recognition and further recruitment of the FA complex (FANCM, FANCD2-FANCI). FANCM also initiates checkpoint response, and FANCD2 coordinates nucleolytic incisions by the nucleotide excision repair (NER) pathway. Unhooking the DNA leaves the cross-linked nucleotides tethered to the complementary strand,

which are then bypassed by translesion synthesis (TLS) polymerases. DNA incisions create a DSB, which is then repaired by the HRR pathway. Adapted from *Konstantinopoulos et al.,*[79].

Specifically, platinum salts enter the cells and immediately react with DNA, generating inter- (ICL) and intra-strand cross-links that lead to single-strand breaks (SSBs) that eventually become DSBs (**Figure 11**). In general, these lesions are efficiently repaired by the sequential intervention of several pathways, such as the Fanconi Anaemia (FA), the nucleotide excision repair (NER) or the translesion synthesis (TLS) pathway, and lately by HR (**Figure 11**). In a context of HRD, platinum adducts block both DNA replication forks (RF) and transcription, resulting in severe cell cycle arrest, apoptosis or necrosis[80].

PARP inhibitors (PARPi)

PARP proteins

PARP enzymes are essential for the detection and repair of DNA SSBs via the base excision repair (BER) pathway (**Figure 12**). Specifically, PARP1, PARP2 and PARP3 sense DNA lesions, bind to the DNA and recruit the repair machinery by adding poly(ADP-ribosylation), PAR, chains to other proteins in a process called PARylation[81,82]. In short, when PARP1 binds to the DNA, there is a conformational change that allows the PARP1 co-factor nicotinamide adenine dinucleotide (NAD^+) to bind to the active site of the enzyme. PARP1 then uses this molecule to create the PAR chains[83]. In addition, PARP1 autoPARylates itself to eventually induce its own release from the site of DNA damage.

PARP inhibitors (PARPi)

PARPi are small molecules that structurally mimic NAD^+ and target the catalytic centre of PARP enzymes, resulting in two general effects on PARP enzymes: i) catalytic inhibition of PARP by preventing the PARylation of other

proteins, and ii) trapping of PARP1 on damaged DNA by inhibiting autoPARylation (**Figure 12**). In the second scenario, trapped PARP1 stalls the replication forks, therefore requiring the HRR pathway to repair it[83,84].

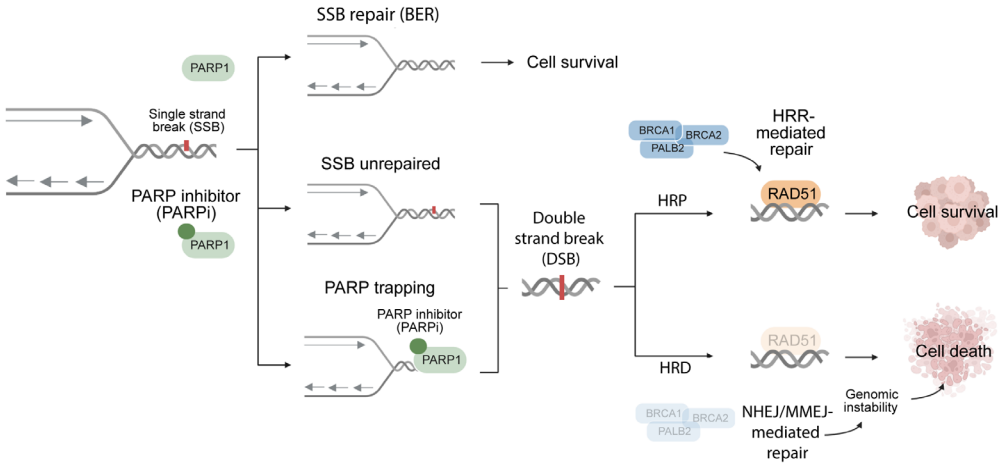


Figure 12. Mechanisms of action of PARP inhibitors.
PARPi are small molecules that inhibit PARP enzymatic activity and therefore SSB repair, and trap PARP1 on DNA damage, leading in both cases to the emergence of a DSB. Only tumours with an intact HRR pathway can safely repair DSBs, while in tumours with HRD, DSBs are repaired by error-prone mechanisms, such as NHEJ or MMEJ, with a consequent increase of genomic instability. Abbreviations: BER: break excision repair; NHEJ: non-homologous end joining; MMEJ: microhomology-mediated end joining. Adapted from F. Pedretti's doctoral thesis.

In 2005, two seminal studies demonstrated that tumour cells lacking *BRCA1* or *BRCA2* are selectively sensitive to PARPi (**Figure 12**)[59,60]. The model proposed to explain the sensitivity of tumours harbouring HRD to inhibitors of the PARP family is based on the concept of synthetic lethality: loss of *BRCA* genes or PARP inhibition separately are not lethal per se as DNA lesions can be repaired by other repair pathways. However, concomitant *BRCA* inactivation and PARP inhibition leads to cell death due to increased genomic instability (**Figure 12**)[83]. To date, several PARPi with different potencies as PARP1 catalytic inhibitors and as PARP trappers have been developed and approved for different clinical indications (**Table 1**).

Table 1. Clinically approved PARP inhibitors.

List of clinically approved PARPi by the regulatory agencies Food and Drug Administration (FDA) and European Medicines Agency (EMA) by the time of the writing of this thesis (04/03/2024). The brand name is indicated in brackets.

PARPi	Treatment	Regulatory agency		Approved indication (to date 04/03/2024)
		FDA	EMA	
Olaparib (Lynparza)				
Ovarian cancer	Monotherapy	X	X	Maintenance treatment of patients with advanced *BRCA1/2* -mutated (germline and/or somatic) high-grade epithelial ovarian, fallopian tube or primary peritoneal cancer who are in response (complete or partial) following completion of first-line platinum-based chemotherapy
		X	X	Maintenance treatment of patients with platinum-sensitive relapsed high-grade epithelial ovarian, fallopian tube or primary peritoneal cancer who are in response (complete or partial) to platinum-based chemotherapy
	In combination with bevacizumab	X	X	Maintenance treatment of patients with advanced high-grade epithelial ovarian, fallopian tube or primary peritoneal cancer who are in response (complete or partial) following HRD-positive status defined by either a *BRCA1/2*- mutation and/or genomic instability, following completion of first-line platinum-based chemotherapy
Breast cancer	Monotherapy	X	X	Adjuvant treatment of patients with germline *BRCA1/2* -mutations who have HER2-negative, high risk early breast cancer previously treated with
	In combination with ET	X	X	
	Monotherapy	X	X	Treatment of patients with germline *BRCA1/2* -mutations who have HER2-negative, locally advanced or metastatic breast cancer
Pancreatic cancer	Monotherapy	X	X	Maintenance treatment of patients with germline *BRCA1/2* -mutations who have metastatic adenocarcinoma of the pancreas and have not progressed after a minimun of 16 weeks of platinum treatment within a first-line chemotherapy regimen
Prostate cancer	Monotherapy		X	Treatment of patients with metastatic castration-resistant prostate cancer (mCRPC) and *BRCA1/2*- mutations (germline and/or somatic) who have progressed following prior therapy that included a new hormonal agent
	In combination with abiraterone and prednisone or prednisolone	X	X	Treatment of patients with mCRPC in whom chemotherapy is not clinically indicated
Rucaparib (Rubraca)				
Ovarian cancer	Monotherapy	X	X	Maintenance treatment of patients with platinum-sensitive relapsed high-grade epithelial ovarian, fallopian tube or primary peritoneal cancer who are in response (complete or partial) to platinum-based chemotherapy
Prostate cancer	Monotherapy	X		Treatment of patients with mCRPC and BRCA1/2-mutations (germline and/or somatic) after treatment with androgen receptor-directed therapy and a taxane-based chemotherapy
Niraparib (Zejula)				
Ovarian cancer	Monotherapy	X	X	Maintenance treatment of patients with platinum-sensitive relapsed high-grade epithelial ovarian, fallopian tube or primary peritoneal cancer who are in response (complete or partial) to platinum-based chemotherapy
			X	Maintenance treatment of patients with advanced high-grade epithelial ovarian, fallopian tube or primary peritoneal cancer who are in response (complete or partial) following completion of first-line platinum-based chemotherapy
		X		Maintenance treatment of patients with advanced *BRCA1/2* -mutated (germline and/or somatic) high-grade epithelial ovarian, fallopian tube or primary peritoneal cancer who are in response (complete or partial) following completion of first-line platinum-based chemotherapy
Talazoparib (Talzenna)				
Breast cancer	Monotherapy	X	X	Treatment of patients with germline *BRCA1/2* -mutations who have HER2-negative, locally advanced or metastatic breast cancer

In 2014, the first-in-class PARPi olaparib was authorized for the maintenance treatment of OvC patients with somatic or germline pathogenic variants in *BRCA1* or *BRCA2*[85]. The success in OvC promoted the use of PARPi in other cancer types, with olaparib and talazoparib approved for metastatic g*BRCA* HER2- BC patients who had previously received lines of CT[76,77]. Notably, in 2022, olaparib was approved for the adjuvant treatment of patients with g*BRCA* HER2- BC who had previously received neoadjuvant CT[86]. Finally, the use of PARPi has been extended to pancreatic and prostate cancers harbouring HRD[87-90]. Of note, numerous clinical trials that could further expand their use are currently ongoing[91].

Developing predictive biomarkers of response to PARPi

Precision medicine approaches have the potential to improve cancer treatment by identifying patients who are more likely to benefit from specific therapies[92]. Therefore, the analytical validation and clinical qualification of biomarkers capable of stratifying patients is critical.

Several biomarkers are being used in the clinic. Firstly, and because sensitivity to platinum and PARPi is associated with HRD, platinum response has been used as a surrogate for PARPi response, particularly in OvC. However, the response to these therapies does not fully overlap, as the pathways involved in repairing damage generated upon treatment with each compound are slightly different[93].

In addition, targeted sequencing allows the identification of alterations in various DDR genes, including *BRCA1* and *BRCA2*, that may lead to HRD, being these tumours more likely be sensitive to PARPi[93]. Therefore, the detection of pathogenic mutations in these genes is another widely used biomarker to select patients that may benefit from the treatment with PARPi, especially in the case of BC.

Thirdly, genomic signatures or scars represent repetitive patterns of DNA alterations that translate an underlying HRD. In particular, the extensive use of the error-prone repair pathways NHEJ or MMEJ in tumours harbouring HRD results in the accumulation of small insertion-deletions and loss-of-heterozygosity (LOH) events[94]. Two assays have been approved as predictive biomarkers of PARPi response in OvC: i) the Foundation Focus CDx BRCA LOH, which tests for germline and somatic mutations in *BRCA* genes and assesses the frequency of LOH[94], and ii) the MyChoice HRD (Myriad), a composite signature of LOH, TAI and large scale transition (LST) events together with the detection of BRCA1 or BRCA2 mutations[95,96]. In addition, and based on the same principle, mutational signatures of HRD have been identified by whole- genome sequencing (WGS). Subsequently, and although not yet approved for clinical use, the HRDetect test has been developed[94,97]. However, these biomarkers are static and do not change when a tumour recovers the HR functionality, presenting the limitation that they may not capture patients who have previously received and progressed on DNA-damaging agents, and therefore, may not be accurate in predicting PARPi sensitivity[83]. In addition, these assays carry some challenges for implementation in the clinical practice as they are technically complex, may require frozen tumour samples and carry a high cost[98].

Thus, a dynamic and functional test to assess HRD was developed by former members of my team using an immunofluorescence-based assay to detect nuclear foci of the downstream HR effector RAD51 together with BRCA1 and γ-H2AX (**Figure 13**)[99,100]. Briefly, *Cruz* and *Castroviejo-Bermejo et al.,* discovered that tumours have enough endogenous DNA damage to activate the HR and, consequently, to exhibit RAD51 foci when the pathway is functional. Thus, the evaluation of RAD51 as a biomarker of HR functionality and, therefore, of PARPi response is feasible in routine formalin-fixed paraffin-embedded (FFPE) tumour samples without prior induction of DNA damage (**Figure 13**).

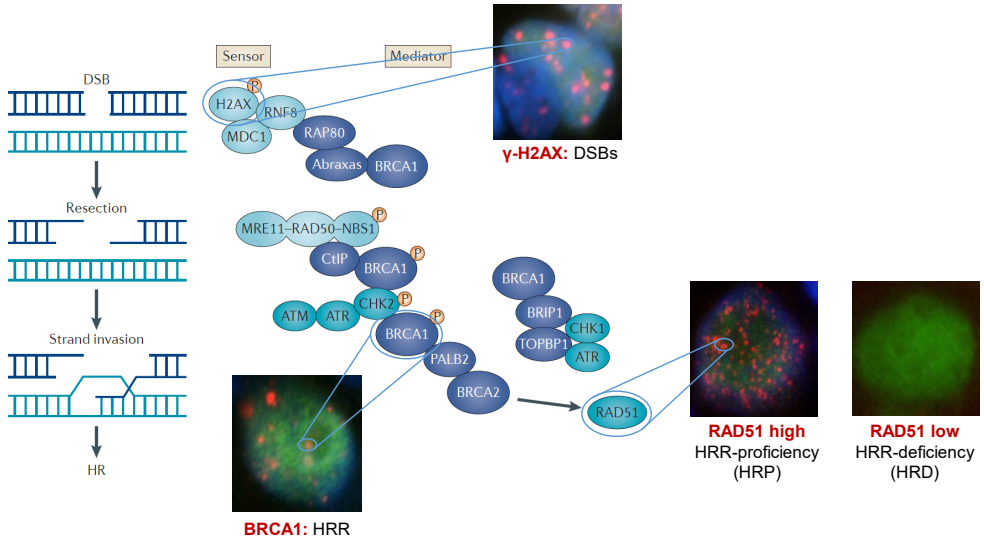


Figure 13. Immunofluorescence-based assay to evaluate the homologous recombination repair (HRR) functionality.

RAD51, BRCA1 and γ-H2AX nuclear foci are quantify in cells that are in the S/G2 phases of the cell cycle (geminin-positive). High levels of RAD51 may indicate HR proficiency (HRP) and, therefore, tumours likely to be resistant to DNA-damaging agents. In contrast, in absence of RAD51 foci, the HRR pathway is likely to be unfunctional, being these tumours more prone to present HR deficiency (HRD) and sensitive to DNA-damaging agents. Nuclear foci of these proteins are seen in red, while geminin is stained in green. Abbreviations: DSB: double-strand break; HRR: homologous recombination repair; HRP: homologous recombination proficiency; HRD: homologous recombination deficiency. Adapted from *Roy et al.,*[16].

Mechanisms of resistance (MoR) to DNA-damaging agents

Platinum-based CT and PARPi frequently elicit a deep initial response, although, eventually, most patients develop resistance and it results in disease relapse. Several mechanisms of resistance (MoR) to these DNA-damaging agents have been described in preclinical and clinical studies and can be divided into three main groups (**Figure 14**)[79,101].

A major MoR is the restoration of the HRR function. This can occur either by secondary mutations that restore the open reading frame and remove the frameshift caused by the original mutation, or by genetic reversion of the inherited mutation, both of which result in the expression of a functional

(nearly) full-length protein (**Figure 14**)[102,103]. Similarly, epigenetic silencing of the HRR-related genes *BRCA1* and *RAD51C* by hypermethylation of promoter regions results in PARPi sensitivity and, therefore, demethylation is associated with BRCA1 and RAD51C re-expression and therapy resistance[104,105]. Expression of functional hypomorphic variants of BRCA1 and BRCA2, although unable to prevent tumour development, has been associated with resistance to platinum and PARPi. Mechanisms such as a downstream translation initiation, transcription of functional splicing variants (such as the Δ11q) or stabilization of the altered variants by the HSP90 chaperone have been described in *BRCA1* RING domain-, exon 11- and BRCT domain-mutated cells, respectively[106-108]. In addition, BRCA1-independent restoration of the HRR pathway functionality has been described based on the emergence of compensatory mutations leading to rewiring or DDR. For instance, dysregulation of the end resection pathway by mutations in key genes of the NHEJ, such as *TP53BP1* or the 53BP1 co-factors, restores DNA end resection in *BRCA1*-deficient cells, rescuing the HR defect and rendering resistance to PARPi. Interestingly, this MoR does not confer cross-resistance to platinum salts, being these examples of PARPi-resistant, platinum-sensitive tumours (**Figure 14**)[79].

An alternative MoR is the replication fork protection, often associated with a slowing of cell cycle progression and the prevention of extensive degradation of the unprotected forks, as BRCA1, BRCA2 and PARP1, among others, play important roles in this pathway (**Figure 14**)[109,110].

Third, mutations in *PARP1* or mechanisms that increase PARylation, such as the loss of PARG, could lead to PARPi resistance by decreasing PARP trapping[111,112]. Finally, increased expression of ATP-binding cassette transporters, such as the P-glycoprotein efflux pump, encoded by *ABCB1*, has been shown to reduce the efficacy of PARPi (**Figure 14**)[113].

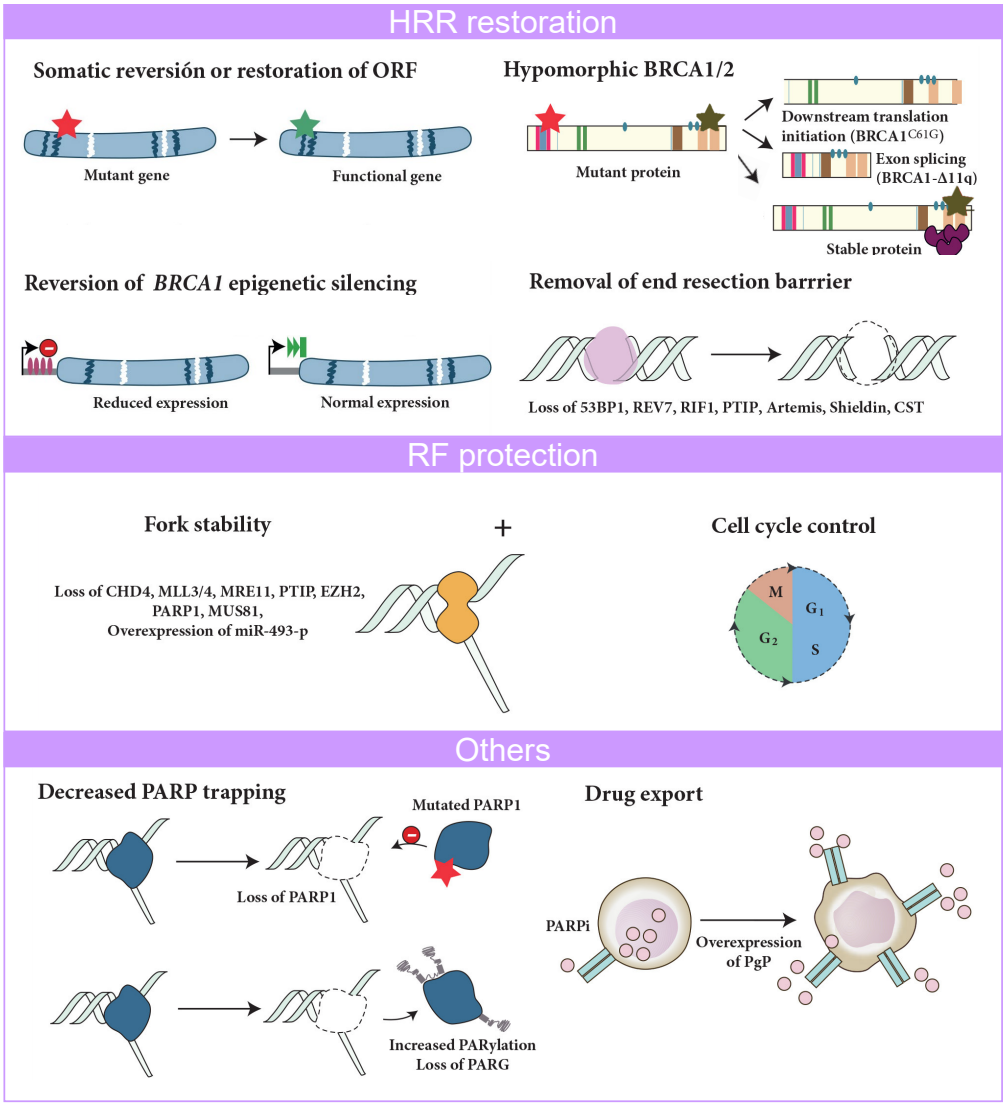


Figure 14. Described mechanisms of resistance (MoR) to PARPi.

The potential mechanisms of resistance to PARPi can be classified in three main groups: i) those that result in restoration of HRR functionality, ii) those leading to mitigation of replication stress commonly together with slower cell cycle progression, and iii) other mechanisms not directly related with an HRR or replication stress pathway but that still alter the response to PARPi, such as mutations in *PARP1* or drug effluxion pumps. Abbreviations: HRR: homologous recombination repair; ORF: open reading frame; RF: replication fork. Adapted from *Mateo et al.*,[83].

Strategies to overcome PARPi resistance

Further studies are needed to develop therapeutic options to combat or delay the emergence of resistance to PARPi. Some potential strategies include the use of more potent next-generation PARP inhibitors or combination therapies aimed at further enhancing the antitumour effects of first-generation PARPi, targeting the acquired vulnerabilities of PARPi-resistant cancers, or suppressing the mutator phenotype that leads the tumour to restore of HRR functionality[91].

AZD5305, a next-generation, selective PARP1 inhibitor and trapper

Currently approved first-generation PARPi, such as olaparib, inhibit both PARP1 and PARP2 (PARP1/2). Importantly, it has been suggested that PARPi that are weak PARP trappers (e.g. veliparib) do not elicit the same level of efficacy compared with effective trappers (e.g. olaparib and talazoparib) in preclinical models[114]. In addition, it has also been described that the solely inhibition of PARP1 and not PARP2 is sufficient to induce synthetic lethality in cancer cells with HRD[115], which also avoids the haematological adverse effects observed in patients receiving first-generation PARPi attributed to the role of PARP2 in hematopoietic renewal[116]. In line with this, the AZD5305 (saruparib), a highly selective PARP1 inhibitor (PARP1i) with potent trapping capacity, has been developed (**Figure 15**)[117,118].

Selective targeting of PARP1 with AZD5305 displays greater differential antiproliferative effects in HRR-mutant vs. WT cells compared to first-generation PARPi[118]. In addition, first-generation PARPi are difficult to combine with other DDR agents due to high levels of toxicity. In the clinic, the PETRA trial (NCT04644068) is a phase I/IIa clinical trial evaluating AZD5305 as monotherapy or in combination with different CT or with ADCs[119].

Targeting acquired vulnerabilities of PARPi-resistant cancers

Several loss-of-function mutations that lead to PARPi resistance have been found to result in increased sensitivity to other therapies. For instance, *BRCA1*-deficient tumours with dysregulation of the end resection pathway have been demonstrated to be dependent on ATR[120]. Therefore, combinations of PARPi and ATR inhibitors (ATRi) are currently being investigated as potential methods to overcome PARPi resistance (AZD6738, **Figure 15**)[121,122]. Additionally, other forms to abrogate cell-cycle checkpoint signalling, for instance through WEE1 kinase inhibitors, have been investigated[122,123].

Tumours with HRD may rely more on alternative DNA damage repair pathways such as the NHEJ or the MMEJ. Therefore, the use of small molecules inhibiting essential proteins of these pathways, such as DNA-PK (AZD7648) or POLθ (AZ'8649 and AZ'1576), might alleviate resistance to PARPi (**Figure 15**)[31,124]. Furthermore, given that the MMEJ is an error-prone mechanism, it has been described to contribute to the emergence of reversion events and therefore, to the restoration of the HRR pathway functionality and PARPi resistance[125]. Thus, POLθ inhibition may be effective, not only in PARPi-resistant tumours a partially functional HR, but also in preventing the emergence of resistance[91].

In addition, the next-generation PARP1i AZD5305 may offer the opportunity to be more easily combined with any of these DNA-damaging agents compared to first-generation PARPi due to its safe profile, high potency and therefore lower administration doses[118].

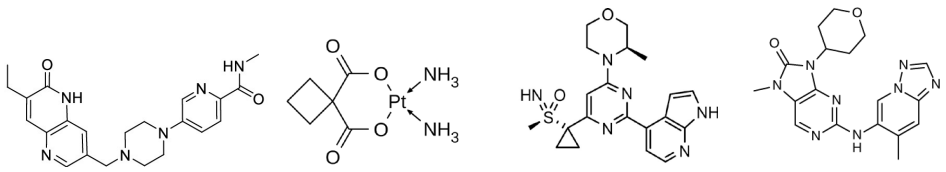


Figure 15. Chemical structure of compounds evaluated to overcome PARPi resistance[31,117,126]

HYPOTHESES AND OBJECTIVES

Tumours with homologous recombination deficiency (HRD), such as those from germline BRCA1/2 mutation carriers, are exquisitely sensitive to DNA-damaging agents, like platinum salts or PARP inhibitors (PARPi). The presence of BRCA1/2 mutations, genomic scars or signatures derived from the inability of these tumours to repair by an error-free mechanism, or sensitivity to platinum agents have been the biomarkers used to select patients that are eligible to receive PARPi. However, 1) up to 40% of the patients who meet these criteria do not respond to the treatment, suggesting a limited positive predictive value; and 2) patients with other HRR pathway defects, such as those with mutations in PALB2 or BRCA1 promoter hypermethylation, may also benefit from PARPi or platinum-based chemotherapy. Therefore, a functional and dynamic test of HRD like the RAD51 test will help identify tumours that are most likely to respond to PARPi.

Also, understanding the mechanisms of primary and acquired resistance is mandatory to help design mechanism-based therapeutic approaches to overcome PARPi resistance.

The major goal of this thesis is to investigate the hypothesis that response to PARPi and platinum-based chemotherapy can be predicted by the combined immunodetection of RAD51 and BRCA1 nuclear foci in tumours from breast cancer. Therefore, we aimed to validate the RAD51 test as a functional biomarker of HRD with a especial focus on i) the validation of cut-offs and ii) determination of the prevalence of functional HRD as well as iii) the study of the predictive value of the test to select patients for PARPi/platinum therapy. Furthermore, it is hypothesised that resistance to first-generation PARPi can be overcome by using DDR-inhibitor combinations. For thesis purposes, we have used patient-derived tumour models and patient samples.

Therefore, the following objectives were established:

Aim 1: Development and characterization of a panel of patient-derived xenografts (PDXs) from breast tumours for the study of biomarkers of response to PARP1/2i and platinum-based chemotherapy.

The specific aims were the following:

1. Develop a panel of PDXs with a special focus on triple-negative breast cancer (TNBC) and other HRR-related gene-associated tumours.
2. Generate a database with the molecular characteristics of these PDXs, including tumour mutations, genomic instability (GIS) and the HRD status by RAD51.
3. Evaluate the antitumour activity of first-generation PARP1/2i and cisplatin in the panel of PDXs.
4. Generate models of acquired resistance and identify the mechanisms of resistance to PARP1/2i.
5. Conduct an analysis of correlation between HRD biomarkers and response to PARP1/2i or platinum salts in the panel of PDXs.

Aim 2: Overcoming first-generation PARPi resistance with a next-generation PARPi or combinations with other DNA-damaging agents.

The specific aims were the following:

1. Evaluate the antitumour activity of the next-generation PARP1i AZD5305 (saruparib) alone or in combination with platinum salts or an ATRi in a panel of HRR-associated PDX models.
2. Investigate if the inhibition of critical proteins of alternative DNA repair pathways, such as DNA-PK (NHEJ) and POLθ (MMEJ), are valid therapeutic options for HRR-altered PARPi-resistant PDXs.
3. Identify mechanisms-based biomarkers of response to the tested treatments.

Aim 3: Study and validation of functional HRD biomarkers in clinical samples of TNBC and tumours harbouring alterations in HRR-related genes.

The specific aims were the following:

1. Establish a cut-off of BRCA1 nuclear foci to evaluate BRCA1 functionality in combination with the RAD51 score by IF.
2. Establish the prevalence of functional HRD by RAD51 in primary high-risk breast cancer
3. Correlate functional HRD by RAD51 scores with treatment response.

MATERIALS AND METHODS

1. Animal models and *in vivo* experiments

1.1 Generation and establishment of patient-derived xenografts (PDXs)

Tumour samples from surgical or biopsy specimens from primary or metastatic patients with HRR-related breast (triple-negative, ER+ or HER2+), ovarian or pancreatic cancer were collected for implantation into the lower flank of 6-week-old female immunocompromised Crl:NOD.Cg-Prkdc^{scid}Il2rg^{tm1Wjl}/SzJ (NSG, Charles River) mice. All the experiments were performed under informed written consent approved by the Ethics Committee for Clinical Research (PR(AG)484/2017) and Animal Research of Vall d'Hebron Hospital (FUE-2020-01541918). The studies were conducted under an institutional review board (IRB)-approved protocol and following the European Union's animal care directive (2010/63/EU), the principles of the WMA Declaration of Helsinki and the Department of Health and Human Services Belmont Report. Clinical information regarding patients' molecular subtype, origin of the biopsies, lines of therapies received before obtaining the tumour biopsies and clinical response was collected.

Animals were housed in air-filtered laminar flow cabinets with a 12-hour light cycle and food and water ad libitum. Mice were continuously supplemented with 1.5 μM 17β-estradiol (Sigma-Aldrich, #E8875) in drinking water. Upon growth of the engrafted tumours, the models were perpetuated by serial transplantation. According to their tumour growth, some PDX models were maintained in NSG and others were further implanted in Rj:NMRI-Foxn1$^{nu/nu}$ (NMRI, Janvier) mice. In each passage, flash-frozen and formalin-fixed paraffin-embedded (FFPE) samples were taken for posterior proteomic and genomic analyses. Three models (STG139, STG316 and STG201, two TNBC and one ER+ breast cancer, BC) were generated in CRUK/UCAM, a member of the EuroPDX consortium (http://www.europdx.eu). The PDX481 (BB3RC31) was generated in the Manchester Breast Centre as previously

described[127]. Most of the PDX models were previously established in the laboratory and were selected for the purpose of this thesis based on their genomic/epigenomic profile.

Two additional cohorts of PDX models whose PARPi response was tested at XenTech (https://www.xentech.eu/) or from Tesaro (START) were used. PDXs from XenTech were generated at Curie Institute (Paris, France) and Paoli Calmette Institute (Marseille, France) under an IRB-approved protocol. The majority of these models were implanted into the interscapular area of 12-week-old female Hsd:Athymic Nude-Foxn1nu (Envigo), and were previously published[128,129].

Patient-derived ductal carcinoma *in situ* (DCIS) mouse-intraductal xenografts (MINDs) were generated in the Netherlands Cancer Institute (NKI, Amsterdam) to study the early stages of BC as described by *Hutten et al.,*[72]. FFPE blocks of biopsies from patients were also collected in the same moment that the samples to generate MINDs.

1.2 *In vivo* experiments

Efficacy studies

To evaluate the sensitivity to targeted therapies, tumour tissue from a PDX model was reimplanted into 4 to 5 mice per treatment arm. Once tumours reached 100-300 mm^3, animals were randomized into the following treatment groups:

- The PARP1/2i olaparib (AZD2281, AstraZeneca) was administered orally (p.o) every day (QD) six times per week in 10%v/v DMSO / 10%w/v kleptose [HP-β-CD] at 50 mg/kg or 100 mg/kg.
- The PARP1/2i niraparib (Tesaro) was administered p.o QD daily in 0.5% methylcellulose at 50 mg/kg or 75 mg/kg.

- The PARP1i AZD5305 (saruparib, AstraZeneca) was administered p.o QD six times per week in water/HCl at pH 3.5-4 at 1 mg/kg.
- Cisplatin was administered intravenously QD once every two weeks unless relative tumour volume (RTV) < 0.5 at 6 mg/kg.
- Carboplatin was administered intraperitoneally QD once a week at 37.5 mg/kg.
- The ATRi AZD6738 (AstraZeneca) was administered p.o QD five times per week in 10% v/v DMSO, 40% v/v PEG300 at 25 mg/kg.
- The DNA-PKi AZD7648 (AstraZeneca) was administered p.o twice daily (BID) six times per week in 0.5% hydroxypropyl methylcellulose / 0.1% Tween80 (HPMC/T) at 75 mg/kg.
- The POLθi AZ'8649 (AstraZeneca) was administered p.o QD six times per week in 5% v/v DMSO, 20% v/v PEG400 at pH 5-6 at 100 mg/kg. In some experiments, the POLθi was switched to AZ'1576 (AstraZeneca), which was administered p.o BID six times per week in 0.5 % HPMC at 100 mg/kg.
- The control group did not receive any vehicle.

Drug administration and dosing schedules were maintained in combinations experiments of either olaparib or AZD5305 plus carboplatin, ATR or DNA-PK inhibitors. In the case of POLθi, the AZ'8649 was given BID six times per week at 50 mg/kg with the PARPi given one hour after the first dose.

Tumour growth was monitored bi-weekly by an electronic calliper from the first day of treatment until the end of the experiment. Tumour volume was calculated as V = (length x width^2) · (π/6). Efficacy experiments contained an untreated control arm with a percentage of change in tumour growth superior to 20% from the initial volume. Antitumour activity was determined by comparing tumour volume on the last day of treatment to its baseline (day 1): % tumour volume change = ($V_{X\ days}$–$V_{baseline}$) / $V_{baseline}$ · 100. Animal welfare was monitored every day based on the following parameters: weight loss,

physical appearance, behaviour and posture, and tumour status. Mice were euthanised at the end of the experiment or if animal welfare was compromised in accordance with institutional guidelines. At the end of the experiment, flash-frozen and FFPE tumours were taken for posterior proteomic and genomic analyses. Samples were collected 2 hours after the administration of olaparib, AZD5305, ATRi, DNA-PKi and POLθi as single agents and one hour after the administration of the PARPi in the case of combinations with POLθi. Upon cisplatin and carboplatin treatments, samples were collected 24 and 2 hours after the administration, respectively.

Treatment response classification

The antitumour response was classified according to the relative change in tumour volume upon treatment, similar to the Response Evaluation Criteria in Solid Tumours (RECIST) and denominated mRECIST (modified RECIST). Complete response (CR) was set as best response ≤-95%; partial response (PR) as -95%<best response≤-30%; stable disease (SD) as -30%<best response≤+20%; and progressive disease (PD) as best response>+20%. Models that displayed a preclinical benefit from treatment (SD, PR, and CR) were categorized as sensitive, whereas all PD models were categorized as resistant. For therapy sensitive PDXs, the best response was defined as the minimum value of % tumour volume change sustained for at least 10 days. For resistant tumours or for control tumours, tumour volume at day 21 was considered.

Pharmacodynamic studies for biomarkers analysis

For pharmacodynamic studies, tumour tissue was reimplanted into 2 mice per treatment arm and, when tumours reached 300-500 mm^3, they were randomized into treatment groups (control, olaparib at 50 mg/kg, olaparib at 100 mg/kg or AZD5305 at 1 mg/kg) and treated for 12 days. Tumours were collected 2 hours after dosage. Flash-frozen and FFPE tumours were taken for posterior biomarker, proteomic and genomic analyses.

1.3 Generation of PDX models of acquired resistance to PARPi

To generate PDX models of acquired resistance to PARPi from those that were originally sensitive (CR, PR, SD), either olaparib or AZD5305 (saruparib) treatment was maintained for up to 150 days. Upon regrowth (100-300 mm^3), PARPi-resistant individual tumours (named “OR” in the case of olaparib-resistant and “SR” in the case of saruparib-resistant tumours) were perpetuated under PARPi treatment pressure.

1.4 Preclinical evaluation of drug antitumour activity in PDXs

Response to therapy was evaluated by measuring different preclinical readouts: preclinical complete response rate (pCRR), preclinical overall response rate (pORR) and preclinical benefit rate (pCBR), calculated over the mean of individual tumours from olaparib-sensitive PDX models showing at least one CR, CR+PR and CR+PR+SD upon PARPi treatment, respectively. More specifically, the pCRR was defined as the fraction of olaparib-sensitive PDXs with at least one individual tumour reaching a CR for at least 10 days. The pORR was defined as the fraction of olaparib-sensitive PDXs with at least one individual tumour reaching a CR or a PR for at least 10 days. Finally, the pCBR as the fraction of olaparib-sensitive PDXs with at least one individual tumour reaching a CR or a PR for at least 10 days or a SD for a minimum of 80 days. Preclinical progression-free survival (pPFS) was defined as the time to disease progression or death from any cause. Preclinical time to progression (pTTP) was defined as the number of days until initially sensitive tumours (CR+PR+SD) regrew.

2. Patient-derived tumour cells (PDCs) and *ex vivo* experiments

2.1 Generation and establishment of PDCs

Patient-derived tumour cells (PDCs) were isolated from PDX through combination of mechanic disruption and enzymatic disaggregation[130]. Briefly, PDX tumours (500-800 mm^3) were freshly collected in DMEM/F12/HEPES (Gibco) after surgery resection, minced using sterile scalpels and dissociated for 1 hour in DMEM/F12/HEPES (Gibco), 1 mg/ml collagenase (Roche), 100 ug/ml hyaluronidase (Sigma-Aldrich), 5% Bovine Serum Albumin (BSA, Sigma-Aldrich), 5 µg/ml insulin and 50 µg/ml gentamycin (Gibco). This was followed by further dissociation using trypsin (Gibco), dispase 5 mg/ml (StemCell technologies) and DNase 1 mg/ml (Sigma-Aldrich). Red blood cell lysis was done by washing the cell pellet with 1X Red Blood Cell (RBC) Lysis Buffer containing ammonium chloride (Invitrogene). To avoid stroma outgrowth, cells were firstly resuspended in DMEM supplemented with 10% of foetal bovine serum (FBS) and cultured 1 hour in a petri dish to let fibroblasts attach to the plastic surface. The non-adherent tumour fraction was then resuspended in RPMI 1640 with GlutaMAX medium (Gibco) supplemented with 2% of heat inactivated FBS (Gibco), 10 µM ROCK inhibitor (Sigma-Aldrich), 1X B-27 Supplement (Invitrogen), 3 µg/ml EGF (Peprotech), 5 µg/ml Insulin (Roche), 1 µg/ml Hydrocortison (Sigma), Gentamycin (Gibco), 15 µg/ml Fungizone (Gibco)[131].

2.2 FFPE blocks from PDCs for biomarker analysis

PDCs were seeded at $2x10^5$ cells/ml in 6-well plates (BD Biosciences). After 24 hours, cells were treated with vehicle (DMSO) or olaparib at 2.5 µM and incubated at 37ºC in 5% of CO_2 for 48 hours. Vehicle and olaparib-treated PDCs were collected into canonical tubes and centrifuged at 2000 rpm for 5 min to obtain cell pellets that were then washed twice with PBS. Pellets were

fixed overnight at 4ºC in 4% paraformaldehyde, which was replaced by 70% ethanol the following day. Then, pellets were centrifuged at 2000 rpm for 10 min and supernatant was discarded. Finally, pellets were extracted using a needle, introduced in cassettes and maintained in 70% ethanol until embedded in paraffin.

2.3 PDCs *ex vivo* experiments

For half maximal inhibitory concentration (IC_{50}) analysis, PDCs were seeded into 96-well plates (2 x 10^3 cells/well, BD Bioscience). After 24 hours, cells were treated with vehicle (DMSO) or different concentrations of olaparib and incubated at 37ºC in 5% of CO_2 for 14 days. Treatments and media were refreshed every 48 hours. Known olaparib-sensitive and -resistant PDCs were included in every batch of analysis as controls. Plates were read with CellTiter Glo® Luminiscent Cell Viability Assay (Promega) in an Infinite M200 PRO plate reader (TECAN). Values at day 14 were subtracted with the mean background signal (no cells), normalized with values at day 0, relativized to controls (not treated cells) and plotted as the percentage inhibition against the log concentration of olaparib. The IC_{50} values were calculated performing a non-linear regression. Each experiment was repeated at least two times with two technical replicates.

3. DNA sequencing

3.1 Targeted-sequencing

VHIO PDX models

All laboratory methods were performed using the manufacturer's protocols. Genomic DNA was isolated from fresh-frozen PDX tissue using the DNeasy Blood & Tissue Kit (Qiagen, #69504). All samples were quantified using the Qubit® dsDNA HS Assay Kit (catalog #Q32851) and Qubit 2.0 fluorometer (Thermo Fisher Scientific, Waltham, MA, USA). Hybridisation, capture and

sequencing of exonic and intronic regions (<±10 bp) of interest were performed using the DNA NGS-based gene panels BRCA Hereditary Cancer MASTR™ Plus (Agilent) or Hereditary Plus OncoKitDx (Healthincode) in a MiSeq device (Illumina). Genes included in each panel are specified in Annex I. In the case of the first kit, coverage range was 100-2240X. Results were analysed with Sophia DDM® platform, which integrates PEPPER™, MUSKAT™ and MOKA™ technologies (minimum coverage of 100 reads per base). In the case of the second kit, the mean coverage was >350X. The bioinformatic analysis of SNVs, insertion/deletions, CNVs and Alus was performed using Data Genomics software (Imegen; v19.1). Potential reversion mutations were verified by manual inspection of alignments in IGV. Variants were described and classified according to HGVS (http://www.hgvs.org) and ACMG/GAMP (2015), with reference hg19 (GRCh37). No variants were detected in regulatory or intronic zones >±10 bp.

XenTech PDX models

For the XenTech PDXs, mutation profiling of 73 genes among the most frequently mutated in cancer according to the COSMIC database was performed at BGI (Beijing, China; see Annex I). Exon trapping was performed on genomic DNA with NimbleGen microarray followed by deep sequencing by using Illumina's HiSeq technology, with at least 50x effective mean coverage for each sample.

3.2 Whole exome-sequencing (WES)

All laboratory methods were performed using the manufacturer's protocols. Genomic DNA was isolated from fresh-frozen PDX tissue using the DNeasy Blood & Tissue Kit (Qiagen, #69504). All samples were quantified using the Qubit® dsDNA BR Assay Kit (Invitrogen, #Q32853) and by Qubit Flex Fluorometer (Invitrogen), DNA purity was determined using a NanoDrop Eight (Thermo Scientific) and DNA integrity was measured using a 4200

Tapestation (Agilent). Exome libraries were constructed using the Illumina DNA Prep with Exome 2.0 Plus Enrichment (Illumina, #20077596). Paired-end sequencing with a read length of 150bp was performed using Illumina NovaSeq 6000 with approximately 10 Gbp per sample for ~200-fold average sequence depth. Library sizes and quantification were determined by 4200 Tapestation (Agilent) and pooled libraries were subsequently pooled equimolar. Each library was loaded onto one lane of an S4 v1.5 flow cell (300 cycles) (Illumina, #20028312).

Sequencing data was demultiplexed, passed through a bcl-to-fastq conversion program (bcl2fastq v2.20.0.422). Fastq files were analyzed using pipeline software bcbio-nextgen v1.2.9 (https://doi.org/10.5281/zenodo.3564938). Reads were aligned to the human hg38 and mouse mm10 reference using bwa mem v0.7.17, and sequencing duplicates for each UMI were collapsed into a single consensus read using fgbio v1.4.0. All software were run using best practice parameters established within the bcbio workflow or in-house (AstraZeneca). Mouse-derived sequences were removed using Disambiguate[132]. Variant calling was performed using VarDict v1.8.2[133], down to a variant allele frequency (VAF) of 1% (before filtering and curation) and variant effects annotated by snpEff 5.0. Filtering of non-cancer variants (i.e. common polymorphisms) was performed as per VarDict best practice.

Additionally, the following filters were applied using the NGS Report App in SolveBio: preset filter: Tissue; Hide Variant Depth (VD) below: 3; Hide Total Depth below: 50; Additional SolveBio filters: “type” does not equal “synonymous_variant” and “dkfzbias” does not equal “strand”.

Copy number analysis was performed using Seq2C v1.3[133]. The change in the normalized Log2 values was used to determine potential copy number changes. Chromosome Y was excluded and only deletions with log2ratio<0 or whole gene amplifications with log2ratio>0 were kept.

Structural variants were reported by manta v1.6.0, and filtered for having annotation_parsed.detail__exact = ON_PRIORITY_LIST, split_read_support_1 > 15, split_read_support_2 > 15.

3.3 Genomic HRD by scars and signatures

Three different genomic scar or signature assays were performed. The Myriad's myChoice® HRD test was carried out at Myriad Genetics on DNA extracted from a subset of Xentech PDX models by using the NucleoBond AXG100 kit (Macherey-Nagel, #740545) according to the manufacturer's protocols and as described by *Abkevich et al.,* and *Timms et al.,*[95,96]. The WGS-based signature named HRDetect and the Genomic Instability Score (GIS, defined as the unweighted sum of loss off heterozygosity (LOH), telomeric allelic imbalance (TAI) and large-scale state transitions (LST) scores) were performed at the Wellcome Trust Sanger Institute on DNA extracted from a subset of VHIO PDX models as described by *Davies et al.,*[94] and *Sztupinszki et al*.,[134].

4. RNA sequencing

4.1 NovaSeq 6000 Illumina

RNA was extracted from 15–30 mg of fresh-frozen tumour from PDX samples by using the RNeasy Mini kit (Qiagen, #74104). RNA concentration was determined by Qubit Flex Fluorometer (Invitrogen), RNA purity was determined using a NanoDrop Eight (Thermo Scientific) and RNA integrity was measured using a 4200 Tapestation (Agilent). Libraries were prepared using NEBNext Ultra II Directional RNA Library Prep Kit for Illumina (New England BioLabs, E7760L) or NEBNext® Ultra™ II RNA Library Prep Kit (New England BioLabs, E7770L) as per manufacturer's guidelines. Ribosomal RNA (rRNA) was removed using the NEBNext® Poly(A) mRNA Magnetic Isolation Module (New England BioLabs, E7490L) or using the NEBNext® rRNA Depletion Kit v2 (Human/Mouse/Rat) (New England

BioLabs, E7400X). Paired-end sequencing with a read length of 150 bp was performed using Illumina NovaSeq 6000. Library sizes and quantification were determined by 4200 Tapestation (Agilent) and libraries were subsequently pooled equimolar. Each library was loaded onto one lane of an S4 v1.5 flow cell (300 cycles) (Illumina, #20028312).

4.2 RNA-sequencing data processing

The RNAseq pipeline implemented in bcbio-nextgen (version 1.2.9) was used for quality control and gene expression quantification. Reads were aligned to the UCSC build GRCh38 Homo sapiens genome, augmented with transcript information from Ensembl release 86 using STAR's 2-pass mapping mode (version 2.6.1d), and to mouse mm10 genome. Alignments were evaluated for evenness of coverage, rRNA content, genomic context of alignments and complexity using a combination of FastQC, Qualimap and custom tools. Transcripts Per Million (tpm) measurements per isoform were generated by alignment-based quantification using the Salmon software (version 1.6.0) and used to estimate abundance of genes. Log2 transformation was used for data analysis.

4.3 *BRCA1* Δ11q splicing variant expression analysis by RT-qPCR

The Δ11q splicing variant expression was analysed in the *BRCA1* exon 11-mutated PDX models included in the AZD5305 study. mRNA from PDX biological replicates was extracted using the RNeasy Mini Kit (Qiagen, #74104) according to the manufacturer’s protocols. An additional step of DNase digestion using the RNase-free DNase Set (Qiagen, #79254) was performed. A total of 200 ng of RNA was retrotranscribed using PrimeScript RT reagent Kit (Takara, RR037B) following the manufacturer’s instructions to finally perform a reverse transcription-quantitative PCR (RT-qPCR). To quantify the *BRCA1* Δ11q isoform transcript levels, 20 ng of cDNA were amplified using TaqMan® MGB probes targeting exon 11 cryptic donor and exon 12 acceptor junction. Additionally, a TaqMan® probe expanding exon

23-24 junction was added to measure *BRCA1* global expression (**Table 2**). The TaqMan Fast Advanced Master Mix (Applied Biosystems, #4444556) was used and samples were run for 40 cycles on a Quant Studio 6 Flex Real-Time PCR System (Applied Biosystems) with the following thermal cycler conditions: 2 min at 50ºC, 20 seconds at 95ºC, 3 seconds at 95ºC and 30 seconds at 60ºC. Relative gene expression of *BRCA1* and, specifically, the Δ11q splicing variant was determined by the comparative Ct method[135]. The geometric means of the expression values for both *RPLP0* and *GAPDH* housekeeping genes were used to normalize the expression and to calculate the normalized standard deviation (SD) of all transcripts analysed. Splicing fraction of the D11q isoform was calculated as $2^{-\Delta Ct(\Delta 11q)}/(2^{-\Delta Ct(23\text{-}24)}) \cdot 100$ as described in *Colombo et al,.*[136].

Table 2. Details of TaqMan® MGB probes used for the RT-qPCR.

Target	Manufacturer	Probe ID	Reporter dye	Quencher
BRCA1 Δ11q	Thermo Fisher Scientific	Custom assay	FAM™	NFQ
BRCA1 global expression	Thermo Fisher Scientific	Hs01556193_m1	FAM™	NFQ
RPLP0	Thermo Fisher Scientific	Hs99999902_m1	VIC™	NFQ
GAPDH	Thermo Fisher Scientific	Hs02758991_g1	VIC™	NFQ

5. *BRCA1* promoter hypermethylation quantitative assays

BRCA1 promoter methylation was quantified using methylation-specific multiplex ligation-dependent probe amplification (MS-MLPA; MRC Holland, Amsterdam, the Netherlands) according to manufacturer's instructions. *BRCA1* epigenetic silencing was further confirmed by lack of *BRCA1* transcript by RNA-sequencing (cut-off ≤ 1 tpm). Two of the PDXs generated in CRUK/UCAM (STG139 and STG201) were previously tested using reduced-representation bisulfite sequencing (RRBS)[130] and further validated using MS-MLPA. Positive controls of tumours with *BRCA1* promoter hypermethylation were used (samples T127 and T162)[137].

6. Protein quantification and biomarker analysis

6.1 Immunohistochemistry (IHC) and biomarker scoring

The molecular characterization of the PDX models was performed by IHC in 3 µM thick FFPE tumour samples. Staining of estrogen receptor (ER), progesterone receptor (PgR), human epidermal growth factor receptor 2 (HER2) and the proliferation marker Ki-67 were undertaken following the protocol provided by Ventana Medical System, Inc and described by *Palafox et al.,*[138] (antibody details in **Table 3**). Positive and negative controls were run along tested slides per each marker. ER, PgR and Ki-67 staining were quantified as the percentage of positive cells with nuclear staining. ER and PgR+ tumours were determined following the recommended cut-off according to the ASCO/CAP guidelines for ER and PgR positivity by IHC (1% of tumour cell nuclei immunoreactive[139]). Tumours were considered as HER2+ if they displayed an intense circumferential membranous staining in >10% of cells[139]. All the scorings were performed with the help of a pathologist.

6.2 PARylation assay

Protein isolation

Flash-frozen pieces of tumours were lysed in ice-cold 1x radioimmunoprecipitation assay buffer (RIPA) containing Tris–HCl pH 8.0 10 mM, EDTA 1 mM, Triton-X-100 0.1%, SDS 0.1%, SDC 0.1% and NaCl 140 mM, supplemented with 1X protease inhibitor cocktail (cOmplete, Roche), NaF 10 mM, Na_2VO_4 200 mM and PMSF 5 mM. Homogenization was performed on ice with a POLYTRON® system PT 1200 E (Kinematica). Lysates were centrifuged at 15.000 *g* at 4ºC for 15 min and supernatants were collected. Protein concentration was calculated using DC™ Protein Assay (Bio-Rad).

Western Blot (WB)

PARylation was determined by WB. Briefly, a total of 20 µg of protein was separated on 8% and 12% SDS-PAGE acrylamide gels at 100 V and transferred to nitrocellulose membrane for 1.5 hours at 100 V. Membranes were blocked for 1 hour in 5% milk in Tris-buffered saline (TBS) with 0.1% Tween20 (T-TBS) and then hybridized using the corresponding primary antibodies in 5% BSA (Sigma-Aldrich, #A9647) with T-TBS overnight at the dilutions detailed in **Table 3**. Membranes were incubated for 1 hour with mouse and rabbit horseradish peroxidase (HRP)-conjugated secondary antibodies (GE Healthcare) in 5% milk in T-TBS, dilution details in **Table 3**. Proteins were detected with Immobilon Western Chemiluminescent HRP substrate (Millipore). Immunoblots were captured at the chemiluminescence imager Amersham Imager 600 (GE Healthcare). Images were captured with FUJIFILM LASS-4000 camera system.

6.2 Immunofluorescence (IF) and biomarker scoring

Staining

IF was performed in 3 µM thick FFPE tumour samples from both PDXs and cancer patients as described by *Cruz et al.,*[100] and *Castroviejo et al.,*[99]. Briefly, for target antigen retrieval, the sections were microwaved (Whirlpool JT479/WH) for 20 min at maximum power in DAKO Antigen Retrieval Buffer pH 9.0. Sections were cooled down in distilled water for 30 min, then permeabilized with DAKO Wash Buffer (contains Tween-20) for 5 min, followed by incubation in blocking buffer (DAKO Wash Buffer with 1% BSA) for 5 min. Primary antibodies were diluted in DAKO Antibody Diluent and incubated at room temperature for 1 hour (dilution details in **Table 3**). Sections were washed for 5 min in DAKO Wash Buffer followed by 5 min in blocking buffer. Secondary antibodies were diluted in blocking buffer (details in **Table 3**) and incubated for 30 min at room temperature. The 2-step washing was repeated followed by 5-min incubation in distilled water.

Dehydration was performed with increasing concentrations of ethanol. Sections were mounted with DAPI ProLong Gold antifading reagent and stored at -20ºC. Positive and negative controls were run along the tested slides per each marker. Image analysis and acquisition were performed using Nikon Ti-2 Eclipse microscope and NIS Elements software.

Biomarker scoring

RAD51, BRCA1, γ-H2AX, pRPA and 53BP1 nuclear foci were counterstained with geminin, a master regulator of cell-cycle progression[140], in order to identify cells in the S/G2 phases of the cell cycle (antibodies details in **Table 3**).

Functional homologous recombination deficiency (HRD) was assessed by the RAD51 score as the percentage of geminin-positive (geminin$^+$) cells with 5 or more nuclear foci of RAD51[99,100]. BRCA1 nuclear foci were quantified for a deeper characterization of the HRR functionality, and nuclear DNA damage was determined by presence of γ-H2AX[141]. pRPA was quantified to determine the levels of replication stress. Finally, activation of the 53BP1 pathway and its recruitment to DNA damage was evaluated by the presence of 53BP1 nuclear foci. Biomarkers were assessed as the percentage of geminin+ cells with 5 or more nuclear foci. One hundred geminin$^+$ cells from at least three representative areas of each sample were analysed. Samples with low γ-H2AX (< 25% of geminin$^+$ cells with γ-H2AX foci) or with < 40 geminin$^+$ cells were not included in the analysis, due to insufficient endogenous DNA damage or tumour cells in the S/G2-phase of the cell cycle, respectively. Genome instability was scored as the percentage of tumour cells with at least one micronucleus based on DAPI staining (micronuclei score). One hundred cells from at least three representative areas of each sample were analysed for the micronuclei score. All scorings were performed blindly onto life images using a 60x-immersion oil lens in a Nikon Ti-2 Eclipse microscope and NIS

Elements software. At least two biological replicates per PDX model were analysed.

Table 3. Details of antibodies used for IHC, WB and IF.

Abbreviations: IHC: immunohistochemistry; WB: western blot; IF: immunofluorescence.

Target	Source	Manufacturer	Reference	Application	Dilution	Diluent
Ki67	Rabbit	Ventana	790-4286	IHC	Ready-to-use	NA
ER	Rabbit	Ventana	790-4325	IHC	Ready-to-use	NA
PR	Mouse	Ventana	790-4296	IHC	Ready-to-use	NA
HER2	Rabbit	Ventana	790-2991	IHC	Ready-to-use	NA
Poly/Mono-ADP Ribose	Rabbit	Cell Signalling	83732	WB	1:1000	5% BSA T-TBS
hGAPDH	Rabbit	Abcam	Ab128915	WB	1:5000	5% BSA T-TBS
Horseradish peroxidase (HRP)-conjugated	Rabbit	GE Healthcare	NA934	WB	1:2000 / 1:10000	5% milk T-TBS
Geminin	Mouse	NovoCastra	NCL-L	IF	1:60	DAKO Antibody Diluent
Geminin	Rabbit	ProteinTech	10802-1-AP	IF	1:400	DAKO Antibody Diluent
RAD51	Rabbit	Abcam	Ab133534	IF	1:1000	DAKO Antibody Diluent
BRCA1 (C-ter)	Mouse	Santa Cruz	Sc-6954	IF	1:50	DAKO Antibody Diluent
BRCA1 (N-ter)	Mouse	Abcam	Ab16780	IF	1:200	DAKO Antibody Diluent
γ-H2AX	Mouse	Millipore	05-636	IF	1:200	DAKO Antibody Diluent
pRPA32 S4/S8	Rabbit	Bethyl	A300-245A	IF	1:500	DAKO Antibody Diluent
53BP1	Rabbit	Cell Signalling	4937	IF	1:200	DAKO Antibody Diluent
Alexa fluor 568	Rabbit	Invitrogen	A-11011	IF	1:500	1% BSA DAKO Wash Buffer
Alexa fluor 488	Rabbit	Invitrogen	A-11008	IF	1:500	1% BSA DAKO Wash Buffer
Alexa fluor 568	Mouse	Invitrogen	A-11004	IF	1:500	1% BSA DAKO Wash Buffer
Alexa fluor 488	Mouse	Invitrogen	A-11001	IF	1:500	1% BSA DAKO Wash Buffer

7. Study and validation of functional HRD biomarkers in clinical samples

7.1 PETREMAC trial (NCT01326880)[142,143]

Study design and patients

In the phase II PETREMAC trial, patients with stage II/III breast cancer were stratified to eight different neoadjuvant treatment regimens based on hormone receptors and HER2 expression, as well as *TP53* mutation status (**Figure 16A** and **B**). The primary aim of the trial was to implement optimal neoadjuvant therapy for high-risk breast cancers, select therapy based on predefined biological parameters and identify novel predictive biomarkers for each individual treatment strategy. Patients with TNBC received initial olaparib monotherapy 300 mg BID for up to 10 weeks, irrespective of *BRCA* and *TP53* mutation status (treatment arms G and H; **Figure 16B**), aiming to shrink tumour size before chemotherapy. Olaparib monotherapy was halted, and chemotherapy was introduced before 10 weeks for patients without evidence of tumour regression[142]. Clinical and radiological evaluation of tumour size was carried out by each local investigator, blinded to knowledge of genomic aberrations, apart from *TP53* mutation status. The median pre-treatment tumour diameter was evaluated by magnetic resonance imaging (MRI).

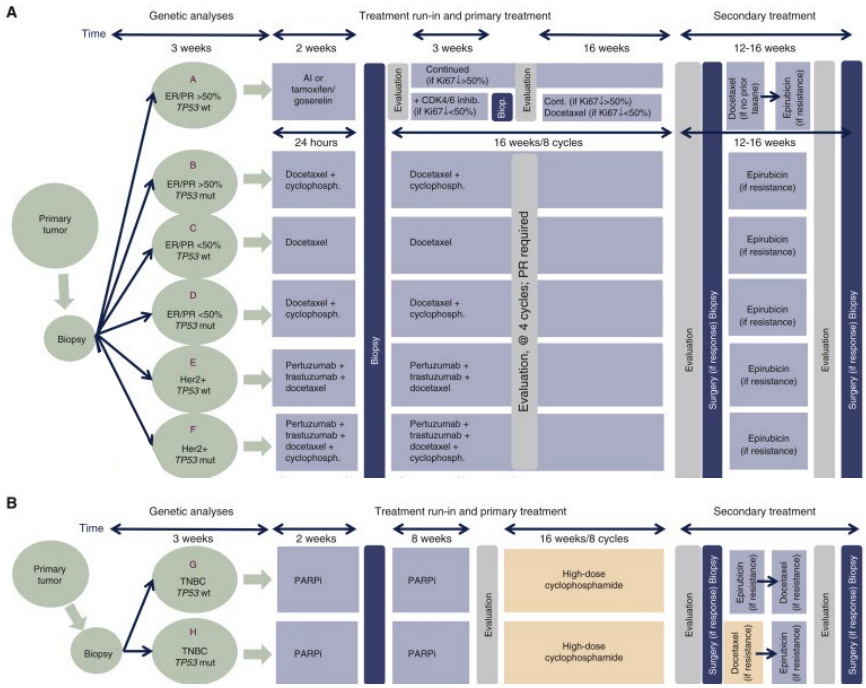


Figure 16. Outline of study arms of the neoadjuvant PETREMAC trial.

A. After informed consent, breast cancer (BC) biopsies were taken and examined for ER, PgR and HER2 expression, in addition to *TP53* mutation status during the screening phase. Based on these results, patients were allocated to the eight study arms to receive personalized neoadjuvant treatment. **B.** Patients with TNBC were allocated to study arms G (*TP53* wild-type; *TP53* wt) and H (*TP53* mutated; *TP53* mut) and received initial olaparib monotherapy with or without subsequent chemotherapy. Abbreviations: AI: aromatase inhibitor; cyclophosph.: cyclophosphamide; ER: estrogen receptor; mut: mutation; wks: weeks; wt: wildtype. Adapted from *Eikesdal et al.,*[142].

Tumour HRR status and RAD51 score

Targeted DNA sequencing applying a 360-gene panel[144] was conducted on tumour biopsies extracted before and after olaparib treatment. Mutations identified in HRR or other DNA damage repair pathways were annotated as likely drivers by predefined criteria[142]. Further analysis of tumour samples for *BRCA1* promoter methylation by methylation-specific quantitative PCR and *BRCAness* by multiplex ligation-dependent probe amplification (MLPA) or an amplicon-based next-generation sequencing assay[144-146] were carried out.

For the non-TNBC cohort, as primary analysis, HRD was defined applying a strict definition (HRD-S) and included mutations in: *BARD1, BRCA1, BRCA2, BRIP1* and *PALB2*. In secondary analyses, a wider definition (HRD-W) was used and included: *ABL1, ATM, ATR, ATRX, BARD1, BLM, BRCA1, BRCA2, BRIP1, CDK12, CHEK1, EMSY, ERCC4, FANCA, FANCC, FANCD2, FANCE, FANCF, FANCG, MEN1, MRE11, NBN, PALB2, PTEN,* and *SETD2*. *BRCA1* promoter methylation analyses were combined with HRR mutations to evaluate the prevalence of HRD by either HRD-W or HRD-S. Furthermore, to call HRD-S status, the HRR mutations had to be deleterious, and somatic HRR mutations or *BRCA1* methylation had to be accompanied by LOH to ascertain biallelic gene inactivation.

Additional methods can be found in *Eikesdal et al.,*[142] *and Yndestad et al.,*[143].

7.2 GeparSixto trial (NCT01326880)[78]

Study design and patients

Patients diagnosed with TNBC who participated in the GeparSixto trial (NCT01426880) were scheduled to receive paclitaxel (80 mg/m^2) plus nonpegylated liposomal doxorubicin (PM, 20 mg/m^2 Myocet; Teva Pharm, North Wales, PA), both administered q1w for 18 weeks, and bevacizumab (15 mg/kg q3w) during all chemotherapy cycles (**Figure 17**). Patients with HER2+ disease were included in the trial and received trastuzumab and lapatinib, but not in the work of this thesis. Patients were randomized to receive simultaneously carboplatin (PMCb) q1w for 18 weeks or no additional treatment[147]. All patients provided written informed consent for trial participation and translational research. Ethical committee approval (119/20) from the University of Marburg, Germany was obtained.

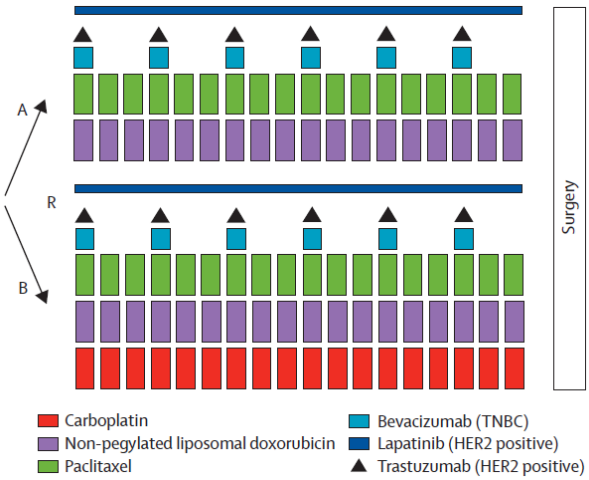


Figure 17. Outline of study arms of the neoadjuvant GeparSixto trial.
Regimens were without (**A**) and with (**B**) carboplatin. Patients with previously untreated, non-metastatic, stage II–III, TNBC and HER2+ breast cancer (BC) were enrolled. Patients were treated for 18 weeks with paclitaxel (80 mg/m² once a week) and non-pegylated liposomal doxorubicin (20 mg/m² once a week). Patients with TNBC received simultaneous bevacizumab (15 mg/kg intravenously every 3 weeks). Patients were randomly assigned in a 1:1 ratio with dynamic allocation and minimisation, stratified by biological subtype and Ki-67 level to receive, at the same time as the backbone regimens, either carboplatin or no carboplatin. Abbreviations: TNBC: triple-negative breast cancer. Adapted from von *Minckwitz et al.,*[147].

The primary endpoint of the GeparSixto study was pCR. Predefined secondary endpoints included disease-free survival (DFS) and overall survival (OS)[148], and a predefined exploratory analysis of HRD biomarkers[95,148,149]. Specifically, we aimed to investigate if the RAD51 score correlates with the t*BRCA* status. A secondary objective was to determine whether RAD51 before therapy initiation correlates with therapy outcome.

Tumour *BRCA* status and RAD51 score

Treatment-naïve FFPE core biopsies were assessed retrospectively for mutations in *BRCA1* and *BRCA2*. The RAD51 test was performed as previously described[98-100].

Additional methods can be found in *Llop-Guevara et al.,*[78].

7.3 Analytical validation and interobserver variability of the RAD51 assay: the RING trial[150]

The evaluation of the RAD51 assay procedure and quantification comprised four European laboratories, i.e., Vall d'Hebron Institute of Oncology (VHIO, Spain), Institute Gustave Roussy (IGR, France), Leiden University Medical Center (LUMC, the Netherlands), and Parma Medical Center (PMC, Italy)[150]. Observers were already trained to stain and score RAD51. The study was divided into a training phase, a evaluation meeting and a testing phase. The study was conducted in accordance with the Declaration of Helsinki, and the protocol was approved by the Ethics Committee of the Leiden University Medical Center (nWMO-D4-2022-030).

Training phase and evaluation meeting

First, 12 high-grade serous ovarian cancer (HGSOC) specimen sections were stained for γ-H2AX/geminin in two laboratories according to local staining procedures[99,100,151]. Next, HGSOC sections were stained for RAD51/geminin in the four academic laboratories applying local staining protocols (**Figure 18A**)[98,151,152]. Moreover, HGSOC specimens were stained four-fold in one of the laboratories according to a central protocol[78,99,100,151] and distributed to participating laboratories for local RAD51 scoring (**Figure 18B**). Thus, training phase specimens were stained and score twice, applying both local and central staining protocols.

RAD51 scoring was performed by a local observer according to a predefined scoring methodology. A comprehensive overview of the RAD51 scoring methodology, including RAD51 scoring form, can be found in *Kramer et al.,*[150]. In this case, RAD51 nuclear foci distribution was determined (heterogeneity).

In the evaluation meeting, the RAD51-stained sections were critically re-reviewed, and features that might underlie the observed variability in RAD51

scores were defined. These features were integrated into an updated RAD51 scoring form.

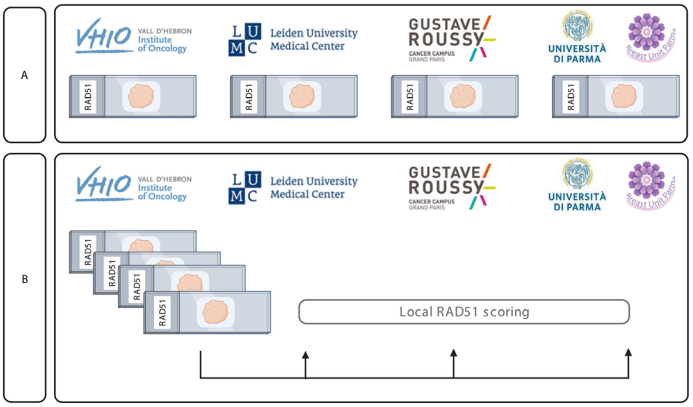


Figure 18. Schematic overview of the design of the training phase of the RING study. **A.** Local staining procedure: each of the n = 12 HGSOC specimens was stained and scored in the academic laboratories according to their local RAD51 staining procedures. **B.** Central staining procedure: each HGSOC specimen was centrally stained four-fold in one centre and distributed to the remining laboratories. Thus, each laboratory provided a final RAD51 score for the same locally and centrally stained section. Adapted from *Kramer et al.,*[150].

Testing phase

In this phase, the interobserver variability was re-determined in an independent set of HGSOC specimens using the updated RAD51 scoring form, provided in *Kramer et al.,*[150]. The RAD51 staining of the testing phase specimens was performed centrally, and stained sections were circulated among participating laboratories for local scoring.

Final RAD51 and γ-H2AX scores were calculated using a foci cut-off of 5 or 2, respectively. On a case level, RAD51 scoring variability was defined as the range of RAD51 scores across observers (highest minus lowest score). If two RAD51 scores were provided by one observer in a heterogeneous case, the highest score was prioritized. The final interobserver variability was defined as the median of RAD51 scoring variabilities. Variability in ranges was

analysed using the first quartile (Q1), median and third quartile (Q3). Specific features were reported if noted by ≥ 3 observers.

8. Statistical analysis

Statistical tests were performed using GraphPad Prism 8.2.1 (GraphPad Software). Details of sample size, replicates, mean, and error bars are provided in figure legends. Normality distribution was assessed with Shapiro-Wilk test in all comparative studies and correlations to assume or not a Gaussian distribution. If the null hypothesis of normal distribution was not rejected, statistical tests were performed using paired and unpaired two-tailed t-test. Otherwise, the non-parametric Mann-Whitney test for unpaired samples or the Wilcoxon matched-pairs signed-rank test for paired samples was used. All analyses were two-tailed unless otherwise stated. The receiver operating characteristic (ROC) curve and the area under the curve (AUC) were calculated to estimate the prediction capacity of the different HRD tests evaluated in this thesis. To calculate association between two variables, linear regression models were fitted to estimate the R^2 with 95% confidence intervals. A linear mixed-effect model was performed to analyse biomarker scores according to response to treatment. For preclinical readouts of response (pCRR, pORR and pCBR), two binomial generalized linear mixed-effects models were performed, both with PDX model as random factor[153]. These models included the preclinical readouts of response as dependent variable and the treatment as fixed factor. In the case of preclinical readouts assessing progression (pPFS, pTBR and pTTP), a mixed-effects cox regression model was performed[154], all of them in R software (https://www.r-project.org/, Team 2023).

RESULTS

Results summary

The work of this thesis has led to the publication of a main article and a second one under review by the time of the writing of this thesis (04/03/2024) with a leading contribution of the PhD candidate. Besides, several papers have been published in which the PhD candidate has contributed.

Aim 1: Development and characterization of a panel of patient-derived xenografts (PDXs) from breast tumours for the study of biomarkers of response to PARP1/2i and platinum-based chemotherapy.

- Results from aim 1 are published in *Cancer Research* (April 2022):

Pellegrino B*, **Herencia-Ropero A*,** Llop-Guevara A, et al. Preclinical In Vivo Validation of the RAD51 Test for Identification of Homologous Recombination-Deficient Tumors and Patient Stratification. *Cancer Res.* 2022;82(8):1646-1657.

*Contributed equally to the article

Aim 2: Overcoming first-generation PARPi resistance with a next-generation PARPi or combinations with other DNA-damaging agents.

- Results from the specific aim 2.1 are under review in *Genome Medicine* by the time of the writing of this thesis (March 2024):

Herencia-Ropero A, Llop-Guevara A, D. Staniszewska A, et al. The PARP1 selective inhibitor saruparib (AZD5305) elicits potent and durable antitumor activity in patient-derived BRCA1, BRCA2 and PALB2-associated cancer models.

- Part of the results from the specific aim 2.2 are published in *Clinical Cancer Research* (October 2022):

Serra V, Wang AT, Castroviejo-Bermejo M, et al. Identification of a Molecularly-Defined Subset of Breast and Ovarian Cancer Models that Respond to WEE1 or ATR Inhibition, Overcoming PARP Inhibitor Resistance. Clin Cancer Res. 2022;28(20):4536-4550. doi:10.1158/1078-0432.CCR-22-0568.

- Part of the specific aim 2.2 and the specific aim 2.3 are unpublished.

Aim 3: Study and validation of functional HRD biomarkers in clinical samples of TNBC and tumours harbouring alterations in HRR-related genes.

- Part of the results from the specific aim 3.2 and 3.3 are published in *JCO Precision Oncology* (December 2023), *Annals of Oncology* (December, 2021) and *The Journal of Pathology: Clinical Research* (November, 2023):

Yndestad S, Engebrethsen C, Herencia-Ropero A, et al. Homologous Recombination Deficiency Across Subtypes of Primary Breast Cancer. *JCO Precis Oncol.* 2023;7:e2300338.

Llop-Guevara A, Loibl S, Villacampa G, et al. Association of RAD51 with homologous recombination deficiency (HRD) and clinical outcomes in untreated triple-negative breast cancer (TNBC): analysis of the GeparSixto randomized clinical trial. *Ann Oncol.* 2021;32(12):1590-1596.

Kramer CJ, Llop-Guevara A, Yaniz-Galende E, et al. RAD51 as a biomarker for homologous recombination deficiency in high-grade serous ovarian carcinoma: robustness and interobserver variability of the RAD51 test. *J Pathol Clin Res.* 2023;9(6):442-448

- Results from the specific aim 3.1 are unpublished.

Finally, other publications out of the scope of this thesis in which the PhD candidate has been involved are referenced in Annex III.

PART 1

Development and characterization of a panel of patient-derived xenografts (PDXs) from breast tumours for the study of biomarkers of response to PARP1/2i and platinum-based chemotherapy

First-generation PARP1/2 inhibitors antitumour activity in a panel of PDX models

Establishment and characterization of a PDX panel from HRR-related cancer patients

In this study, we aimed to test the accuracy of the immunofluorescence-based RAD51 assay to predict response to PARPi and platinum in comparison with two well-established HRD tests, with further validation in clinical samples, to eventually support the RAD51 assay in clinical practice.

It is well known that PDXs capture the genomic, transcriptomic and proteomic heterogeneity of patient tumours and faithfully recapitulate response to targeted therapies[155,156]. To study the antitumour activity of first-generation PARP1/2 inhibitors (PARP1/2i) and platinum salts, as well as to validate biomarkers of response to these therapies, a panel of PDXs was developed. From 2010 to 2021, a total of 109 PDX models of HRR-related cancers,

namely breast (BC), ovarian (OvC) and pancreatic cancer (PaC), were established upon subcutaneous engraftment of fresh tumour biopsies into immunodeficient mice. BC PDXs were characterised by IHC to determine the molecular subtype according to ER, PgR, HER2 and Ki-67 expression, which, in addition, was analysed in OvC and PaC models. Thus, we successfully generated a first cohort of 96 PDX models, of which 65 were triple-negative (TN, 72%), 24 hormone receptor-positive (HR+, 27%) and 1 HER2+ (1%) BC, 4 were high-grade serous ovarian cancer (HGSOC, 4%) and 2 were pancreatic adenocarcinomas (PaC, 2%; **Supplementary Table 1**). Regarding tumour setting, 44 of the 96 models (46%) were derived from primary tumours, while 41 (43%) were obtained from metastatic lesions (**Figure 19A, Supplementary Tables 1** and **2**). The stage of 11 tumours (11%) from Tesaro was unknown. Regarding prior treatment, 33 (34%) and 56 (58%) PDXs were obtained from treatment-naïve and previously treated patients, respectively (**Figure 19B, Supplementary Tables 1** and **3**). The list of treatments received by 7 patients from Tesaro (7%) before the generation of the PDXs was unknown.

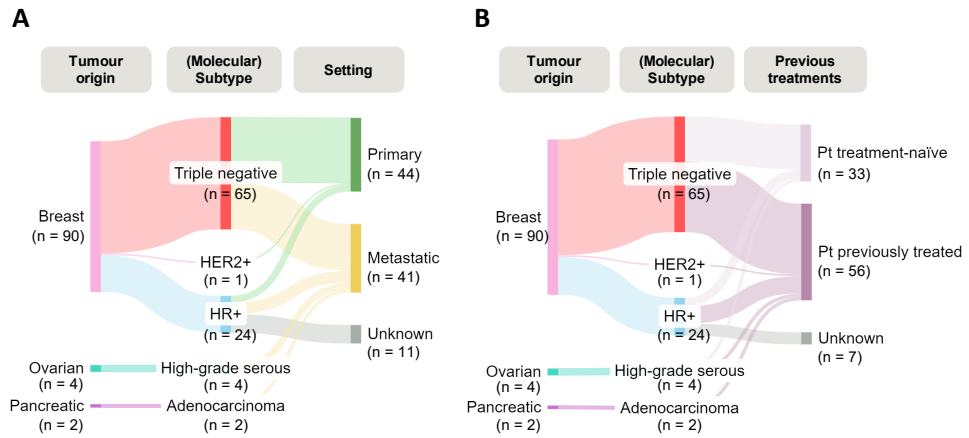


Figure 19. Disease characteristics of the PDX cohort.

Sankey plots showing the PDX tumour origin, PDX molecular subtype (based on the IHC) and **A**. tumour setting, or **B.** previous treatments received by patients before the generation of the matched PDX model (n = 96). Abbreviations: Pt: patient.

We then aimed to further characterise the cohort of PDXs at the genetic level. DNA targeted- and/or whole-exome sequencing (WES) was performed to identify HRR alterations. Fifty-six of the 96 models (58%) harboured alterations in HRR-related genes, 37 of which were TNBC (57%). More specifically, pathogenic biallelic variants in *BRCA1* and *BRCA2* were identified in 25 (26%) and 13 (13.5%) models, respectively (**Figure 20**). Of note, the majority of *BRCA2*-mutated tumours (7/13, 54%) were ER+ BC, as expected[157,158]. In addition, *BRCA1* epigenetic silencing, assessed by absence of *BRCA1* transcript by RNA sequencing (cut-off ≤1 tmp) and further confirmed by lack of functional BRCA1 nuclear foci by IF in paraffin sections (cut-off ≤10%, see results Part-3), was found in 13 PDXs (13.5%, "*BRCA1*-low" in **Figure 20**). Furthermore, we identified biallelic frameshift mutations in *PALB2* in 3 BC models (3%, PDX093, T298, ST897) and homozygous loss of the genes encoding the RAD51 paralogs *XRCC2* and *XRCC3* in two models (2%, PDX350 and HBCx14, labelled as "Other HRR genes" in **Figure 20** and **Supplementary Table 1**).

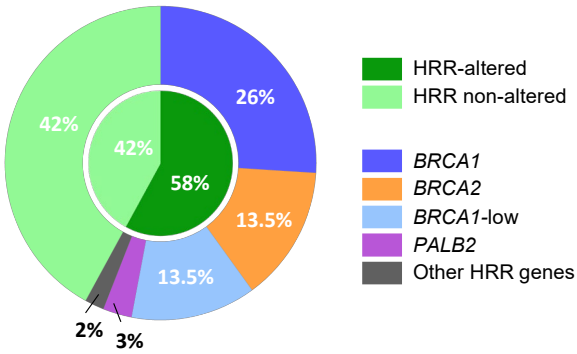


Figure 20. Frequencies of homologous recombination repair (HRR)-related gene alterations in the PDX cohort.

Pie chart indicating the distribution of the HRR functional status and the HRR alterations in 96 PDX models, with *BRCA1* being the most frequently mutated, followed by *BRCA2* and *BRCA1*-low. Abbreviations: HRR: homologous recombination repair.

Since HRR-altered tumours may have a reduced ability to repair DNA damage compared to the non-altered ones, we characterised the

endogenous levels of double-strand breaks (DSBs) in models with and without alterations in the HRR pathway by quantifying γ-H2AX nuclear foci in paraffin-embedded untreated samples. Interestingly, high levels of DNA damage were observed in both HRR-altered and non-altered (WT) models, with no significant differences in γ-H2AX score (%) observed between the two groups (median of 67% vs. 64%, p=0.4; **Supplementary Figure 1A**). Of note, two PDXs showed low endogenous levels (γ-H2AX score < 25%) of DNA damage (HBCx39 and ST1363). Therefore, we successfully generated a characterised a representative cohort of PDX models with and without HRR-related gene alterations that can be used as a platform to study PARPi antitumour activity.

Association of *BRCA1*, *BRCA2* or *PALB2* mutations with PARPi response in PDXs

Since the detection of mutations in *BRCA1* or *BRCA2* is currently one of the main biomarkers used to identify patients who may benefit from PARPi[76,77], we investigated the relationship between the presence of mutations in these genes, together with *PALB2*, known to be frequently mutated in patients with HBOC syndrome, and response to PARP1/2i (olaparib and niraparib) in the cohort of PDX models.

Tumours treated with DNA-damaging agents greatly increase their baseline levels of DSBs[141]. Therefore, we first wanted to interrogate target engagement and the dynamics of DNA damage levels upon treatment with PARPi. As expected, PARPi-treated tumours exhibited significantly higher levels of γ-H2AX than the untreated ones, confirming target engagement of the treatment and subsequent activation of DNA damage repair pathways (median of 65% vs. 83%, p<0.0001; **Supplementary Figure 1B**). Alike untreated tumours, no differences were observed between HRR-altered or non-altered models when analysing the levels of DNA damage upon olaparib

treatment according to the HRR-gene status (median of 82% vs. 83%, p=0.6; **Supplementary Figure 1C**).

Upon treatment *in vivo*, the best response according to modified RECIST criteria was complete response (CR) in 12, partial response (PR) in 10 and stable disease (SD) in 7 PDX models, totalling 29 out of 96 (30%) sensitive models (**Figure 21A**). Among PARPi-sensitive PDXs, 10 were derived from metastatic lesions (35%) and 19 from primary tumours (65%), supporting studies investigating the use of PARPi in the primary setting[86,142]. Interestingly, 55% of the PARPi-sensitive models were derived from previously treated patients, meaning that PARPi were potent enough to hit tumours previously exposed to DNA-damaging agents. As expected, the 29 PARPi-sensitive models harboured alterations in the HRR pathway, of which 10 were *BRCA2*-, 9 were *BRCA1*- and 3 were *PALB2*-mutated PDXs (**Figure 21A** and **B**). Sixty-seven of 96 PDX models were PARPi-resistant (70%, PD, progressive disease as best response), of which 31 were obtained from metastatic lesions (46%) that had received prior lines of treatment (28 out of 31, 90%, **Supplementary Figure 1D**). Twenty-seven of the 67 PARPi-resistant models (40%) were HRR-altered tumours, with *BRCA1* as the most frequently mutated (21 out of 40, 53%). In addition to the 96 original models, 13 olaparib-resistant models were generated from 9 olaparib-sensitive PDXs after prolonged exposure and steep treatment progression (models named OR, “olaparib-resistant”), making a total of 109 (96 original + 13 OR) models. Interestingly, models harbouring *BRCA1* genetic mutations acquired olaparib resistance more frequently (5/13) compared to tumours harbouring mutations in other HRR-related genes, but preclinical progression-free survival (pPFS) was not observed to be associated with the type of HRR alteration (**Supplementary Figure 1E** and **F**). Therefore, considering only HRR-altered PDXs, 29 out of 69 (56 original + 13 OR, 42%) were PARPi-sensitive, while 40 (27 original + 13 OR, 58%) were PARPi-resistant (**Figure 21B**). In total, 80 (67 original + 13 OR) out of 109 (73%) models were resistant to PARPi.

Thus, although the detection of mutations in *BRCA1*, *BRCA2* or *PALB2* captured an HRD prevalence of 45% (49/109) in the cohort of PDXs, only 45% of them (22/49) were sensitive to PARPi. These results indicate that this test does not accurately predict response to PARPi and, in consequence, that there is an unmet need to find more robust biomarkers (**Figure 21A** and **Table 4**). We therefore wanted to further explore the accuracy of other HRD tests, such as genomic scars, signatures and the RAD51 assay.

We finally sought to gain further insight into the mechanisms of resistance to PARPi present in the cohort of PDXs. Since genetic, transcriptomic and protein-based mechanisms of resistance to PARPi have been described, we used WES, bulk RNA-sequencing and BRCA1 nuclear foci IF to cover all these three possibilities. Of the HRR-altered PDXs (n = 69, including models of acquired resistance), 40 (58%) were found to be resistant (**Figure 21B**). Among them, three (PDX093OR6, PDX332 and PDX405OR100) harboured mutations in *PALB2* or *BRCA2* that were compatible with reversions of the original pathogenic mutations. Three *BRCA1*-mutant models harboured alterations in the 53BP1 pathway, which have been shown to confer PARPi resistance (HBCx28, PDX127, PDX230OR1; **Figure 21C** and **Supplementary Table 1**)[159,160]. Additionally, the presence of BRCA1 proteins lacking relevant domains in *BRCA1*-mutated tumours has been associated with resistance to PARPi[106,107,161]. Interestingly, BRCA1 nuclear foci (cut-off≤10%, see Results Part-3) were detected by IF in 7 out of 25 *BRCA1*-mutant models, underscoring the high prevalence of BRCA1 proteins lacking relevant domains (hypomorphic BRCA1) in this panel (**Supplementary Table 1**). Moreover, two models had both alterations in the 53BP1 pathway (STG316 and PDX341, with a mutation in *TP53BP1* and a downregulation of *SHLD1,* respectively) and hypomorphic BRCA1 as assessed by nuclear foci scoring. In addition, BRCA1 nuclear foci were detected in 4 out of 13 initially sensitive *BRCA1*-low models upon acquisition of PARPi resistance. Historically, the presence of RAD51 nuclear foci by IF has been widely used

to determine HRR functionality[162]. We therefore scored RAD51 in untreated paraffin-embedded samples from all models to unravel whether resistance to PARPi was due to a restoration of the HRR pathway functionality. All the previously mentioned PARPi-resistant models exhibited high levels of RAD51, suggesting that the resistance was HRR-dependent. However, the mechanism of intrinsic or acquired resistance to PARPi was unknown in 21 out of the 40 models. Of these, 18 exhibited high levels of RAD51, meaning that the most likely mechanism was based on the restoration of HRR pathway functionality (labelled as “Other RAD51-dependent in **Figure 21C**). The three remaining models (PDX124OR, PDX377OR1 and PDX377OR2) were PARPi-resistant without substantial HRR restoration according to their levels of BRCA1 and RAD51 nuclear foci compared to their sensitive counterparts (PDX124 and PDX377, respectively; “RAD51-independent” in **Figure 21C**). Taken together, the genomic, transcriptomic and BRCA1 protein foci analyses identified likely mechanisms of PARPi resistance in half of the HRR-altered, resistant models.

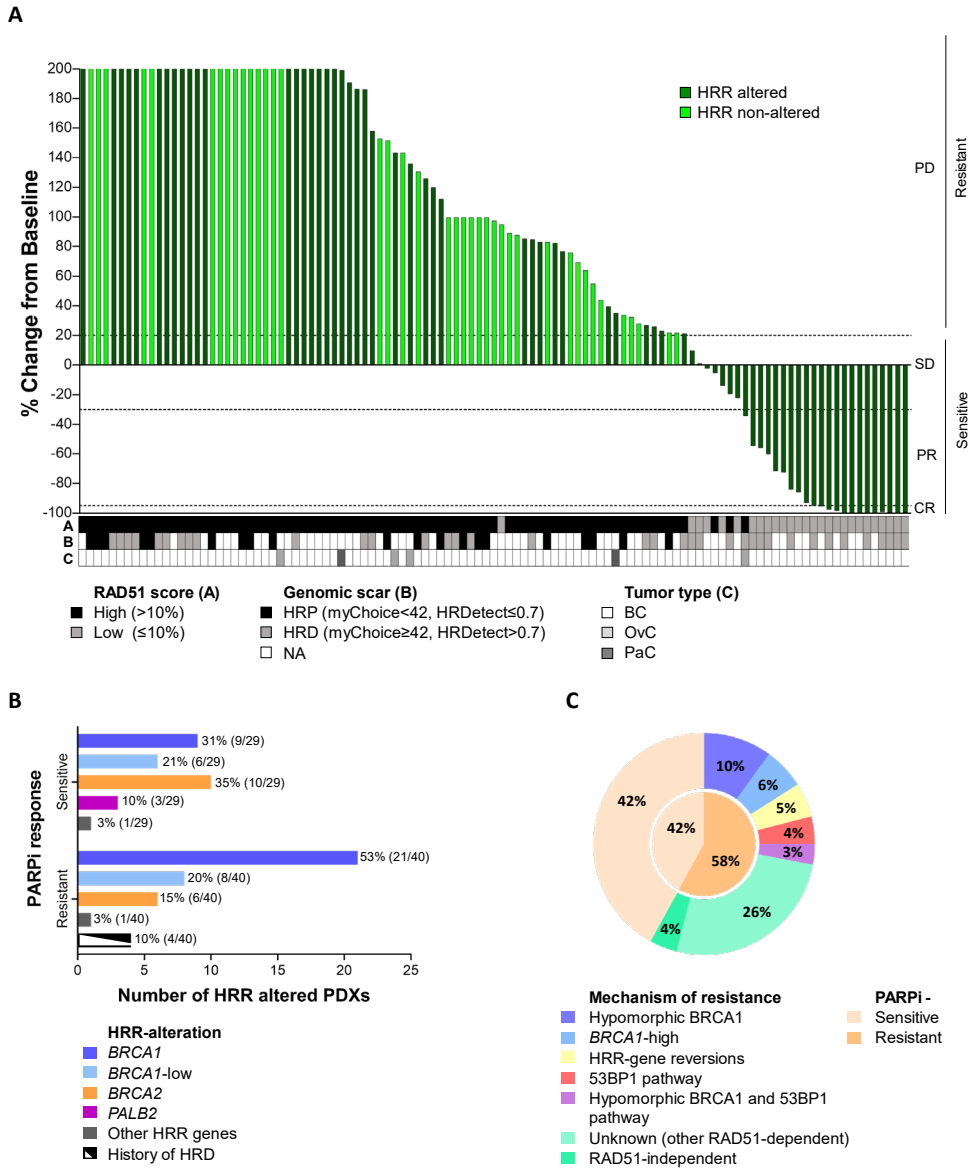


Figure 21. Antitumour activity of PARPi in PDXs.

A. Waterfall plot showing the best response to the PARPi olaparib or niraparib in N = 109 PDX models, measured as percentage of tumour volume change, compared to the tumour volume on day 1. Each bar indicates the mean and SEM of at least three biological replicates. +20%, −30%, -95% are marked by dashed lines to indicate the range of PD (resistant), SD, PR, CR (sensitive), respectively. The box summarizes the RAD51 score (A), the genomic scars (based on Myriad myChoice® or HRDetect) (B) and the tumour type (C, n = 62). **B.** Response to PARPi according to the HRR-gene alteration (PARPi-sensitive, n = 20; PARPi-resistant, n = 40). **C**.

Pie chart indicating the distribution of the sensitivity to PARPi in HRR-altered PDXs and the mechanisms of resistance in PARPi-resistant models (n = 69). Abbreviations: HRR: homologous recombination repair; PD: progressive disease; SD: stable disease; PR: partial response; CR: complete response; HRP: homologous recombination proficiency; HRD: homologous recombination deficiency; NA: non-available; BC: breast cancer; OvC: ovarian cancer; PaC: pancreatic cancer. Adapted from *Pellegrino & Herencia et al.,*[98].

Table 4. Homologous recombination deficiency (HRD) prevalence according to different HRD tests compared to the proportion of PARPi-sensitive tumours.
Abbreviations: HRD: homologous recombination pathway

Biomarkers of PARPi response	*BRCA1/2*, *PALB2* mutations	Genomic HRD score (≥42)	RAD51 score (≤10%)
HRD prevalence (%)	45% (49/109)	59% (24/41)	26% (28/109)
PARPi-sensitive tumours (%)	45% (22/49)	50% (12/24)	93% (26/28)

Biomarkers of homologous recombination deficiency (HRD) and sensitivity to DNA-damaging agents

Detection of HRR-related gene mutations as a biomarker of HRD and PARPi sensitivity in PDX models

We then calculated the sensitivity, specificity, positive predictive value (PPV) and negative predictive value (NPV) of the presence of HRR-related gene mutations (*BRCA1/2* or *PALB2*) described above. Additionally, we calculated the same test performance values for low *BRCA1* expression (mRNA or nuclear foci) to predict PARPi response in the cohort of PDXs (**Table 5**). In line with previous results, these two HRD biomarkers showed similar performance with relatively low robustness, confirming that genetic and epigenetic alterations in HRR-related genes had limited accuracy in predicting PARPi sensitivity (67% and 69%, respectively).

Table 5. Test performance values for the indicated HRD biomarkers predicting PARPi response.

Abbreviations: HRD: homologous recombination deficiency; PPV: positive predictive value; NPV: negative predictive value. Adapted from *Pellegrino & Herencia et al.,*[98].

Biomarkers of PARPi response	*BRCA1/2*, *PALB2* mutations (n = 109)	*BRCA1-low* mRNA/foci (n = 108)	Genomic HRD score (≥42) (n = 41)	RAD51 score (≤10%) (n = 109)	Platinum response (n = 56)
Sensitivity	76%	38%	100%	90%	73%
Specificity	64%	81%	59%	98%	49%
PPV	43%	42%	50%	93%	26%
NPV	88%	78%	100%	96%	88%
Accuracy	67%	69%	71%	95%	54%

Quantification of genomic HRD and association with PARPi response in PDX models

The Myriad myChoice® genomic scar HRD test is widely used to determine the HRD status in OvC patients and provides information on the magnitude of benefit for PARPi[163]. We then investigated the performance of this HRD biomarker and its association with PARPi response in the cohort of PDXs. Genomic HRD was quantified in a subset of 41 PDX models, 11 of which harboured a mutation in *BRCA1/2* or *PALB2*. When we analysed the genomic HRD score according to the HRR-gene status, we observed that all HRR-mutated samples were HRD-positive (cut-off≥42; **Supplementary Figure 2A, Supplementary Table 1**). In addition, the test identified as HRD-positive three HRR non-altered (WT) models, probably due to other alterations in the HRR pathway that have not yet been detected or genomic instability produced from other sources beyond HRD. According to the response to PARPi, all sensitive PDXs were HRD-positive and the median of HRD values was higher in PARPi-sensitive than in PARPi-resistant models (median of 67 vs. 36, p=0.0002; **Figure 22A**). Nevertheless, 12 out of 29 PARPi-resistant PDXs were also HRD-positive: the 3 HRR-WT models mentioned above together with 9 tumours lacking *BRCA1* expression. Among those 9 *BRCA1*-altered PDXs, six were known to have or previously had *BRCA1* promoter

hypermethylation (labelled as "*BRCA1*-low" and "WT with history of HRD" in **Figure 22A**, respectively)[164], and three harboured *BRCA1*-mutations. Interestingly, only one model was derived from a metastatic lesion (HBCx12) and two were obtained from previously treated patients (HBCx12 and HBCx8). The remaining discordant *BRCA1*-altered PDXs were derived from primary, treatment-naïve patients (**Supplementary Tables 1**, **2** and **3**). Overall, the genomic HRD test captured an HRD prevalence of 59% (**Table 4**), of which only half of the models (50%) were found to be PARPi-sensitive, suggesting and overestimation of HRD tumours in the cohort as in the case of detection of HRR-related gene alterations. Accordingly, the genomic HRD test showed limited accuracy in predicting PARPi response (71%), similar to HRR-gene mutations or assessment of *BRCA1* expression by mRNA expression or BRCA1 nuclear foci (**Table 5**).

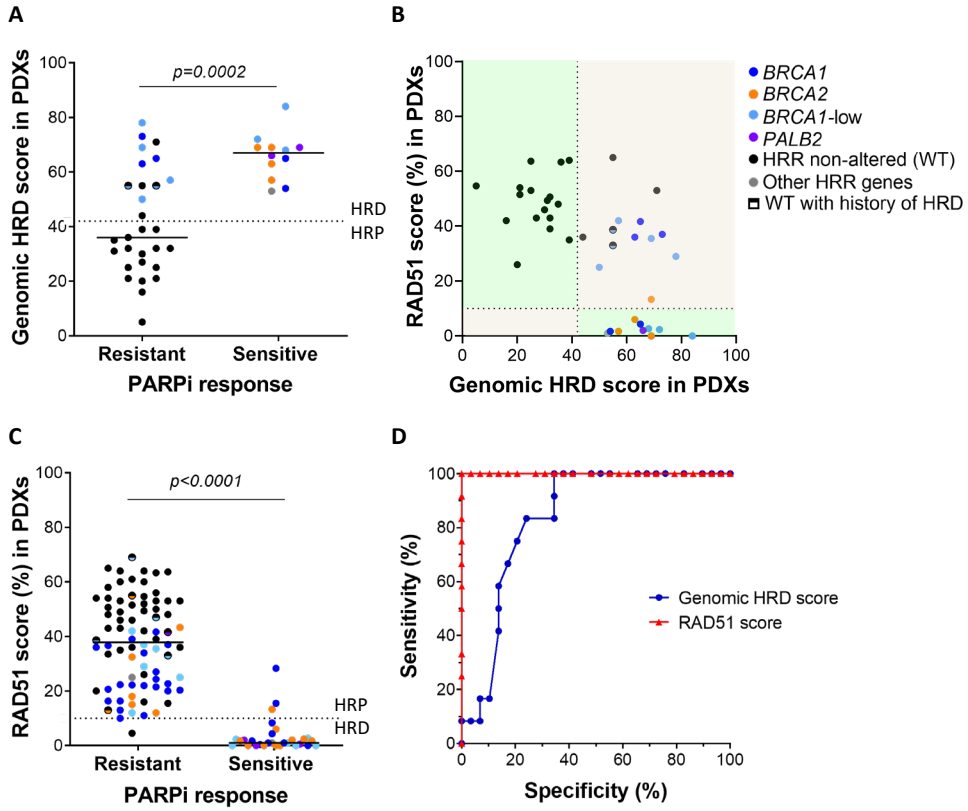


Figure 22. HRD tests scoring according to response to PARPi.

A. Genomic HRD score in PARPi-sensitive and resistant models (n = 41), measured with Myriad myChoice®. **B.** Comparison of the RAD51 score with the genomic HRD score (n = 41). Green and brown areas indicate HRD concordant and discordant cases according to tests' cut-offs, respectively. **C.** Distribution of the RAD51 score according to PARPi response (n = 109). Each dot represents the mean of at least three tumours for each PDX model in panels B and C. Lines represent the mean of PARPi-sensitive or -resistant models in panels A and C. Dashed line indicates the tests' cut-offs in panels A-C (HRD≥42; low RAD51≤10%). An unpaired t-test was applied in panels A and C. **D.** Comparison of ROC curves for the RAD51 and Myriad myChoice® scores for PARPi response in PDXs (n = 41). Abbreviations: HRD: homologous recombination deficiency; HRP: homologous recombination proficiency; WT: wild-type. Adapted from *Pellegrino & Herencia et al.,*[98].

We also performed the Genome Instability Score (GIS), defined as the unweighted sum of LOH, TAI and LST scores, in an independent cohort of 13 PDX models, 10 of which harboured HRR-related gene alterations. We observed similar results compared to the genomic HRD test: HRR-altered tumours showed higher scores than HRR non-altered. Regarding PARPi response, sensitive PDXs showed high GIS values compared to resistant models (median of 76 vs. 73, p=0.3; **Supplementary Figure 2B**). Notably, the 6 PARPi-resistant models with high GIS were those harbouring *BRCA1* mutations.

Although not approved for its use in the clinic, the whole genome-sequencing (WGS)-derived HRD signature, named HRDetect, has shown promise as a predictor of PARPi response and for patient stratification based on HRR status[94]. We therefore evaluated the HRDetect test in the same subset of PDXs as the GIS along with two models of acquired resistance to olaparib (OR, n = 15), 10 of which harboured *BRCA1/2*-alterations (**Supplementary Table 1**). As observed with the Myriad myChoice® HRD test, all PDXs derived from patients with *BRCA1/2*-associated tumours showed high HRDetect values (HRD>0.7)[94]. Also, all PARPi-sensitive and 8 of the 11 PARPi-resistant tumours showed high HRDetect values (**Supplementary Figure 2C**). When comparing the results of the GIS with the HRDetect scores, we found a high

concordance in tumour stratification (**Supplementary Figure 2D**). Noteworthy, 6 out of 8 PARPi-resistant, *BRCA1*-altered models were derived from metastatic lesions and all were obtained from heavily treated patients (**Supplementary Tables 1**, **2** and **3**), which may explain the discordance between the HRD signature/GIS and response to PARPi. In summary, these results show that genomic HRD tests provide very high sensitivity and NPV, but limited specificity and PPV for predicting PARPi response. These data suggest that DNA-based HRD tests accurately capture HRR-altered tumours but are poor at identifying those that may benefit from PARPi treatment.

Association of functional HRD by RAD51 and PARPi sensitivity in PDX models

As mentioned above, genomic HRD tests show limited accuracy in predicting PARPi response due to their static nature. Therefore, the development of functional dynamic tests able to identify patients who may or may not benefit from PARPi treatment is an urgent clinical need. Thus, we further aimed to investigate the functional HRD status of this PDX cohort by scoring the percentage of tumour cells with RAD51 nuclear foci in the S/G2-phase of the cell cycle (geminin-positive, geminin+)[99,100]. When analysing RAD51 according to the presence of HRR-gene status, we noted that HRR-altered models had significantly lower RAD51 scores than HRR-WT PDXs (median of 16% vs. 50%, $p<0.0001$, **Supplementary Figure 3A**). Using the pre-established cut-off for RAD51 (RAD51≤10%)[162], 61% of HRR-gene altered tumours exhibited high RAD51 scores and, similarly, 54% of tumours identified as positive for genomic HRD had high RAD51 scores (**Supplementary Figure 3A** and **Figure 22B**).

We then explored the potential of the RAD51 assay and the pre-established cut-off to predict PARPi response. PARPi-sensitive models showed a significantly lower percentage of RAD51-positive cells than PARPi-resistant ones (median of 1% vs. 38% respectively, $p<0.0001$), with 26/29 (90%)

PARPi-sensitive PDXs exhibiting scores ≤ 10% (**Figure 22C**). In addition, we observed an increase of the RAD51 score in the 13 models of acquired PARPi resistance derived under laboratory conditions compared to their sensitive counterparts (median of 33% vs. 1%, p=0.0006, **Supplementary Figure 3B**), highlighting the dynamic nature of the assay. Of the remaining 67 PARPi-resistant models, 66 (99%) had RAD51 scores above 10%. Overall, the prevalence of HRD by the RAD51 assay in the cohort of PDXs was 26% (28/109), of which 93% were found to be PARPi-sensitive (**Table 4**).

Importantly, the RAD51 assay (cut-off≤10%)[162] demonstrated high sensitivity (90%) and specificity (98%), along with a well-balanced PPV (93%) vs. NPV (96%) (**Table 5**). The accuracy of RAD51 to predict PARPi response was significantly higher than the one obtained with the genomic HRD test (95% vs. 71%, p<0.001). Specifically, the RAD51 assay predicted PARPi response in PDXs harbouring *BRCA1, BRCA2* or *PALB2* mutations (accuracy 95%, **Supplementary Figure 3C**) and in PDXs without mutations in these genes (accuracy 98%, **Supplementary Figure 3D**). Notably, discordant models showed intermediate responses to PARPi (PARPi-sensitive PDX196, PDX384 and HBCx17 and PARPi-resistant PDX432; **Supplementary Figure 4A** and **B,** respectively).

A comparative receiver operating characteristic (ROC) analysis was conducted for RAD51 scores and the Myriad myChoice® HRD test in a subset of 41 samples and revealed that the ROC AUC for the RAD51 assay was superior to the genomic HRD score one (0.97 vs. 0.81, p=0.03; **Figure 22D**). Collectively, these data validate the pre-established RAD51 assay score cut-off and demonstrate that assessment of RAD51 nuclear foci by immunofluorescence is the most accurate and dynamic HRD biomarker for predicting PARPi response (**Table 5**).

Platinum response as biomarker of PARPi sensitivity

As PARPi are approved for their use in platinum-sensitive ovarian cancer patients, we assessed cisplatin response in a subset of 56 PDXs with known response to PARPi (**Figure 23A**). Most of the PARPi-sensitive models were also sensitive to cisplatin (18/21, 86%). However, three PARPi-sensitive models showed resistance to cisplatin: two models with *BRCA2* mutations (PDX474.2 and PDX481) and a model with a *BRCA1* promoter hypermethylation (HBCx6). Interestingly, PDX474.2 was obtained after clinical progression to CDK4/6i, which has been described to confer to cross-resistance to platinum-salts[165,166]. Of note, PDX474.1, collected from the same patient as PDX474.2 before clinical progression to CDK4/6i, showed sensitivity upon cisplatin treatment. In addition, PDX474.2 showed a heterogeneous response to cisplatin *in vivo* (**Supplementary Figure 5A**). With respect to PDX481, and in contrast to what was observed for the rest of PDXs, the levels of DNA damage after treatment with cisplatin, measured as γ-H2AX nuclear foci, remained the same as that observed in the control arm (76% vs. 71%, p=0.2; **Supplementary Figure 5B**). Therefore, we evaluated whether PDX481 exhibited an upregulation of the platinum-related efflux pumps that prevent drug intake, such as *ATP7A*, *ATP7B*[167] or *ABCC2*[168]. However, no increased expression was observed in any of these genes in PDX481 (data not shown). We also investigated the presence of *CCNE1* amplification/upregulation in both PDX474.2 and PDX481 as it has been described to be indicative to platinum resistance[169], but we did not detect an increased expression (data not shown). Due to lack of material of tumour HBCx6, no further assessments could be performed to try to elucidate its mechanisms of resistance to cisplatin. Thus, the mechanisms of platinum resistance of PDX481 and HBCx6 still remain unknown. Consistently, none of the PARPi-resistant PDXs that restored HRR pathway functionality (i.e. tumours with HRR-gene reversions, loss of *BRCA1* promoter hypermethylation ("*BRCA1*-high") and BRCA1 hypomorphic protein) were

platinum sensitive (0/8, 0%). As expected, the two 53BP1-dependent PARPi-resistant models were platinum-sensitive (2/2, 100%)[170]. The two PARPi-resistant models PDX341 and STG316 showing hypomorphic BRCA1 and alterations in the 53BP1 pathway were resistant and sensitive to cisplatin, respectively. Of note, PDX341 exhibited a downregulation in *SHLD1*, which may lead to a milder dysregulation of the pathway and explain the resistance to cisplatin. Thus, we concluded that, when assessing platinum sensitivity as a biomarker of response to PARPi, we observed a lower accuracy than the RAD51 score (54% vs. 95%, **Table 5**).

After having compared several HRD biomarkers (i.e. detection of *BRCA1*, *BRCA2* or *PALB2* mutations, loss of *BRCA1* expression, genomic scars, genomic signatures, RAD51 and response to platinum), we conclude that the RAD51 test shows the highest accuracy to predict PARPi response in the cohort of PDX models.

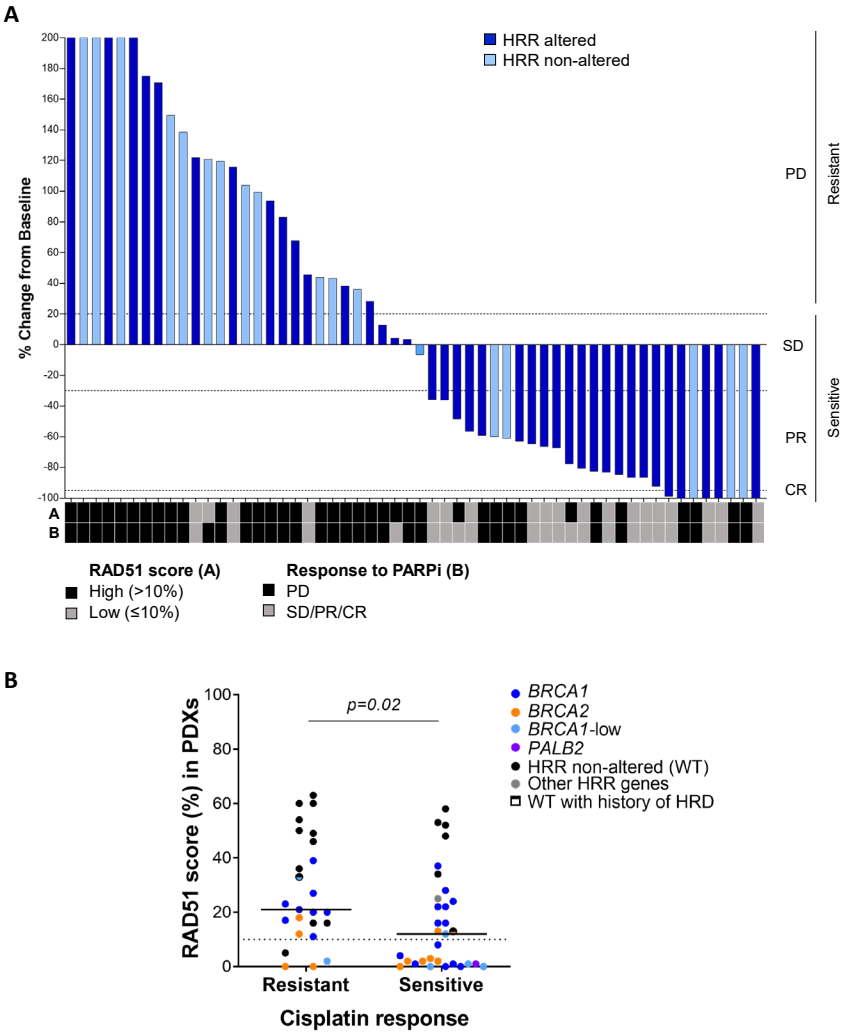


Figure 23. Antitumour activity of cisplatin in PDXs.

A. Waterfall plot showing the best response to cisplatin in N = 56 PDXs as the percentage of tumour volume change compared to the tumour volume on day 1. Each bar indicates the mean and SEM of at least three biological replicates. +20%, −30%, -95% are marked by dashed lines to indicate the range of PD (resistant), SD, PR, CR (sensitive), respectively. The box summarizes the RAD51 score (A) and the response to PARPi (B). **B.** Distribution of the RAD51 score in platinum-sensitive and resistant models (n = 56). Each dot represents the mean of at least three tumours for each PDX model. Dashed line indicates the test cut-off (low RAD51≤10%). Lines represent the mean of resistant or sensitive models in panel B. An unpaired t-test was applied in panel B. Abbreviations: WT: wild-type; HRR: homologous recombination repair; HRD: homologous recombination deficiency. Adapted from *Pellegrino & Herencia et al.,*[98].

Association of functional HRD by RAD51 and platinum sensitivity

Although platinum-based chemotherapy is widely used in the clinic for the treatment of different types of cancer, there is still no reliable predictive biomarkers to identify patients who may benefit from this therapeutic option. Given the fact that, as mentioned earlier, sensitivity to PARPi overlaps with sensitivity to platinum salts both in the clinic and in our hands, we aimed to investigate the performance of the RAD51 assay to predict response to cisplatin. We observed that cisplatin-sensitive models exhibited overall lower RAD51 scores than cisplatin-resistant PDXs (median of 12% vs 21%, p=0.02, **Figure 23B**). However, 16/31 (52%) of the cisplatin-sensitive models had high RAD51 scores, which suggests that they may have deficiencies in other DNA repair pathways involved in the repair of platinum-induced damage (e.g. nucleotide excision repair or Fanconi anaemia pathway[80]). The accuracy of the RAD51 assay to predict cisplatin response was similar to that of HRR-related gene mutations (*BRCA1*, *BRCA2* or *PALB2*) or *BRCA1* epigenetic silencing (64%, 61% and 63%, respectively; **Table 6**). These results suggest that the RAD51 assay may help to identify patients who are likely to respond to platinum-based treatments with similar accuracy to other HRD tests currently used in clinical practice, in contrast to what was observed regarding PARPi, in which the RAD51 score was superior.

Table 6. **Test performance values for the indicated HRD biomarkers predicting platinum response.**

Abbreviations: PPV: positive predictive value; NPV: negative predictive value. Adapted from *Pellegrino & Herencia et al.,*[98].

Biomarkers of platinum response	*BRCA1/2*, *PALB2* mutations (n = 56)	*BRCA1-low* mRNA/foci (n = 56)	RAD51 score (≤10%) (n = 56)
Sensitivity	68%	42%	48%
Specificity	52%	88%	84%
PPV	64%	81%	79%
NPV	57%	55%	57%
Accuracy	61%	63%	64%

Patient-derived models recapitulate patient's HRD status and *in vivo* response to PARPi

After having validated the RAD51 score as a promising biomarker to identify patients that respond to PARPi in PDX models, we aimed to study its performance *ex vivo* and to demonstrate that there is high concordance with the results obtained *in vivo*. Patient-derived tumour organoids from HGSOC are being established to assess responses to targeted drugs in a real time[171]. Therefore, we evaluated the ability of patient-derived tumour cells (PDCs) to recapitulate the HRD status and *in vivo* responses of PDXs to PARPi in a cohort of 14 models. As observed in PDXs, untreated PDCs already presented high levels of DNA damage, indicating that the cells had sufficient DNA damage to activate DNA repair pathways. After treatment with olaparib, PDCs greatly increased levels of DSBs (median of 68% vs. 84%, p=0.005; **Supplementary Figure 6A**). We then aimed to quantify the RAD51 score to interrogate the ability of PDCs to activate HRR and compare it to the corresponding PDXs. The RAD51 score in PDCs was highly concordant with the score in PDXs (R^2=0.74, p<0.0001) both when the models were PARPi-treated (kappa coefficient=0.68) or left untreated (kappa coefficient=0.74; **Figure 24A** and **Supplementary Figure 6B**). A lower correlation was observed in the case of γ-H2AX, as levels were higher in PDCs than in PDX models both when treated with PARPi or left untreated (R^2=0.1, p=0.09, **Supplementary Figure 6C**). Consistently, treatment with olaparib resulted in lower half-maximal inhibitory concentration (IC_{50}) values in PDCs derived from PARPi-sensitive than from resistant PDXs (10^2nM vs. $10^{2.9}$nM, p=0.017; **Figure 24B** and **C**). In summary, we showed that both PDXs and PDCs recapitulate the HRD status of patients and *in vivo* response to PARPi.

Finally, as the reproducibility and fidelity of patient-derived models compared to patient characteristics has been widely questioned, we interrogated whether RAD51 scores in PDXs recapitulated what was observed in the

corresponding patient samples. The RAD51 status in PDXs was highly concordant with the patient's tumour samples, taken at the same timepoint as the establishment of the patient-derived xenograft model (n = 20, Cohen's kappa=0.93, **Figure 24D**). In agreement, the responses of the PDXs to PARPi or platinum salts were also highly concordant with the responses of the patients to the respective therapy (30 out of 36, 83% concordance, **Supplementary Table 3**).

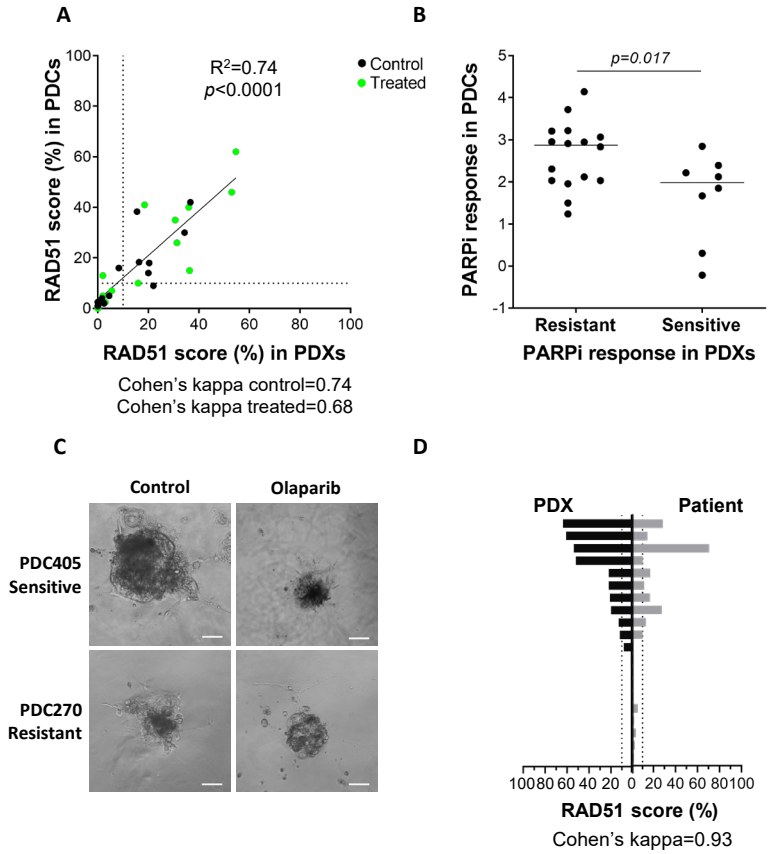


Figure 24. **Homologous recombination repair functionality and PARPi sensitivity is concordant in PDXs, PDCs and patients.**

A. Distribution of the RAD51 score in PDXs and their corresponding PDCs treated with PARPi (green) or left untreated (black, n = 14). Each dot represents the mean of at least three tumours for each PDX model. A linear regression model and a Cohen's kappa coefficient was calculated. **B.** Representation of the logarithm of the half maximal inhibitory concentration (IC_{50}) of PDCs treated with olaparib according to PARPi response in PDXs (n = 24). Lines

represent the mean of resistant or sensitive models. An unpaired t-test was applied. **C.** Bright-field microscopic images showing one PARPi-sensitive (PDC405) and one PARPi-resistant model (PDC270) untreated (control) and treated with olaparib 2.5 μM for 14 days. **D.** RAD51 scores in PDXs and in patient's tumour samples (grey) concurrent to the PDX establishment (black, n = 20). A Cohen's kappa coefficient was calculated. Dashed line indicates the test cut-off (low RAD51≤10%) in panels A and D. Adapted from *Pellegrino & Herencia et al.,*[98].

RAD51 as an HRD biomarker in ductal carcinoma *in situ* (DCIS)

Due to the clinical success in the metastatic setting and their recent approval for their use as adjuvant therapy in BC[86], other studies are investigating the use of PARPi as a therapeutic option in other scenarios within the primary setting, such as part of the neoadjuvant therapy[142]. Accordingly, it has been described that women with germline *BRCA1* or *BRCA2* mutations have an increased risk of developing pre-malignant lesions such as ductal carcinoma *in situ* (DCIS, 0.8% and 2.4%, respectively), as these are the driver mutations that lead to this non-invasive breast carcinoma[172]. Therefore, the use of PARPi in this context could be further extended to this early stage of the disease. However, the prevalence of HRD in unselected populations of DCIS still reminds unknown. In addition, and in line with this, there is also the unmet need to find biomarkers to select those patients who may benefit from adding PARPi to their early treatment regimen.

Having validated the RAD51 score cut-off and its increased accuracy to predict PARPi response in the cohort of primary and metastatic PDX models, we aimed to explore the HRD prevalence in an independent subset of 22 patient-derived DCIS mouse-intraductal xenografts (MIND, **Supplementary Table 4**)[72]. Although data were limited (n = 12), we found that tumours were predominantly HR+ (8, 67%), followed by HER2+ (2, 16.5%) and TNBC (2, 16.5%). In addition, 67% progressed to invasive disease (**Supplementary Figure 7A**). Moreover, *Hutten et al.,* found a high concordance between the

original patient samples and the DCIS-MIND models for the expression of HR, Ki-67, and the surrogate molecular DCIS subtypes: luminal A, luminal B, HER2+, and basal DCIS[72].

When analysing DNA damage, MINDs accumulated high levels of γ-H2AX nuclear foci (**Figure 25A**), suggesting that, even at very early stages of the disease, pre-malignant DCIS lesions already exhibit sufficient DNA damage to activate the HRR pathway. We then set out to investigate the HRR pathway as a mechanism for repairing these DSBs. Interestingly, 5 out of the 22 (23%) MINDs had low levels of RAD51 levels and were, therefore, predicted to be HRD (**Figure 25A**). These data suggest that treatment-induced DNA damage is not required to assess RAD51 in pre-malignant lesions. Furthermore, these results were comparable to the proportion of HRD by RAD51 in more advanced invasive breast cancer in our hands (**Table 4**) and by HRD signatures and/or genomic scars[72,94]. Of note, one out of the 5 (20%) HRD tumours showed low levels of BRCA1 nuclear foci, probably due to a genetic or epigenetic alteration in this gene (**Figure 25A**). We then explored whether HRD was associated with the tumours molecular subtype or their ability to invade neighbour tissues. As expected, we observed that tumours with lower RAD51 levels were those with a TN and non-invasive profile (**Supplementary Figure 7B** and **C**).

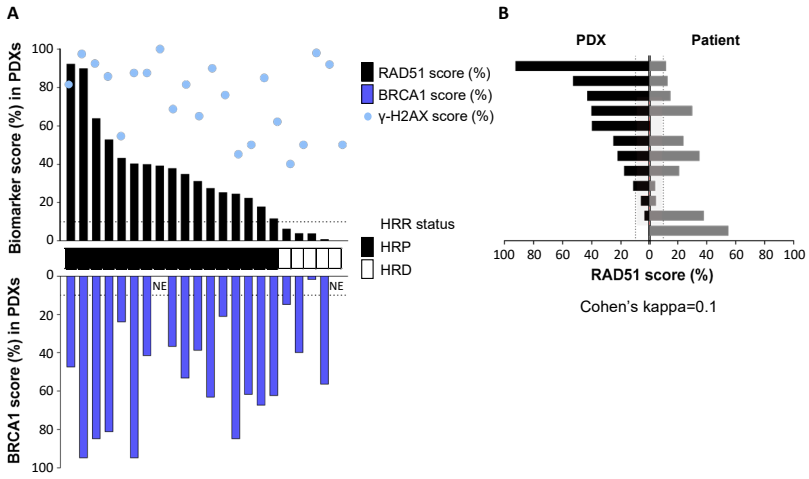


Figure 25. Analysis of HRD tumour biomarkers by immunofluorescence (IF) in untreated patient-derived DCIS mouse-intraductal xenografts (MINDs).
A. The percentages of geminin+ tumour cells with RAD51 (upper black bars), BRCA1 (bottom blue bars) and γ-H2AX (blue dots) nuclear foci in 22 DCIS-MINDs samples are shown. The box summarises the HRR status (HRP or HRD). **B.** RAD51 scores in PDXs and in patient tumour samples (grey) concurrent to the PDX establishment (black, n = 12). Dashed line indicates the tests' cut-offs (low RAD51≤10%; low BRCA1≤10%). A Cohen's kappa coefficient was calculated in panel B. Abbreviations: NE: non-evaluable; HRD: homologous recombination deficiency; HRP: homologous recombination proficiency. Adapted from *Hutten et al.,*[72].

As we demonstrated the high concordance between biomarker scoring in PDXs vs. patients the cohort of invasive preclinical models (**Figure 24D**), we then aimed to assess RAD51 levels in the patient tumour samples taken at the same timepoint as the samples to generate the PDXs and compare them. In this way, we evaluated whether the MIND injection technique used in this study to generate the PDX biobank recapitulated clinical features. Of the 12 paired tumours, 8 PDXs (67%) showed concordant HRD classification (kappa coefficient=0.1, **Figure 25B**) and RAD51 scores (**Supplementary Figure 7D**) with their corresponding patient samples. Of note, one of the discordant cases was likely explained by the low levels of γ-H2AX nuclear foci observed in the patient sample (**Supplementary Figure 7E**) and another PDX was known to present a heterogeneous pattern with respect to RAD51.

In conclusion, in the first part of the thesis, we evaluated the RAD51 assay, an immunofluorescence-based test, as a biomarker of response to PARPi and platinum salts in more than 100 PDX models derived from early stage, primary and metastatic HRR-associated BC, OvC and PaC. We validated the RAD51 score cut-off (≤10%) and compared the performance of this assay with other HRD detection methods such as the detection of HRR-gene mutations, genomic HRD tests and platinum sensitivity. We confirmed the superior predictive value and accuracy of the RAD51 assay to identify (i) patients with germline *BRCA1/2* (g*BRCA1/2*) or germline *PALB2* (g*PALB2*) mutations who are likely to be PARPi-resistant and (ii) patients without

g*BRCA1/2* or g*PALB2* with HRD-positive tumours who are likely to be PARPi-sensitive. When comparing preclinical models with their corresponding patient samples, we observed a high concordance in biomarker scores. In line with this, and given the supportive clinical data[78,142,173,174], we propose to continue the analytical validation and the clinical qualification of the RAD51 assay in larger cohorts of breast cancer patients treated with PARPi or platinum salts.

PART 2

Overcoming first-generation PARPi resistance with a next-generation PARPi or combinations with other DNA-damaging agents

As previously described in the clinic and further demonstrated in the cohort of PDXs[98], despite the initial sensitivity to first-generation PARPi in tumours with HRD, resistance emerges as the major obstacle to their clinical efficacy in tumours with HRD[101,175]. Thus, the lack of therapeutic options for patients with tumours with intrinsic or acquired resistance to first-generation PARPi underlines the urgency of developing additional treatments. We therefore investigated different strategies to find therapeutic approaches and overcome PARPi resistance, namely the use of next-generation selective PARP1i or combinations with other DNA-damaging agents.

The PARP1 selective inhibitor AZD5305 elicits more potent and durable antitumour activity than olaparib in patient-derived *BRCA/PALB2*-associated cancer models

As it has been described that PARP1 inhibition alone is sufficient to induce synthetic lethality in tumours with HRD and that trapping of PARP2 may not be required for anticancer activity[115,176], PARP1 selective inhibitors, such as AZD5305 (saruparib), are being developed. PARP2 has been described to play an essential role in hematopoietic renewal and thus, its inhibition may contribute towards the haematological adverse effects observed in patients

treated with first-generation PARPi. It is expected that selective PARP1 inhibition will result in a safer profile that facilitates its combination with other DNA damage repair inhibitors. Therefore, we aimed to characterise the antitumour activity of AZD5305 in a cohort of HRR-mutated PDX models compared to the first generation PARP1/2 inhibitor olaparib and to identify mechanisms of resistance to this novel compound.

AZD5305 shows potent and durable antitumour response in HRR-altered PDX models

The antitumour activity of AZD5305 was evaluated in a panel of 13 PDX models derived from five triple-negative (TN), one ER+ and one HER2+ breast cancer (BC), as well as one high-grade serous ovarian cancer (OvC) and one pancreatic adenocarcinoma (**Figure 26A**). All PDX models harboured the patient germline pathogenic alterations in HRR pathway genes: six in *BRCA1*, two in *BRCA2* and one in *PALB2* (**Supplementary Table 5**). Only two PDXs from the initial cohort, namely PDX230 and PDX173, were collected from primary BC patients. One ER+ BC model was generated from a clinical progression to talazoparib (PDX474.7). PDX196 was generated from the pericardial effusion of an OvC patient on treatment with PARPi shortly before clinical progression, and PDX168 was generated from a platinum-refractory pancreatic cancer patient (**Supplementary Table 3**). Additionally, three olaparib-resistant models (OR) were generated from initially sensitive tumours after prolonged exposure and steep progression to olaparib (PDX173OR3, PDX230OR5 and PDX474.2OR2). We identified a plausible mechanism of resistance to olaparib in two models, namely a reversion mutation in *BRCA2* in PDX474.2OR2, and the expression of a potentially hypomorphic BRCA2 protein in PDX474.7 (**Supplementary Figure 8** and **Supplementary Table 5**)[177]. We did not identify the specific genetic mechanism of resistance to PARPi for PDX173OR3 nor for

PDX230OR5, but all resistant models exhibited functional HRR, suggesting restoration of the HRR pathway functionality (RAD51 > 10%; **Figure 26A**).

AZD5305 treatment revealed antitumour activity in 7 PDX models: complete response (CR) in four PDXs (PDX230, PDX124, PDX474.2 and PDX173), partial response (PR) in two (PDX179 and PDX196) and stable disease (SD) in one PDX (PDX341; **Figure 26A**). Notably, PDX179 showed a significantly superior response to AZD5305 compared to olaparib. Progression upon AZD5305 treatment was observed in two models with primary resistance to olaparib (PDX127 and PDX168), likely due to loss of *FAM35A/SHLD2* leading to defects in the 53BP1 pathway[160] or lack of gene-specific loss of heterozygosity (gsLOH) of the *PALB2* pathogenic mutation, respectively (**Supplementary Table 5**). The three olaparib-resistant models showed resistance to AZD5305, as did the model generated from the clinical progression to talazoparib (PDX474.7).

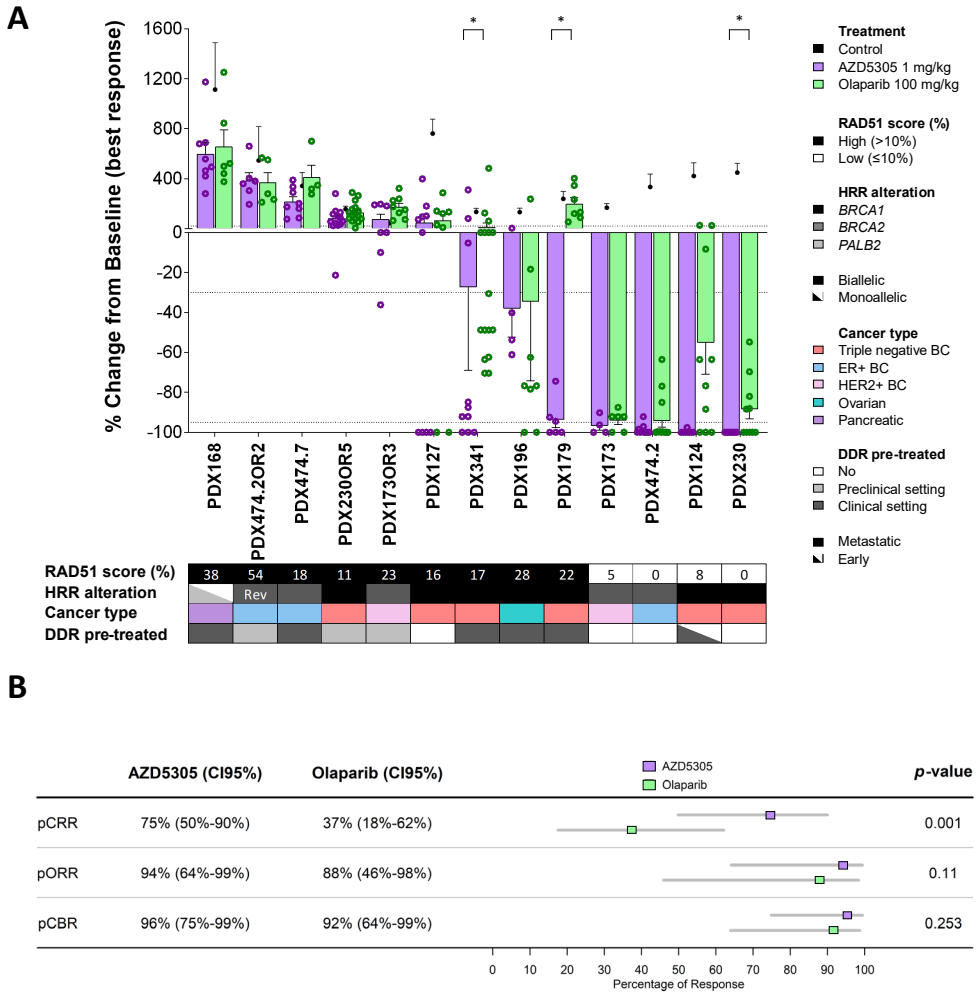


Figure 26. Antitumour activity of AZD5305 and olaparib in PDXs.

A. Waterfall plot showing the antitumour activity of AZD5305 and olaparib in N = 13 PDX models, measured as percentage of tumour volume change compared with the tumour volume on day 1. Each bar indicates the mean and SEM of at least three biological replicates (open circles). The mean of control tumours (n ≥ 3) is represented with solid circles. +20%, -30%, -95% are marked by dotted lines to indicate the range of PD (resistant), SD, PR and CR (sensitive), respectively. The lower box summarizes the RAD51 score (%), the specific gene alteration harboured by each model, the cancer type, and previous treatment history with DNA-damaging agents. A Wilcoxon test corrected for multiple testing was performed. *, *p*-value ≤ 0.05. **B.** Comparison of preclinical mRECIST criteria-based readouts to evaluate response to PARPi. Percentage of tumours, 95% confidence intervals (CI95%), forest plot and *p*-values (generalized linear mixed-effects model) are shown. Abbreviations: Rev: reversion mutation;

DDR: DNA damage repair; pCRR: preclinical complete response rate; pORR: preclinical overall response rate; pCBR: preclinical benefit rate.

Focusing on PARPi-sensitive tumours, AZD5305 as single agent showed superior antitumour activity than the first-generation PARPi in terms of preclinical CR rate (pCRR, 75%, 95% CI: 50%-90% vs. 37%, 95% CI: 18%-62%; p=0.001). However, similar preclinical overall response rate (pORR, 94%; 95% CI: 64%-99% vs. 88%; 95% CI: 46%-98%; p=0.11) and preclinical benefit rate (pCBR, 96%; 95% CI: 75%-99% vs. 92%; 95% CI: 64%-99%; p=0.25) were observed upon treatment with AZD5305 and olaparib (**Figure 26B**).

We then sought to investigate the long-term benefit of either PARPi. Consistent with the higher pCRR rate, a higher percentage of tumours remained in response while on treatment or after treatment discontinuation with AZD5305 compared to olaparib-treated tumours (36/45 with AZD5305 (80%) vs. 20/50 with olaparib (40%), p<0.0001, **Figure 27A, Supplementary Figure 9A** and **Supplementary Table 6**). In addition, the median pPFS was significantly longer in the AZD5305 group compared to the olaparib group (>386 days vs. 90 days; hazard ratio for progression or death, 0.39; 95% CI: 0.23-0.66; p<0.001; **Figure 27B** and **C**). Preclinical time to progression (pTTP) was also longer with AZD5305 compared to olaparib in sensitive tumours (172 days vs. 113 days; hazard ratio of 0.51; 95% CI: 0.33-0.78; p=0.002; **Figure 27C** and **Supplementary Figure 9B**). Taken together, these data demonstrated that treatment with AZD5305 results in a higher preclinical CR rate and a more durable response than treatment with a first-generation PARPi.

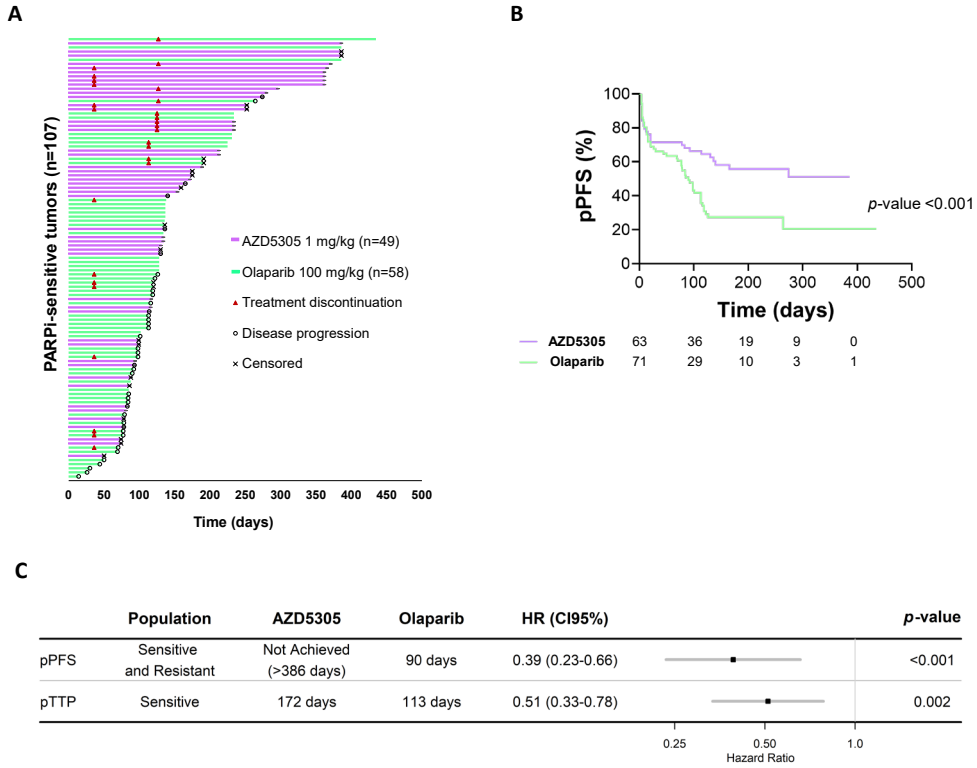


Figure 27. Analysis of response to AZD5305 and olaparib in PDXs.

A. Swimmer plot showing the timeline of the *in vivo* experiments with individual PARPi-sensitive tumours. **B.** Kaplan-Meier curve showing pPFS for AZD5305- and olaparib-treated individual tumours. **C.** Analysis of response and forest plot for pPFS in PARPi-sensitive and resistant tumours (AZD5305, n = 63; olaparib, n = 71) and pTTP in PARPi-sensitive tumours (AZD5305, n = 45; olaparib, n = 50). A mixed-effects Cox model was performed. Abbreviations: pPFS: preclinical progression-free survival; pTTP: preclinical time to progression; HR: hazard ratio.

RAD51 foci captures PARPi sensitivity and restoration of HRR functionality

Next, we aimed to determine whether the functional status of HRD by RAD51 foci was associated with response to PARP1 selective inhibition in the cohort of 13 PDXs. Models resistant to AZD5305 exhibited a significantly higher RAD51 score than sensitive tumours at baseline (median of 27% vs. 11%, p=0.046; **Supplementary Figure 10A**). Of note, some of the AZD5305-

sensitive PDXs with high RAD51 levels (>10%) harbour pathogenic alterations in the exon 11 of *BRCA1*, for which PARP1/2 inhibitors can elicit an intermediate antiproliferative response[107]. We also observed that the RAD51 score correlated with pTTP upon AZD5305 and olaparib treatment (R^2=0.55, p=0.004 and R^2=0.43, p=0.01, respectively), with no differences between the two (p=0.66, **Supplementary Figure 10B** and **C**). These results indicated that tumours with a functional HRD by RAD51 progress later than tumours with HRP.

We then wanted to gain further insight into the mechanisms leading to acquired resistance of tumours from models that were initially sensitive. We first studied the functional HRR status of these tumours at progression by RAD51 and observed that all acquired-resistant tumours enhanced HRR functionality regardless of the specific PARPi compared to their sensitive controls (9/9 AZD5305- (p-value=0.02) and 30/30 olaparib-progressing tumours (p-value=0.02); **Figure 28A** and **Supplementary Figure 11**). This data suggests that these tumours became resistant to PARPi through HRR-dependent mechanisms.

When we assessed the specific mechanisms of resistance, reversion mutations in *BRCA1* or *BRCA2* were seen in 5/30 tumours that progressed to olaparib, while no reversions were observed in those progressing to AZD5305 (**Figure 28B, C** and **Supplementary Table 6**).

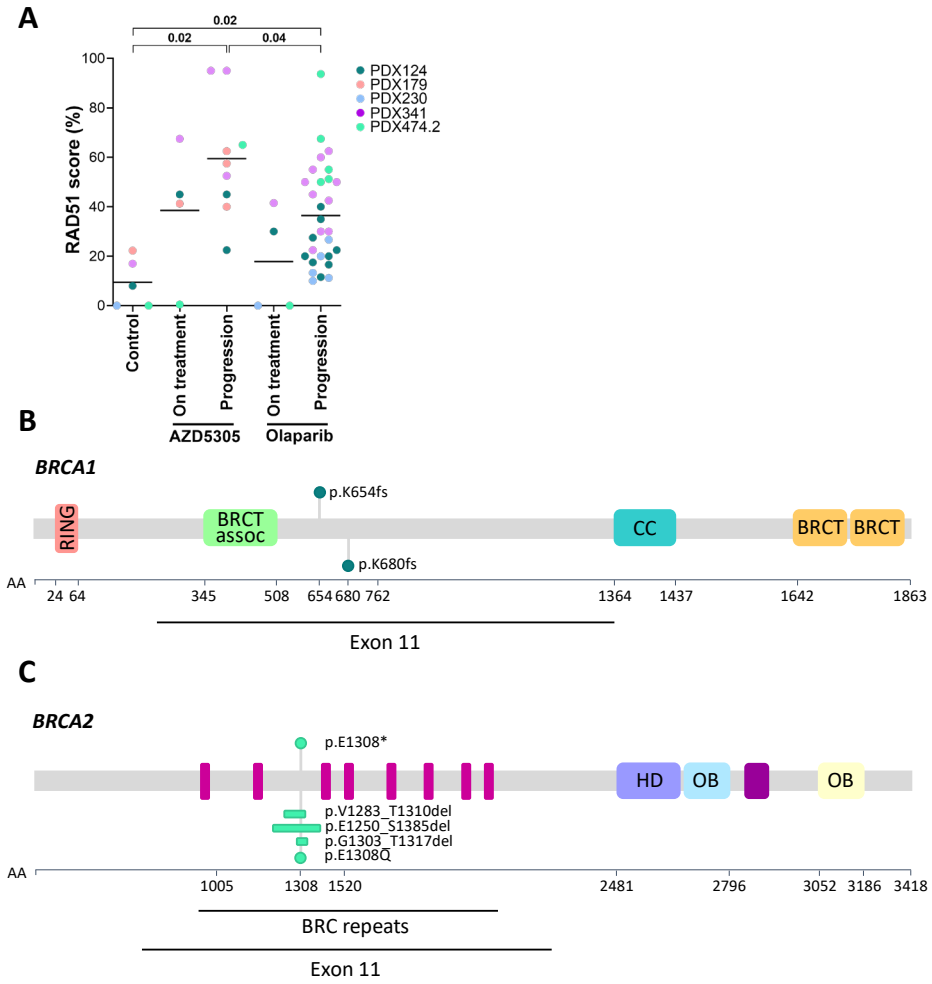


Figure 28. Mechanisms of resistance to AZD5305 and olaparib in PDXs.

A. Quantification by IF of the RAD51 score in tumours that progressed under treatment with either PARPi, compared to untreated controls. *P*-values are shown. Location of pathogenic (up) and reversion (down) mutations on the domain structure of **B.** *BRCA1* and **C.** *BRCA2*. Each square/dot represents a patient. **D.** Pie chart indicating the distribution of the resistance mechanisms detected in individual tumours that had progressed to AZD5305 and olaparib in purple and green, respectively.

The prevalence of reversion mutations was high in tumours from certain PDX models, such as the ER+ *BRCA2*-mutant model PDX474.2, in which 4/5 (80%) olaparib-progressing tumours exhibited reversion mutations (**Supplementary Table 6**). Remarkably, patient 474 had not received any

platinum drug that could have induced subclonal reversion mutations prior to establishing the PDX model. We then aimed to investigate whether this predisposition was due to an increased mutational rate or usage of microhomology mediated end joining (MMEJ) as a backup mechanism to repair DSBs in the absence of HRR[125,178]. Overall, we did not observe an increased mutational rate in PDX474.2 tumours progressing to PARPi (**Figure 29A**), but 3/4 (75%) olaparib-progressing tumours with reversion mutations from this PDX presented microhomology signatures (progressions #26, #28 and #29, **Figure 29B**). Interestingly, out of the 9 olaparib-progressing and 2 AZD5305-progressing tumours from the *BRCA1*-mutant PDX124, one olaparib-progressing tumour exhibited a reversion mutation that, in addition, was found to present microhomology signatures (progression #3, **Figure 29B**). Although we observed an increased mutational rate in this tumour, it was comparable with the mutational rate of its control tumour (**Figure 29A**).

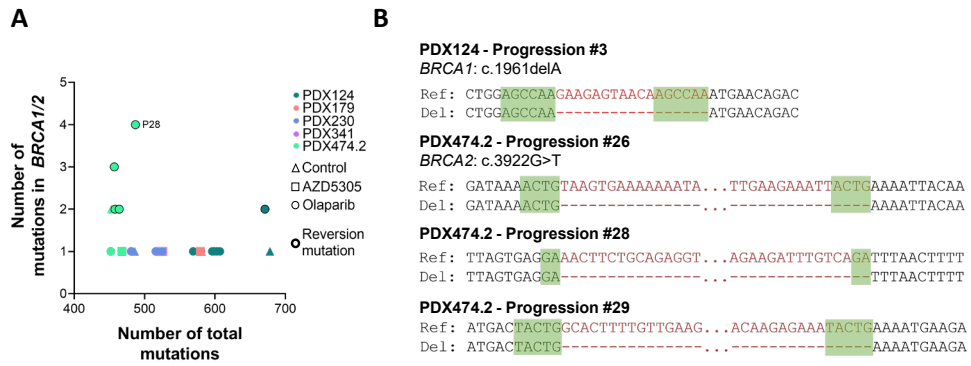


Figure 29. Characterization of *BRCA1/2* genetic-based mechanisms of resistance to PARPi in PDXs.

A. Number of mutations detected in *BRCA1* or *BRCA2* vs. total number of mutations detected by whole exome sequencing. Untreated controls, AZD5305- and olaparib-progressing tumours of each PDX are depicted (AZD5305, n = 9; olaparib, n = 30). PARPi-progressing tumours harbouring a reversion mutation are highlighted. **B.** Illustrations of the reversion mutations associated with the usage of microhomology as a backup mechanism to repair DSBs detected in PARPi-progressing tumours. The reference (Ref) and the sequence with the deletion (Del)

are shown. Deleted sequences are labelled in red, and dashes indicate deleted base pairs. Microhomology regions are labelled in green.

It has been described that tumours with *BRCA1*-exon 11 mutations are prone to generate splicing isoforms, such as the Δ11q, leading to the expression of a hypomorphic BRCA1 protein and to PARPi resistance[107]. Therefore, we investigated the emergence of hypomorphic BRCA1 and noted that BRCA1 C-terminal nuclear foci were increased above the baseline levels in two *BRCA1*-exon 11 mutated models (PDX124 and PDX341), namely in 4/5 tumours progressing to AZD5305 and in 14/19 (including the tumour harbouring a *BRCA1* reversion mutation) tumours progressing to olaparib (**Figure 30A**). Moreover, increased levels of BRCA1 foci in the tumours that had progressed on either PARPi were accompanied by increased levels of RAD51 foci, suggesting that there was a concomitant enhanced HRR functionality (R^2=0.24, p=0.01, **Figure 30B**). We further confirmed by RT-qPCR that the increased expression of BRCA1 Δ11q-splicing mRNA isoforms was not a common mechanism leading to enhanced BRCA1 foci formation, as only three out of 17 (18%) olaparib-progressing tumours with high levels of BRCA1 foci showed transcriptional upregulation of the *BRCA1* Δ11q isoform (**Figure 30C** and **Supplementary Figure 12**).

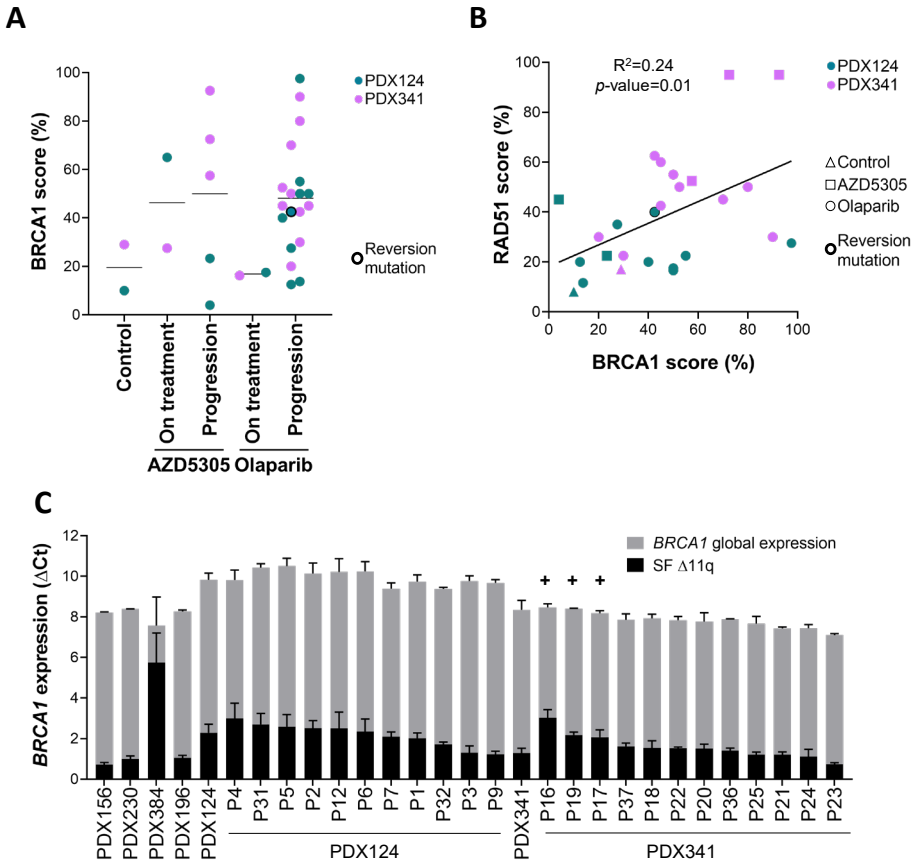


Figure 30. Evaluation of the presence of BRCA1 hypomorphic protein as a mechanism of resistance to PARPi in the *BRCA1* exon 11-mutated PDX124 and PDX341.

A. Quantification by IF of the BRCA1 score in the AZD5305- and olaparib-progressing tumours (AZD5305, n = 5; olaparib, n = 19) compared to untreated controls. PARPi-progressing tumours harbouring a reversion mutation are highlighted. **B.** Correlation analysis of the RAD51 score vs. the BRCA1 score of AZD5305- progressing (n = 5), olaparib-progressing (n = 18) and untreated tumours. PARPi-progressing tumours harbouring a reversion mutation are highlighted. **C.** Splicing fraction of the Δ11q isoform over the global *BRCA1* expression measured as the ΔCt of the probe expanding exon 23-24 junction. The splicing fraction of the control tumours PDX124 and PDX341 is shown as reference. Tumours in which the splicing fraction of the Δ11q isoform > 1.5 the splicing fraction of the untreated control of the corresponding tumour are indicated with "+". Untreated PDX156 (*BRCA1*-wild-type), PDX230 (*BRCA1* RING domain-mutated), PDX384 (*BRCA1* exon 11-mutated with Δ11q isoform overexpression) and PDX196 (*BRCA1* exon 11-mutated) are shown as controls. Abbreviations: SF: Splicing fraction; P: Progression.

Finally, we reviewed the presence of mutations on other PARPi resistance factors such as *TP53BP1, RIF1, PAXIP1* and members of the Shieldin complex. We noted that one AZD5305-progressing tumour from PDX124 showed lack of 53BP1 nuclear foci formation (**Supplementary Figure 11**). In addition, a mutation in *SHLD3* was found in an additional olaparib-progressing tumour from PDX124 at an allele frequency of 0.2, which was accompanied by low expression of *SHLD3* by RNA sequencing (**Supplementary Table 6**).

Interestingly, 2/3 AZD5305-progressing tumours from PDX179 (progressions #33 and #35) showed an upregulation of *ABCB1*, encoding for a known efflux pump that removes toxic compounds from the cells[179], which was concomitant with a reduction in the levels of DNA damage in these tumours (progressions #33 and #35 with 45% and 44%, respectively, vs. 87.5%, p=0.02; **Supplementary Figure 13A** and **B**). The third AZD5305-progressive tumour from this PDX (progression #34) exhibited a downregulation of the drug target *PARP1* (**Supplementary Figure 13C**). Although these results need to be further validated at the protein level, they rise the possibility that tumours may become resistant to AZD5305 through HRR-independent mechanisms. No other alterations in genes associated with PARPi resistance were identified (**Supplementary Table 7**).

In summary, these data show that restoration of HRR is commonly associated with resistance to PARPi, and that the most prevalent mechanisms are *BRCA1/2* reversion mutations in the case of olaparib-progressing tumours (10% vs. 0% of AZD5305-progressing tumours) and the accumulation of hypomorphic BRCA1 (9% and 26% in AZD5305 and olaparib-progressing tumours, respectively; **Figure 31**).

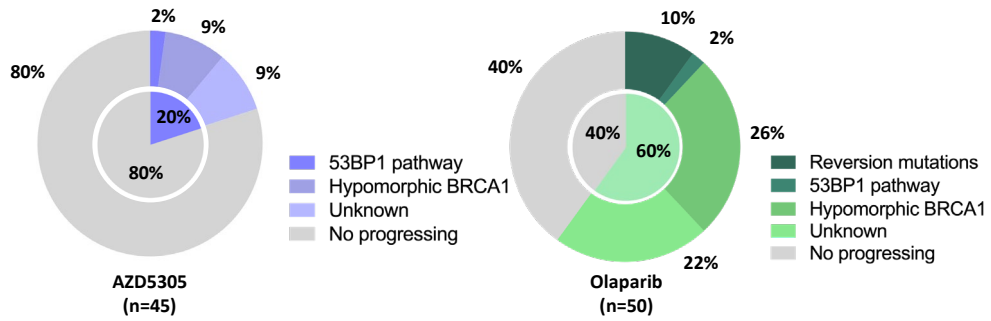


Figure 31. Distribution of the resistance mechanisms detected in individual tumours that progressed to AZD5305 and olaparib in purple and green, respectively.

AZD5305 inhibits PARylation and enhances biomarkers of DNA damage and replication stress

We next analysed potential differences in the mode of action of PARP1 selective vs. PARP1/2 inhibition in an attempt to identify the key mechanism leading to the incremental response observed with AZD5305, compared to olaparib. Firstly, we analysed the effect on protein poly ADP-ribosylation (PARylation) after twelve days of treatment with both compounds in a subset of 4 models. Inhibition of PARylation was observed in both AZD5305-resistant (PDX168 and PDX474.7) and -sensitive (PDX179 and PDX124) tumours treated with either AZD5305 or olaparib, indicating similar target engagement in both cases (**Supplementary Figure 14**). Likewise, DNA damage accumulation, as measured by γ-H2AX nuclear foci, increased upon treatment with both PARPi in AZD5305-resistant and -sensitive models (**Figure 32A**). AZD5305 is also a potent and selective PARP1 trapper, leading to the accumulation of replication stress derived from stalled and collapsed DNA replication forks[118]. In this sense, phosphorylation of RPA3 on Ser-4/8 (pRPA) is a good marker of collapsed replication forks[180]. Higher levels of pRPA were observed in AZD5305-sensitive PDXs treated with AZD5305 compared to baseline, with no significant difference in AZD5305-resistant models or olaparib-treated, suggesting a poorer capacity of the sensitive models resolving the replication stress produced by PARP1 trapped on

chromatin (**Figure 32B**). Finally, we quantified DNA-containing micronuclei as marker of genomic instability due to mitotic progression following DNA damage[181]. Interestingly, treatment with AZD5305 significantly increased micronuclei only in AZD5305-sensitive models (**Figure 32C**). In summary, the PARP1 selective inhibitor AZD5305 induces more replication stress and genomic instability than the PARP1/2 inhibitor olaparib in PARPi-sensitive tumours compared to vehicles.

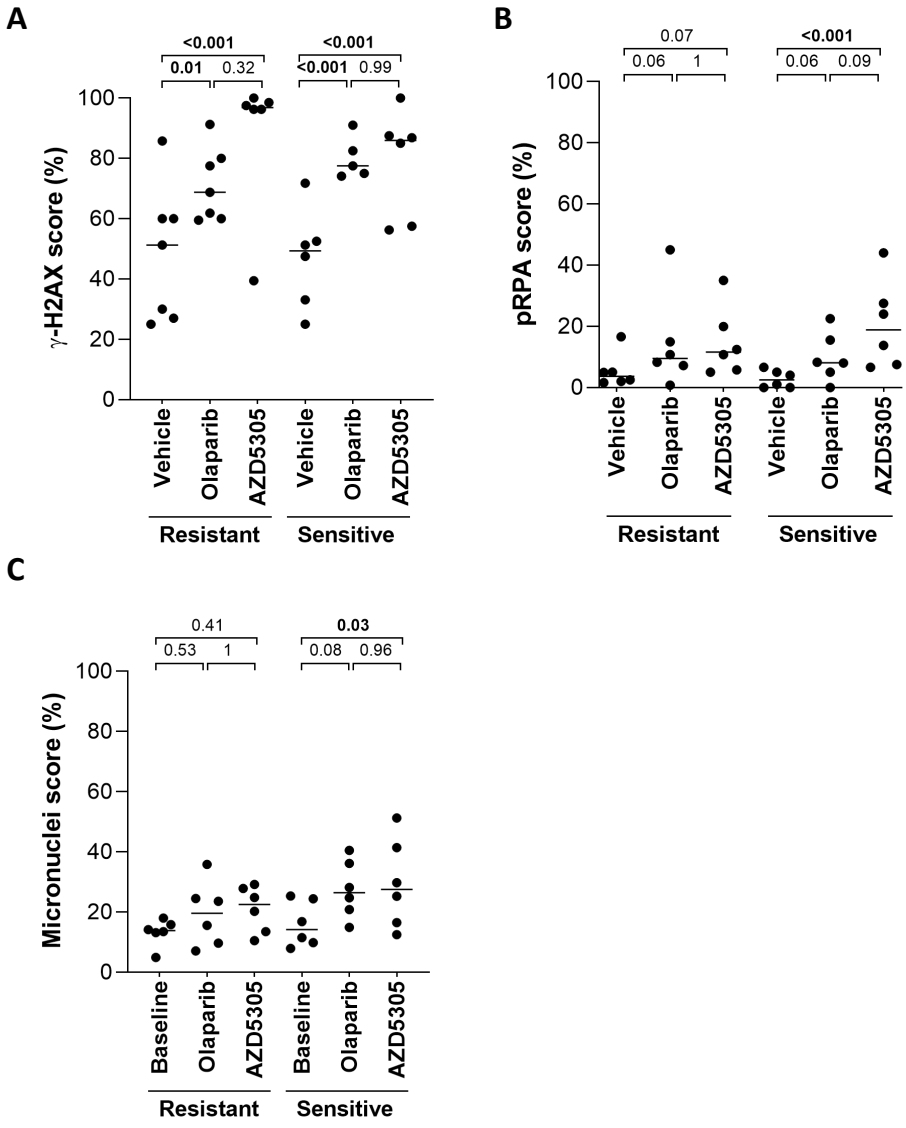


Figure 32. Biomarkers of DNA damage and replication stress in PDX models at baseline or treated with olaparib or AZD5305.
Quantification of the percentage of tumour cells **A**. in S/G2-phase (geminin+) with γ-H2AX nuclear foci, **B.** in S/G2-phase (geminin+) with phospho-RPA nuclear foci, or **C.** with at least one micronucleus in AZD5305-resistant (n = 6) and sensitive (n = 6) available PDX models, untreated or treated for 12 days with olaparib 100 mg/kg and AZD5305 1 mg/kg. Black lines indicate the biomarker mean of each group. A linear mixed-effects model was performed in all panels. *P*-values are indicated with significant values labelled in bold.

Understanding the combination potential of carboplatin or an ATRi with PARP1i in *BRCA*-mutated models

Because PARP1 is involved in both the base-excision repair (BER) and in the nucleotide-excision repair (NER) pathways[182], namely in the repair of inter and intrastrand cross-links (ICL) generated by platinum salts, synergy between PARPi and platinum drugs is anticipated[179]. Specifically, *Illuzzi et al.,* demonstrated that treatment with AZD5305 in combination with carboplatin in preclinical models results in rapid recovery of red blood cell parameters, contrary to the sustained loss observed with olaparib plus carboplatin[118]. We therefore investigated whether the antitumour activity of AZD5305 could be increased by adding carboplatin in a subset of six BC PDXs with a range of responses to AZD5305 (**Figure 33A**). AZD5305 plus carboplatin induced tumour regression (CR) in two models with primary resistance to both PARPi, namely PDX127 and PDX341, as well as in one model sensitive to AZD5305 (PDX124). Durable responses were observed upon combination treatment in PDX127 (**Supplementary Figure 15A**). However, the combination did not induce tumour regression in any of the PDXs with acquired resistance to olaparib (PDX474.2OR2, PDX474.7 or PDX230OR5).

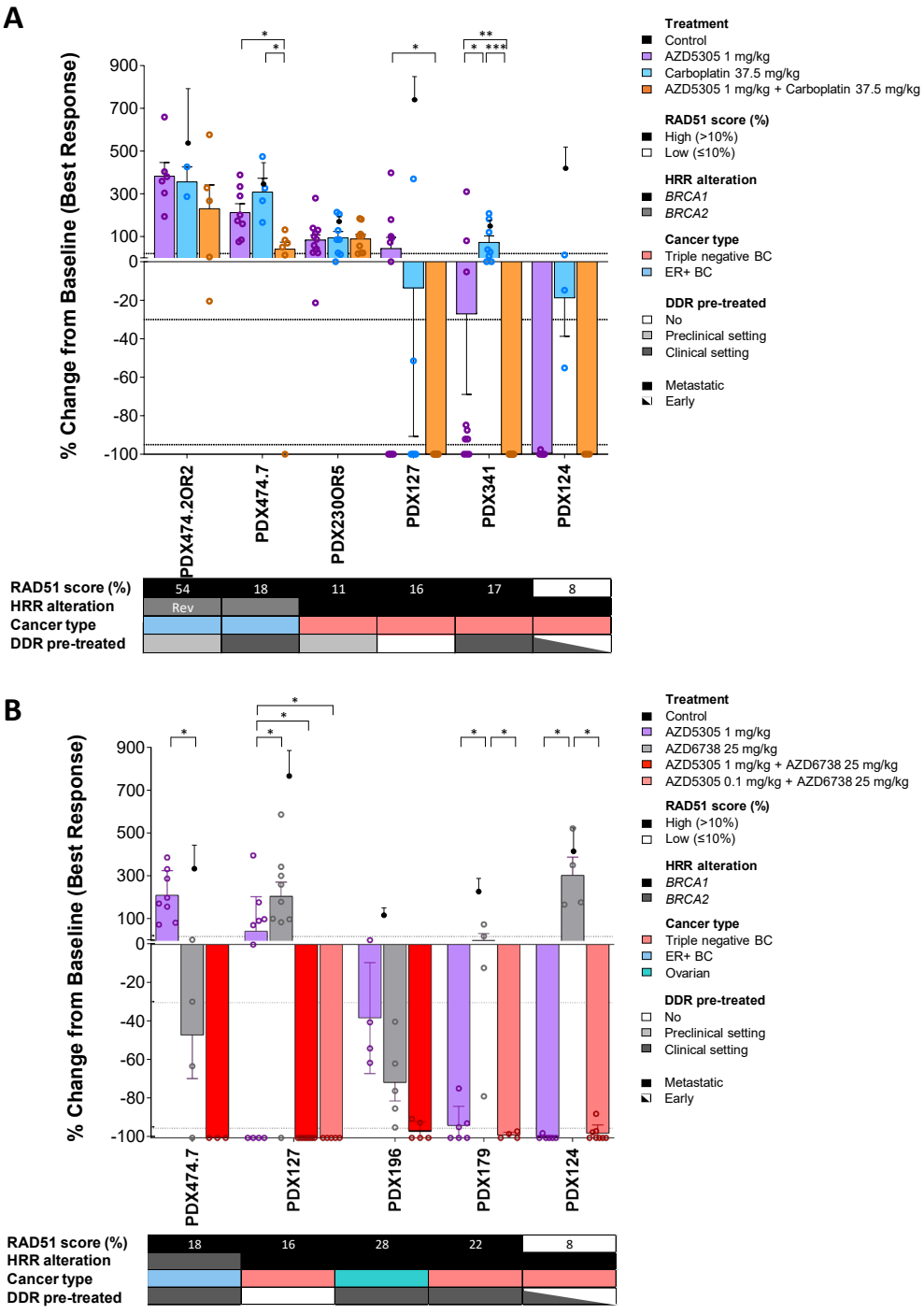


Figure 33. Antitumour activity of AZD5305 as single agent or in combination with other DNA-damaging agents.

Waterfall plots showing the antitumour activity of AZD5305 with **A.** carboplatin as single agent or in combination in n = 6 PDX models and with **B.** AZD6738 as single agent or in combination in n = 5 models, measured as percentage of tumour volume change, compared with the tumour volume on day 1. Each bar indicates the mean and SEM of at least three biological replicates (open circles). The mean of control tumours (n ≥ 3) is represented with solid circles. +20%, -30%, -95% are marked by dotted lines to indicate the range of PD (resistant), SD, PR and CR (sensitive), respectively. The lower box summarizes the RAD51 score, the specific gene alteration harboured by each model, the cancer type, and previous treatment history with DNA-damaging agents. A pairwise Wilcoxon test corrected for multiple testing was performed in all the panels. *, *p*-value ≤ 0.05; **, *p*-value ≤ 0.01; ***, *p*-value ≤ 0.001. Abbreviations: Rev: reversion mutation; DDR: DNA damage repair.

Similar to carboplatin, ATR inhibition has the potential to synergize with PARPi since trapped PARP1 can lead to replication fork stalling, which requires ATR for resolution[122,183]. Thus, we explored the antitumour activity of the PARP1i AZD5305 in combination with the ATRi ceralasertib (AZD6738) in a subset of five PDXs, four from breast and one from ovarian cancer. Ceralasertib is a highly selective, ATP-competitive inhibitor that, in combination with AZD5305, induced tumour regression (CR) in PDX127, a model with primary resistance to either PARPi due to a dysregulation of the end resection pathway (**Figure 33B** and **Supplementary Table 1**). Interestingly, this combination also resulted in CR in PDX474.7, a model obtained after the clinical progression to talazoparib, and that was resistant to the combination of AZD5305 plus carboplatin. Furthermore, the combination with ATRi increased the magnitude and the duration of response in three AZD5305-sensitive models (PDX124, PDX179 and PDX196) without compromising tolerability (**Figure 33B** and **Supplementary Figure 15B-G**). Of note, PDX474.7 harboured a *CDKN2A* deletion, considered as a high replicative stress biomarker[184], and PDX196 a pathogenic variant in *ATM,* also known to promote ATRi sensitivity[122], which might contribute to their sensitivity to the ATRi plus PARPi combination. Taken together, these results demonstrate that response to AZD5305 can be improved by combining it with carboplatin or an ATRi, with superior activity of the latter.

Overcoming PARPi resistance by inhibiting alternative DNA damage repair pathways: POLθ and DNA-PK inhibitors

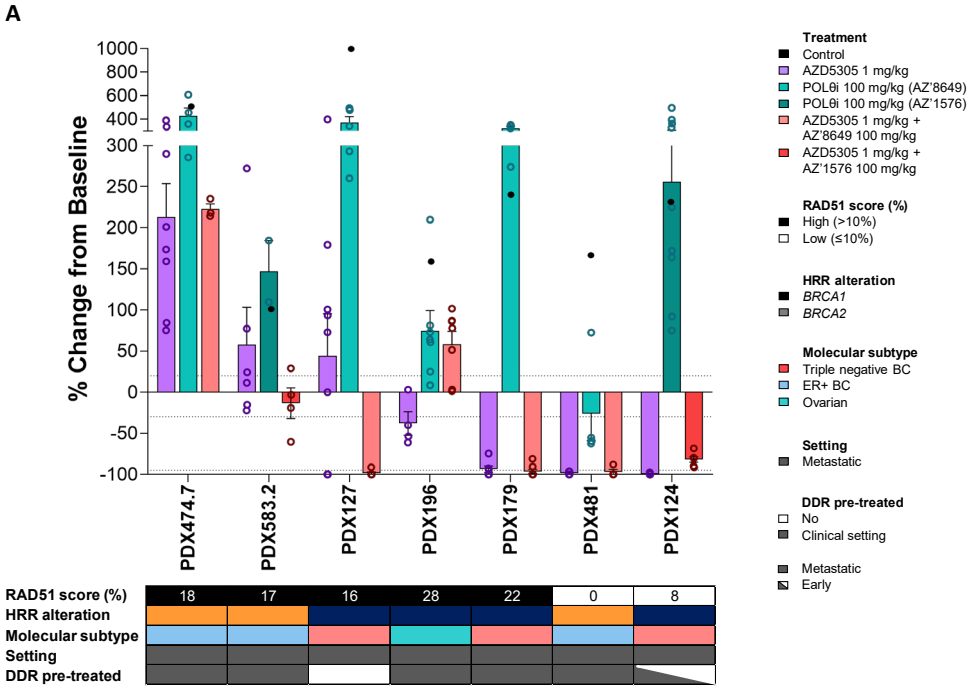
Tumours with defects in the HRR pathway, an error-free mechanism to repair DSBs, rely on alternative error-prone pathways such as the microhomology-mediated end-joining (MMEJ) or the non-homologous end-joining (NHEJ)[14,18,59,124]. Accordingly, failure to repair DSBs by these backup mechanisms, even if they do so in a non-faithful manner, is synthetic lethal with alterations in HRR. Therefore, inhibitors of key proteins of the MMEJ and NHEJ, such as POLθ and DNA-PK, respectively, have emerged as new promising drug targets for the treatment of PARPi-resistant tumours with HRD. Here, we aimed to evaluate the antitumour activity of POLθi and DNA-PKi alone and in combination with PARPi as therapeutic options for PARPi-resistant tumours.

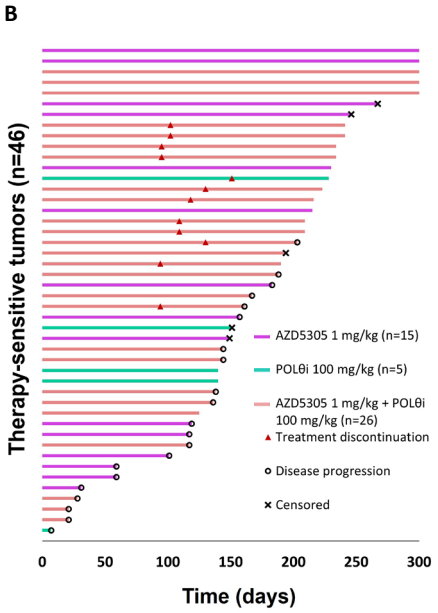
Dissecting the antitumour response of POLθ inhibitors in combination with PARP1i in *BRCA*-associated PDXs

Establishment and characterization of a PDX panel from *BRCA*-associated cancer patients

DNA polymerase theta (POLθ, encoded by *POLQ*) displays several functions in maintaining genomic stability and preventing tumourigenesis[185]. In particular, POLθ is a critical enzyme in the mutagenic MMEJ repair of DSBs[186] and its depletion has been described to be synthetic lethal with HRD[14,124]. As a result, POLθ inhibitors (POLθi) have emerged as a promising targeted therapy for the treatment of *BRCA*-altered tumours. In addition, first-generation PARPi-resistant *BRCA*-deficient tumours are known to be sensitive to POLθi treatment[187]. Based on this preliminary evidence, we sought to study POLθi as a strategy to improve the efficacy and durability of responses observed with the next-generation PARP1i AZD5305 alone and to overcome AZD5305 resistance. To this end, a panel of 7 previously well-

characterised *BRCA*-associated PDXs was selected according to their molecular characteristics and response to PARPi. Specifically, we selected 3 TN, 3 HR+ and 1 HGSOC models. All PDXs were obtained from metastatic patients who had received prior treatment (**Supplementary Table 8**). Regarding the HRR status, 4 PDXs harboured mutations in *BRCA1* and 3 in *BRCA2,* with 5 out of 7 PDXs showing intermediate/high RAD51 levels, which suggests that at least a partially functional HRR pathway in these models (**Figure 34A, Supplementary Table 8**). Regarding response to PARPi, 4 models were sensitive to AZD5305 (PDX124, PDX481, PDX179 and PDX196) and 3 were resistant (PDX127, PDX583.2 and PDX474.7; **Figure 34A**).





C

	AZD5305	AZD5305+ POLθi	*p* - value
No progressing	7	14	0.6
Progressing	8	12	
Total	15	26	41

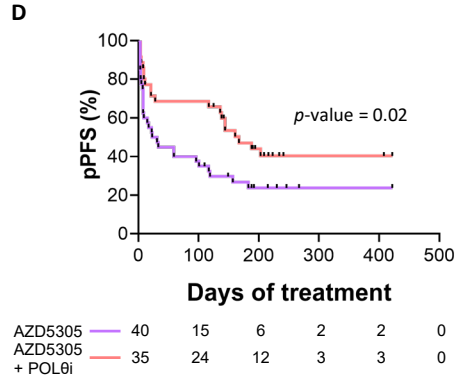


Figure 34. Evaluation of POLθi antitumour activity as single agent or in combination with the PARP1 selective inhibitor AZD5305.

A. Waterfall plot showing the best response to AZD5305 and POLθi (either AZ'8649 or AZ'1576) as single agents or in combination in 7 PDXs as the percentage of tumour volume change compared to the tumour volume on day 1. Each bar indicates the mean and SEM of at least three biological replicates (open circles). The mean of control tumours (n ≥ 3) is represented with solid circles. +20%, −30%, -95% are marked by dashed lines to indicate the range of PD (resistant), SD, PR, CR (sensitive), respectively. The legend summarizes the RAD51 score, the genetic alteration, molecular subtype, setting and previous treatment with DNA-damaging agents. **B.** Swimmer plot showing the timeline of the *in vivo* experiments with individual therapy-sensitive tumours (n = 46). Time at which treatment discontinuation, disease progression or animal censoring occurred are labelled. **C.** Number of initially sensitive tumours that eventually progressed upon treatment. A chi-squared test was performed. Total sample size and *p*-values are shown. **D.** Kaplan-Meier curve showing pPFS for AZD5305- and AZD5305+POLθi-treated individual tumours. A mixed-effects cox regression model was performed in panel D. Abbreviations: pPFS: preclinical progression-free survival.

POLθi in combination with AZD5305 showed improved efficacy in *BRCA1*-deficient PARPi-resistant PDX models

Having established the PDX cohort and the response of these models to the PARP1i AZD5305 as a single agent, we evaluated whether improved efficacy in terms of best response *in vivo* could be achieved by treatment with POLθi (two compounds used: AZ'8649 or AZ'1576) both as a single agent or in combination with AZD5305, particularly in those models with intermediate response or resistance to AZD5305. Notably, 6/7 models were resistant to POLθi as a single agent. Indeed, the only tumour that showed sensitivity (SD) to POLθi, PDX481, exhibited 0% RAD51, which suggests that a completely non-functional HRR pathway may be required for POLθi to be effective (**Figure 34A**).

By contrast, better responses were observed following treatment with the combination of POLθi plus AZD5305, as 5 out of 7 PDXs were sensitive to therapy (**Figure 34A** and **Table 7**). Surprisingly, among combination-sensitive tumours, the AZD5305-resistant HR-proficient PDX127 and PDX583.2 achieved CR and SD, respectively. Interestingly, PDX127 harboured an alteration in *FAM35A*, a key gene involved in the NHEJ repair pathway (**Supplementary Table 1**). The fact that PDX127 has two of the three DNA repair pathways not fully functional (NHEJ and HRR) could lead to an increased reliability on MMEJ and thus sensitivity to POLθi. The three remaining combination-sensitive models (PDX124, PDX481 and PDX179) achieved CR on AZD5305 as single agent, indicating that the sensitivity observed to the combination is likely due to the PARPi activity.

Table 7. Antitumour activity and durability of response of the POLθi plus AZD5305 combination vs. AZD5305 as single agent in combination-sensitive models.
Abbreviations: combo: POLθi plus AZD5305 combination; PD: Progressive disease; SD: Stable disease; PR: Partial response; CR: Complete response.

PDX models	Best response (mRECIST)		Durability of response (days)		Number of tumours progressing/total (%)	
	Combo	AZD5305	Combo	AZD5305	Combo	AZD5305
PDX124	PR	CR	149	151	6/6 (100%)	5/6 (83%)
PDX481	CR	CR	362	301	0/4 (0%)	0/5 (0%)
PDX179	PR	CR	194	91	3/8 (38%)	3/4 (75%)
PDX127	CR	PD	238	-	0/4 (0%)	-
PDX583.2	SD	PD	49	-	3/4 (75%)	-

Treatment with POLθi in combination with AZD5305 elicited durable responses in two HR-proficient PDX models

Following the efficacy analysis, we sought to evaluate the durability of response to POLθi as a single agent or in combination with AZD5305 in therapy-sensitive models. POLθi single agent did not improve durability of response in the only POLθi-sensitive model, PDX481, compared to AZD5305 alone (133 days vs. 301 days, respectively, **Supplementary Figure 16A**).

Regarding the combination, tumours from 1/3 sensitive models showed an increased durability of response with the combination with respect to AZD5305 alone (PDX481, 362 days vs. 301 days, p=0.03; PDX179, 194 days vs. 91 days, p=0.09; PDX124, 149 days vs. 151 days, p=0.9; **Figure 34B** and **Table 7**). No regrowth was observed in tumours from the HR-deficient PDX481 nor the HR-proficient PDX127 on treatment with the combination (0/4 in both cases). However, tumours from the combination-sensitive PDX124 and PDX179, as well as from the combination-resistant PDX583.2 eventually progressed upon treatment (**Table 7**). Therefore, 14 out of 26 (54%) tumours treated with the combination and 7 out of 15 (47%) tumours

treated with AZD5305 alone remained sensitive after treatment (p=0.6; **Figure 34C**).

Overall, preclinical time to progression (pTTP) was longer with POLθi plus AZD5305 compared to AZD5305 alone, although results were not significant (122 days vs. 103 days, p=0.4; **Supplementary Figure 16B**). Finally, preclinical PFS (pPFS) was superior with the combination of POLθi plus AZD5305 compared to AZD5305 alone (median pPFS of 161 days vs. 23 days, p=0.02; **Figure 34D**).

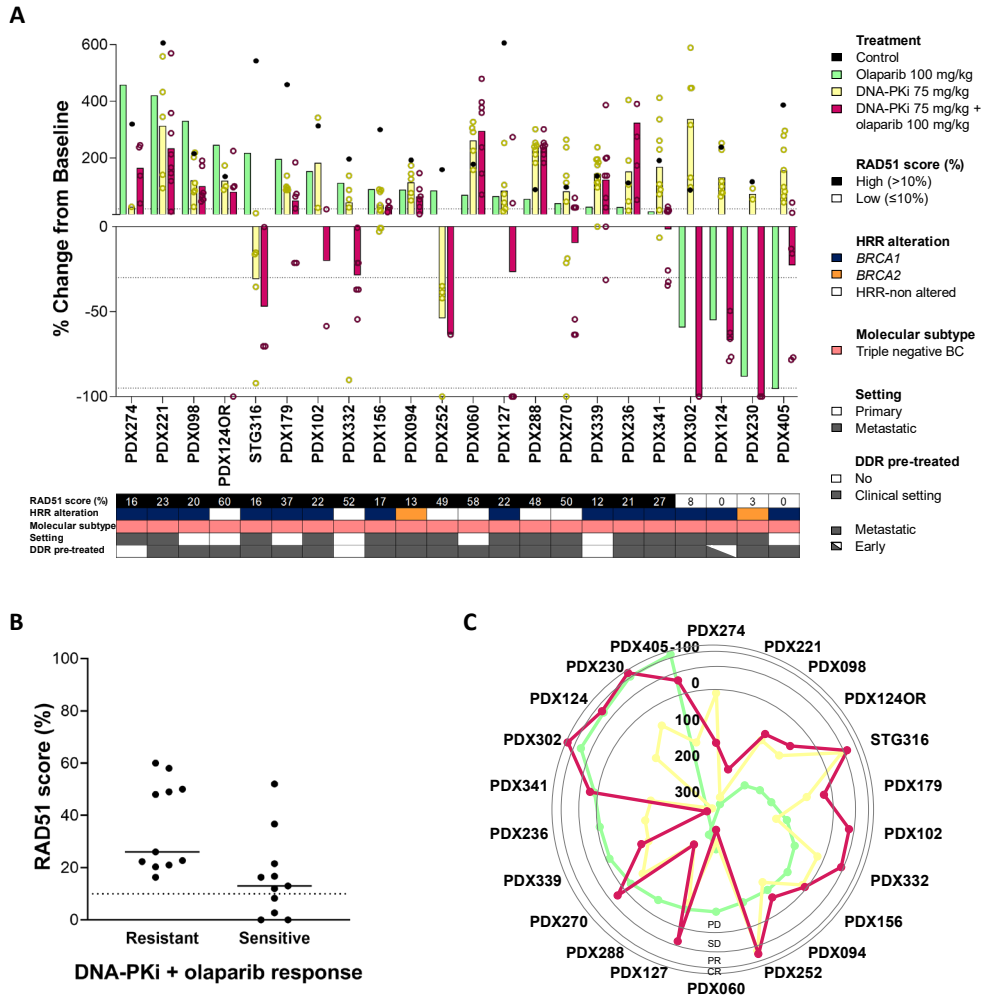
Collectively, these results indicate that, in contrast to POLθi as a single agent, the combination of POLθi plus AZD5305 resulted in improved antitumour activity, durability of response and progression rate in *BRCA*-associated PDX models compared to AZD5305 alone.

Dissecting the antitumour response of DNA-PK inhibitors in TNBC PDXs

Establishment and characterization of a PDX panel from TNBC patients

Inhibition of NHEJ has been described as an important additional approach to overcome PARPi resistance as it is the major pathway used to repair DSBs in *BRCA*-deficient cells[31]. More specifically, inhibitors of the DNA-PK kinase activity, a key player in the NHEJ, are an effective strategy when combined with radiation or topoisomerase I inhibition, two standard-of-care therapies for TNBC. Therefore, after having evaluated the effect of inhibiting MMEJ by POLθi in *BRCA*-associated PDXs, we aimed to assess sensitivity to the inhibition of the third DNA damage repair pathway NHEJ using AZD7648, a potent and selective DNA-PK inhibitor, in a panel of 22 TNBC PDXs. Seven of the 22 (32%) were obtained from primary tumours, while sixteen (68%) were derived from metastatic lesions, most of which had received prior treatment with DNA-damaging agents (20/22, 91%; **Figure 35A; Supplementary Table 9**). Regarding the HRR status, the majority of models

harboured alterations in *BRCA1* (14/22, 64%), 2/22 (9%) in *BRCA2* and 6 showed an intact HRR pathway (27%). In terms of olaparib response, 5/22 models were sensitive (4 PR and 1 SD), while 17/22 models were resistant (**Figure 35A**).



D

	Olaparib	Olaparib + DNA-PKi	*p*-value
No progressing	16	16	<0.0001
Progressing	30	0	
Total	46	16	62

E

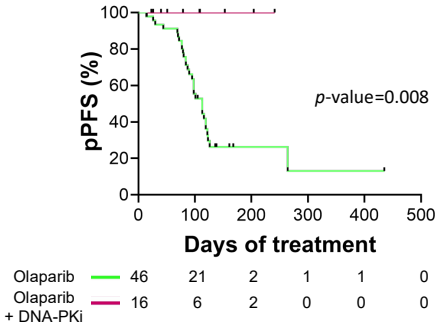


Figure 35. Evaluation of DNA-PKi antitumour activity as single agent or in combination with olaparib.

A. Waterfall plot showing the best response to olaparib and the DNA-PKi AZD7648 as single agents or in combination in 22 PDXs as the percentage of tumour volume change compared to the tumour volume on day 1. Each bar indicates the mean and SEM of at least three biological replicates (open circles). The mean of control tumours (n ≥ 2) is represented with solid circles. +20%, −30%, -95% are marked by dashed lines to indicate the range of PD (resistant), SD, PR, CR (sensitive), respectively. The legend summarizes the RAD51 score, the genetic alteration, molecular subtype, setting and previous treatment with DNA-damaging agents. **B.** Distribution of the RAD51 score according to the response to DNA-PKi+olaparib (n = 22). Each dot represents the mean of at least three tumours for each PDX model. Lines represent the mean of treatment-resistant or sensitive models. Dashed line indicates the test's cut-off (low RAD51≤10%). **C.** Radar plot showing the best response to olaparib and the DNA-PKi AZD7648 as single agents or in combination in 22 PDXs as the percentage of tumour volume change compared to the tumour volume on day 1. **D.** Number of initially sensitive tumours that eventually progressed upon treatment. Total sample size and *p*-values are shown. **E.** Kaplan-Meier curve showing pPFS for olaparib- and combination-treated individual tumours. A mixed-effects cox regression model was performed in panel E. Abbreviations: pPFS: preclinical progression-free survival.

DNA-PK inhibitors enhance the antitumour activity of the PARPi olaparib and reduce progression rate

We then evaluated whether improved efficacy in terms of best response *in vivo* was achieved in the cohort of PDXs by treatment with the DNA-PKi AZD7648, both as a single agent or in combination with olaparib, with particular interest in olaparib-resistant PDXs. Two of the 17 olaparib-resistant

models (12%) exhibited sensitivity (PR) to AZD7648, namely PDX252 and STG316, two *BRCA1*-mutated PDXs (**Figure 35A**). Of note, PDX252 showed an alteration in *ATM* (c.2756G>C; p.R919T; variant allele frequency, VAF: 0.3), which has previously been described to confer sensitivity to DNA-PKi as its absence favours the use of NHEJ to repair DSBs[188-190]. In addition, STG316 showed a predicted likely deleterious missense variant in *POLQ* (c.724C>T; p.R242W; VAF: 0.5) accompanied by an upregulation of the *PRKCD* gene, which encodes for the DNA-PK kinase, measured by RNA sequencing (**Supplementary Figure 17A**). These findings indicate that this tumour is likely to rely on NHEJ to repair DSBs due to the pathogenic *BRCA1* and *POLQ* mutations in the HRR and the MMEJ pathways, respectively.

When combining DNA-PKi with PARPi, six olaparib-resistant models showed sensitivity: two PR and four SD (**Figure 35A**). Regarding olaparib-sensitive models, better responses were shown in 2 PDXs compared to PARPi as a single agent (PDX230 and PDX302).

It has been described that several factors may play a role in the pathway selection decision following a DSB, such as the cell cycle phase[191,192] or the availability of the key factors that modulate each pathway, namely BRCA1 and 53BP1 for HRR and NHEJ, respectively[27]. Therefore, we aimed to evaluate the response to the combination according to the HRR pathway functionality by RAD51, and to establish a correlation between HRD and NHEJ usage. As expected, combination-resistant tumours showed high RAD51 scores (11/11, 100%), indicating that the HRR was the mechanism of choice to repair DSBs, while HR-deficient models were sensitive to treatment (4/4, 100%), likely because they rely more on NHEJ due to their inability to repair by HRR (**Figure 35B**). Interestingly, 7/11 combination-sensitive PDXs (64%) were HRP, which confirms that sensitivity to a NHEJ inhibitor does not completely overlap with sensitivity to olaparib (i.e. those models that are unable to repair by HRR and hence rely more on NHEJ) and therefore does not depend solely on HRR functionality (**Figure 35C**). In the specific cases of

the combination-sensitive PDX127 and STG316, which harboured alterations in *FAM35A* and *TP53BP1*, respectively, partially functional NHEJ could explain the observed sensitivity.

A significant difference was observed between the combination and olaparib in terms of tumour progression. All the initially sensitive tumours remained sensitive to the combination, compared to the 30/46 (65%) that progressed after olaparib treatment (p>0.0001; **Figure 35D** and **Supplementary Figure 17B**), meaning that the combination was superior at preventing tumour regrowth. However, no differences were observed in terms of overall pTTP (89 days vs. 109 days, p=0.09; **Supplementary Figure 17C**). Finally, pPFS was superior with the combination compared to olaparib as a single agent (median pPFS of > 266 days vs. 101 days, p=0.008; **Figure 35E**). In summary, the combination of a DNA-PKi with olaparib was shown to target olaparib resistance and achieve more profound responses with a lower rate of progression, having a broad potential as an anticancer agent as it acts as a sensitiser to PARPi.

In conclusion, although the emergence of intrinsic and acquired resistance to first-generation PARPi still reminds a clinical hurdle, the data described in this thesis, along with further results generated by us[122], have shown that the use of selective PARP1 inhibitors or combinations of PARPi plus other DNA-damaging agents rescued 13/23 (57%) of the HRR-altered PARPi-resistant PDXs, with the combination of AZD5305 plus ATRi as the more potent option (**Table 8** and **Supplementary Figure 18**). Although this study supports the use of other therapeutic combination approaches in PARPi-resistant tumours, further studies with increased sample sizes are needed.

Table 8. Response rate (RR) observed upon treatment with the different DNA-damaging agents alone vs. in combination with PARPi assessed in this thesis.
The overall RR achieved with each treatment, as well as the RR obtained with combinations beyond the one observed with PARPi in monotherapy is indicated. Abbreviations: RR: response rate; CR: complete response; PR: partial response.

Compound	Treatment	N PDX	RR (CR+PR)	ΔRR from monotherapy
Olaparib	First-generation PARP1/2i	109	20% (22/109)	-
AZD5305	Next-generation PARP1i	13	46% (6/13)	-
Carboplatin	Platinum-based CT	6	0% (0/6)	-
AZD5305 + carboplatin	-	6	50% (3/6)	33% (2/6)
AZD6738	ATRi	5	40% (2/5)	-
AZD5305 + ATRi	-	5	100% (5/5)	40% (2/5)
AZ'8649/AZ'1576	POLϑi	7	0% (0/7)	-
AZD5305 + POLϑi	-	7	57% (4/7)	14% (1/7)
AZD7648	DNA-PKi	22	9% (2/22)	-
Olaparib + DNA-PKi	-	22	23% (5/22)	9% (2/22)

Dysregulation of the end resection pathway is associated with DNA-damaging agents in combination with PARPi in *BRCA1*-mutated tumours

Loss of function of specific BRCA1 domains leads to specific mechanisms of resistance to PARPi

The roles of BRCA1 and BRCA2 in preserving genomic stability can be uncoupled and that they are carried out by different protein domains. Thus, this separation-of-function structure suggests that mutations in specific locations of these genes could lead to different outcomes in terms of PARPi response depending on the function affected.

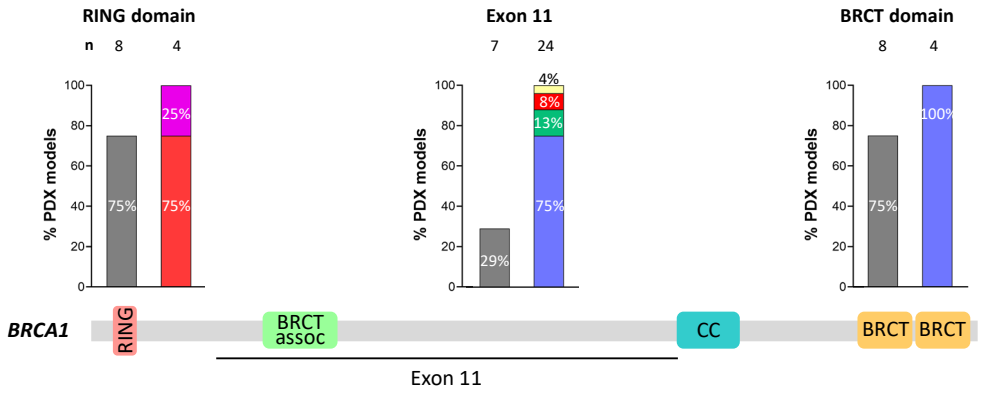
Briefly, BRCA1 contains four main domains: the N-terminal RING domain, the central region encoded by the exon 11, a coiled-coil domain and the C-terminal region (BRCT domain)[43,193]. In this line, we sought to investigate the

correlation between the location of the mutation within the gene, and consequently the lack of a specific function, with PARPi response. We have previously described that models with mutations in *BRCA1* are more prone to show primary and acquired resistance to olaparib than tumours with alterations in other HRR-related genes (53% and 73%, respectively; **Figure 21B**). We observed that 75% (6/8) of the RING and 75% (6/8) of the BRCT domain-mutated models were resistant to PARPi (including models with intrinsic resistance and excluding models with acquired resistance to olaparib, OR; labelled with grey bars in **Figure 36A** and **Supplementary Figure 19**). Indeed, of all PARPi-resistant *BRCA1*-mutated models, 43% had mutations in the RING and 43% in the BRCT domain (**Figure 36B**). In contrast, PDXs harbouring mutations in the exon 11 of *BRCA1* were predominantly PARPi-sensitive (5/7, 71%), with only 14% of *BRCA1*-mutated PARPi-resistant tumours presenting mutations in this region (**Figure 36A** and **B**).

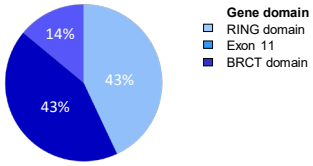
When we studied the proportion of models with acquired resistance to PARPi according to the presence of alterations in the different BRCA1 domains we found that, while 27/40 (68%) harboured the mutation in the exon 11 and 13/40 (32%) in the RING domain, none of the PDXs had a mutation in the BRCT domain (highlighted in pink in **Supplementary Figure 19**).

These results indicate that, while the RING and BRCT domains are not essential to preserve BRCA1 functionality and tumours with mutations in these regions can immediately progress to PARPi treatment, the exon 11 is more relevant for the HRR pathway to be functional, as these models are more prone to be initially sensitive. However, upon selective pressure through treatment, exon 11-mutated tumours exhibited a higher proportion of tumours with acquired resistance.

A



B



C

PDX	HRR alteration	Gene domain	PARPi	Response to PARPi	MoR	Platinum salts	Carbo + AZD5305	AZD6738 (ATRi)	ATRi + PARPi	AZD1775 (WEE1i)	WEE1i + Olaparib	AZD7648 (DNA-PKi)	DNA-PKi + Olaparib	POLθi	POLθi + AZD5305
PDX339	*BRCA1*	RING	Olaparib	PD	Unknown	PD		PD	SD			PD	PD		
PDX629	*BRCA1*	RING	Olaparib	PD	Unknown	PD									
PDX230OR2	*BRCA1*	RING	Olaparib	PD	Unknown	PD									
PDX230OR8	*BRCA1*	RING	Olaparib	PD	Unknown										
PDX230OR5	*BRCA1*	RING	Olaparib	PD	Unknown	PD	PD								
PDX230OR1	*BRCA1*	RING	Olaparib	PD	53BP1 pt										
STG316	*BRCA1*	RING	Olaparib	PD	53BP1+B1	SD		PD	SD	SD	SD	PR	PR		
HBCx8	*BRCA1*	RING	Olaparib	PD	Unknown										
PDX127	*BRCA1*	RING	Olaparib	PD	53BP1 pt	PR	CR	PD	CR	PD	PD	PD	SD	PD	CR
HBCx28	*BRCA1*	RING	Olaparib	PD	53BP1 pt										
10	*BRCA1*	RING	Olaparib	PD	Unknown										
11	*BRCA1*	RING	Olaparib	PD	Unknown										
12	*BRCA1*	RING	Olaparib	PD	Unknown										
13	*BRCA1*	RING	Olaparib	PD	Unknown										
14	*BRCA1*	RING	Olaparib	PD	Unknown										
15	*BRCA1*	RING	Olaparib	PD	Unknown										
33	*BRCA1*	RING	Olaparib	PD	Unknown										
34	*BRCA1*	RING	AZD5305	PD	Unknown										
35	*BRCA1*	RING	AZD5305	PD	Unknown										

D

PDX	HRR alteration	Gene domain	PARPi	Response to PARPi	MoR	Platinum salts	Carbo + AZD5305	AZD6738 (ATRi)	ATRi + PARPi	AZD1775 (WEE1i)	WEE1i + Olaparib	AZD7648 (DNA-PKi)	DNA-PKi + Olaparib	POLθi	POLθi + AZD5305
PDX236	*BRCA1*	BRCT	Olaparib	PD	Hyp BRCA1	PD		PD	PD	CR	CR	PD			
PDX641.1	*BRCA1*	BRCT	Olaparib	PD	Unknown										
PDX252	*BRCA1*	BRCT	Olaparib	PD	Unknown	PR		PD	PD		PR	PR	PR		
PDX397	*BRCA1*	BRCT	Olaparib	PD	Hyp BRCA1	PD									
PDX418	*BRCA1*	BRCT	Olaparib	PD	Hyp BRCA1	PD									
PDX221	*BRCA1*	BRCT	Olaparib	PD	Hyp BRCA1	PD		PD	PD	PD	PR	PD	PD		

E

PDX	HRR alteration	Gene domain	PARPi	Response to PARPi	MoR	Platinum salts	Carbo + AZD5305	AZD6738 (ATRi)	ATRi + PARPi	AZD1775 (WEE1i)	WEE1i + Olaparib	AZD7648 (DNA-PKi)	DNA-PKi + Olaparib	POLθi	POLθi + AZD5305
PDX064	*BRCA1*	Exon 11	Olaparib	PD	Hyp BRCA1										
PDX377OR1	*BRCA1*	Exon 11	Olaparib	PD	RAD51-i										
HBCx11	*BRCA1*	Exon 11	Olaparib	PD	Unknown										
PDX377OR2	*BRCA1*	Exon 11	Olaparib	PD	RAD51-i										
PDX124OR	*BRCA1*	Exon 11	Olaparib	PD	RAD51-i							PD	PD		
1	*BRCA1*	Exon 11	Olaparib	PD	53BP1 pt										
2	*BRCA1*	Exon 11	Olaparib	PD	Hyp BRCA1										
3	*BRCA1*	Exon 11	Olaparib	PD	Reversion										
4	*BRCA1*	Exon 11	Olaparib	PD	Hyp BRCA1										
5	*BRCA1*	Exon 11	Olaparib	PD	Hyp BRCA1										
6	*BRCA1*	Exon 11	Olaparib	PD	Hyp BRCA1										
7	*BRCA1*	Exon 11	Olaparib	PD	Hyp BRCA1										
8	*BRCA1*	Exon 11	Olaparib	PD	Unknown										
9	*BRCA1*	Exon 11	Olaparib	PD	Hyp BRCA1										
16	*BRCA1*	Exon 11	Olaparib	PD	Hyp BRCA1										
17	*BRCA1*	Exon 11	Olaparib	PD	Unknown										
18	*BRCA1*	Exon 11	Olaparib	PD	Unknown										
19	*BRCA1*	Exon 11	Olaparib	PD	Hyp BRCA1										
20	*BRCA1*	Exon 11	Olaparib	PD	Hyp BRCA1										
21	*BRCA1*	Exon 11	Olaparib	PD	Hyp BRCA1										
22	*BRCA1*	Exon 11	Olaparib	PD	Hyp BRCA1										
23	*BRCA1*	Exon 11	Olaparib	PD	Unknown										
24	*BRCA1*	Exon 11	Olaparib	PD	Hyp BRCA1										
25	*BRCA1*	Exon 11	Olaparib	PD	Hyp BRCA1										
31	*BRCA1*	Exon 11	Olaparib	PD	Hyp BRCA1										
32	*BRCA1*	Exon 11	Olaparib	PD	53BP1 pt										
36	*BRCA1*	Exon 11	AZD5305	PD	Hyp BRCA1										
37	*BRCA1*	Exon 11	AZD5305	PD	Hyp BRCA1										
38	*BRCA1*	Exon 11	AZD5305	PD	Hyp BRCA1										

PARPi-resistance
- Intrinsic
- Acquired

HRR alteration
- *BRCA1*

Gene domain
- RING domain
- Exon 11
- BRCT domain

PARPi
- Olaparib
- AZD5305

Mechanism of resistance (MoR) to PARPi
- Hypomorphic BRCA1
- HRR-gene reversions
- 53BP1 pathway
- 53BP1 pathway and hypomorphic BRCA1
- RAD51-independent
- Unknown (other RAD51-dependent)

Response to therapy (mRECIST)
- CR
- PR
- SD
- PD
- NA

Figure 36. Evaluation of DNA-damaging agents antitumour activity as single alone or in combination with PARPi according to the affected gene domain in PARPi-resistant *BRCA1*-mutated PDX models.

A. Percentage of PARPi-resistant PDX models with mutations in each *BRCA1* domain (RING domain, exon 11 and BRCT domain; grey bars). Coloured bars indicate the percentage of these PARPi-resistant models developing specific mechanisms of resistance within each group. **B.** Pie chart indicating the distribution of *BRCA1*-gene mutated domains among PARPi-resistant models (n = 24). DNA-damaging agents activity in PARPi-resistant PDXs harbouring mutations in **C.** the RING domain, **D.** the BRCT domain and **E.** the exon 11. The mechanism of resistance to PARPi and response to therapy according to the mRECIST criteria are shown. White boxes indicate non-available cases. Abbreviations: MoR: mechanisms of resistance; carbo: carboplatin; NA: non-available; CR: complete response; PR: partial response; SD: stable disease; PD: progressive disease; Hyp BRCA1: hypomorphic BRCA1; 53BP1 pt: 53BP1 pathway; 53BP1+B1: 53BP1 pathway and hypomorphic BRCA1; RAD51-i: RAD51-independent.

We further analysed the mechanism of resistance to PARPi in these models, that was identified in 4/19 (21%) RING domain-, 24/29 (83%) exon 11- and 4/6 (67%) BRCT domain-mutated PDXs (including models with acquired resistance to olaparib, OR; **Supplementary Figure 19**). We found that all

RING domain-mutated models (4/4, 100%) were resistant to PARPi mainly by BRCA1-independent mechanisms and likely due to a dysregulation of the 53BP1/end resection pathway (**Figure 36A** and **C**).

In contrast, all tumours with mutations in the BRCT domain of BRCA1 (4/4, 100%) showed increased levels of hypomorphic protein (**Figure 36A** and **D**). Similarly, most of the models harbouring mutations in the exon 11 (18/24, 75%) showed high levels of hypomorphic BRCA1 (chi-squared test, p=0.0007). Other mechanisms were observed among exon 11-mutated tumours, namely 1/24 (4%) with a *BRCA1* reversion mutation, 2/24 (8%) with a dysregulation of the 53BP1/end resection pathway and 3/24 (13%) became resistant through RAD51-independent mechanisms (**Figure 36A** and **E**). These results highlight that mutations in specific regions of *BRCA1* may lead to different mechanisms of resistance to PARPi.

PARPi-resistant tumours harbouring a dysregulation of the 53BP1/end resection pathway are highly sensitive to DNA-damaging combinations

We further aimed to investigate if there was an association between the specific mechanism of resistance and sensitivity to any DDR drug. **Supplementary Figure 19** shows a summary of the data obtained in this thesis and related publications[122]. As expected, and as previously noted for all HRR-altered models (**Supplementary Figure 18**), platinum resistance overlapped with PARPi resistance in 8/11 (73%) *BRCA1*-altered models (**Supplementary Figure 19**). As expected, 2/3 PARPi-resistant, platinum-sensitive models harboured a mutation in the RING domain and were resistant to PARPi due to a dysregulation of the 53BP1/end resection pathway (**Figure 36C**). Similar results were observed when targeting replication stress with the ATRi AZD6738, as it showed antitumour activity in combination with PARPi only in models with mutations in the RING domain (3/3, 100%), and not in BRCT-mutated tumours (0/3, 0%; **Figure 36D**). In contrast, models harbouring mutations in the BRCT domain were the most sensitive to the

WEE1i AZD1775 in combination with olaparib (3/3, 100%). Remarkably, among the WEE1i-sensitive PDXs, 2/3 BRCT-mutated and 1/1 RING domain-mutated (total 3/5, 60%) showed increased levels of hypomorphic BRCA1, suggesting that partially functional BRCA1 may be involved in sensitivity to this therapy (**Figure 36C** and **D**). Finally, 3/6 (50%) and 1/1 (100%) tumours showed sensitivity to treatment with DNA-PK or POLθ plus PARP inhibitors, respectively, two of which were RING domain-mutated with dysregulation of the 53BP1/end resection pathway. Importantly, only two of the models exhibiting sensitivity to these DDRi, namely STG316 and PDX252 in the neoadjuvant and the metastatic setting, respectively, were obtained from patients who had received prior platinum-based treatment. Thus, these results demonstrate that alterations in the 53BP1 pathway are associated sensitivity to combinations of DNA-damaging agents plus PARPi, rising the need to find functional biomarkers to identify these tumours that may benefit from these therapeutic options. Finally, further efforts are needed to identify possible patterns of sensitivity in tumours harbouring mutations in the exon 11 of *BRCA1* (**Figure 36E**).

In conclusion, these results suggest that, in tumours harbouring mutations in the RING domain of *BRCA1*, the most likely PARPi-resistance mechanism is through a dysregulation of the end resection pathway, which leads to sensitivity to platinum salts and combinations of PARPi with other DDRi such as ATR, POLθ or DNA-PK inhibitors. In contrast, tumours with mutations in the BRCT domain were more sensitive to WEE1 inhibitors[122]. Further research in larger cohorts of tumours is required to robustly confirm these associations.

PART 3

Study and validation of functional HRD biomarkers in clinical samples of TNBC and tumours harbouring alterations in HRR-related genes

We robustly demonstrated the high accuracy of the histopathology-based test based on the detection of RAD51 nuclear foci in predicting response to PARPi and cisplatin in a cohort of more than 100 untreated PDX models (see Results-Part 1)[98]. Therefore, our next aim was to demonstrate the clinical feasibility and utility of the RAD51 test in FFPE from patients with TNBC or tumours with alterations in HRR-related genes. In addition, we sought to establish the prevalence of HRD in primary breast cancer. Briefly, the use of DNA-damaging agents such as PARPi or platinum-based chemotherapies has increased in the recent years mainly in the metastatic setting[175]. To find out the potential benefit of these therapies in early stages of the disease, molecular and/or clinical biomarkers are required. Therefore, the purpose of this study was two-fold. Firstly, we wanted to investigate the feasibility and robustness of the RAD51 test in clinical samples. Secondly, we sought to explore the prevalence of functional HRD by RAD51 in the different scenarios within the primary setting and, therefore, to eventually predict and evaluate the benefit of adding DNA-damaging agents to treatments in the primary setting (**Figure 37**). Thus, several cohorts of non-invasive pre-malignant lesions (in collaboration with the Netherlands Cancer Institute, NKI, Amsterdam) and primary invasive breast (in collaboration with Bergen

University[142,143] and the German Breast Group, GBG[78]) have been analysed (**Figure 37**).

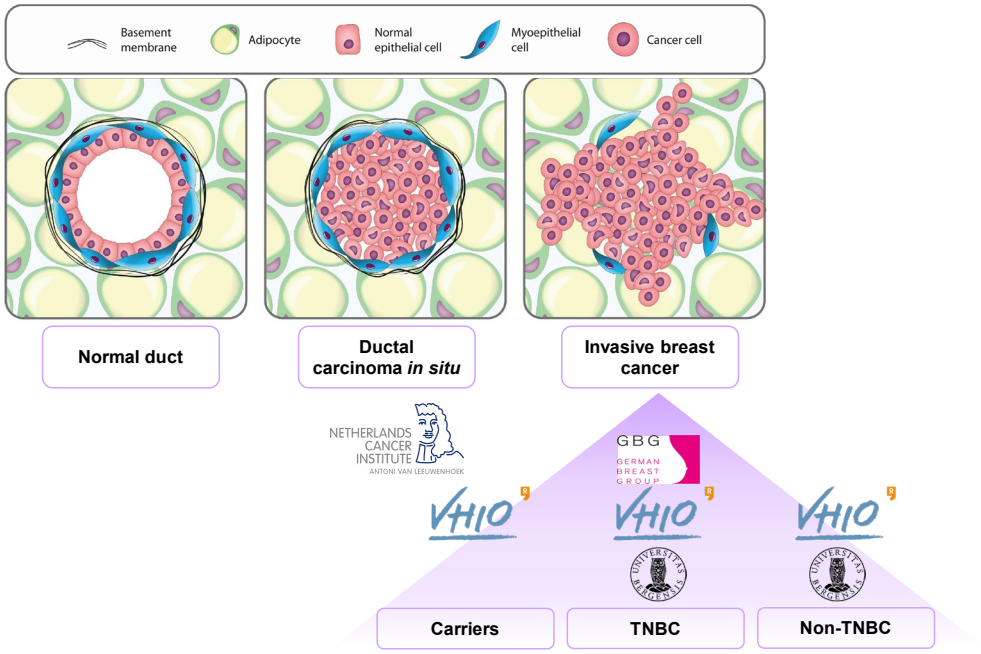


Figure 37. Schematic overview of the patients' cohorts used to validate the RAD51 assay in different scenarios within the primary setting of breast cancer.
The RAD51 assay was performed to estimate the HRD prevalence and to predict response to DNA-damaging agents in ductal carcinoma *in situ* (NKI) and in carrier (VHIO), TN (GBG, VHIO, Bergen University) and non-TN (VHIO, Bergen University) invasive breast cancer patients. Abbreviations: TNBC: triple-negative breast cancer. Adapted from *Gibson et al.*,[194].

Additionally, since the last objective of our project is the implementation of the RAD51 test in the clinical practice, the RING trial was conducted, which involved an analytical validation to assess staining procedures and interobserver variability among European expert laboratories.

Together with the validation of the 10% cut-off of the RAD51 assay, the establishment of the BRCA1 nuclear foci cut-off by IF that determines protein functionality was a priority in this thesis. Once it was established, the BRCA1

cut-off was applied to evaluate HRR functionality along with RAD51 in results from Part 1, 2 and 3.

Establishment of the BRCA1 cut-off to evaluate HRR functionality in combination with RAD51 by IF

As previously explained, the RAD51 assay measures the nuclear foci of three different proteins in geminin^{+} (S/G2-phase) cells: γ-H2AX as a marker of DNA damage (and as a quality check of the test), BRCA1 as a key protein of the pathway, and RAD51. The cut-offs used to determine levels of DNA damage by γ-H2AX were formerly established by *Cruz et al.,* and *Castroviejo-Bermejo et al.,*[99,100].

BRCA1 is known to be the most frequently mutated gene in tumours from HBOC syndrome patients, one of the main scenarios in which PARPi are clinically approved. In addition, it has been described that up to 60% of sporadic TNBC tumours can present *BRCA1* silencing through promoter hypermethylation[195]. Regarding protein levels, in the context of PARPi sensitivity, tumours harbouring *BRCA1* epi/genetic alterations may show low levels of BRCA1 foci, leading to low RAD51 scores. Nevertheless, tumours with alterations in other HRR-related genes, such as *BRCA2* or *PALB2*, would exhibit high BRCA1 foci levels and still present HRD. Regarding PARPi-resistant tumours, although they usually present high levels of BRCA1 foci due to the presence of genetic reversions in *BRCA1* or to the presence of BRCA1 hypomorphic protein, BRCA1-independent mechanisms of resistance, such as the dysregulation of the 53BP1/end resection pathway, can contribute to HRP in the absence of BRCA1 foci. Therefore, beyond being able to capture the functional HRD by RAD51 foci, which, as previously mentioned, is dynamic, there is the need to determine the reason behind the obtained status. Thus, in this thesis, we aimed to establish the cut-off of BRCA1 nuclear foci that determines BRCA1 functionality by IF.

In order to do so, we first evaluated the distribution and amount of BRCA1 nuclear foci in tumour cells from a subset of 39 PDX models. We quantified the percentage of geminin^{+} cells with 0, 1-2, 3-4 or ≥5 BRCA1 nuclear foci per nucleus and observed that, although tumours harbour certain heterogeneity, most of tumour cells exhibited none or ≥5 foci (**Supplementary Figure 20A**). In addition, BRCA1 nuclear foci perfectly overlapped with RAD51 foci by IF, as BRCA1 is directly involved in RAD51 recruitment to the DSBs (**Supplementary Figure 20B**). Therefore, we selected the threshold of ≥5 foci as a criterion to determine BRCA1 functionality within a tumour cell.

We then aimed to assess the percentage of geminin+ cells in a tumour with ≥5 BRCA1 foci with respect to the HRD status by RAD51. In this way, we were able to determine the level of BRCA1 required for a tumour to exhibit HRR functionality, namely >10% geminin^{+} cells presenting ≥5 RAD51 foci foci[98-100]. We scored RAD51 in a homogeneous cohort of 346 primary untreated FFPE samples from BC patients and observed that 166/346 (48%) presented low RAD51 scores, while 180 (52%) showed high scores. Next, we quantified BRCA1 nuclear foci in consecutive sections. While HRR-deficient tumours (low RAD51 scores) showed a wide range of BRCA1 scores, all HRR-proficient tumours (180/180, 100%, high RAD51 scores) presented levels of BRCA1 above 10% (**Figure 38A** and **Supplementary Figure 20C**). Hence, in the context of primary setting with no selective pressure (untreated), tumours require more than 10% of cells in the S/G2 phases showing 5 or more BRCA1 nuclear foci to be HRR-proficient. The biomarker achieved a sensitivity of 60% and a specificity of 100% when this threshold was applied.

Therefore, we have selected 10% as the BRCA1 nuclear foci cut-off to distinguish between HRR-proficient and deficient cells, which complements RAD51 score.

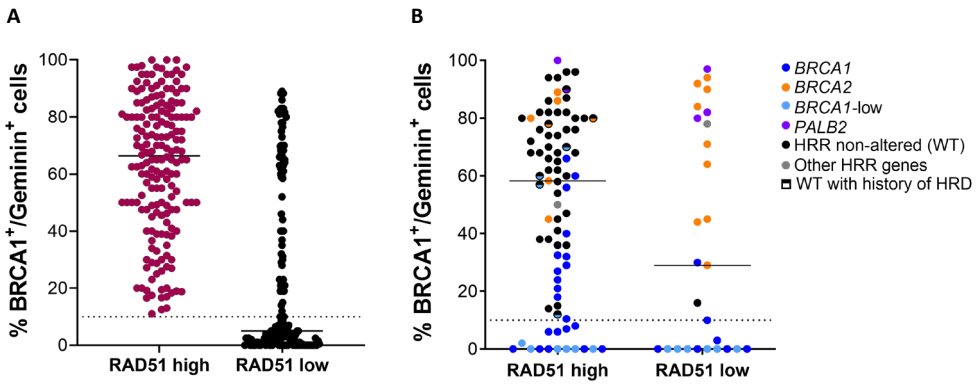


Figure 38. Establishment of BRCA1 nuclear foci cut-off in tumour samples.

A. Distribution of the percentage of geminin+ cells presenting 5 or more BRCA1 nuclear foci per nucleus according to RAD51 scores (RAD51 high > 10%; RAD51 low ≤ 10%) in a cohort of untreated primary BC patients. Each dot represents a single tumour. **B.** Validation of the pre-established 10% BRCA1 foci cut-off in a subset of PDX models. Each dot represents the mean of at least three tumours for each PDX model. Lines represent the mean of each group and dashed lines indicate the test pre-established cut-off (BRCA1 ≤ 10%) in all panels. Abbreviations: HRR: homologous recombination repair pathway; WT: wild-type; HRD: homologous recombination deficiency.

We then aimed to validate the pre-established 10% cut-off of BRCA1 in the cohort of PDX models. The analysis of the percentage of geminin+ cells with 5 or more BRCA1 foci according to RAD51 levels revealed that, among RAD51-low tumours, 12 out of 13 *BRCA1*-altered tumours presented levels below 10%. The remaining tumour, which harboured a mutation in the exon 11, partly in charge of the HRR functionality, showed 30% of BRCA1 and 4% of RAD51 foci, probably due to a skipping mechanism affecting this exon. As expected, RAD51-low tumours harbouring mutations in other HRR-related genes, such as *BRCA2* or *PALB2,* showed high levels of BRCA1 (**Figure 38B, Supplementary Table 1**). Additionally, among RAD51-high tumours, it was observed that 15 out of the 27 *BRCA1*-altered tumours (56%) showed BRCA1 levels below 10%, coinciding with models harbouring unknown or BRCA1-independent mechanisms of resistance to PARPi. The remaining 12 *BRCA1*-altered models having levels above 10% of both BRCA1 and RAD51 foci were classified as PARPi-resistant due to the presence of hypomorphic

BRCA1 or reversion mutations. These models exhibited similar BRCA1 levels to other non-*BRCA1*-mutated tumours (*BRCA2*, *PALB2* or HRR non-altered, **Figure 38B**).

In summary, we have established the cut-off of BRCA1 nuclear foci by IF in 10% of geminin+ cells harbouring 5 or more BRCA1 nuclear foci. This cut-off was further applied in the analyses of results Parts 1, 2 and 3 of this thesis.

Prevalence of HRD in non-invasive ductal carcinoma *in situ* (DCIS)

Following the establishment of the RAD51 and BRCA1 cut-offs and their validation in PDX models, we aimed to assess the HRD prevalence in non-invasive DCIS, which represents the earliest form of breast lesions.

The RAD51 assay along with the γ-H2AX and BRCA1 IF stainings was performed in a cohort of 28 untreated samples, of which the HRR-gene status was unknown. It was confirmed that all but one sample showed high levels of γ-H2AX (≥ 25%), meaning that, at early stages of the disease, there are levels of DNA damage comparable to those observed in later settings (**Figure 39**). Upon analysis of RAD51 scores, we observed that 5 out of the 28 samples had low levels, indicating that HRD is present in 18% of the DCIS of the cohort (**Figure 25A**). It is worth noting that, even in the sample with low γ-H2AX level (16%), high RAD51 scores were still observed, indicating that the HRR pathway was anyhow active. Furthermore, we confirmed that 3/5 (60%) low RAD51 samples also exhibited low levels of BRCA1 nuclear foci, which suggests that HRD may be caused by *BRCA1* alterations in these tumours (**Figure 39**).

Overall, these results demonstrate that the RAD51 assay is a feasible option for detecting tumours with HRD in untreated FFPE samples and that functional HRD appears to be prevalent in early non-invasive breast lesions.

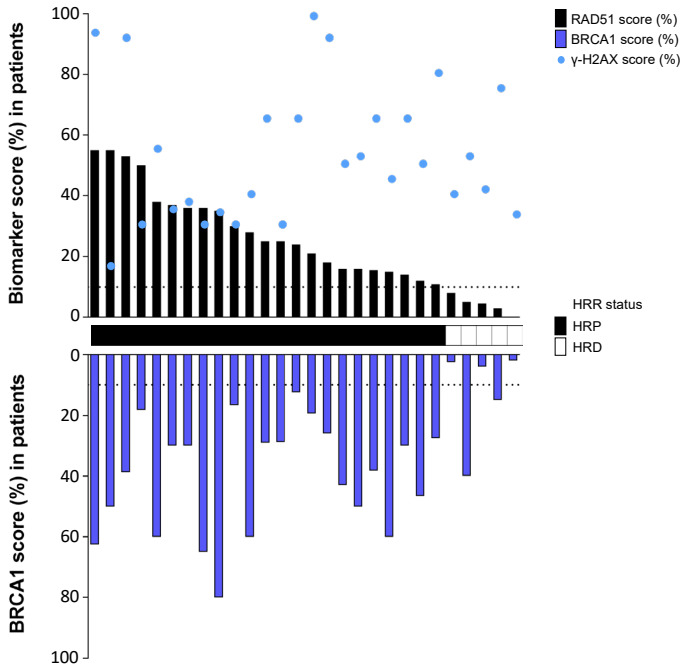


Figure 39. Analysis of homologous recombination deficiency (HRD) biomarkers by immunofluorescence (IF) in ductal carcinoma *in situ* (DCIS) clinical samples.

The percentages of geminin+ tumour cells with RAD51 (upper black bars), BRCA1 (bottom blue bars) and γ-H2AX (blue dots) nuclear foci in 28 DCIS clinical samples are shown. HRR status (HRP or HRD) is indicated. Dashed line indicates the tests' cut-offs (low RAD51≤10; low BRCA1≤10). Abbreviations: HRR: homologous recombination repair; HRD: homologous recombination deficiency; HRP: homologous recombination proficiency.

Prevalence of HRD and predictive value of the RAD51 assay in primary invasive breast cancer patients

Prevalence of HRD in mutation carriers vs. unselected TN and non-TNBC patients: HUVH, PETREMAC and GeparSixto clinical trials[78,142,143]

Prevalence of HRD in mutation carriers

We then wanted to establish the HRD prevalence in primary invasive breast cancer patient samples. Within this context, we conducted an analysis of

several different scenarios. Firstly, we aimed to determine the functional HRD prevalence among carriers of mutations in HRR-related genes (**Figure 40**). To do so, we evaluated RAD51 in untreated tumour samples from the diagnostic biopsy or untreated surgery of patients from Vall d'Hebron University Hospital (HUVH). As expected, a significant proportion of patients with germline mutations in *BRCA1*, *BRCA2* and *PALB2* demonstrated low levels of RAD51 (91%, 92% and 95%, respectively).

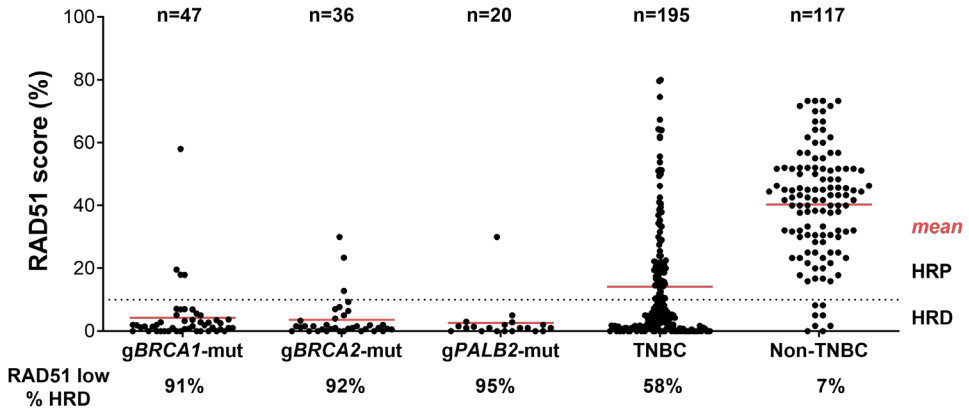


Figure 40. Prevalence of homologous recombination deficiency (HRD) by RAD51 in untreated primary invasive breast cancer patients.

Distribution of the RAD51 score according to the presence of detected germline HRR-related gene mutations (g*BRCA1*, g*BRCA2* or g*PALB2* from HUVH), or the molecular subtype (TNBC from the PETREMAC and the GeparSixto trials; non-TNBC from HUVH and the PETREMAC trial). The percentage of RAD51 low tumours, classified as HRD, as well as sample sizes and the mean of each group is indicated. Each dot represents a single tumour. Dashed lines indicate the test cut-off (low RAD51 ≤ 10%). Abbreviations: g: germline; TNBC: triple-negative breast cancer; HRD: homologous recombination deficiency; HRP: homologous recombination proficiency.

HRD in unselected TNBC patients[78,142]

We then investigated the prevalence of HRD in unselected primary untreated TNBC patients enrolled in two clinical trials, namely the PETREMAC (NCT02624973) and the GeparSixto (NCT01426880) trials (see Materials and Methods)[78,142].

Results from the PETREMAC trial cohort showed that all 30 TNBC patients analysed presented high levels of γ-H2AX (**Figure 41** and **Supplementary Table 10**). We observed that 57% (17/30) of TNBC exhibited low RAD51 scores, with 47% (14/30) of them harbouring an HRR-gene alteration[142]. Of note, there was a high prevalence of tumours presenting epigenetic alterations in *BRCA1* in this cohort (10/30, 33%), with most of them showing low RAD51 scores (9/10, 90%).

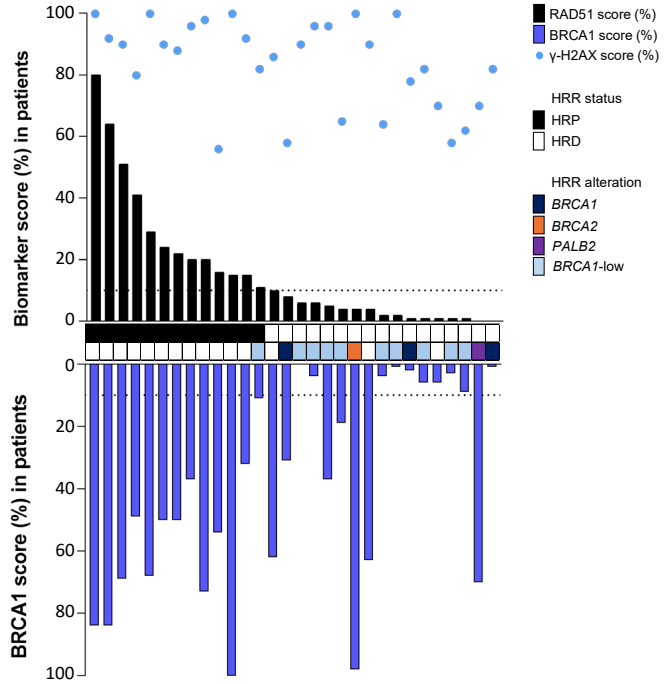


Figure 41. Analysis of homologous recombination deficiency (HRD) biomarkers by immunofluorescence (IF) in untreated triple-negative breast cancer (TNBC) patients from the PETREMAC trial.

The percentages of geminin+ tumour cells with RAD51 (upper black bars) and BRCA1 (bottom blue bars) nuclear foci in 30 untreated TNBC samples are shown. HRR status (HRP or HRD) is indicated. Dashed line indicates the test cut-off (low RAD51≤10; low BRCA1≤10). Abbreviations: HRR: homologous recombination repair; HRD: homologous recombination deficiency; HRP: homologous recombination proficiency.

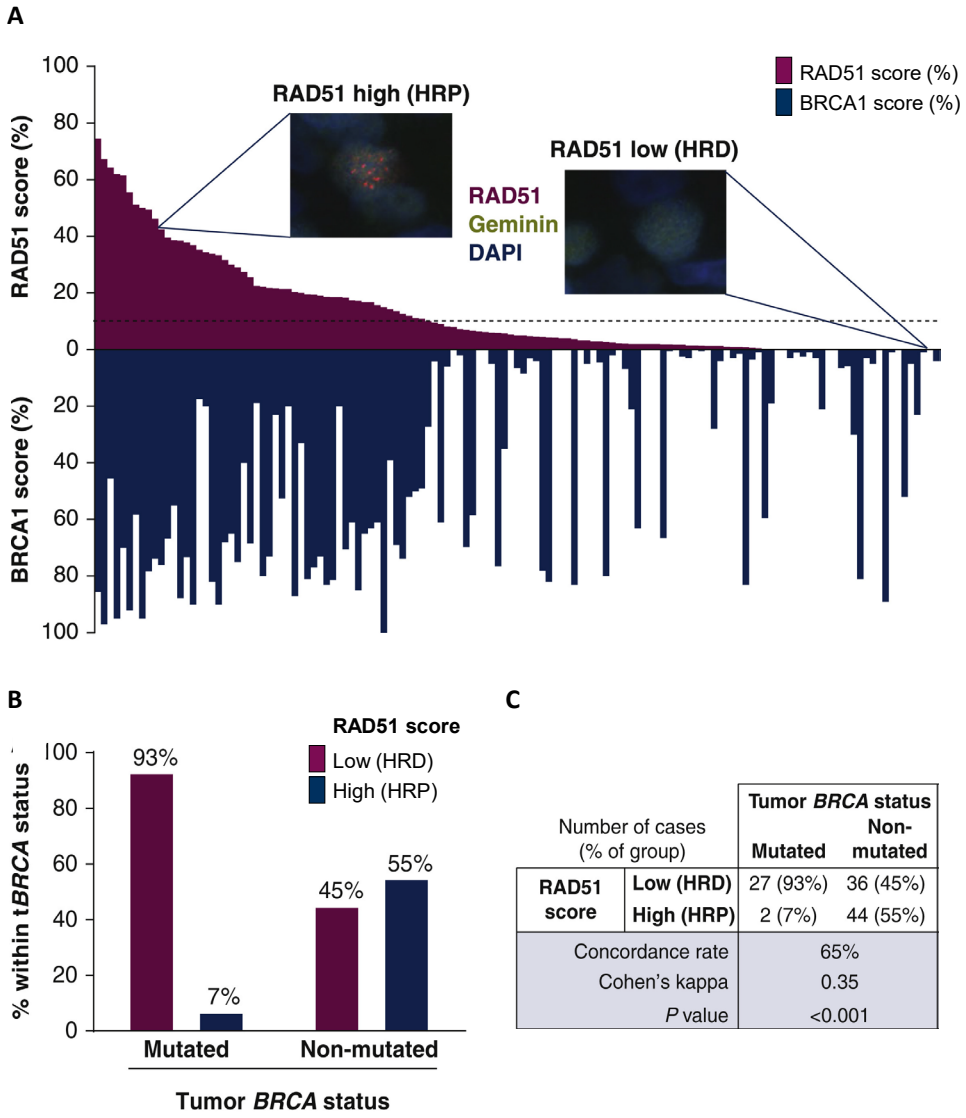
When analysing BRCA1 nuclear foci in this cohort, we observed that 10/17 (59%) tumours with low RAD51 levels presented also low BRCA1 scores. Out

of these, 2 patients had genetic and 7 had epigenetic alterations in *BRCA1,* which may explain the observed BRCA1 levels. Two RAD51-low tumours with a genetic and an epigenetic alteration in BRCA1, respectively, showed high BRCA1 foci levels, together with two additional tumours with a *BRCA2* and a *PALB2* mutation, respectively. It is noteworthy that there were three RAD51-low tumours with no alterations found in the HRR pathway, one of them accompanied by low BRCA1 score (**Figure 41**)[142].

Regarding the GeparSixto trial, 259 TNBC tumour samples laid on tissue microarrays (TMAs) were considered for biomarker analyses. Fifty-nine cases were excluded due to absence/insufficient tumour cells. It is worth noting that RAD51, BRCA1 and γ-H2AX nuclear foci were successfully scored in 133 out of 200 cores (67%). The γ-H2AX score was found to be high in all tumours[78]. Functional HRD by RAD51 was found in 81/133 tumours (61%, **Figure 42A**). Additionally, the BRCA1 score was low in 43% of tumours, all of which exhibited low RAD51 values.

RAD51 identified as HRD 93% of *BRCA1/2*-mutated tumours and 45% of *BRCA1/2*-WT tumours, which could be attributed to mutations in other genes or epigenetic alterations in *BRCA1* (**Figure 42B** and **C**)[78].

Collectively, these findings suggest that, although inferior to the one observed in carriers of HRR-related gene mutations (91-95%), there is a high prevalence of HRD by RAD51 among unselected primary untreated TNBC patients (57-61%,**Figure 40**).



C

Number of cases (% of group)		Tumor *BRCA* status: Mutated	Tumor *BRCA* status: Non-mutated
RAD51 score	Low (HRD)	27 (93%)	36 (45%)
	High (HRP)	2 (7%)	44 (55%)
Concordance rate		65%	
Cohen's kappa		0.35	
P value		<0.001	

Figure 42. Analysis of homologous recombination deficiency (HRD) in TMA preparations biomarkers by immunofluorescence (IF) of untreated triple-negative breast cancer (TNBC) patients from de GeparSixto trial.

A. The percentages of geminin+ tumour cells with RAD51 (upper blue bars) and BRCA1 (bottom green bars) nuclear foci in 133 samples are shown. Insert images depict representative geminin+ cells with and without RAD51 foci. Dashed line indicates the test cut-off (low RAD51≤10%). **B.** Association of the RAD51 score with *BRCA1/2* status. Bars represent the percentage of cases in each indicated group. A logistic regression model was performed in panel B. **C.** Summary table with the numbers of individual cases (and percentage within each

column group) as well as statistics showing the concordance between RAD51 and *BRCA1/2* status. A Cohen's kappa coefficient was calculated in panel C. Abbreviations: HRD: homologous recombination deficiency; HRP: homologous recombination proficiency. Adapted from *Llop-Guevara et al.,*[78]

HRD in unselected non-TNBC patients[143]

Although genetic aberrations associated with HRD have been identified in non-TNBC[196-201], the prevalence of HRD in this context remains to be elucidated. Then, we aimed to explore the prevalence of HRD by RAD51 in the non-TNBC cohort of patients from HUVH and those enrolled in the PETREMAC trial (**Figure 16**)[143].

In the HUVH non-TNBC cohort (n = 59), 4 tumours showed low levels of RAD51, resulting in a HRD prevalence of 7% (**Figure 40**). Regarding the PETREMAC cohort, out of the 201 tumours collected (32 TN and 169 non-TNBC), RAD51 was analysed in 100 samples (30 previously analysed TN and 70 non-TNBC). However, 12 non-TNBC tumours were not evaluable due to the low number of geminin+ cells or low levels of γ-H2AX. We observed that only 4/58 (7%) had low RAD51 levels, whereas 54/58 (92%) presented high RAD51 levels (**Figure 40** and **Supplementary Table 12**), being consistent with what was observed in the HUVH cohort.

When applying the HRD definitions established in the PETREMAC study (wide and strict HRD, HRD-W and HRD-S, respectively, see Materials and Methods), we found a 23% prevalence (39/169) of HRD-W in the non-TNBC subgroup, being this prevalence higher than the one captured by the RAD51 test. Of these, 25 had HRR mutations and five had *BRCA1* promoter hypermethylation[143]. Using the stricter definition (HRD-S), 5% (9/169) were classified as HRD. Among them, we found two tumours with *BRCA1*, two with *BRCA2* and one with *PALB2* mutations. Additionally, 4 revealed *BRCA1* promoter hypermethylation (**Supplementary Table 11**). In the case of HRD-S, the prevalence captured was similar to the one found by the RAD51 assay,

suggesting a weak role of most of the genes included in the wider HRD definition in the HRR pathway[143].

Taken together, the HRD data from the PETREMAC trial in TN and non-TNBC indicate that the concordance between HRD-S and functional HRD status by RAD51 low was 95.5%, with sensitivity, specificity and positive predictive value of 0.94, 0.96 and 0.85, respectively.

In conclusion, these data demonstrate the feasibility of the RAD51 assay in untreated FFPE samples from BC patients. The prevalence of HRD within the primary setting captured by the RAD51 assay varies by context, being over 90% in tumours from HRR-related gene mutation carriers and decreasing in unselected TNBC and non-TNBC (**Figure 40**).

Predictive value of the RAD51 assay in unselected primary TNBC patients: PETREMAC and GeparSixto clinical trials

Having established the prevalence of HRD in different BC subtypes within the primary setting, we aimed to investigate the predictive value of the RAD51 test to response to DNA-damaging agents. To do so, we used the same cohorts of patients from the PETREMAC (olaparib) and GeparSixto (carboplatin) trials[78,142].

We observed that tumours with low RAD51 scores showed a better response to treatment with olaparib, as measured by the percentage change in tumour on magnetic resonance imaging (MRI), than tumours with high RAD51 levels (median of -49% vs. -8%, respectively, $p<0.0001$; **Figure 43A**). These results suggest that primary BC tumours with HRD by RAD51 may benefit from the addition of PARPi to their neoadjuvant treatment.

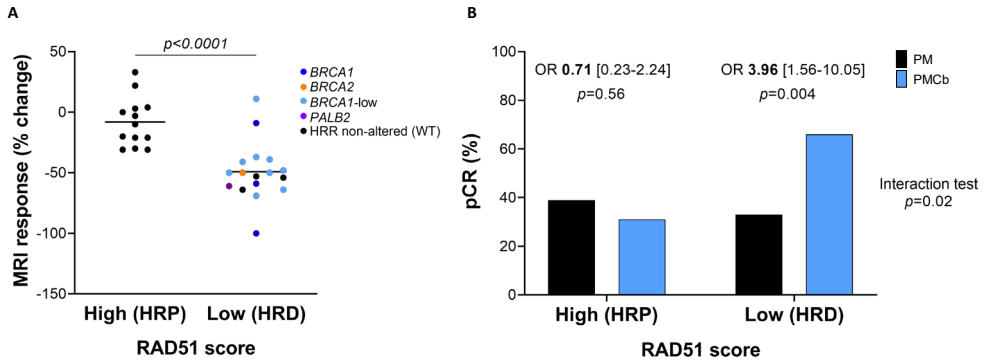


Figure 43. Association of the RAD51 score with clinical outcomes.

A. Response to olaparib measured as percentage of change of MRI response according to RAD51 scores in untreated TNBC patients from the PETREMAC trial (n = 30). An unpaired t-test was applied in panel A. **B.** Response to paclitaxel plus Myocet-nonpegylated liposomal doxorubicin (PM, n = 52) or PM plus carboplatin (PMCb, n = 81) according to RAD51 scores in untreated TNBC patients from the GeparSixto trial. A logistic regression model (interation test) was applied in panel B. *P*-values are shown. Abbreviations: HRP: homologous recombination proficiency; HRD: homologous recombination deficiency; WT: wild-type; OR: odd ration; Cb: carboplatin. Adapted from *Eikesdal et al.,*[142] and *Llop-Guevara et al.,*[78], respectively.

For platinum-based chemotherapy, pathological complete response (pCR) in patients with RAD51-high tumours was similar between the two treatment arms in the GeparSixto trial (paclitaxel plus myocet-nonpegylated liposomal doxorubicin plus carboplatin, PMCb 31% vs. PM 39%, OR=0.71, 95% CI 0.23-2.24, p=0.56; **Figure 43B**). In contrast, patients with RAD51-low tumours benefited significantly from PMCb (pCR PMCb 66% vs. PM 33%, OR=3.96, 95% CI 1.56-10.05, p=0.004). Thus, the RAD51 test was able to significantly discriminate tumours sensitive to carboplatin (interaction test, p=0.02).

In conclusion, these studies support the clinical validity of the RAD51 assay as a functional HRD test and a predictive biomarker of response to DNA-damaging agents in untreated primary TNBC.

Inter-laboratory analytical validation of the RAD51 test: RING trial150

The strong clinical validity of RAD51 as an HRD biomarker has already been established by several European laboratories[78,99,100,142,151,152,202]. However, the robustness and reproducibility of the RAD51 assay when applied in different research laboratories has not been explored. Therefore, we wanted to investigate the effect of local analytical variation on RAD51 test results and the interobserver variability through an international exchange of high-grade serous ovarian cancer (HGSOC) samples[150]. The study consisted of two phases: the training and the testing phases (see Materials and Methods).

Training phase

Our first objective was to evaluate the robustness of the RAD51 assay by analysing the influence of local protocol differences on the final test results. The first quality control step of the RAD51 assay, γ-H2AX/geminin co-staining, was performed in two laboratories using different techniques: immunohistochemistry (IHC) and IF (**Supplementary Figure 21A** and **B**). The median range of γ-H2AX scores between the two centres was 8% (Q1: 4%, Q3: 21%, **Supplementary Figure 21C**), indicating a high concordance.

Next, we investigated the effect of local staining protocol differences on the RAD51 scores. The fact that all HGSOC samples were stained according to the central but also each local staining protocol allowed for a side-by-side comparison. At the case level, the median difference in RAD51 scores between locally and centrally stained sections was 5% (Q1: 1%, Q3: 9.5%), demonstrating that local protocol differences were trivial and did not affect the RAD51 scores.

In the initial training phase, interobserver variability was assessed using centrally stained sections. **Figure 44A** illustrates the RAD51 scores of all four observers per training cohort case, ranked from highest (25%) to lowest (0%)

interobserver variability in RAD51 scores. The median interobserver variability in RAD51 scores was 13.5% (Q1: 9%, Q3: 19%).

In 6 out of 12 cases, ≥ 3 observers noted complicating features, including weak geminin (case ID #6) or high RAD51 signal-to-noise ratio (case IDs #2 and #11; **Figure 44A**).

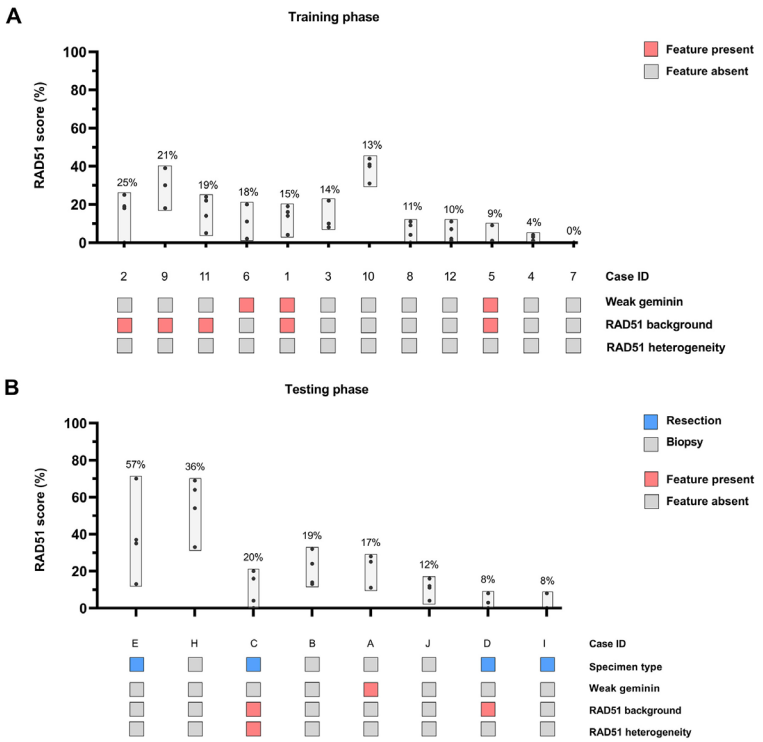


Figure 44. RAD51 scores of individual observers per A. training phase and B. testing phase cases, sorted from largest to smallest RAD51.
Box plots indicate the variability of RAD51 score across observers. Case ID and staining features in RAD51 scores are shown below the graphs. The presence or absence of weak geminin, RAD51 background or RAD51 heterogeneity is described if it was reported by at least three of the four observers. Taken from *Kramer et al.,*[150].

An on-site evaluation meeting was then organised to re-evaluate cases from the training cohort to identify features that may underlie the observed RAD51 scoring variability. Technical and biological features, such as weak geminin expression, high RAD51 signal-to-noise ratio, and RAD51 heterogeneity,

were defined as potential difficulties to score RAD51 and were incorporated into a refined RAD51 scoring form (**Supplementary Figure 22**).

Testing phase

In the testing phase, the RAD51 assay was performed on an independent cohort of HGSOC samples enriched for biopsy specimens to gain insight into the effect of tumour tissue size on RAD51 scores. As the training phase demonstrated that local staining protocol differences did not affect the final RAD51 scores, HGSOC sections from the testing cohort were only stained centrally, and stained sections were circulated among academic laboratories.

Two HGSOC cases (case IDs F and G) were non-evaluable based on low γ-H2AX scores by ≥ 3 observers and were excluded from further analyses. Regarding RAD51 scoring, the median range of RAD51 scoring variability was 18% (Q1: 9%, Q3: 32%; **Figure 44B**). In three cases (case IDs C, A, and D), previously defined complicating features appeared to affect scoring accuracy, although RAD51 variability was not higher in cases with (median: 17%) compared to those without quality issues (median: 19%). Finally, RAD51 scoring variability was not higher in large resection specimens (median: 14%) than in smaller biopsy specimens (median: 18%), indicating that variability was not explained by HGSOC tissue size.

Thus, these results suggest that the subtle differences in staining procedures resulted in low variability in RAD51 and γ-H2AX scores, demonstrating the robustness of these biomarkers[150].

In conclusion, in the third part of this thesis we showed that the RAD51 test is a useful tool to establish the HRD prevalence in different scenarios of the primary setting, which might contribute to the accurate selection of patients who may benefit from DNA-damaging agents-based regimes. In line, we demonstrated that RAD51 is a robust predictive biomarker of response to PARPi or carboplatin in the neoadjuvant setting. Finally, we proved that it is

a feasible assay that can successfully be performed across different laboratories with minimum impact in the results.

DISCUSSION

Cancer represents the leading cause of death and a major obstacle to increasing life expectancy worldwide[61]. Traditionally, conventional chemotherapy has been barely the only strategy to combat this aggressive disease, leading to low success and high mortality rates. In the recent years, however, the concept of personalised medicine has been introduced. In particular, the shift from traditional therapies to more targeted strategies, selected according to tumour characteristics, together with high-quality prevention and early detection, have accelerated the decline in breast cancer mortality. Accordingly, treatment decisions are made based on the precise molecular changes in the tumour, using these specific characteristics to attack it by using targeted therapies.

The use of Poly(ADP)-ribose polymerase 1 and 2 inhibitors (PARPi) in homologous recombination (HR)-deficient tumours is one of the best examples of a targeted therapy that has been successfully translated into the clinic[91]. Based on the phenomenon of synthetic lethality, PARPi have emerged as a promising strategy, approved to treat patients including those with germline *BRCA1 or BRCA2* mutations (g*BRCA1/2*), by inducing DNA damage and further genomic instability that these tumours are unable to repair, leading to tumour cell death[59,60]. However, despite their success, there is a need to i) expand the population to include patients with alterations in other HR repair (HRR) pathway-related genes beyond *BRCA1/2*, such as *PALB2*, and ii) refine patient selection and improve clinical efficacy, as the emergence of resistance in g*BRCA1/2*-mutated tumours remains a clinical hurdle.

Diagnostic tests have been developed to better identify cancers that present HR deficiency (HRD) and, therefore, that are more likely to be sensitive to PARPi and other DNA-damaging agents, such as platinum-based chemotherapy. These HRD tests are based on the detection of i) mutations in HRR-related genes, ii) genomic scars or mutational signatures that are accumulated in cancers with HRD independent of the underlying defect and

iii) functional assays with the potential to provide a real-time readout of the HRD status. Notably, the HRD status has been shown to be dynamic, as tumours have the ability to restore the HRR pathway functionality through multiple mechanisms. Concordantly, HRD tests with a static nature, such as DNA-based tests, fail to provide an accurate functional status of the HRR pathway and cannot identify tumours that may or may not benefit from treatment with DNA-damaging agents.

Our laboratory has developed the RAD51 assay, an immunofluorescence-based HRD test in which the detection of RAD51 nuclear foci as a key downstream effector of HRR determines the pathway functionality and, consequently, sensitivity to DNA-damaging agents[99,100].

In the **first part** of this thesis, we validated the predictive value of the RAD51 test for response to first-generation PARP1/2i and platinum-based chemotherapies in preclinical mouse models that recapitulate patient characteristics, HRD status and response to therapy. We employed a panel of more than one hundred patient-derived xenografts (PDXs) from the four canonical HRD-related cancers: breast cancer (n = 103), high-grade serous ovarian cancer (n = 4) and pancreatic cancer (n = 2, **Figure 19**).

The first-generation PARPi olaparib is approved for metastatic and primary breast cancer patients with g*BRCA1/2* pathogenic variants together with talazoparib, which is approved only in the metastatic setting. Nevertheless, the overall response rate is in the range of 60%[76,77]. Consistently, while 45% of the models in the cohort had a mutation in *BRCA1/2* or *PALB2*, and 59% had HRD due to genomic scars, only 45% and 50% of them were sensitive to PARPi, respectively (**Figure 20** and **Table 4**). As expected, PARPi-sensitive PDXs were often obtained from treatment-naïve primary lesions that had not been under selective pressure. In contrast, the high proportion of PARPi resistance observed among HRR-altered models may be explained by the fact that most of them were collected from metastatic patients who had

received prior lines of DNA damaging treatment (**Supplementary Figure 1D**, **Supplementary Table 2**). The selective pressure to which these tumours had been exposed may have led to the expansion of resistant subclones. Taken together, these data highlight the unmet medical need to optimise the use of DNA-damaging agents and, therefore, to identify biomarkers of response beyond DNA. Remarkably, the RAD51 test demonstrated a higher positive predictive value compared to genetic and genomic HRD tests (PPV, 93% vs. 43% vs. 50%, respectively), suggesting a better ability to identify PARPi-sensitive tumours. In addition, RAD51 was also able to identify tumours that become PARPi-resistant after restoration of HRR functionality (**Table 5**). Alike genomic HRD tests, RAD51 identified HRD in tumours with likely epigenetic silencing of *BRCA1*, as evidenced by concomitant low *BRCA1* mRNA expression or low BRCA1 nuclear foci (**Figure 22C**).

The lack of PPV of DNA-based tests lies upon the heterogeneity of the HRD nature. Also, they cannot distinguish between HRR restoration or genomic instability arising from other sources that do not affect the HRR pathway, such as prior treatment with other therapies inducing DNA damage, like CDK4/6 inhibitors[203]. This scenario or the presence of unknown non-canonical HRR alterations might explain the case of the HRR-WT, PARPi-resistant tumours that we found to be HRD-positive based on the genomic HRD score by Myriad myChoice® (**Figure 22A**). In contrast, a dynamic functional biomarker like RAD51 can capture this heterogeneity and dynamism, as shown in paired models with acquired resistance to PARPi (**Supplementary Figure 3B**). The discordance between genomic HRD tests and RAD51 foci is observed in half of the PDXs, particularly in models harbouring *BRCA1* epigenetic silencing, likely reflecting the “soft” status of the phenotype (**Figure 22A**). This observation is in line with the TBCRC009 and TNT trials for platinum [204,205]. In addition, given that we discarded that *BRCA1*-mutated, PARPi-resistant tumours with high HRD scores were derived from metastatic and/or

previously treated patients, protein-based intrinsic resistance mechanisms may explain their phenotype.

It is well known that *BRCA1* is the most frequently mutated gene among patients diagnosed with HBOC syndrome[56]. Additionally, *BRCA1* epigenetic silencing has been described as a common phenomenon among patients with sporadic triple negative breast cancer (TNBC), being present in up to 60% of them[195]. On the other hand, resistance to PARPi due to the restoration of BRCA1 functionality, but also through BRCA1-independent mechanisms, has been described in *BRCA1*-altered tumours. Therefore, due to this dynamism, there is a clear need to find ways to characterise and monitor BRCA1 status along the progression of the disease, mainly to find therapeutic approaches according to tumour vulnerabilities. Thus, we established the percentage of tumour cells in the S/G2 phases (geminin+) harbouring the BRCA1 nuclear foci (BRCA1-positive, BRCA1+) required to exhibit a functional HR by immunofluorescence (IF) in a homogeneous cohort of untreated primary tumours so that we got rid of the complexity driven by metastasis under the selective pressure of treatment with DNA-damaging agents. We found that all tumours with HR-proficiency (HRP) by RAD51 exhibited more than 10% BRCA1+ cells. In contrast, HR-deficient tumours showed more heterogeneous results (**Figure 38A**). This could be explained by the fact that several mechanisms beyond *BRCA1* alterations may explain HRD. For instance, we found that tumours with pathogenic alterations in other HRR-related genes leading to a HRD phenotype, such as mutations in *BRCA2* or *PALB2*, were able to form high levels of BRCA1 foci, even more than HRR-WT tumours, likely to compensate for the absence of the altered protein. Therefore, from these data, we established that tumours with low BRCA1 foci levels (≤10%) may be HRD, while those with high BRCA1 levels (>10%) may be HRP or harbour alterations in other HRR-related genes. In line with this, a major limitation of this study is that the *BRCA* status of the tumours in which we established the cut-off is unknown. Therefore, we cannot determine the

reason behind the BRCA1 score of each RAD51-low tumour (**Figure 38A**). When we moved from clinical to preclinical samples, we observed that the BRCA1 10% cut-off recapitulated all these possibilities in our PDX models and, in addition, identified RAD51-high tumours with low levels of BRCA1, likely due to a BRCA1-independent restoration of the HRR functionality (**Figure 38B**). Further study and validations are needed in well characterised cohorts of tumours to confirm this cut-off.

Together with the established BRCA1 foci cut-off, RAD51 also helped to identify mechanisms of resistance and determine their dependence on the HRR functionality. In this way, we identified the potential mechanism of resistance in half of the PARPi-resistant models, encompassing the restoration of HRR-gene function in 21% (**Figure 21C**). Although reversion mutations restoring the open reading frame of *BRCA1/2* have been observed as a recurrent mechanism to restore HRR function and lead to PARPi resistance in the clinic[206], restoration of BRCA1 functionality by the presence of hypomorphic protein or loss of promoter hypermethylation were the most common mechanism in the cohort (10% and 6%, respectively). Nevertheless, our results recapitulated previous data supporting that reversion mutations are more prevalent in *BRCA2*-mutated tumours[178], as the reversions that we observed happened in this gene. In addition, end resection recovery mediated by the 53BP1 pathway was present in 7% of the models, and RAD51-independent mechanisms in 4%. Regarding the latter, we suspect that replication fork protection, which is mediated by HRR-related proteins such as BRCA1 and BRCA2, is a plausible mechanism of resistance, as tumours exhibited intermediate levels of both RAD51 and BRCA1 nuclear foci in the PARPi-sensitive and -resistant counterparts (**Supplementary Table 1**). Still, and although RAD51 may help to narrow down the possibilities, RAD51-independent mechanisms of PARPi resistance represent a limitation to the accuracy of the RAD51 test. As an example, increased PARP trapping causes PARPi toxicity irrespective of HRD, such as in tumours with impaired

ribonucleotide or base excision repair due to defects in *RNaseH2* or *XRCC1*, respectively[207,208]. Impairment of enzymes involved in other base damage repair pathways, such as the loss of *ALC1* nucleosome remodelling, also confers PARP1 sensitivity[209]. The clinical relevance of these mechanisms is yet to be established. In 26% of the PDXs in the cohort, the mechanism of resistance to PARPi was not revealed by WES, but it was consistent with restoration of HRR by RAD51 nuclear foci formation. Accordingly, although we were able to characterise *BRCA1*-related resistance mechanisms using several approaches, but mainly by IF, a major obstacle to reducing the proportion of tumours with an unknown mechanism of resistance in the cohort was the study of BRCA2. In fact, DNA-sequencing is still the only strategy to study *BRCA2* today due to the lack of efficient tools to assess the presence of functional protein. Therefore, further research is needed to find strategies to efficiently detect BRCA2 hypomorphic protein and, along with RAD51 levels, to help identifying other HRR-dependent, but also -independent resistance mechanisms in which BRCA2 plays an essential role, such as the replication fork protection.

Interestingly, regarding platinum response and breast cancer, and despite cisplatin sensitivity may occur beyond HRD[210], our preclinical data showed that the RAD51 assay may help select patients who will benefit from this treatment, thus providing a “targeted” therapy option for g*BRCA1/2* WT patients, as it showed similar accuracy to HRR-related gene mutations (64% vs. 61%; **Table 6**).

Finally, we demonstrated that the RAD51 test is not only feasible in invasive breast cancer, but also in earlier stages of the disease, such as in pre-malignant ductal carcinoma *in situ* (**Figure 25**). These data, together with the safe profile of PARPi, may contribute to establish PARPi-based preventive treatment in these patients, as defects in the HRR pathway may be the drivers of the invasive lesion.

In summary, a functional test like RAD51 offers an improved performance to predict response to DNA-damaging agents, as it captures the different sources of HRD and their dynamic evolution. The test is also useful for understanding the mechanisms leading to the emergence of resistance, which is a key aspect for the rational design of subsequent therapies. In the context of metastatic breast cancer patients with known germline conditions, in which PARPi are approved, a functional test that measures the tumour HRD status prior to treatment initiation would likely improve patient selection for PARPi monotherapy. This would optimise the prescription of effective drugs to patients whose tumours have restored HRR.

Having validated a test to predict response to PARPi, as well as to identify the mechanisms of resistance, our next goal was to evaluate the performance of other therapeutic options to overcome first-generation PARPi resistance. Therefore, in the **second part** of the thesis, we evaluated the antitumour activity of i) the more potent selective new-generation PARP1 inhibitor (PARP1i) AZD5305 and ii) combinations of PARPi with other DNA-damaging agents selected to target acquired vulnerabilities of the tumours resistant to the single agents. Accordingly, we observed patterns of response among specific tumours and, therefore, we further associated the lack of specific *BRCA1* domains with specific mechanisms of resistance and sensitivity to other DNA-damaging agents.

AZD5305 (recently named saruparib) is a potent and highly selective PARP1 inhibitor and trapper[117] that has previously been shown to have greater target engagement and antiproliferative activity than first-generation PARP1/2i in cells with HRD[118]. Consistently, we demonstrated that AZD5305 elicits more potent and durable antitumour activity *in vivo* than olaparib across a panel of *BRCA1/2*- and *PALB2*-mutated PDXs. Specifically, AZD5305 showed superior activity to olaparib in tumours with intermediate HRR capacity (PDX179 and PDX341, **Figure 26A**). We reasoned that residual HRR is sufficient to limit responses to olaparib but may be overwhelmed by the

greater PARP1 trapping and DNA-damaging properties of AZD5305, leading to responses. It is interesting to note that, in the phase I/IIa PETRA trial (NCT04644068), preliminary results have been reported and antitumour activity was observed in both PARPi-naïve patients and patients who had received prior PARP1/2i-containing treatment but not necessarily progressed on PARPi[119]. In addition, we also confirmed that AZD5305-sensitive models show lower levels of RAD51 than the resistant ones and that enhancement of HRR functionality is ubiquitous in models of acquired resistance. However, our study suggests that AZD5305 as single agent does not exhibit antitumour activity in preclinical models of acquired resistance to the first-generation PARP1/2i olaparib or talazoparib, where resistance involved restoration of HRR. However, Another interesting aspect of our results is the observation that treatment with AZD5305 delivers a higher complete response rate and longer-term responses as single agent than olaparib (**Figure 26B**). This would be potentially relevant in the advanced and early breast cancer setting, where *BRCA1/2* carriers could potentially gain further overall survival benefit, as has already been demonstrated for olaparib[86].

Mechanistically, AZD5305 induces DNA damage and elicits a replication stress response along with an increase in markers of genomic instability, as measured by the induction of γ-H2AX, pRPA and DNA-containing micronuclei, respectively (**Figure 32**). This is consistent with cell line data showing selective and more potent PARP1 trapping in the low nanomolar range of AZD5305, compared to olaparib[118]. We acknowledge that the acute measurements obtained from the short-term pharmacodynamic experiments conducted in the PDXs may not fully capture all the longer-term effects of AZD5305 on DNA that may translate into the observed preclinical benefit. In addition, the accumulation of genomic instability produced by treatment with DNA-damaging agents such as PARPi results in the activation of the STING pathway, promoting an innate immune response[211]. However, the effects on the immune response may not be fully reproduced in these short-term

experiments. Further research is needed to characterise the antitumour immune response elicited by treatment with AZD5305 in syngeneic mouse models and human samples.

Notably, acquired resistance to PARP1 selective inhibition occurs in a smaller fraction of tumours compared to PARP1/2 inhibition (**Figure 27**). In contrast to our previous work[98], we identified two putative HRR-independent mechanisms of resistance, namely upregulation of efflux pumps encoded by the *ABCB1* gene in two and downregulation of the compound's target *PARP1* in one AZD5305-progressing tumour (**Supplementary Figure 13**). This raises the question of whether PARPi that selectively target PARP1 and that have an enhanced ability to trap it on the DNA may more frequently lead to mechanisms of resistance beyond restoration of HRR, also considering that other molecular pathways may be involved in attenuating their antitumour activity. In addition, we identified the presence of mechanisms of PARPi resistance that restore HRR functionality, including hypomorphic BRCA1/2 and loss of 53BP1 pathway components, all being captured with the RAD51 foci assay **(Figure 28A** and **D**). While 10% of acquired resistance to olaparib was due to reversion mutations (specifically, in PDX474.2 and PDX124), none were observed upon progression to AZD5305, likely due to the relatively small sample size used in this study (**Figure 28D**). However, our preclinical data suggest that models harbouring baseline reversion mutations are intrinsically resistant to AZD5305 (**Figure 26A**). This fact is of critical importance since we speculate that *BRCA1/2* reversion mutations may become more prevalent in breast cancer patients in the near future based on the current treatment regimens that include platinum in the early setting and the observation of a relatively high frequency of reversion mutations in patients receiving platinum[212]. To our knowledge, this is the first study that describes mechanisms of resistance to the next-generation PARP1i AZD5305 and, in particular, that mentions HRR-independent pathways. Accordingly, further research with larger sample sizes is needed to confirm

these data and to determine whether RAD51 alone may predict response to AZD5305.

PARP1 selective inhibitors are expected to differ from first-generation PARP1/2 inhibitors (PARP1/2i) in several aspects: i) it would be desirable that they lead to improved clinical response by overcoming resistance to former drugs by providing a wider therapeutic window, and ii) they offer the opportunity to be more easily combined with other DNA damaging agents to overcome drug resistance.

Interestingly, it has been described that a large proportion of reversion mutations in the context of HRD is likely to be mediated by MMEJ repair[125,206]. Consistently, our data showed that most of reversion mutations acquired upon olaparib treatment exhibited MMEJ signatures (**Figure 29B**). In addition, we speculate that the emergence of mutations in the 53BP1 complex in *BRCA1*-altered tumours, another common mechanism of resistance to PARPi, might also be the result of an increased usage of MMEJ. Importantly, inhibitors of the MMEJ-related polymerase theta (POLθ inhibitors, POLθi) have recently been developed. The use of these compounds in combination with AZD5305 might prevent or delay the emergence of genetic-based mechanisms of resistance and, therefore, palliate a large proportion of DNA-damaging agents-progressing tumours. Unfortunately, we were not able to evaluate the performance of this combination in the *BRCA2*-mutated PDX474.2, one of the PARPi-sensitive PDXs known to generate MMEJ-based reversion mutations upon continuous treatment (**Figure 29B** and **Supplementary Table 5**). Unexpectedly, when we analysed the emergence of progressions following treatment with AZD5305 alone or in combination with POLθi in the *BRCA1*-mutated PDX124, another model known to generate 53BP1-related progressions and MMEJ-based reversion mutations, we observed no differences in progression rate and time to progression between the two treatment arms (**Table 7**). Although we do not yet have the results of the DNA and RNA sequencing of these tumours, we propose two

possibilities to explain these results. Firstly, resistance to AZD5305 alone might be the result of mechanisms such as the occurrence of reversion mutations and/or 53BP1 alterations following MMEJ usage, while progressions to the combination might be explained by other mechanisms beyond those, as the MMEJ is inhibited. Secondly, if we confirm the presence of MMEJ-mediated resistance mechanisms in tumours that progress to the combination, we expect that there must be other DNA repair pathways besides MMEJ that generate them. Additionally, we did not find an increased mutational rate in tumours with high prevalence of reversion mutations, probably because single nucleotide variants (SNVs) are not considered direct microhomology signatures and, therefore, are not a good MMEJ reporter, as this pathway is known to generate larger rearrangements (**Figure 29A**). In the case of PDX179 (*BRCA1*-mutated), in which we observed 50% and 75% of tumours progressing to AZD5305 by unknown mechanisms in two different experiments, the combination of AZD5305 with POLθi prevented the emergence of progression in 5/8 tumours (63%). The same was observed in PDX127 (*BRCA1*-mutated), in which none of the tumours treated with the combination (0/4) relapsed (**Table 7**). It will be of great interest to perform further long-term *in vivo* experiments to elucidate whether POLθ inhibition might lead to more durable responses in tumours known to be frequent users of the MMEJ repair pathway and to further assess the emergence of progressions. Sequencing of new progressive tumours to both AZD5305 alone and in combination with POLθi will allow us to assess the proportion of relapses arising from *BRCA1* reversion mutations and whether they present microhomology signatures[125]. These data will help to better understand the mechanisms that lead, not only to acquired resistance to AZD5305 and its combination with POLθi, but also to the emergence of reversion mutations beyond MMEJ and, therefore, to explore new mechanisms and therapeutic options for them.

In terms of antitumour activity, the combination of AZD5305 plus POLθi rescued two models with intrinsic resistance to PARPi (PDX127 and PDX583.2). In PDX127, we found a recurrent sensitivity to DNA-damaging agents. The most plausible reason is the dysregulation of the 53BP1/end resection pathway and the resulting partially functional HRR pathway (**Supplementary Table 1**)[187,213]. Therefore, the use of alternative error-prone DNA repair pathways which, ultimately, may not faithfully repair DNA damage, may be essential for the survival of this tumour. Specifically, it has been described that treatment of tumours exhibiting partial HRR functionality with POLθi leads to toxic RAD51, as POLθ is responsible of preventing excessive resection and subsequent RAD51 accumulation[187]. Consistently, this event can be easily analysed in PDX127 by measuring the size and the duration of the RAD51 nuclear foci it exhibits under POLθi treatment.

Similarly, PDX127 also showed sensitivity to combinations of PARPi with inhibitors of the NHEJ key protein DNA-PK (DNA-PKi), with 2/7 tumours progressing on treatment (**Figure 35A**). Consistent with this, the combination of olaparib with DNA-PKi rescued five additional models that were resistant to the single agents, significantly increasing the mean pPFS, which was not even achieved at the end of the study (> 290 days, **Figure 35E**). When analysing the HRR pathway functionality, we observed that all PDXs resistant to the combination showed high RAD51 levels, as expected, since these models may rely on this error-free mechanism to repair DNA damage (**Figure 35B**). In a putative scenario of tumours with HRD but resistant to the combination of PARPi plus DNA-PKi, it would be useful to know whether they are sensitive to the combination with POLθi, as they may rely on the MMEJ to repair DSBs. In contrast, we observed that tumours that were sensitive to the DNA-PKi plus AZD5305 combination had both low, as expected, and high levels of RAD51. However, in this context, one might expect tumours harbouring a defective HRR pathway and, therefore, with a high reliability on the NHEJ for repair. The fact that we observe both RAD51-low and -high

tumours requires further research, but we hypothesise that these RAD51-high models might be, at least in part, i) arrested in G1, when the NHEJ is functional, ii) in a state of senescence, in which repairing is stopped or iii) harbouring high levels of replication stress, the elimination of which has been described to be DNA-PK-dependent[214].

It will be interesting to further evaluate the antitumour activity of PARPi plus DNA-PKi in tumours with intermediate levels of RAD51 to see to what extent they trust in alternative DSB repair pathways, as it was seen before that they appeared to be sensitive to inhibition of POLθ plus AZD5305 (**Figure 34A**). The triple combination of PARPi plus POLθi and DNA-PKi may be considered as an option if toxicity permits[215].

We further showed that the addition of carboplatin or an ATR inhibitor (ATRi) overcomes PARPi resistance. Specifically, we observed CR in two models that exhibited primary resistance and SD upon treatment with AZD5305 alone, namely PDX127 and PDX341, with no tumour regrowth (**Figure 33A** and **Supplementary Figure 15A**). In contrast, models with acquired resistance to first-generation PARPi were prone to re-express BRCA2 variants (PDX474.2OR2 and PDX474.7) and were resistant to AZD5305 plus carboplatin.

Interestingly, the combination of AZD5305 with an ATR inhibitor (ATRi) resulted in complete responses in all models tested, including PDX127 (**Figure 33B**). These results are consistent with previous literature suggesting that tumours with 53BP1 pathway alterations are more susceptible to replication stress inducing agents due to their partial HRR functionality and residual mutational burden[120]. This combination also led to profound responses in one of the models with acquired resistance to talazoparib that was not rescued by the combination of AZD5305 plus carboplatin (PDX474.7). Finally, a CR was achieved upon treatment with the combination in an ovarian cancer model with a mutation in *ATM* (PDX196), described to

lead to ATRi sensitivity[122], compared to the partial response obtained after treatment with AZD5305 alone. Again, no tumour progression was observed, suggesting that combinations of PARPi plus a DNA-damaging agent induce more profound and durable responses, with ATRi being the most promising. Therefore, our data warrant further investigation of this combination in the clinic. It will also be important to go one step further and evaluate the antitumour activity of these combinations in models with acquired resistance to AZD5305. The PETRA trial will provide information on the safety and signs of AZD5305 activity in advanced patients with *BRCA1/2, PALB2* or *RAD51C/D* mutations.

Having evaluated the antitumour activity of DNA-damaging agents in the cohort of PDX models, we noticed that there were certain patterns of response and mechanisms of resistance worth investigating. Accordingly, in 2020, *Pettitt et al.,* and others showed that reversion mutations are more frequent when the original pathogenic mutations are located in certain regions of *BRCA1*, shedding light on the functional importance of the different protein domains in conferring resistance to treatment[125,178]. However, little is known about the behaviour of these mutations with respect to other resistance mechanisms and further susceptibility to other DNA-damaging agents. In this work, we found that, in contrast to tumours with mutations in the exon 11 of *BRCA1*, models lacking the RING or BRCT domains were more likely to be resistant to PARPi (**Figure 36A** and **B**). This demonstrates that, although these conserved domains are essential to prevent tumour development, their absence is rapidly compensated and overcome by other mechanisms to maintain a partially functional HRR pathway, rendering tumours resistance to DNA-damaging agents.

In addition, we showed a correlation between the absence of specific *BRCA1* regions and the development of certain mechanisms of resistance to PARPi, as might be expected given the different uncoupled roles of BRCA1 domains in tumour suppression[16,41]. More specifically, we observed that the resistance

mechanisms developed by tumours with mutations in the RING or the BRCT domains went beyond reversion mutations, one of the most frequent events in the clinic, especially in tumours with mutations in the exon 11[178], the emergence of which often leads to the loss of part of the sequence (**Figure 36A**). This may be explained by the fact that these are very well conserved domains and, therefore, there must be less flexibility in the amino acid changes that can occur in these regions without affecting the BRCA1 function. Accordingly, the only reversion mutation detected in a *BRCA1*-mutated tumour had a pathogenic variant in the exon 11 (progression #3 from PDX124). Several other mechanisms of resistance to PARPi have been described, such as the presence of hypomorphic BRCA1 protein. In our hands, this mechanism was also frequent among exon 11-mutated tumours (75%, **Figure 36A**), partly due to the overexpression of the exon 11 functional splicing variant Δ11q. Interestingly, tumours with mutations in the RING domain have been described to be able to initiate translation downstream of the lesion (at methionine 297, Met297), resulting in a smaller, undamaged peptide[161]. When we analysed BRCA1 nuclear foci with an antibody directed against the RING domain of the protein (amino acid 304), we found that no signal was detected (**Supplementary Table 1**). This might be due to two facts: i) the antibody does not detect a protein starting at Met297 although it is generated, or ii) even with a more downstream initiation of translation, BRCA1 is degraded, as the N-terminal part is essential for the protein to be functional. The second option seems more plausible, as we analysed BRCA1 nuclear foci with an antibody directed against the C-terminal part of the protein and no signal was detected. In contrast, we showed that these tumours harbouring mutations in the RING domain were more likely to become resistant through an alteration in the 53BP1 pathway (**Figure 36A** and **C**). According to what we mentioned earlier, the dysregulation of the 53BP1/end resection pathway might be the only known mechanism derived from an increased usage of MMEJ in which no *BRCA1* sequence is lost. Therefore, we suggest that tumours with mutations in the RING domain might have

increased activity of POLθ and reliability on MMEJ that lead to the emergence of mutations in the 53BP1 pathway. Consistently, sensitivity to the combination of PARPi plus POLθi is expected in these models, and so was observed in the two RING domain-mutated models studied (PDX179 and PDX127, **Figure 34A**). Further research in larger cohorts is needed to corroborate these data and to find an explanation for this potential increased MMEJ activity in tumours with this profile.

It was in the case of models with mutations in the BRCT domain that we observed hypomorphic BRCA1 as the most prevalent mechanism of resistance, probably explained by the fact that mutations at the end of the sequence might more easily lead to a functional protein without losing amino acids (**Figure 36A** and **D**). Indeed, it has been described that BRCT-altered BRCA1 can be stabilised by HSP90, leading to PARPi resistance[108]. Investigating whether this is the mechanism behind the high prevalence of hypomorphic BRCA1 among the BRCT-mutated models would allow us to target it, for example, with HSP90 inhibitors.

As mentioned above, different protein domains of BRCA1 have been shown to play specific roles in preserving genomic instability[216,217], and this may be advantageous in finding therapeutic options by targeting vulnerabilities in each case. For instance, tumours with mutations in the RING domain, which has been shown to have a role in replication fork protection, would be more susceptible to agents inducing replication stress[178]. Consistently, we observed that RING domain-mutated tumours were more sensitive to platinum salts, ATRi and WEE1i (**Figure 36C**). In addition, due to the potentially increased MMEJ activity and consequent dysregulation of the end resection pathway that these tumours often exhibit, their partially functional HRR pathway makes them dependent on MMEJ and NHEJ for repair, leading to POLθi and DNA-PKi sensitivity. Thus, the search for biomarkers that identify tumours with these characteristics, namely mutations in the RING domain itself or other biomarkers that capture the dysregulation of the end

resection pathway as a mechanism of PARPi resistance, is critical for predicting further response to other DNA-damaging agents.

Among BRCT-domain mutated tumours, sensitivity to WEE1i was the most frequent response, which can be explained by the role of this domain in DNA damage repair during replication (**Figure 36D**)[16].

Other novel combinations with PARPi are currently being investigated, such as checkpoint blockade immunotherapy, as PARP inhibition modulates the tumour immune microenvironment by several mechanisms, for instance the formation of neoantigents and the induction of interferon-related genes such as PD-L1. On the other hand, the improved therapeutic index of antibody-drug conjugates (ADCs) makes them an appealing combination partner for PARPi, being those carrying a topoisomerase 1 (TOP1) inhibitor payload the most promising[218]. Indeed, in the PETRA trial, the PARP1i AZD5305 is investigated as monotherapy or in combination with other compounds, such as ADCs. Finally, in *BRCA1/2*-WT preclinical models, co-inhibition of bromodomain and extraterminal (BET) proteins, which regulate HRR gene expression, and PARP led to enhanced antitumour activity. Further efforts will be made to unravel mechanisms of action, biomarkers of response and mechanisms of resistance to these combinations in order to improve clinical outcomes of patients whose tumours are resistant to PARPi alone.

Beyond PARP inhibitors, novel agents acting as dual inhibitors of PARP1 and intracellular molecules (e.g. histone deacetylases, topoisomerases or PI3K pathway effectors), PARP1 degraders based on proteolysis targeting chimera technology and PARP1-targeting prodrugs are under development[218].

Finally, in the **third part** of this thesis, we demonstrated that the RAD51 assay, which included the assessment of RAD51, BRCA1 and γ-H2AX nuclear foci, was a robust predictive biomarker of response to DNA-damaging agents in the clinic. Specifically, the test was able to estimate the prevalence of HRD in several contexts, including the primary setting (carriers of HRR-

related gene mutations, and unselected populations of TN and non-TNBC) and patients with non-invasive lesions such as ductal carcinoma *in situ* (**Figure 37**). Consistently, the test identified patients that may benefit from both PARPi and platinum-based chemotherapy in the early setting[78,142]. As it is well known that PARPi are mostly approved for their use in the metastatic setting, unravelling the HRD prevalence beyond is of critical importance to reveal whether this targeted therapy may be beneficial in other scenarios.

In particular, given the positive safety profile of PARPi and preliminary efficacy data in early breast cancer, it is expected that PARPi will be incorporated as part of the neoadjuvant treatment regimens[219], especially following the approval of olaparib in the adjuvant setting[86]. Accordingly, we have shown that data supporting the use of the RAD51 test as a predictive biomarker of PARPi response in early breast cancer is encouraging[142,173]. In this regard, we started exploring the potential of the RAD51 test to identify HRD tumours in pre-malignant lesions (DCIS) and found that even at this early stage of the disease, tumours with HRR-deficient tumours can be identified (**Figure 39**). HRD prevalence capture pre-clinically was similar to the one observed in clinical samples (23% vs. 18%). As already observed in PDXs, these results demonstrate that DNA damage induced by treatment is not a pre-requisite for scoring RAD51 in pre-malignant lesions.

A similar scenario is expected for early breast cancer patients harbouring germline pathogenic alterations in *BRCA1/2* or *PALB2*, among whom the HRD prevalence is estimated to be over 90% and who are also sensitive to PARPi[198,220]. Efforts are also underway to expand the patient population that may benefit from PARPi beyond those with germline HRR-related gene pathogenic variants. In treatment-naïve, unselected primary TNBC, RAD51 independently predicted clinical benefit from the addition of olaparib or carboplatin to the neoadjuvant regimen[78,142]. Further studies are needed to confirm the clinical validity of the RAD51 assay in predicting long-term

treatment benefit and to verify if the test can predict response to treatments with similar mechanisms of action.

Functional biomarkers of HRD are also needed for the management of tumour types beyond TNBC, such as other BC subtypes, high-grade serous ovarian cancer (HGSOC), prostate cancer or pancreatic cancer (PaC). Despite quality of tumour genetic testing and interpretation of variants' effect have greatly improved in recent years, there is still a scarcity of implementation of tumour genetic testing beyond the ovarian cancer population. Platinum salts still remind the standard treatment for HGSOC patients. Consistent with what was previously explained for breast cancer, it has been recently published that the RAD51 test robustly predicts platinum chemotherapy response and survival in HGSOC[152,174]. Regarding platinum-sensitive HGSOC, PARPi have been approved as first- and second-line maintenance therapy[221,222]. Recently, the European Medicines Agency (EMA) approved olaparib in combination with bevacizumab (an anti-VEGF monoclonal antibody) as first-line therapy in patients with HRD-positive platinum-sensitive HGSOC, using an HRD diagnostic test with proven clinical validity[223]. This setting provides an opportunity to clinically validate the RAD51 assay. In prostate cancer, the PARPi olaparib and rucaparib are now approved for men with metastatic disease[88-90], but significant intra-patient variability in clinical outcomes has been observed, particularly in those with alterations in genes beyond *BRCA2*. A functional assay such as RAD51 may be relevant to assess the clinical value of less-frequent alterations in other DNA damage repair genes, such as *PALB2*, and to guide patient stratification[224]. Finally, olaparib is the first targeted therapy approved for g*BRCA1/2*-mutated pancreatic tumours that previously responded to platinum salts[87]. Accordingly, in these contexts, the RAD51 assay could be helpful to: i) avoid platinum-based chemotherapy as a selection biomarker, thus reducing toxicities in patients who may not benefit from it; ii) select patients who would otherwise need to be tested for g*BRCA1/2* status, given the low incidence of mutations in this subset of

patients; and iii) increase the number of patients who may benefit from PARPi beyond those with g*BRCA1/2* mutations.

We anticipate that the RAD51 test will have some limitations in relation with PARPi response: i) it will not identify tumours whose sensitivity to DNA-damaging agents lies on a DNA repair deficiency outside the HRR core pathway (i.e., alterations in the Fanconi anaemia or nucleotide excision repair pathway, genes encoding proteins involved in PARP trapping repair, *ATM*, *RNAseH2*, *XRCC1*, *ALC1*); and ii) it will not identify acquired resistance when the mechanism does not involve restoration of HRR (i.e., replication fork stabilisation, efflux pumps).

As future steps, the automatization of the staining protocol and the biomarker scoring should be a priority in the following years so that the test can successfully be implemented in the clinic. In addition, since tumour biopsies are not always feasible and cannot be taken repeatedly to monitor patients' progression. Therefore, as future steps, we propose i) to develop a RAD51 assay that can be used in liquid biopsies (i.e. in circulating tumour cells) and to test its capacity to predict PARPi sensitivity in g*BRCA1/2* mutation carriers with breast cancer, and ii) to develop an in-house assay to detect *BRCA1/2* reversion mutations in circulating tumour DNA. This will allow the monitoring of treatment responses in a dynamic and less invasive way, improving patient's quality of life and reducing healthcare costs. In this line, the RADIOLA trial, a prospective phase II clinical trial which aims to predict olaparib sensitivity in patients with unresectable locally advanced/metastatic HER2- breast cancer with HRR-related gene mutations or RAD51-low scores, will additionally explore the performance of the test in liquid biopsy.

In conclusion, the RAD51 assay could help to identify i) patients with gB*RCA1/2* or g*PALB2* mutations who are likely to be PARPi-resistant and ii) patients without germline *BRCA1/2* or *PALB2* mutations with HRD-positive tumours who are likely to be PARPi-sensitive. Using PDXs, we confirmed the

superior predictive value of an immunofluorescence-based test detecting RAD51 nuclear foci in preclinical models to predict PARPi response when compared with HRR-gene mutations, genomic HRD tests and platinum sensitivity. Given the supportive clinical data[78,142,173,174], we propose to continue the analytical validation and clinical qualification of the RAD51 assay in predicting response to PARPi but also other DNA-damaging agents in larger cohorts of breast cancer patients and beyond. The RAD51 test will facilitate the implementation of personalised medicine by guiding the prescription of most beneficial treatment regimens and reduce unnecessary, non-effective treatments.

CONCLUSIONS

PART 1

- First-generation PARP inhibitors (PARP1/2i) and platinum-based chemotherapy show antitumour activity in breast, ovarian and pancreatic cancers with homologous recombination (HR) deficiency (HRD).
- DNA-based HRD tests, such as the detection of HRR-related gene alterations, genomic scars or signatures, are static biomarkers of response to DNA-damaging agents that do not capture restoration of the HRR functionality and further acquired resistance.
- The RAD51 test is a protein-based dynamic biomarker that, by using a 10% cut-off, identifies tumours harbouring HRD, showing higher accuracy in predicting response to PARPi than other HRD tests.
- The RAD51 test identifies tumours that are likely to respond to platinum-based chemotherapy with similar accuracy to other HRD tests.
- The RAD51 test identifies HRD in both invasive and pre-malignant lesions such as ductal carcinoma *in situ* (DCIS).
- PDXs recapitulate the HRD status and PARPi responses of patients.

PART 2

- The new and more potent PARP1 selective inhibitor AZD5305 (PARP1i, saruparib) shows profound antitumour response in HRR-altered PDX models from breast, ovarian and pancreatic cancer.
- Treatment with AZD5305 results in lower progression rates and, therefore, more durable responses than treatment with first-generation PARPi.
- The RAD51 test captures sensitivity to PARP1i and restoration of the HRR functionality.

- The presence of hypomorphic BRCA1 is the most prevalent mechanism of acquired resistance to AZD5305 and olaparib in the cohort of PDX models. In addition, HRR-independent mechanisms can lead to AZD5305 resistance.
- Mechanistically, AZD5305 inhibits PARylation and enhances biomarkers of DNA damage and replication stress.
- Treatment with AZD5305 elicits profound and durable responses in combination with carboplatin or an ATR inhibitor (ATRi) in tumours exhibiting resistance to PARPi alone.
- Treatment with inhibitors of the microhomology-mediated end joining (MMEJ)-related polymerase theta (POLθi) induces durable responses in combination with AZD5305 in HR-proficient (HRP) tumours.
- Treatment with inhibitors of the non-homologous end joining's key protein DNA-PK (DNA-PKi) enhances the antitumour activity of olaparib and elicits durable responses.
- PARPi in combination with other DNA-damaging agents rescue resistance to PARPi as single agent.
- Dysregulation of the end resection pathway predicts sensitivity to DNA-damaging agents in combination with PARPi in *BRCA1*-mutated tumours, particularly in those harbouring mutations in the RING domain.

PART 3

- BRCA1 nuclear foci in combination with RAD51 help characterising the HRR functionality and capture mechanisms of resistance to DNA-damaging agents.
- Already in early stages of the breast disease, functional HRD can be captured by the RAD51 test.

- There is a high prevalence of functional HRD among HRR-related gene mutation carriers and unselected TNBC patients. Although in less extent, HRD is also observed among non-TNBC patients.
- The RAD51 test shows high accuracy in predicting benefit from adding neoadjuvant olaparib or carboplatin.
- Although there is variability in terms of RAD51 scoring among readers, further efforts in defining HRD scoring must be done in order to implement the test in the clinical routine.

REFERENCES

1. Hanahan D, Weinberg RA. TheHallmarksofCancer. *Cell.* 2000;100:50-70.
2. Hanahan D, Weinberg RA. Hallmarks of cancer: the next generation. *Cell.* 2011;144(5):646-674.
3. Hanahan D. Hallmarks of Cancer: New Dimensions. *Cancer Discov.* 2022;12(1):31-46.
4. Negrini S, Gorgoulis VG, Halazonetis TD. Genomic instability--an evolving hallmark of cancer. *Nat Rev Mol Cell Biol.* 2010;11(3):220-228.
5. Salk JJ, Fox EJ, Loeb LA. Mutational heterogeneity in human cancers: origin and consequences. *Annu Rev Pathol.* 2010;5:51-75.
6. Kastan MB. DNA damage responses: mechanisms and roles in human disease: 2007 G.H.A. Clowes Memorial Award Lecture. *Mol Cancer Res.* 2008;6(4):517-524.
7. Jackson SP, Bartek J. The DNA-damage response in human biology and disease. *Nature.* 2009;461(7267):1071-1078.
8. Lane DP. p53, guardian of the genome *Nature.* 1992;358.
9. Sigal A, Rotter V. Oncogenic Mutations of the p53 Tumor Suppressor: The Demons of the Guardian of the Genome. *Cancer Research.* 2000;60.
10. Harper JW, Elledge SJ. The DNA damage response: ten years after. *Mol Cell.* 2007;28(5):739-745.
11. Moynahan ME, Jasin M. Mitotic homologous recombination maintains genomic stability and suppresses tumorigenesis. *Nat Rev Mol Cell Biol.* 2010;11(3):196-207.
12. Scully R, Panday A, Elango R, Willis NA. DNA double-strand break repair-pathway choice in somatic mammalian cells. *Nat Rev Mol Cell Biol.* 2019;20(11):698-714.
13. Deriano L, Roth DB. Modernizing the nonhomologous end-joining repertoire: alternative and classical NHEJ share the stage. *Annu Rev Genet.* 2013;47:433-455.
14. Ceccaldi R, Rondinelli B, D'Andrea AD. Repair Pathway Choices and Consequences at the Double-Strand Break. *Trends Cell Biol.* 2016;26(1):52-64.
15. Ciccia A, Elledge SJ. The DNA damage response: making it safe to play with knives. *Mol Cell.* 2010;40(2):179-204.
16. Roy R, Chun J, Powell SN. BRCA1 and BRCA2: different roles in a common pathway of genome protection. *Nat Rev Cancer.* 2011;12(1):68-78.
17. Pilch DR, Sedelnikova OA, Redon C, Celeste A, Nussenzweig A, Bonner WM. Characteristics of gamma-H2AX foci at DNA double-strand breaks sites. *Biochem Cell Biol.* 2003;81(3):123-129.
18. Symington LS, Gautier J. Double-strand break end resection and repair pathway choice. *Annu Rev Genet.* 2011;45:247-271.

19. Chapman JR, Taylor MR, Boulton SJ. Playing the end game: DNA double-strand break repair pathway choice. *Mol Cell.* 2012;47(4):497-510.
20. Chang HHY, Pannunzio NR, Adachi N, Lieber MR. Non-homologous DNA end joining and alternative pathways to double-strand break repair. *Nat Rev Mol Cell Biol.* 2017;18(8):495-506.
21. Dynan WS, Yoo S. Interaction of Ku protein and DNA-dependent protein kinase catalytic subunit with nucleic acids. *Nucleic Acids Res.* 1998;26:1551-1559.
22. Chapman JR, Barral P, Vannier JB, et al. RIF1 is essential for 53BP1-dependent nonhomologous end joining and suppression of DNA double-strand break resection. *Mol Cell.* 2013;49(5):858-871.
23. Xu G, Chapman JR, Brandsma I, et al. REV7 counteracts DNA double-strand break resection and affects PARP inhibition. *Nature.* 2015;521(7553):541-544.
24. He YJ, Meghani K, Caron MC, et al. DYNLL1 binds to MRE11 to limit DNA end resection in BRCA1-deficient cells. *Nature.* 2018;563(7732):522-526.
25. Gupta R, Somyajit K, Narita T, et al. DNA Repair Network Analysis Reveals Shieldin as a Key Regulator of NHEJ and PARP Inhibitor Sensitivity. *Cell.* 2018;173(4):972-988 e923.
26. Mirman Z, Lottersberger F, Takai H, et al. 53BP1-RIF1-shieldin counteracts DSB resection through CST- and Polalpha-dependent fill-in. *Nature.* 2018;560(7716):112-116.
27. Bunting SF, Callen E, Wong N, et al. 53BP1 inhibits homologous recombination in Brca1-deficient cells by blocking resection of DNA breaks. *Cell.* 2010;141(2):243-254.
28. Xie A, Hartlerode A, Stucki M, et al. Distinct roles of chromatin-associated proteins MDC1 and 53BP1 in mammalian double-strand break repair. *Mol Cell.* 2007;28(6):1045-1057.
29. Zimmermann M, de Lange T. 53BP1: pro choice in DNA repair. *Trends Cell Biol.* 2014;24(2):108-117.
30. Neal JA, Meek K. Choosing the right path: does DNA-PK help make the decision? *Mutat Res.* 2011;711(1-2):73-86.
31. Fok JHL, Ramos-Montoya A, Vazquez-Chantada M, et al. AZD7648 is a potent and selective DNA-PK inhibitor that enhances radiation, chemotherapy and olaparib activity. *Nat Commun.* 2019;10(1):5065.
32. Kurosawa A, Adachi N. Functions and regulation of Artemis: a goddess in the maintenance of genome integrity. *J Radiat Res.* 2010;51(5):503-509.
33. Ramsden DA. Polymerases in Nonhomologous End Joining: Building a Bridge over Broken Chromosomes. *Antioxidants and redox signaling* 2011;14.
34. Gu J, Lu H, Tippin B, Shimazaki N, Goodman MF, Lieber MR. XRCC4:DNA ligase IV can ligate incompatible DNA ends and can ligate across gaps. *EMBO J.* 2007;26(4):1010-1023.

35. Wang H. DNA Ligase III as a Candidate Component of Backup Pathways of Nonhomologous End Joining. *Cancer Res.* 2005;65.
36. Patterson-Fortin J, D'Andrea AD. Exploiting the Microhomology-Mediated End-Joining Pathway in Cancer Therapy. *Cancer Res.* 2020;80(21):4593-4600.
37. Newman JA, Cooper CDO, Aitkenhead H, Gileadi O. Structure of the Helicase Domain of DNA Polymerase Theta Reveals a Possible Role in the Microhomology-Mediated End-Joining Pathway. *Structure.* 2015;23(12):2319-2330.
38. Simsek D, Brunet E, Wong SY, et al. DNA ligase III promotes alternative nonhomologous end-joining during chromosomal translocation formation. *PLoS Genet.* 2011;7(6):e1002080.
39. Della-Maria J, Zhou Y, Tsai MS, et al. Human Mre11/human Rad50/Nbs1 and DNA ligase IIIalpha/XRCC1 protein complexes act together in an alternative nonhomologous end joining pathway. *J Biol Chem.* 2011;286(39):33845-33853.
40. Garcin EB, Gon S, Sullivan MR, et al. Differential Requirements for the RAD51 Paralogs in Genome Repair and Maintenance in Human Cells. *PLoS Genet.* 2019;15(10):e1008355.
41. Nacson J, Di Marcantonio D, Wang Y, et al. BRCA1 Mutational Complementation Induces Synthetic Viability. *Mol Cell.* 2020;78(5):951-959 e956.
42. Wu LC. Identification of a RING protein that can interact in vivo with the BRCA1 gene product. *Nat Genet.* 1996;4.
43. Meza JE, Brzovic PS, King M-C, Klevit RE. Mapping the Functional Domains of BRCA1. *The Journal of Biological Chemistry.* 1999;274:5659-5665.
44. Sy SMH. PALB2 is an integral component of the BRCA complex required for homologous recombination repair. *PNAS.* 2009;106.
45. Zhang F, Ma J, Wu J, et al. PALB2 links BRCA1 and BRCA2 in the DNA-damage response. *Curr Biol.* 2009;19(6):524-529.
46. Zhang F, Fan Q, Ren K, Andreassen PR. PALB2 functionally connects the breast cancer susceptibility proteins BRCA1 and BRCA2. *Mol Cancer Res.* 2009;7(7):1110-1118.
47. Cantor SB. BACH1, a novel helicase-like protein, interacts directly with BRCA1 and contributes to its DNA repair function. *Cell.* 2001;105.
48. Yu X, Wu LC, Bowcock AM, Aronheim A, Baer R. The C-terminal (BRCT) domains of BRCA1 interact in vivo with CtIP, a protein implicated in the CtBP pathway of transcriptional repression. *J Biol Chem.* 1998;273(39):25388-25392.
49. Bochar DA. BRCA1 is associated with a human SWI/SNF-related complex: linking chromatin remodelling to breast cancer *Cell.* 2000;102.
50. Anderson SF. BRCA1 protein is linked to the RNA polymerase II holoenzyme complex via RNA helicase A. *Nature Genetics* 1998;19.

51. Venkitaraman AR. Cancer susceptibility and the functions of BRCA1 and BRCA2. *Cell.* 2002;108.
52. Tutt A, Ashworth A. The relationship between the roles of BRCA genes in DNA repair and cancer predisposition *Trends in Molecular Medicine* 2002;8.
53. Kuchenbaecker KB, Hopper JL, Barnes DR, et al. Risks of Breast, Ovarian, and Contralateral Breast Cancer for BRCA1 and BRCA2 Mutation Carriers. *JAMA.* 2017;317(23):2402-2416.
54. Kast K, Rhiem K, Wappenschmidt B, et al. Prevalence of BRCA1/2 germline mutations in 21 401 families with breast and ovarian cancer. *J Med Genet.* 2016;53(7):465-471.
55. Chen S, Parmigiani G. Meta-analysis of BRCA1 and BRCA2 penetrance. *J Clin Oncol.* 2007;25(11):1329-1333.
56. Turner N. Signatures of DNA-Repair Deficiencies in Breast Cancer. *The New England Journal of Medicine* 2017;377.
57. Turner N, Tutt A, Ashworth A. Hallmarks of "BRCAness" in sporadic cancers. *Nature reviews.* 2004;4.
58. Greenblatt MS. TP53 mutations in breast cancer associated with BRCA1 or BRCA2 germline mutations: Distinctive spectrum and structural distribution. *Cancer Res.* 2001;61.
59. Farmer H, McCabe N, Lord CJ, et al. Targeting the DNA repair defect in BRCA mutant cells as a therapeutic strategy. *Nature.* 2005;434.
60. Bryant HE. Specific killing of BRCA2-deficient tumours with inhibitors of poly(ADP-ribose) polymerase. *Nature.* 2005;434.
61. Sung H, Ferlay J, Siegel RL, et al. Global Cancer Statistics 2020: GLOBOCAN Estimates of Incidence and Mortality Worldwide for 36 Cancers in 185 Countries. *CA Cancer J Clin.* 2021;71(3):209-249.
62. Loibl S, Poortmans P, Morrow M, Denkert C, Curigliano G. Breast cancer. *Lancet.* 2021;397(10286):1750-1769.
63. Bray F, Laversanne M, Weiderpass E, Soerjomataram I. The ever-increasing importance of cancer as a leading cause of premature death worldwide. *Cancer.* 2021;127(16):3029-3030.
64. Nielsen FC, van Overeem Hansen T, Sorensen CS. Hereditary breast and ovarian cancer: new genes in confined pathways. *Nat Rev Cancer.* 2016;16(9):599-612.
65. Loibl S, Andre F, Bachelot T, et al. Early breast cancer: ESMO Clinical Practice Guideline for diagnosis, treatment and follow-up. *Ann Oncol.* 2024;35(2):159-182.
66. Voduc KD, Cheang MC, Tyldesley S, Gelmon K, Nielsen TO, Kennecke H. Breast cancer subtypes and the risk of local and regional relapse. *J Clin Oncol.* 2010;28(10):1684-1691.
67. Curigliano G, Burstein HJ, Gnant M, et al. Understanding breast cancer complexity to improve patient outcomes: The St Gallen International Consensus Conference for the Primary Therapy of Individuals with Early Breast Cancer 2023. *Ann Oncol.* 2023;34(11):970-986.

68. Perou CM. Molecular portraits of human breast tumours. *Nature.* 2000;406.
69. Parker JS, Mullins M, Cheang MC, et al. Supervised risk predictor of breast cancer based on intrinsic subtypes. *J Clin Oncol.* 2009;27(8):1160-1167.
70. Cancer Genome Atlas N. Comprehensive molecular portraits of human breast tumours. *Nature.* 2012;490(7418):61-70.
71. Harbeck N, Penault-Llorca F, Cortes J, et al. Breast cancer. *Nat Rev Dis Primers.* 2019;5(1):66.
72. Hutten SJ, de Bruijn R, Lutz C, et al. A living biobank of patient-derived ductal carcinoma in situ mouse-intraductal xenografts identifies risk factors for invasive progression. *Cancer Cell.* 2023;41(5):986-1002 e1009.
73. van Seijen M, Lips EH, Thompson AM, et al. Ductal carcinoma in situ: to treat or not to treat, that is the question. *Br J Cancer.* 2019;121(4):285-292.
74. Sessa C, Balmana J, Bober SL, et al. Risk reduction and screening of cancer in hereditary breast-ovarian cancer syndromes: ESMO Clinical Practice Guideline. *Ann Oncol.* 2023;34(1):33-47.
75. Gennari A, Andre F, Barrios CH, et al. ESMO Clinical Practice Guideline for the diagnosis, staging and treatment of patients with metastatic breast cancer. *Ann Oncol.* 2021;32(12):1475-1495.
76. Robson M, Im SA, Senkus E, et al. Olaparib for Metastatic Breast Cancer in Patients with a Germline BRCA Mutation. *N Engl J Med.* 2017;377(6):523-533.
77. Litton JK, Rugo HS, Ettl J, et al. Talazoparib in Patients with Advanced Breast Cancer and a Germline BRCA Mutation. *N Engl J Med.* 2018;379(8):753-763.
78. Llop-Guevara A, Loibl S, Villacampa G, et al. Association of RAD51 with homologous recombination deficiency (HRD) and clinical outcomes in untreated triple-negative breast cancer (TNBC): analysis of the GeparSixto randomized clinical trial. *Ann Oncol.* 2021;32(12):1590-1596.
79. Konstantinopoulos PA, Ceccaldi R, Shapiro GI, D'Andrea AD. Homologous Recombination Deficiency: Exploiting the Fundamental Vulnerability of Ovarian Cancer. *Cancer Discov.* 2015;5(11):1137-1154.
80. Ghosh S. Cisplatin: The first metal based anticancer drug. *Bioorg Chem.* 2019;88:102925.
81. De Vos M, Schreiber V, Dantzer F. The diverse roles and clinical relevance of PARPs in DNA damage repair: current state of the art. *Biochem Pharmacol.* 2012;84(2):137-146.
82. Caldecott KW. Protein ADP-ribosylation and the cellular response to DNA strand breaks. *DNA Repair (Amst).* 2014;19:108-113.
83. Mateo J, Lord CJ, Serra V, et al. A decade of clinical development of PARP inhibitors in perspective. *Ann Oncol.* 2019;30(9):1437-1447.

84. Hopkins TA, Shi Y, Rodriguez LE, et al. Mechanistic Dissection of PARP1 Trapping and the Impact on In Vivo Tolerability and Efficacy of PARP Inhibitors. *Mol Cancer Res.* 2015;13(11):1465-1477.
85. Moore K, Colombo N, Scambia G, et al. Maintenance Olaparib in Patients with Newly Diagnosed Advanced Ovarian Cancer. *N Engl J Med.* 2018;379(26):2495-2505.
86. Tutt ANJ, Garber JE, Kaufman B, et al. Adjuvant Olaparib for Patients with BRCA1- or BRCA2-Mutated Breast Cancer. *N Engl J Med.* 2021;384(25):2394-2405.
87. Golan T, Hammel P, Reni M, et al. Maintenance Olaparib for Germline BRCA-Mutated Metastatic Pancreatic Cancer. *N Engl J Med.* 2019;381(4):317-327.
88. de Bono J, Mateo J, Fizazi K, et al. Olaparib for Metastatic Castration-Resistant Prostate Cancer. *N Engl J Med.* 2020;382(22):2091-2102.
89. Abida W. Rucaparib in Men With Metastatic Castration-Resistant Prostate Cancer Harboring a BRCA1 or BRCA2 Gene Alteration. *Journal of Clinical Oncology.* 2020.
90. Clarke NW, Armstrong AJ, Thiery-Vuillemin A, et al. Abiraterone and Olaparib for Metastatic Castration-Resistant Prostate Cancer. *NEJM Evidence.* 2022;1(9).
91. Dias MP, Moser SC, Ganesan S, Jonkers J. Understanding and overcoming resistance to PARP inhibitors in cancer therapy. *Nat Rev Clin Oncol.* 2021;18(12):773-791.
92. Ganguly B, Dolfi SC, Rodriguez-Rodriguez L, Ganesan S, Hirshfield KM. Role of Biomarkers in the Development of PARP Inhibitors. *Biomark Cancer.* 2016;8(Suppl 1):15-25.
93. Stover EH, Konstantinopoulos PA, Matulonis UA, Swisher EM. Biomarkers of Response and Resistance to DNA Repair Targeted Therapies. *Clin Cancer Res.* 2016;22(23):5651-5660.
94. Davies H, Glodzik D, Morganella S, et al. HRDetect is a predictor of BRCA1 and BRCA2 deficiency based on mutational signatures. *Nat Med.* 2017;23(4):517-525.
95. Timms KM, Abkevich V, Hughes E, et al. Association of BRCA1/2 defects with genomic scores predictive of DNA damage repair deficiency among breast cancer subtypes. *Breast Cancer Res.* 2014;16(6):475.
96. Abkevich V, Timms KM, Hennessy BT, et al. Patterns of genomic loss of heterozygosity predict homologous recombination repair defects in epithelial ovarian cancer. *Br J Cancer.* 2012;107(10):1776-1782.
97. Alexandrov LB, Nik-Zainal S, Wedge DC, et al. Signatures of mutational processes in human cancer. *Nature.* 2013;500(7463):415-421.
98. Pellegrino B, Herencia-Ropero A, Llop-Guevara A, et al. Preclinical In Vivo Validation of the RAD51 Test for Identification of Homologous Recombination-Deficient Tumors and Patient Stratification. *Cancer Res.* 2022;82(8):1646-1657.

99. Castroviejo-Bermejo M, Cruz C, Llop-Guevara A, et al. A RAD51 assay feasible in routine tumor samples calls PARP inhibitor response beyond BRCA mutation. *EMBO Mol Med.* 2018;10(12).
100. Cruz C, Castroviejo-Bermejo M, Gutierrez-Enriquez S, et al. RAD51 foci as a functional biomarker of homologous recombination repair and PARP inhibitor resistance in germline BRCA-mutated breast cancer. *Ann Oncol.* 2018;29(5):1203-1210.
101. Lord CJ, Ashworth A. Mechanisms of resistance to therapies targeting BRCA-mutant cancers. *Nat Med.* 2013;19(11):1381-1388.
102. Norquist B, Wurz KA, Pennil CC, et al. Secondary somatic mutations restoring BRCA1/2 predict chemotherapy resistance in hereditary ovarian carcinomas. *J Clin Oncol.* 2011;29(22):3008-3015.
103. Kondrashova O, Nguyen M, Shield-Artin K, et al. Secondary Somatic Mutations Restoring RAD51C and RAD51D Associated with Acquired Resistance to the PARP Inhibitor Rucaparib in High-Grade Ovarian Carcinoma. *Cancer Discov.* 2017;7(9):984-998.
104. Kondrashova O, Topp M, Nesic K, et al. Methylation of all BRCA1 copies predicts response to the PARP inhibitor rucaparib in ovarian carcinoma. *Nat Commun.* 2018;9(1):3970.
105. Nesic K, Kondrashova O, Hurley RM, et al. Acquired RAD51C Promoter Methylation Loss Causes PARP Inhibitor Resistance in High-Grade Serous Ovarian Carcinoma. *Cancer Res.* 2021;81(18):4709-4722.
106. Drost R, Dhillon KK, van der Gulden H, et al. BRCA1185delAG tumors may acquire therapy resistance through expression of RING-less BRCA1. *J Clin Invest.* 2016;126(8):2903-2918.
107. Wang Y, Bernhardy AJ, Cruz C, et al. The BRCA1-Delta11q Alternative Splice Isoform Bypasses Germline Mutations and Promotes Therapeutic Resistance to PARP Inhibition and Cisplatin. *Cancer Res.* 2016;76(9):2778-2790.
108. Johnson N, Johnson SF, Yao W, et al. Stabilization of mutant BRCA1 protein confers PARP inhibitor and platinum resistance. *Proc Natl Acad Sci U S A.* 2013;110(42):17041-17046.
109. Schlacher K, Wu H, Jasin M. A distinct replication fork protection pathway connects Fanconi anemia tumor suppressors to RAD51-BRCA1/2. *Cancer Cell.* 2012;22(1):106-116.
110. Lomonosov M, Anand S, Sangrithi M, Davies R, Venkitaraman AR. Stabilization of stalled DNA replication forks by the BRCA2 breast cancer susceptibility protein. *Genes Dev.* 2003;17(24):3017-3022.
111. Pettitt SJ, Krastev DB, Brandsma I, et al. Genome-wide and high-density CRISPR-Cas9 screens identify point mutations in PARP1 causing PARP inhibitor resistance. *Nat Commun.* 2018;9(1):1849.
112. Gogola E, Duarte AA, de Ruiter JR, et al. Selective Loss of PARG Restores PARylation and Counteracts PARP Inhibitor-Mediated Synthetic Lethality. *Cancer Cell.* 2018;33(6):1078-1093 e1012.

113. Vaidyanathan A, Sawers L, Gannon AL, et al. ABCB1 (MDR1) induction defines a common resistance mechanism in paclitaxel- and olaparib-resistant ovarian cancer cells. *Br J Cancer.* 2016;115(4):431-441.
114. Murai J, Pommier Y. PARP Trapping Beyond Homologous Recombination and Platinum Sensitivity in Cancers. *Annual Review of Cancer Biology.* 2019;3(1):131-150.
115. Murai J, Huang SY, Das BB, et al. Trapping of PARP1 and PARP2 by Clinical PARP Inhibitors. *Cancer Res.* 2012;72(21):5588-5599.
116. Farres J, Martin-Caballero J, Martinez C, et al. Parp-2 is required to maintain hematopoiesis following sublethal gamma-irradiation in mice. *Blood.* 2013;122(1):44-54.
117. Johannes JW, Balazs A, Barratt D, et al. Discovery of 5-4-[(7-Ethyl-6-oxo-5,6-dihydro-1,5-naphthyridin-3-yl)methyl]piperazin-1-yl-N-methylpyridine-2-carboxamide (AZD5305): A PARP1-DNA Trapper with High Selectivity for PARP1 over PARP2 and Other PARPs. *J Med Chem.* 2021;64(19):14498-14512.
118. Illuzzi G, Staniszewska AD, Gill SJ, et al. Preclinical Characterization of AZD5305, A Next-Generation, Highly Selective PARP1 Inhibitor and Trapper. *Clin Cancer Res.* 2022;28(21):4724-4736.
119. Yap TA. PETRA: A first-in-class, first-in-human trial of the next-generation PARP1-selective inhibitor AZD5305 in patients with BRCA1/2, PALB2 or RAD51C/D mutations. . In. AACR Annual Meeting, New Orleans2022.
120. Yazinski SA, Comaills V, Buisson R, et al. ATR inhibition disrupts rewired homologous recombination and fork protection pathways in PARP inhibitor-resistant BRCA-deficient cancer cells. *Genes Dev.* 2017;31(3):318-332.
121. Tutt A. VIOLETTE: Randomised phase II study of olaparib (ola) + ceralasertib (cer) or adavosertib (ada) vs ola alone in patients (pts) with metastatic triple-negative breast cancer (mTNBC). In. Annals of Oncology 2022.
122. Serra V, Wang AT, Castroviejo-Bermejo M, et al. Identification of a Molecularly-Defined Subset of Breast and Ovarian Cancer Models that Respond to WEE1 or ATR Inhibition, Overcoming PARP Inhibitor Resistance. *Clin Cancer Res.* 2022;28(20):4536-4550.
123. Westin SN. EFFORT: EFFicacy Of adavosertib in parp ResisTance: A randomized two-arm non-comparative phase II study of adavosertib with or without olaparib in women with PARP-resistant ovarian cancer. In. Journal of Clinical Oncology2021.
124. Ceccaldi R, Liu JC, Amunugama R, et al. Homologous-recombination-deficient tumours are dependent on Poltheta-mediated repair. *Nature.* 2015;518(7538):258-262.
125. Pettitt SJ, Frankum JR, Punta M, et al. Clinical BRCA1/2 Reversion Analysis Identifies Hotspot Mutations and Predicted Neoantigens

Associated with Therapy Resistance. *Cancer Discov.* 2020;10(10):1475-1488.
126. Foote KM, Nissink JWM, McGuire T, et al. Discovery and Characterization of AZD6738, a Potent Inhibitor of Ataxia Telangiectasia Mutated and Rad3 Related (ATR) Kinase with Application as an Anticancer Agent. *J Med Chem.* 2018;61(22):9889-9907.
127. Simões BM, O'Brien CS, Eyre R, et al. Anti-estrogen Resistance in Human Breast Tumors Is Driven by JAG1-NOTCH4-Dependent Cancer Stem Cell Activity. *Cell Rep.* 2015;12(12):1968-1977.
128. Marangoni E, Vincent-Salomon A, Auger N, et al. A new model of patient tumor-derived breast cancer xenografts for preclinical assays. *Clin Cancer Res.* 2007;13(13):3989-3998.
129. Charafe-Jauffret E, Ginestier C, Bertucci F, et al. ALDH1-positive cancer stem cells predict engraftment of primary breast tumors and are governed by a common stem cell program. *Cancer Res.* 2013;73(24):7290-7300.
130. Bruna A, Rueda OM, Greenwood W, et al. A Biobank of Breast Cancer Explants with Preserved Intra-tumor Heterogeneity to Screen Anticancer Compounds. *Cell.* 2016;167(1):260-274 e222.
131. Driehuis E, Kretzschmar K, Clevers H. Establishment of patient-derived cancer organoids for drug-screening applications. *Nat Protoc.* 2020;15(10):3380-3409.
132. Ahdesmaki MJ, Gray SR, Johnson JH, Lai Z. Disambiguate: An open-source application for disambiguating two species in next generation sequencing data from grafted samples. *F1000Res.* 2016;5:2741.
133. Lai Z, Markovets A, Ahdesmaki M, et al. VarDict: a novel and versatile variant caller for next-generation sequencing in cancer research. *Nucleic Acids Res.* 2016;44(11):e108.
134. Sztupinszki Z, Diossy M, Krzystanek M, et al. Migrating the SNP array-based homologous recombination deficiency measures to next generation sequencing data of breast cancer. *NPJ Breast Cancer.* 2018;4:16.
135. Schmittgen TD, Livak KJ. Analyzing real-time PCR data by the comparative C(T) method. *Nat Protoc.* 2008;3(6):1101-1108.
136. Colombo M, Lopez-Perolio I, Meeks HD, et al. The BRCA2 c.68-7T > A variant is not pathogenic: A model for clinical calibration of spliceogenicity. *Hum Mutat.* 2018;39(5):729-741.
137. Ter Brugge P, Kristel P, van der Burg E, et al. Mechanisms of Therapy Resistance in Patient-Derived Xenograft Models of BRCA1-Deficient Breast Cancer. *J Natl Cancer Inst.* 2016;108(11).
138. Palafox M, Monserrat L, Bellet M, et al. High p16 expression and heterozygous RB1 loss are biomarkers for CDK4/6 inhibitor resistance in ER(+) breast cancer. *Nat Commun.* 2022;13(1):5258.
139. Allison KH, Hammond MEH, Dowsett M, et al. Estrogen and Progesterone Receptor Testing in Breast Cancer: American Society

of Clinical Oncology/College of American Pathologists Guideline Update. *Arch Pathol Lab Med.* 2020;144(5):545-563.
140. Ballabeni A, Zamponi R, Moore JK, Helin K, Kirschner MW. Geminin deploys multiple mechanisms to regulate Cdt1 before cell division thus ensuring the proper execution of DNA replication. *Proc Natl Acad Sci U S A.* 2013;110(30):E2848-2853.
141. Rogakou EP, Pilch DR, Orr AH, Ivanova VS, Bonner WM. DNA double-stranded breaks induce histone H2AX phosphorylation on serine 139. *J Biol Chem.* 1998;273(10):5858-5868.
142. Eikesdal HP, Yndestad S, Elzawahry A, et al. Olaparib monotherapy as primary treatment in unselected triple negative breast cancer. *Ann Oncol.* 2021;32(2):240-249.
143. Yndestad S, Engebrethsen C, Herencia-Ropero A, et al. Homologous Recombination Deficiency Across Subtypes of Primary Breast Cancer. *JCO Precis Oncol.* 2023;7:e2300338.
144. Yates LR, Gerstung M, Knappskog S, et al. Subclonal diversification of primary breast cancer revealed by multiregion sequencing. *Nat Med.* 2015;21(7):751-759.
145. Nikolaienko O, Eikesdal HP, Ognedal E, et al. Prenatal BRCA1 epimutations contribute significantly to triple-negative breast cancer development. *Genome Med.* 2023;15(1):104.
146. Nikolaienko O, Lonning PE, Knappskog S. epialleleR: an R/Bioconductor package for sensitive allele-specific methylation analysis in NGS data. *Gigascience.* 2022;12.
147. von Minckwitz G, Schneeweiss A, Loibl S, et al. Neoadjuvant carboplatin in patients with triple-negative and HER2-positive early breast cancer (GeparSixto; GBG 66): a randomised phase 2 trial. *Lancet Oncol.* 2014;15(7):747-756.
148. Loibl S, Weber KE, Timms KM, et al. Survival analysis of carboplatin added to an anthracycline/taxane-based neoadjuvant chemotherapy and HRD score as predictor of response-final results from GeparSixto. *Ann Oncol.* 2018;29(12):2341-2347.
149. Hahnen E, Lederer B, Hauke J, et al. Germline Mutation Status, Pathological Complete Response, and Disease-Free Survival in Triple-Negative Breast Cancer: Secondary Analysis of the GeparSixto Randomized Clinical Trial. *JAMA Oncol.* 2017;3(10):1378-1385.
150. Kramer CJ, Llop-Guevara A, Yaniz-Galende E, et al. RAD51 as a biomarker for homologous recombination deficiency in high-grade serous ovarian carcinoma: robustness and interobserver variability of the RAD51 test. *J Pathol Clin Res.* 2023;9(6):442-448.
151. van Wijk LM, Kramer CJH, Vermeulen S, et al. The RAD51-FFPE Test; Calibration of a Functional Homologous Recombination Deficiency Test on Diagnostic Endometrial and Ovarian Tumor Blocks. *Cancers (Basel).* 2021;13(12).

152. Blanc-Durand F, Yaniz-Galende E, Llop-Guevara A, et al. A RAD51 functional assay as a candidate test for homologous recombination deficiency in ovarian cancer. *Gynecol Oncol.* 2023;171:106-113.
153. Bates D, Mächler M, Bolker B, Walker S. Fitting Linear Mixed-Effects Models Usinglme4. *Journal of Statistical Software.* 2015;67(1).
154. Therneau TM. Mixed Effects Cox Models. 2022.
155. Dobrolecki LE, Airhart SD, Alferez DG, et al. Patient-derived xenograft (PDX) models in basic and translational breast cancer research. *Cancer Metastasis Rev.* 2016;35(4):547-573.
156. Izumchenko E, Paz K, Ciznadija D, et al. Patient-derived xenografts effectively capture responses to oncology therapy in a heterogeneous cohort of patients with solid tumors. *Ann Oncol.* 2017;28(10):2595-2605.
157. Mavaddat N, Barrowdale D, Andrulis IL, et al. Pathology of breast and ovarian cancers among BRCA1 and BRCA2 mutation carriers: results from the Consortium of Investigators of Modifiers of BRCA1/2 (CIMBA). *Cancer Epidemiol Biomarkers Prev.* 2012;21(1):134-147.
158. Larsen MJ, Thomassen M, Gerdes AM, Kruse TA. Hereditary breast cancer: clinical, pathological and molecular characteristics. *Breast Cancer (Auckl).* 2014;8:145-155.
159. Jaspers JE, Kersbergen A, Boon U, et al. Loss of 53BP1 causes PARP inhibitor resistance in Brca1-mutated mouse mammary tumors. *Cancer Discov.* 2013;3(1):68-81.
160. Dev H, Chiang TW, Lescale C, et al. Shieldin complex promotes DNA end-joining and counters homologous recombination in BRCA1-null cells. *Nat Cell Biol.* 2018;20(8):954-965.
161. Wang Y, Krais JJ, Bernhardy AJ, et al. RING domain-deficient BRCA1 promotes PARP inhibitor and platinum resistance. *J Clin Invest.* 2016;126(8):3145-3157.
162. Graeser M, McCarthy A, Lord CJ, et al. A marker of homologous recombination predicts pathologic complete response to neoadjuvant chemotherapy in primary breast cancer. *Clin Cancer Res.* 2010;16(24):6159-6168.
163. Miller RE, Leary A, Scott CL, et al. ESMO recommendations on predictive biomarker testing for homologous recombination deficiency and PARP inhibitor benefit in ovarian cancer. *Ann Oncol.* 2020;31(12):1606-1622.
164. Coussy F, El-Botty R, Château-Joubert S, et al. BRCAness, SLFN11, and RB1 loss predict response to topoisomerase I inhibitors in triple-negative breast cancers. *Science Translational Medicine* 2020.
165. Iyengar M, O'Hayer P, Cole A, et al. CDK4/6 inhibition as maintenance and combination therapy for high grade serous ovarian cancer. *Oncotarget* 2018;9(21):15658-15672.
166. Coffman LG, Orellana TJ, Liu T, et al. Phase I trial of ribociclib with platinum chemotherapy in ovarian cancer. *JCI Insight.* 2022;7(18).

167. Safaei R. Role of copper transporters in the uptake and efflux of platinum containing drugs. *Cancer Lett.* 2006;234(1):34-39.
168. Comsa E, Nguyen K-A, Loghin F, et al. Ovarian cancer cells cisplatin sensitization agents selected by mass cytometry target ABCC2 inhibition. *Future Medicinal Chemistry.* 2018.
169. Gorski JW, Ueland FR, Kolesar JM. CCNE1 Amplification as a Predictive Biomarker of Chemotherapy Resistance in Epithelial Ovarian Cancer. *Diagnostics (Basel).* 2020;10(5).
170. Bunting SF, Callen E, Kozak ML, et al. BRCA1 functions independently of homologous recombination in DNA interstrand crosslink repair. *Mol Cell.* 2012;46(2):125-135.
171. Farkkila A, Rodriguez A, Oikkonen J, et al. Heterogeneity and Clonal Evolution of Acquired PARP Inhibitor Resistance in TP53- and BRCA1-Deficient Cells. *Cancer Res.* 2021;81(10):2774-2787.
172. Claus EB, Petruzella S, Matloff E, Carter D. Prevalence of BRCA1 and BRCA2 Mutations in Women Diagnosed with Ductal Carcinoma In Situ. *JAMA Oncology.* 2005;293.
173. Chopra N, Tovey H, Pearson A, et al. Homologous recombination DNA repair deficiency and PARP inhibition activity in primary triple negative breast cancer. *Nat Commun.* 2020;11(1):2662.
174. Compadre AJ, van Biljon LN, Valentine MC, et al. RAD51 Foci as a Biomarker Predictive of Platinum Chemotherapy Response in Ovarian Cancer. *Clinical Cancer Research.* 2023;29(13):2466-2479.
175. Lord CJ, Ashworth A. PARP inhibitors: Synthetic lethality in the clinic. *Science.* 2017.
176. LaFargue CJ, Dal Molin GZ, Sood AK, Coleman RL. Exploring and comparing adverse events between PARP inhibitors. *Lancet Oncol.* 2019;20(1):e15-e28.
177. Park PH, Yamamoto TM, Li H, et al. Amplification of the Mutation-Carrying BRCA2 Allele Promotes RAD51 Loading and PARP Inhibitor Resistance in the Absence of Reversion Mutations. *Mol Cancer Ther.* 2020;19(2):602-613.
178. Tobalina L, Armenia J, Irving E, O'Connor MJ, Forment JV. A meta-analysis of reversion mutations in BRCA genes identifies signatures of DNA end-joining repair mechanisms driving therapy resistance. *Ann Oncol.* 2021;32(1):103-112.
179. Rottenberg S. High sensitivity of BRCA1-deficient mammary tumors to the PARP inhibitor AZD2281 alone and in combination with platinum drugs. *PNAS.* 2008;105:17079–17084.
180. Glanzer JG, Liu S, Wang L, Mosel A, Peng A, Oakley GG. RPA inhibition increases replication stress and suppresses tumor growth. *Cancer Res.* 2014;74(18):5165-5172.
181. Harding SM, Benci JL, Irianto J, Discher DE, Minn AJ, Greenberg RA. Mitotic progression following DNA damage enables pattern recognition within micronuclei. *Nature.* 2017;548(7668):466-470.

182. Flohr C, Burkle A, Radicella JP, Epe B. Poly(ADP-ribosyl)ation accelerates DNA repair in a pathway dependent on Cockayne syndrome B protein. *Nucleic Acids Res.* 2003;31(18):5332-5337.
183. Pommier Y. Laying a trap to kill cancer cells: PARP inhibitors and their mechanisms of action. *Science Translational Medicine.* 2016.
184. Konstantinopoulos PA, da Costa A, Gulhan D, et al. A Replication stress biomarker is associated with response to gemcitabine versus combined gemcitabine and ATR inhibitor therapy in ovarian cancer. *Nat Commun.* 2021;12(1):5574.
185. Wood RD, Doublie S. DNA polymerase theta (POLQ), double-strand break repair, and cancer. *DNA Repair (Amst).* 2016;44:22-32.
186. Chan SH, Yu AM, McVey M. Dual roles for DNA polymerase theta in alternative end-joining repair of double-strand breaks in Drosophila. *PLoS Genet.* 2010;6(7):e1001005.
187. Zhou J, Gelot C, Pantelidou C, et al. A first-in-class Polymerase Theta Inhibitor selectively targets Homologous-Recombination-Deficient Tumors. *Nat Cancer.* 2021;2(6):598-610.
188. Callen E, Jankovic M, Wong N, et al. Essential role for DNA-PKcs in DNA double-strand break repair and apoptosis in ATM-deficient lymphocytes. *Mol Cell.* 2009;34(3):285-297.
189. Riabinska A. Therapeutic Targeting of a Robust Non-Oncogene Addiction to PRKDC in ATM-Defective Tumors. *Science Translational Medicine.* 2013;5(189).
190. Bhargava R, Carson CR, Lee G, Stark JM. Contribution of canonical nonhomologous end joining to chromosomal rearrangements is enhanced by ATM kinase deficiency. *Proc Natl Acad Sci U S A.* 2017;114(4):728-733.
191. Bennardo N, Cheng A, Huang N, Stark JM. Alternative-NHEJ is a mechanistically distinct pathway of mammalian chromosome break repair. *PLoS Genet.* 2008;4(6):e1000110.
192. Yun MH, Hiom K. CtIP-BRCA1 modulates the choice of DNA double-strand-break repair pathway throughout the cell cycle. *Nature.* 2009;459(7245):460-463.
193. Huen MS, Sy SM, Chen J. BRCA1 and its toolbox for the maintenance of genome integrity. *Nat Rev Mol Cell Biol.* 2010;11(2):138-148.
194. Gibson SV, Roozitalab RM, Allen MD, Jones JL, Carter EP, Grose RP. Everybody needs good neighbours: the progressive DCIS microenvironment. *Trends Cancer.* 2023;9(4):326-338.
195. Zhu X, Shan L, Wang F, et al. Hypermethylation of BRCA1 gene: implication for prognostic biomarker and therapeutic target in sporadic primary triple-negative breast cancer. *Breast Cancer Res Treat.* 2015;150(3):479-486.
196. Litton JK. Neoadjuvant Talazoparib for Patients With Operable Breast Cancer With a Germline BRCA Pathogenic Variant. *J Clin Oncol.* 2019.

197. Spring LM, Han H, Liu MC, et al. Neoadjuvant study of niraparib in patients with HER2-negative, BRCA-mutated, resectable breast cancer. *Nat Cancer.* 2022;3(8):927-931.
198. Gruber JJ, Afghahi A, Timms K, et al. A phase II study of talazoparib monotherapy in patients with wild-type BRCA1 and BRCA2 with a mutation in other homologous recombination genes. *Nat Cancer.* 2022;3(10):1181-1191.
199. Ballot E, Galland L, Mananet H, et al. Molecular intrinsic subtypes, genomic, and immune landscapes of BRCA-proficient but HRD-high ER-positive/HER2-negative early breast cancers. *Breast Cancer Res.* 2022;24(1):80.
200. Heeke AL, Xiu J, Elliott A, et al. Actionable co-alterations in breast tumors with pathogenic mutations in the homologous recombination DNA damage repair pathway. *Breast Cancer Res Treat.* 2020;184(2):265-275.
201. Luen SJ, Viale G, Nik-Zainal S, et al. Genomic characterisation of hormone receptor-positive breast cancer arising in very young women. *Ann Oncol.* 2023;34(4):397-409.
202. van Wijk LM, Nilas AB, Vrieling H, Vreeswijk MPG. RAD51 as a functional biomarker for homologous recombination deficiency in cancer: a promising addition to the HRD toolbox? *Expert Rev Mol Diagn.* 2022;22(2):185-199.
203. Simpson; Fabrice Andre; Sarah-Jane Dawson; Richard Pearson; Sherene Loi CTvGZLTPSSJLKACSSKJCFCKJ. SPEN is a biomarker for CDK4/6 inhibitor resistance in patients with metastatic hormone receptor positive (HR+)/HER2- breast cancer. In: Symposium SABC, ed. San Antonio, USA, March 01 2023: San Antonio Breast Cancer Symposium; 2023.
204. Isakoff SJ, Mayer EL, He L, et al. TBCRC009: A Multicenter Phase II Clinical Trial of Platinum Monotherapy With Biomarker Assessment in Metastatic Triple-Negative Breast Cancer. *J Clin Oncol.* 2015;33(17):1902-1909.
205. Tutt A, Tovey H, Cheang MCU, et al. Carboplatin in BRCA1/2-mutated and triple-negative breast cancer BRCAness subgroups: the TNT Trial. *Nat Med.* 2018;24(5):628-637.
206. Lukashchuk N AJ, Luis Tobalina T. BRCA reversion mutations mediated by microhomology-mediated end joining (MMEJ) as a mechanism of resistance to PARP inhibitors in ovarian and breast cancer. In. ASCO Annual Meeting, Chicago, USA2022.
207. Horton JK, Stefanick DF, Prasad R, Gassman NR, Kedar PS, Wilson SH. Base excision repair defects invoke hypersensitivity to PARP inhibition. *Mol Cancer Res.* 2014;12(8):1128-1139.
208. Zimmermann M, Murina O, Reijns MAM, et al. CRISPR screens identify genomic ribonucleotides as a source of PARP-trapping lesions. *Nature.* 2018;559(7713):285-289.

209. Hewitt G, Borel V, Segura-Bayona S, et al. Defective ALC1 nucleosome remodeling confers PARPi sensitization and synthetic lethality with HRD. *Mol Cell.* 2021;81(4):767-783 e711.
210. Postel-Vinay S, Soria J-C. ERCC1 as Predictor of Platinum Benefit in Non–Small-Cell Lung Cancer. *Journal of Clinical Oncology.* 2017;25.
211. Parkes EE, Humphries MP, Gilmore E, et al. The clinical and molecular significance associated with STING signaling in breast cancer. *NPJ Breast Cancer.* 2021;7(1):81.
212. Harvey-Jones E, Raghunandan M, Robbez-Masson L, et al. Longitudinal profiling identifies co-occurring BRCA1/2 reversions, TP53BP1, RIF1 and PAXIP1 mutations in PARP inhibitor-resistant advanced breast cancer. *Ann Oncol.* 2024.
213. Zatreanu D, Robinson HMR, Alkhatib O, et al. Poltheta inhibitors elicit BRCA-gene synthetic lethality and target PARP inhibitor resistance. *Nat Commun.* 2021;12(1):3636.
214. Buisson R, Boisvert JL, Benes CH, Zou L. Distinct but Concerted Roles of ATR, DNA-PK, and Chk1 in Countering Replication Stress during S Phase. *Mol Cell.* 2015;59(6):1011-1024.
215. Kumar RJ, Chao HX, Simpson DA, et al. Dual inhibition of DNA-PK and DNA polymerase theta overcomes radiation resistance induced by p53 deficiency. *NAR Cancer.* 2020;2(4):zcaa038.
216. Shakya R. BRCA1 Tumor Suppression Depends on BRCT Phosphoprotein Binding, But Not Its E3 Ligase Activity. *Nature.* 2011;334(6055).
217. Drost R, Bouwman P, Rottenberg S, et al. BRCA1 RING function is essential for tumor suppression but dispensable for therapy resistance. *Cancer Cell.* 2011;20(6):797-809.
218. Morganti S, Marra A, De Angelis C, et al. PARP Inhibitors for Breast Cancer Treatment: A Review. *JAMA Oncol.* 2024.
219. Fasching PA, Link T, Hauke J, et al. Neoadjuvant paclitaxel/olaparib in comparison to paclitaxel/carboplatinum in patients with HER2-negative breast cancer and homologous recombination deficiency (GeparOLA study). *Ann Oncol.* 2021;32(1):49-57.
220. Tung NM. TBCRC 048: Phase II Study of Olaparib for Metastatic Breast Cancer and Mutations in Homologous Recombination-Related Genes. *Journal of Clinical Oncology.* 2020;38.
221. Ledermann J, Harter P, Gourley C, et al. Olaparib maintenance therapy in patients with platinum-sensitive relapsed serous ovarian cancer: a preplanned retrospective analysis of outcomes by BRCA status in a randomised phase 2 trial. *Lancet Oncol.* 2014;15(8):852-861.
222. Ledermann JA, Harter P, Gourley C, et al. Overall survival in patients with platinum-sensitive recurrent serous ovarian cancer receiving olaparib maintenance monotherapy: an updated analysis from a randomised, placebo-controlled, double-blind, phase 2 trial. *Lancet Oncol.* 2016;17(11):1579-1589.

223. Ray-Coquard I, Pautier P, Pignata S, et al. Olaparib plus Bevacizumab as First-Line Maintenance in Ovarian Cancer. *N Engl J Med.* 2019;381(25):2416-2428.
224. Carreira S, Porta N, Arce-Gallego S, et al. Biomarkers Associating with PARP Inhibitor Benefit in Prostate Cancer in the TOPARP-B Trial. *Cancer Discov.* 2021;11(11):2812-2827.

ANNEXES

Annex I: Genes included in the panels (targeted sequencing) performed

BRCA Hereditary Cancer MASTR™ Plus (Agilent)

BRCA1, BRCA2, STK11, TP53, PTEN, BLM, CDH1, CHEK2, MLH1, MSH2, MSH6, ATM, BARD1, NBN, PALB2, PMS2, RAD50, RAD51C, RAD51D, BRIP1, MRE11A, XRCC2, MUTYH, MEN1, EPCAM, and *FAM175A.*

Hereditary Plus OncoKitDx (Healthincode)

ABRAXAS1 (FAM175A), ACD, AIP, AKT1, ALK, APC (incl. 5' UTR), *ATM, ATR, AXIN2, BAP1, BARD1, BLM, BMPR1A, BRCA1, BRCA2, BRIP1, CDC73, CDH1, CDK4, CDKN1B, CDKN1C, CDKN2A, CHEK2, CTNNA1, CYLD, DICER1, EPCAM (incl. 3' UTR), FANCC, FANCG, FANCM, FH, FLCN, GALNT12, GALNT14, GDNF, GEN1, GREM1, HABP2, HOXB13, KIF1B, KLLN, LZTR1, MAX, MC1R, MEN1, MET, MITF, MLH1, MLH3, MRE11A, MSH2, MSH3, MSH6, MUTYH, NBN, NF1, NF2, NTHL1, PALB2, PHOX2B, PIK3CA, PMS2, POLD1, POLE, POT1, PRKAR1A, PRSS1, PTCH1, PTEN, RAD50, RAD51, RAD51B, RAD51C, RAD51D, RB1, RECQL4, RET, RINT1, SDHA, SDHAF2, SDHB, SDHC, SDHD, SEC23B, SLX4, SMAD4, SMARCA4, SMARCB1, SMARCE1, SPRED1, STK11, SUFU, TERF2IP, TERT, TMEM127, TP53, TSC1, TSC2, VHL, WT1 and XRCC2.*

Panel designed according to the COSMIC database

CTNNB1, TP53, CDKN2A-p16 (INK4a), CDKN2A-p14ARF, PTEN, KRAS, PIK3CA, BRAF, RB1, EGFR, MLH1, NF1, PIK3R1, STK11, APC, ATM, BRCA2, FBXW7, GPC3, HRAS, KDM6A, MAP2K4, MLL3, MSH2, MSH6,

NF2, SMARCA4, AKAP9, ARID1A, BRCA1, CREBBP, EP300, FGFR2, FGFR3, HNF1A, ITK, KDM5C, KIT, MET, MLL2, NOTCH1, NRAS, NTRK1, PBRM1, PTCH1, ROS1, RUNX1T1, SMAD4, VHL, AKT1, ASXL1, ATRX, CDH1, CDKN2C, CHEK2, ERBB2, FAM123B, FOXL2, GATA3, GNA11, GNAS, IDH1, IDH2, KDR, MEN1, MYH11, NCOA2, PPP2R1A, RNF213, SETD2, SMARCB1, TSC1, TSC2.

Annex II: Supplementary tables

List of supplementary tables

Supplementary Table 1. Clinical and molecular characteristics of the PDX cohort. Modified from *Pellegrino and Herencia et al.,*

Supplementary Table 2. Clinical characteristics of the PDXs and the corresponding patients. Modified from *Pellegrino and Herencia et al.,*

Supplementary Table 3. Clinical and demographic characteristics of patients from which PDXs were generated. Modified from *Pellegrino and Herencia et al.,*

Supplementary Table 4. Characterization of PDX models of ductal carcinoma *in situ* (DCIS).

Supplementary Table 5. Clinical and molecular characteristics of the PDX cohort used to evaluate the AZD5305 antitumour activity alone or in combination with carboplatin or an TR inhibitor (AZD6738).

Supplementary Table 6. Molecular characteristics of tumors with acquired resistance to AZD5305 and olaparib.

Supplementary Table 7. Mechanisms of resistance to PARPi evaluated inthe cohort of PDX models.

Supplementary Table 8. Clinical and molecular characteristics of the PDX cohort used to evaluate POLθi antitumour activity.

Supplementary Table 9. Clinical and molecular characteristics of the PDX cohort used to evaluate DNA-PKi antitumour activity.

Supplementary Table 10. Clinical and molecular characteristics of TNBC patients enrolled in the PETREMAC clinical trial. *Modified from Eikesdal et al.,*

Supplementary Table 11. Clinical and molecular characteristics of non-TNBC patients enrolled in the PETREMAC clinical trial. *Modified from Yndestad et al.,*

Supplementary Table 1. Clinical and molecular characteristics of the PDX cohort. Modified from *Pellegrino and Herencia et al.,*

PDX	Cancer subtype	Primary/Metastatic (P/M) tumor	Patient previous treatment	HRR alteration	cDNA change	AA change	Domain	Variant effect	BRCA1 promoter hypermethylation	BRCA1 foci	RAD51 foci	HRDetect	HRD score (Myriad)	GIS	Mechanism of Resistance to PARPi	Drug	Dose (mg/kg)	Response to PARPi (mRECIST criteria)
PDX168	PaC	M	Yes	*PALB2*	c.1965dupT	p.P656fs	Ring	Frameshift	-	38	94	NA	NA	NA	No gsLOH	Olaparib	100	Resistant
PDX474.2OR2	ER+	M	Yes	*BRCA2*	c.3922G>T	p.E1308*	Non recognized domain region	Nonsense	-	43	65	NA	NA	NA	*BRCA2* reversion (c.3848_3931delTAAGTGAAAAAAATAATAAATGCCAACTGATATTACAAAATAATATTGAAATGACTACTGGCACTTTTGTTGAAGAAATTACTG)	Olaparib	100	Resistant
PDX405OR50	TNBC	P	Yes	*BRCA2*	c.5909C>A	p. S1970*	Non recognized domain region	Nonsense	-	86	15	NA	NA	NA	Unknown	Olaparib	50	Resistant
T180R	TNBC	P	No	-	-	-	-	-	-	66	39	NA	32	NA	-	Niraparib	75	Resistant
HBCx33	TNBC	P	No	-	-	-	-	-	-	80	50,7	NA	32	NA	-	Niraparib	75	Resistant
HBCx27	TNBC	P	No	-	-	-	-	-	-	80	43	NA	27	NA	-	Niraparib	75	Resistant
HBCx28	TNBC	P	No	*BRCA1*	c.212+3A>G	-	Intronic variant	Splicing	-	0	36	NA	63	NA	53BP1 pathway dysregulation (FAM35A homodel)	Niraparib	75	Resistant
HBCx16	TNBC	P	No	*BRCA1*	-	-	-	-	NA	0	42	NA	57	NA	Unknown	Niraparib	50	Resistant
PDX127	TNBC	M	No	*BRCA1*	c.185delAG	p.E23fs	Ring	Frameshift	-	0	16,3	0,999983359	NA	87	53BP1 pathway dysregulation (FAM35A homodel)	Olaparib	50	Resistant
PDX274	TNBC	M	Yes	*BRCA1*	Homoloss	-	-	-	-	12	22,7	0,999883399	NA	76	Hypomorphic BRCA1	Olaparib	50	Resistant
HBCx2	TNBC	M	No	-	-	-	-	-	-	74	63,3	NA	36	NA	-	Niraparib	50	Resistant
HBCx31	TNBC	P	No	-	-	-	-	-	-	82	53	NA	25	NA	-	Niraparib	75	Resistant
HBCx24	TNBC	P	No	*BRCA1*	-	-	-	-	Yes	12	38,7	NA	55	NA	Loss of *BRCA1* promoter hypermethylation	Niraparib	75	Resistant
PDX221	TNBC	P	Yes	*BRCA1*	c.5027delT	p.L1676fs	BRCT	Frameshift	-	66	20,3	0,999829767	NA	83	Hypomorphic BRCA1	Olaparib	50	Resistant
PDX474.7	ER+	M	Yes	*BRCA2*	c.3922G>T	p.E1308*	Non recognized domain region	Nonsense	-	89	18	NA	NA	NA	Unknown	Olaparib	100	Resistant
HBCx9	TNBC	P	No	*BRCA1*	-	-	-	-	Yes	60	33	NA	55	NA	Loss of *BRCA1* promoter hypermethylation	Olaparib	50	Resistant
HBCx1	TNBC	P	No	*BRCA1*	-	-	-	-	NA	0	25	NA	50	NA	Unknown	Niraparib	50	Resistant
HBCx8	TNBC	P	Yes	*BRCA1*	-	p.Q81*	Ring	Nonsense	-	0	41,7	NA	65	NA	Unknown	Niraparib	50	Resistant
PDX302OR2	TNBC	M	Yes	*BRCA1*	-	-	-	-	-	70	69	NA	NA	NA	Loss of *BRCA1* promoter hypermethylation	Olaparib	50	Resistant
HBCx30	TNBC	P	No	-	-	-	-	-	-	68	51,5	NA	21	NA	-	Niraparib	75	Resistant
PDX098	TNBC	P	Yes	-	-	-	-	-	-	94	60	NA	NA	NA	-	Olaparib	50	Resistant
PDX467	TNBC	P	Yes	-	-	-	-	-	-	82	64	NA	NA	NA	-	Olaparib	50	Resistant
STG139	TNBC	P	Yes	-	-	-	-	-	-	15	53	NA	NA	NA	-	Olaparib	50	Resistant
HBCx39	TNBC	P	Yes	-	-	-	-	-	-	14	43	NA	32	NA	-	Niraparib	75	Resistant
T311R	TNBC	P	No	-	-	-	-	-	-	62	63,7	NA	25	NA	-	Niraparib	75	Resistant
PDX549	TNBC	P	Yes	-	-	-	-	-	-	54	61	NA	NA	NA	-	Olaparib	50	Resistant
PDX137	TNBC	M	Yes	-	-	-	-	-	-	84	56	NA	NA	NA	-	Olaparib	50	Resistant
T381	TNBC	P	Yes	-	-	-	-	-	-	62	46	NA	30	NA	-	Niraparib	75	Resistant
PDX445	OvC	M	No	-	-	-	-	-	-	94	60	NA	NA	NA	-	Olaparib	100	Resistant
PDX124OR	TNBC	M	Yes	*BRCA1*	c.1961delA	p.K654fs	Exon 11	Frameshift	-	10,5	16,3	NA	NA	NA	Suspected replication fork	Olaparib	100	Resistant
HBCx23	TNBC	P	No	*BRCA1*	-	-	-	-	NA	0	35,5	NA	69	NA	Unknown	Niraparib	75	Resistant
PDX093OR6	TNBC	P	No	*PALB2*	-	-	-	-	-	90	41,6	NA	NA	NA	HRR genetic reversion (VAF > 0.1)	Olaparib	100	Resistant
STG316	TNBC	P	Yes	*BRCA1*	c.134+3A>C	-	Intronic variant	Splicing	-	26	36,7	NA	NA	NA	Hypomorphic BRCA1 and 53BP1 pathway dysregulation (53BP1 homodel)	Olaparib	50	Resistant

PDX	Cancer subtype	Primary/Metastatic (P/M) tumor	Patient previous treatment	HRR alteration	cDNA change	AA change	Domain	Variant effect	BRCA1 promoter hypermethylation	BRCA1 foci	RAD51 foci	HRDetect	HRD score (Myriad)	GIS	Mechanism of Resistance to PARPi	Drug	Dose (mg/kg)	Response to PARPi (mRECIST criteria)
PDX474.2OR1	ER+	M	Yes	*BRCA2*	c.3922G>T	p.E1308*	Non recognized domain region	Nonsense	-	76,6	43,3	NA	NA	NA	Unknown	Olaparib	100	Resistant
PDX377OR2	TNBC	M	Yes	*BRCA1*	c.1912delG	p.E638fs	Exon 11	Frameshift	-	21	13	NA	NA	NA	Suspected replication fork	Olaparib	100	Resistant
PDX179	TNBC	M	Yes	*BRCA1*	c.185delAG	p.E23fs	Ring	Frameshift	-	7	22,3	NA	NA	NA	Unknown	Olaparib	100	Resistant
PC-PDX060	PaC	M	Yes	*BRCA2*	c.1909+1G>A	-	Intronic variant	Splicing	-	45	12	NA	NA	NA	Unknown	Olaparib	100	Resistant
STG201OR	ER+	M	Yes	*BRCA1*	-	-	-	-	-	57	47	NA	NA	NA	Loss of *BRCA1* promoter hypermethylation	Olaparib	50	Resistant
PDX418	ER+	M	Yes	*BRCA1*	c.5266dupC	p.Q1756Pfs*74	BRCT	Nonsense	-	32	19,5	NA	NA	NA	Hypomorphic BRCA1	Olaparib	50	Resistant
PDX230OR1	TNBC	P	Yes	*BRCA1*	c.185delAG	p.E23fs	Ring	Frameshift	-	6	20,7	0,999978059	NA	NA	53BP1 pathway dysregulation (53BP1 c.5294_5305+33delAAGAAGAGGAGGGTAAGGCCTTAGGAAGCCCTGGGAGCTCTGACA)	Olaparib	100	Resistant
PDX173OR3	HER2+	P	HER2+	BRCA2	c.9808delG	p.A3270Pfs*5	NLS	Nonsense	-	82,5	33	NA	NA	NA	Unknown	Olaparib	100	Resistant
HBCx11	TNBC	P	No	*BRCA1*	c.1961delA	p.K654fs	Exon 11	Frameshift	-	40	37	NA	73	NA	Hypomorphic BRCA1	Niraparib	50	Resistant
PDX230OR5	TNBC	P	Yes	*BRCA1*	c.185delAG	p.E23fs	Ring	Frameshift	-	0,5	11	NA	NA	NA	Unknown	Olaparib	100	Resistant
PDX102	TNBC	P	No	-	-	-	-	-	-	82	52	NA	NA	NA	-	Olaparib	50	Resistant
HBCx7	TNBC	M	Yes	-	-	-	-	-	-	36	54,7	NA	5	NA	-	Niraparib	50	Resistant
PDX280	OvC	M	Yes	*BRCA1*	Homoloss	-	-	-	-	0	24,3	NA	NA	NA	Unknown	Olaparib	50	Resistant
PDX044	TNBC	M	Yes	-	-	-	-	-	-	68	54	NA	NA	NA	-	Olaparib	50	Resistant
PDX397	OvC	M	No	*BRCA1*	c.5108A>C	p.Y1703S	BRCT	Missense	-	27	39	NA	NA	NA	Hypomorphic BRCA1	Olaparib	50	Resistant
T174	TNBC	P	No	-	-	-	-	-	-	96	49,3	NA	31	NA	-	Niraparib	75	Resistant
HBCx12B	TNBC	M	Yes	*BRCA1*	-	-	-	-	NA	0	29	NA	78	NA	Unknown	Niraparib	50	Resistant
PDX341	TNBC	M	Yes	*BRCA1*	c.2404delGA	p.R762fs	Exon 11	Frameshift	-	29	16,7	NA	NA	NA	Hypomorphic BRCA1 and 53BP1 pathway dysregulation (C20orf196 downregulation)	Olaparib	50	Resistant
PDX332	TNBC	M	Yes	*BRCA2*	c.7796A>G	p.E2599G	DNA binding (Helical domain)	Missense	-	80	13	0,05659481	NA	39	HRR genetic reversion (VAF > 0.1)	Olaparib	50	Resistant
ST1363	ER+	Unknown	Unknown	-	-	-	-	-	-	38	53	NA	71	NA	-	Niraparib	50	Resistant
ST1557	ER+	Unknown	Unknown	-	-	-	-	-	-	86	65	NA	55	NA	-	Niraparib	50	Resistant
ST231	ER+	Unknown	Unknown	-	-	-	-	-	-	74	48	NA	35	NA	-	Niraparib	50	Resistant
ST941	ER+	Unknown	Yes	-	-	-	-	-	-	76	36	NA	44	NA	-	Niraparib	50	Resistant
ST1248	ER+	Unknown	Unknown	-	-	-	-	-	-	80	54	NA	21	NA	-	Niraparib	50	Resistant
HBCx21	ER+	P	No	-	-	-	-	-	-	96	42	NA	16	NA	-	Niraparib	50	Resistant
PDX457	TNBC	M	Yes	-	-	-	-	-	-	34	33,5	NA	NA	NA	-	Olaparib	50	Resistant
PDX432	TNBC	M	Yes	-	-	-	-	-	-	16	4,5	NA	NA	NA	Unknown	Olaparib	100	Resistant
PDX583.2	ER+	M	Yes	*BRCA2*	c.8954-5A>G	-		Splicing	-	45	17	NA	NA	NA	Unknown	Olaparib	100	Resistant
PDX156	TNBC	M	Yes	-	-	-	-	-	-	68	49	NA	NA	NA	-	Olaparib	50	Resistant
PDX094	TNBC	P	Yes	-	-	-	-	-	-	58	58	NA	NA	NA	-	Olaparib	50	Resistant
PDX405OR100	TNBC	P	Yes	*BRCA2*	c.5909C>A	p. S1970*	Non recognized domain region	Nonsense	-	78	55	NA	NA	NA	HRR genetic reversion (VAF > 0.1)	Olaparib	100	Resistant
PDX230OR8	TNBC	P	Yes	*BRCA1*	c.185delAG	p.E23fs	Ring	Frameshift	-	0	11	NA	NA	NA	Unknown	Olaparib	100	Resistant
PDX252	TNBC	M	Yes	*BRCA1*	c.5123C>A	p.A1708E	BRCT	Missense	-	0	21,5	0,997235532	NA	70	Unknown	Olaparib	50	Resistant
PDX230OR2	TNBC	P	Yes	*BRCA1*	c.185delAG	p.E23fs	Ring	Frameshift	-	6	11,1	NA	NA	NA	Unknown	Olaparib	50	Resistant
PDX291	TNBC	M	Yes	-	-	-	-	-	-	76	53	0,578303258	NA	39	-	Olaparib	50	Resistant
PDX377OR1	TNBC	M	Yes	*BRCA1*	c.1912delG	p.E638fs	Exon 11	Frameshift	-	32,5	10	NA	NA	NA	Suspected replication fork	Olaparib	50	Resistant
PDX629	PaC	M	Yes	*BRCA1*	c.185delAG	p.E23fs	Ring	Frameshift	-	0	1,25	NA	NA	NA	Unknown	Olaparib	100	Resistant
PDX350	ER+	M	Yes	*XRCC2*	Homoloss	-	-	-	-	50	25	NA	NA	NA	Unknown	Olaparib	100	Resistant

PDX	Cancer subtype	Primary/Metastatic (P/M) tumor	Patient previous treatment	HRR alteration	cDNA change	AA change	Domain	Variant effect	BRCA1 promoter hypermethylation	BRCA1 foci	RAD51 foci	HRDetect	HRD score (Myriad)	GIS	Mechanism of Resistance to PARPi	Drug	Dose (mg/kg)	Response to PARPi (mRECIST criteria)
PDX453	TNBC	M	Yes	-	-	-	-	-	-	68	36	NA	NA	NA	-	Olaparib	100	Resistant
PDX060	TNBC	M	Yes	-	-	-	-	-	-	47,1	48	NA	NA	NA	-	Olaparib	50	Resistant
PDX641.1	Gastric	M	Yes	*BRCA1*	c.5266dupC	p.Q1756Pfs*74	BRCT	Nonsense	-	0	0	NA	NA	NA	Unknown	Olaparib	100	Resistant
ST1337	ER+	Unknown	Unknown	-	-	-	-	-	-	36	35	NA	39	NA	-	Niraparib	50	Resistant
PDX288	TNBC	M	Yes	-	-	-	-	-	-	65	50	0,695911274	NA	33	-	Olaparib	50	Resistant
PDX440	TNBC	M	Yes	-	-	-	-	-	-	41	46	NA	NA	NA	-	Olaparib	100	Resistant
PDX270	TNBC	P	No	*BRCA1*	-	-	-	-	Yes	0	12	NA	NA	NA	Unknown	Olaparib	50	Resistant
PC-PDX064	PaC	M	Yes	*BRCA1*	c.3839_3843delinsAGGC	p.S1280*	Exon 11	Nonsense	-	24	22,2	NA	NA	NA	Hypomorphic BRCA1	Olaparib	100	Resistant
ST1799	ER+	Unknown	Yes	-	-	-	-	-	-	60	26	NA	20	NA	-	Niraparib	50	Resistant
PDX427	TNBC	M	Yes	-	-	-	-	-	-	87	15,5	NA	NA	NA	-	Olaparib	100	Resistant
ST455B	ER+	Unknown	Yes	-	-	-	-	-	-	NA	20	NA	NA	NA	-	Niraparib	50	Resistant
PDX339	TNBC	M	Yes	*BRCA1*	c.211A>G	p.R71G	Ring	Missense	-	8	21	0,9998763	NA	84	Unknown	Olaparib	100	Resistant
PDX236	TNBC	M	Yes	*BRCA1*	c.5194-12G>A	-	Intronic variant	Splicing	-	60	27	0,984120074	NA	58	Hypomorphic BRCA1	Olaparib	50	Resistant
PDX071OR	ER+	P	No	*BRCA2*	c.3264dupT	p.Q1089fs	Non recognized domain region	Frameshift	-	80	32,5	NA	NA	NA	Unknown	Olaparib	50	Resistant
ST1337B	ER+	Unknown	Unknown	-	-	-	-	-	-	72	64	NA	39	NA	-	Niraparib	50	Resistant
PDX509	TNBC	M	Yes	-	-	-	-	-	-	45	16	NA	NA	NA	-	Olaparib	100	Resistant
PDX302OR	TNBC	M	Yes	*BRCA1*	-	-	-	-	Yes	0	37	0,993005023	NA	NA	Unknown	Olaparib	50	Resistant
HBCx34	ER+	P	No	*BRCA2*	c.7976+2dupC	-	Intronic variant	Splicing	-	92	0	NA	69	NA	-	Niraparib	50	Sensitive
HBCx22	ER+	P	No	*BRCA2*	c.6405_6409del	p.N2135Kfs*3	Non recognized domain region	Nonsense	-	64	6	NA	63	NA	-	Olaparib	100	Sensitive
PDX124	TNBC	M	Yes	*BRCA1*	c.1961delA	p.K654fs	Exon 11	Frameshift	-	10	8,3	NA	NA	NA	-	Olaparib	50	Sensitive
PDX384	TNBC	M	Yes	*BRCA1*	c.791-794delGTTC	p.S264Mfs*33	Exon 11	Frameshift	-	38	15,5	NA	NA	NA	-	Olaparib	50	Sensitive
PDX173	HER2+	P	Yes	*BRCA2*	c.9808delG	p.A3270Pfs*5	NLS	Nonsense	-	29	0	NA	NA	NA	-	Olaparib	100	Sensitive
HBCx17	TNBC	P	No	*BRCA2*	c.6033_6034delTT	p.F2011fs	Non recognized domain region	Frameshift	-	100	13,3	NA	69	NA	-	Niraparib	50	Sensitive
PDX539	TNBC	P	No	*BRCA1*	c.4843dupG	p.A1615Gfs*7	BRCT	Nonsense	-	0	1	NA	NA	NA	-	Olaparib	100	Sensitive
PDX196	OvC	M	Yes	*BRCA1*	c.1961delA	p.K654fs	Exon 11	Frameshift	-	68	28,3	0,99967619	NA	72	-	Olaparib	100	Sensitive
T298	TNBC	P	No	*PALB2*	-	-	-	-	-	82	2	NA	66	NA	-	Olaparib	100	Sensitive
ST897	ER+	Unknown	No	*PALB2*	c.3549C>G	p.Y1183*	Non recognized domain region	Nonsense	-	80	0	NA	69	NA	-	Niraparib	50	Sensitive
PDX302	TNBC	M	Yes	*BRCA1*	-	-	-	-	Yes	0	0	0,993121792	NA	58	-	Olaparib	50	Sensitive
PDX474.1	ER+	M	Yes	*BRCA2*	c.3922G>T	p.E1308*	Non recognized domain region	Nonsense	-	71	1,5	NA	NA	NA	-	Olaparib	100	Sensitive
BB3RC31/PDX481	ER+	M	Yes	*BRCA2*	c.7976+1G>C	-	Intronic variant	Splicing	-	78	0	NA	NA	NA	-	Olaparib	100	Sensitive
ST1099	ER+	Unknown	Unknown	*BRCA1*	-	-	-	-	NA	0	0	NA	84	NA	-	Niraparib	50	Sensitive

PDX	Cancer subtype	Primary/Metastatic (P/M) tumor	Patient previous treatment	HRR alteration	cDNA change	AA change	Domain	Variant effect	BRCA1 promoter hypermethylation	BRCA1 foci	RAD51 foci	HRDetect	HRD score (Myriad)	GIS	Mechanism of Resistance to PARPi	Drug	Dose (mg/kg)	Response to PARPi (mRECIST criteria)
PDX474.2	ER+	M	Yes	*BRCA2*	c.3922G>T	p.E1308*	Non recognized domain region	Nonsense	-	45	0	NA	NA	NA	-	Olaparib	100	Sensitive
STG201	ER+	M	Yes	*BRCA1*	-	-	-	-	Yes	0	0	NA	NA	NA	-	Olaparib	50	Sensitive
HBCx10	TNBC	P	No	*BRCA2*	c.9106C>T	p.Q3036*	DNA binding (OB3)	Nonsense	-	84	1,7	NA	57	NA	-	Olaparib	100	Sensitive
PDX405	TNBC	M	Yes	*BRCA2*	c.5909C>A	p. S1970*	Non recognized domain region	Nonsense	-	90	2,7	NA	NA	NA	-	Olaparib	50	Sensitive
T330	TNBC	P	No	*BRCA1*	c.3839_3844 delins5	p.S1280*	Exon 11	Nonsense	-	30	4,3	NA	65	NA	-	Niraparib	75	Sensitive
PDX473	TNBC	P	Yes	*BRCA1*	c.5123C>A	p.A1708E	BRCT	Missense	-	0	1	NA	NA	NA	-	Olaparib	100/50	Sensitive
PDX230	TNBC	P	Yes	*BRCA1*	c.185delAG	p.E23fs	Ring	Frameshift	-	0	0,3	0,999977931	NA	83	-	Olaparib	50	Sensitive
PDX093	TNBC	P	No	*PALB2*	c.886dupA	p.M296fs	Non recognized domain region	Frameshift	-	97	0,5	NA	NA	NA	-	Olaparib	50	Sensitive
PDX197	TNBC	P	Yes	*BRCA1*	-	-	-	-	Yes	0	1	NA	NA	NA	-	Olaparib	50	Sensitive
PDX071	ER+	P	No	*BRCA2*	c.3264dupT	p.Q1089fs	Non recognized domain region	Frameshift	-	64	1,7	0,998978372	NA	92	-	Olaparib	50	Sensitive
PDX377	TNBC	M	Yes	*BRCA1*	c.1912delG	p.E638fs	Exon 11	Frameshift	-	24,5	0	NA	NA	NA	-	Olaparib	50	Sensitive
T168	TNBC	P	No	*BRCA1*	-	p.S1524L	-	Missense	-	0	1,7	NA	54	NA	-	Niraparib	75	Sensitive
HBCx6	TNBC	P	No	*BRCA1*	-	-	-	-	Yes	0	2,3	NA	72	NA	-	Olaparib	100	Sensitive
HBCx14	TNBC	P	Yes	*XRCC3*	Homoloss	-	-	-	-	78	1	NA	53	NA	-	Olaparib	100	Sensitive
HBCx15	TNBC	P	No	*BRCA1*	-	-	-	-	Yes	0	2,7	NA	68	NA	-	Olaparib	100	Sensitive

Supplementary Table 2. Clinical characteristics of the PDXs and the corresponding patients. Modified from *Pellegrino and Herencia et al.,*

	BIOPSY for PDX								PDX				
ID_PDX	BIOPSY_LOCATION	BIOPSY_TYPE (primary/met/lymph node)	REPEATED_MOLECULAR_SUBTYPING? (Y/N)	ER status AT PDX BIOPSY	PR status AT PDX BIOPSY	HER2_STATUS AT PDX BIOPSY	Ki67%	MOLECULAR_PDX_SUBTYPE_STGALLEN	ER status (%)	PR status (%)	HER2 status (0-3;FISH)	Ki67 (%)	MOLECULAR_PDX_SUBTYPE_STGALLEN
PDX044	LYMPH NODE	METASTASES	Y	NEGATIVE	NEGATIVE	NEGATIVE	90	TNBC	NEGATIVE	NEGATIVE	NEGATIVE	90	TNBC
PDX060	SKIN	METASTASES	N	NE	NE	NE	NE	NE	POSITIVE	NEGATIVE	NEGATIVE	70	LUMINAL B
PC-PDX060	PANCREAS	PRIMARY TUMOR	-	-	-	-	-	-	NEGATIVE	NEGATIVE	NEGATIVE	70	-
PC-PDX064	LIVER	METASTASES	-	-	-	-	-	-	NEGATIVE	NEGATIVE	NEGATIVE	90	-
PDX071	BREAST	PRIMARY TUMOR	Y	POSITIVE	POSITIVE	NEGATIVE	30	LUMINAL B	POSITIVE	NEGATIVE	ISH non-ampli	20	LUMINAL B
PDX093	BREAST	PRIMARY TUMOR	Y	NEGATIVE	NEGATIVE	NEGATIVE	30	TNBC	NEGATIVE	NEGATIVE	NEGATIVE	90	TNBC
PDX094	BREAST	PRIMARY TUMOR	Y	POSITIVE	NEGATIVE	NEGATIVE	20	LUMINAL B	NEGATIVE	NEGATIVE	NEGATIVE	98	TNBC
PDX098	BREAST	PRIMARY TUMOR	Y	POSITIVE	NEGATIVE	NEGATIVE	80	LUMINAL B	POSITIVE	NEGATIVE	NEGATIVE	90	LUMINAL B
PDX102	BREAST	PRIMARY TUMOR	Y	POSITIVE	POSITIVE	NEGATIVE	90	LUMINAL B	NEGATIVE	NEGATIVE	NEGATIVE	80	TNBC
PDX124	SKIN	METASTASES	N	NE	NE	NE	NE	NE	NEGATIVE	NEGATIVE	NEGATIVE	80	TNBC
PDX127	SKIN	METASTASES	N	NE	NE	NE	NE	NE	NEGATIVE	NEGATIVE	NEGATIVE	80	TNBC
PDX137	SKIN	METASTASES	N	NE	NE	NE	NE	NE	NEGATIVE	NEGATIVE	NEGATIVE	90	TNBC
PDX156	SKIN	METASTASES	N	NE	NE	NE	NE	NE	NEGATIVE	NEGATIVE	NEGATIVE	60	TNBC
PDX173	BREAST	PRIMARY TUMOR	Y	POSITIVE	POSITIVE	POSITIVE	20	HER2	POSITIVE	POSITIVE	POSITIVE	90	HER2-amplified
PDX179	SKIN	METASTASES	N	NE	NE	NE	NE	NE	NEGATIVE	NEGATIVE	NEGATIVE	90	TNBC
PDX168	LIVER	METASTASES	N	NE	NE	NE	NE	NE	NEGATIVE	NEGATIVE	NEGATIVE	70	-
PDX196	PERICARDIAL	METASTASES	NA	NA	NA	NA	NA	NA	-	-	-	-	HGSOC
PDX197	BREAST	PRIMARY TUMOR	Y	POSITIVE	NEGATIVE	NEGATIVE	85	LUMINAL B	NEGATIVE	NEGATIVE	NEGATIVE	90	TNBC
PDX221	BREAST	PRIMARY TUMOR	Y	NEGATIVE	NEGATIVE	NEGATIVE	95	TNBC	NEGATIVE	NEGATIVE	NEGATIVE	90	3
PDX230	BREAST	PRIMARY TUMOR	Y	NEGATIVE	NEGATIVE	NEGATIVE	85	TNBC	NEGATIVE	NEGATIVE	NEGATIVE	70	TNBC
PDX236	SKIN	METASTASES	N	NE	NE	NE	NE	NE	NEGATIVE	NEGATIVE	NEGATIVE	60	TNBC
PDX252	SKIN	METASTASES	N	NE	NE	NE	NE	NE	NEGATIVE	NEGATIVE	NEGATIVE	90	TNBC
PDX270	BREAST	PRIMARY TUMOR	Y	NEGATIVE	NEGATIVE	NEGATIVE	70	TNBC	NEGATIVE	NEGATIVE	NEGATIVE	90	TNBC
PDX274	SKIN	METASTASES	N	NE	NE	NE	NE	NE	NEGATIVE	NEGATIVE	NEGATIVE	90	TNBC
PDX280	LYMPH NODE	METASTASES	NA	NA	NA	NA	NA	NA	-	-	-	80	HGSOC
PDX288	SKIN	METASTASES	N	NE	NE	NE	NE	NE	NEGATIVE	NEGATIVE	NEGATIVE	70	TNBC
PDX291	SKIN	METASTASES	N	NE	NE	NE	NE	NE	NEGATIVE	NEGATIVE	NEGATIVE	85	TNBC
PDX302	SKIN	METASTASES	N	NE	NE	NE	NE	NE	NEGATIVE	NEGATIVE	NEGATIVE	90	TNBC
PDX332	AUTOPSY	METASTASES	N	NE	NE	NE	NE	NE	NEGATIVE	NEGATIVE	NEGATIVE	100	TNBC
PDX339	BONE	METASTASES	N	NE	NE	NE	NE	NE	NEGATIVE	NEGATIVE	NEGATIVE	90	TNBC
PDX341	LYMPH NODE	METASTASES	Y	NEGATIVE	NEGATIVE	NEGATIVE	45	TNBC	NEGATIVE	NEGATIVE	NEGATIVE	80	TNBC
PDX350	BREAST	METASTASES	Y	POSITIVE	POSITIVE	NEGATIVE	50	LUMINAL B	POSITIVE	POSITIVE	NEGATIVE	50	LUMINAL B
PDX377	BREAST	PRIMARY TUMOR	Y	NEGATIVE	NEGATIVE	NEGATIVE	70	TNBC	NEGATIVE	NEGATIVE	NEGATIVE	75	TNBC
PDX384	LYMPH NODE	METASTASES	N	NE	NE	NE	NE	NE	NEGATIVE	NEGATIVE	NEGATIVE	70	TNBC
PDX397	LIVER	METASTASES	-	-	-	-	-	-	-	-	POSITIVE	50	HGSOC
PDX405	NA	NA	NA	NA	NA	NA	NA	NA	NEGATIVE	NEGATIVE	NEGATIVE	80	TNBC
PDX418	SKIN	METASTASES	Y	POSITIVE	NEGATIVE	NEGATIVE	90	LUMINAL B	POSITIVE	NEGATIVE	NEGATIVE	90	TNBC
PDX427	BREAST	METASTASES	N	NE	NE	NE	NE	NE	NEGATIVE	NEGATIVE	NEGATIVE	70	TNBC
PDX432	SKIN	METASTASES	N	NE	NE	NE	NE	NE	NEGATIVE	NEGATIVE	NEGATIVE	80	TNBC
PDX440	SKIN	METASTASES	N	NE	NE	NE	NE	NE	POSITIVE (10%)	NEGATIVE	NEGATIVE	70	LUMINAL B
PDX445	LIVER	METASTASES	-	-	-	-	-	-	-	-	-	60	HGSOC
PDX453	BREAST	METASTASES	N	NE	NE	NE	NE	NE	NEGATIVE	NEGATIVE	NEGATIVE	60	TNBC
PDX457	BONE	METASTASES	Y	NEGATIVE	NEGATIVE	NEGATIVE	NE	TNBC	NEGATIVE	NEGATIVE	NEGATIVE	80	TNBC
PDX467	BREAST	PRIMARY TUMOR	Y	NEGATIVE	NEGATIVE	NEGATIVE	90	TNBC	NEGATIVE	NEGATIVE	NEGATIVE	80	TNBC
PDX473	BREAST	PRIMARY TUMOR	N	NE	NE	NE	NE	NE	NEGATIVE	NEGATIVE	NEGATIVE	80	TNBC
PDX474.1	BREAST	PRIMARY TUMOR	Y	POSITIVE	POSITIVE	NEGATIVE	80	LUMINAL B	POSITIVE	POSITIVE	NEGATIVE	60	LUMINAL B
PDX474.2	BREAST	PRIMARY TUMOR	Y	POSITIVE	POSITIVE	NEGATIVE	90	LUMINAL B	POSITIVE	POSITIVE	NEGATIVE	85	LUMINAL B
PDX474.7	SKIN	METASTASES	N	NE	NE	NE	NE	NE	POSITIVE	POSITIVE	NEGATIVE	75	LUMINAL B
PDX509	LYMPH NODE	METASTASES	Y	NEGATIVE	NEGATIVE	NEGATIVE	75	TNBC	POSITIVE (1%)	NEGATIVE	NEGATIVE	70	LUMINAL B
PDX539	BREAST	PRIMARY TUMOR	Y	NEGATIVE	NEGATIVE	NEGATIVE	90	TNBC	NEGATIVE	NEGATIVE	NEGATIVE	60	TNBC
PDX549	BREAST	PRIMARY TUMOR	Y	NEGATIVE	NEGATIVE	NEGATIVE	95	TNBC	POSITIVE	NEGATIVE	NEGATIVE	80	LUMINAL B
STG201	BREAST	PRIMARY TUMOR	NA	NA	NA	NA	NA	NA	POSITIVE	NEGATIVE	NEGATIVE	90	TNBC
STG316	BREAST	PRIMARY TUMOR	NA	NA	NA	NA	NA	NA	NEGATIVE	NEGATIVE	NEGATIVE	90	TNBC

Supplementary Table 3. Clinical and demographic characteristics of patients from which PDXs were generated. Modified from *Pellegrino and Herencia et al.,*

ID_PDX	PATIENT'S TREATMENTS LIST	GENDER	TUMOR_TYPE	pTNM	ER_status	PR_status	HER2_status	Ki67%	MOLECULAR_SUBTYPE_ST_GALLEN	PRE-PDX_NEOADJ_TREAT	PRE-PDX_ADJ_TREAT	PRE-PDX_MET_TREAT	RELEVANT PATIENT VS PDX TREATMENT	TIME-POINT OF IMPLANTATION VS RELEVANT TREATMENT	NUMBER OF TREATMENT LINES BETWEEN PDX IMPLANTATION AND RELEVANT TREATMENT	PATIENT'S BEST RESPONSE TO RELEVANT TREATMENT	PDX RESPONSE TO RELEVANT TREATMENT
PDX044	DOXORUBICIN + CYCLOPHOSPHAMIDE + DOCETAXEL + RADIOTHERAPY; CT TCD11418 (NCT 01045304); CAPECITABINE + VINORELBINE	FEMALE	BREAST	TXNXM0	NEGATIVE	NEGATIVE	NEGATIVE	30	TNBC	-	DOXORUBICIN + CYCLOPHOSPHAMIDE + DOCETAXEL + RADIOTHERAPY	CT TCD11418 (NCT01045304)	CT TCD11418 (NCT01045304: CARBOPLATIN + INIPARIB + GEMCITABINE)	WHILE ON TREATMENT (C2D1)	0	SENSITIVE (PR)	PD (CISPLATIN)
PDX060	DOXORUBICIN + CYCLOPHOSPHAMIDE; DOCETAXEL; CAPECITABINE + RADIOTHERAPY; TAMOXIFEN; CT CBKM 120X2101 (NCT01068483)	FEMALE	BREAST	T4N2M0	POSITIVE	NEGATIVE	NEGATIVE	10	LUMINAL A	DOXORUBICIN + CYCLOPHOSPHAMIDE; DOCETAXEL	-	CAPECITABINE + RADIOTHERAPY; TAMOXIFEN	-	-	-	-	-
PC-PDX060	GEMCITABINE + OXALIPLATIN; CT POLO (NCT02184195); GEMCITABINE + OXALIPLATIN	MALE	PANCREAS	TXNXM1	-	-	-	-	-	-	-	-	OLAPARIB	PRE	1	SENSITIVE (SD for 6 months)	PD (OLAPARIB)
PC-PDX064	FOLFIRINOX; NAB-PACLITAXEL; GEMCITABINE; OLAPARIB; ATEZOLIZUMAB	FEMALE	PANCREAS	TXNXM1	-	-	-	-	-	-	-	-	OLAPARIB	PRE	0	RESISTANT (PD)	PD (OLAPARIB)
PDX071	DOXORUBICIN + CYCLOPHOSPHAMIDE; DOCETAXEL + CARBOPLATIN + RADIOTHERAPY; TAMOXIFEN; LETROZOL	FEMALE	BREAST	T3N2M0	POSITIVE	POSITIVE	NEGATIVE	30	LUMINAL B	-	-	-	DOXORUBICIN + CYCLOPHOSPHAMIDE + DOCETAXEL + CARBOPLATIN	PRE	0	SENSITIVE (No relapse >10y)	CR (CISPLATIN)
PDX093	DOXORUBICIN + CYCLOPHOSPHAMIDE; DOCETAXEL	FEMALE	BREAST	T2N0M0	NEGATIVE	NEGATIVE	NEGATIVE	30	TNBC	-	-	-	-	-	-	-	-
PDX094	DOXORUBICIN + CYCLOPHOSPHAMIDE; DOCETAXEL; CAPECITABINE + GEMCITABINE; TAMOXIFEN; RADIOTHERAPY; PACLITAXEL + BEVACIZUMAB; CT MO22998 (NCT01250379); CAPECITABINE + VINORELBINE	FEMALE	BREAST	T2N1M0	POSITIVE	NEGATIVE	NEGATIVE	20	LUMINAL B	-	-	-	-	-	-	-	-
PDX098	DOXORUBICIN + CYCLOPHOSPHAMIDE; PACLITAXEL; RADIOTHERAPY; LETROZOL; CAPECITABINE + VINORELBINE; CARBOPLATIN + GEMCITABINE; CT ET-B-031-10 (EUDRACT 2010-022968-13)	FEMALE	BREAST	T1N1M0	POSITIVE	NEGATIVE	NEGATIVE	80	LUMINAL B	DOXORUBICIN + CYCLOPHOSPHAMIDE; PACLITAXEL	-	-	CARBOPLATIN + GEMCITABINE	PRE	2	RESISTANT (PD)	PD (CISPLATIN)
PDX102	LETROZOL	FEMALE	BREAST	T1N0M0	POSITIVE	POSITIVE	NEGATIVE	90	LUMINAL B	-	-	-	-	-	-	-	-
PDX124	DOXORUBICIN + DOCETAXEL; CISPLATIN + VINORELBINE + RADIOTHERAPY; PACLITAXEL + BEVACIZUMAB; VINORELBINE + CAPECITABINE + BEVACIZUMAB; CISPLATIN + OLAPARIB (CT D0810C00021 (NCT00782574)); CT L00070 IN 308 B0 (NCT01091168); DOXORUBICIN	FEMALE	BREAST	T3N1M0	NEGATIVE	NEGATIVE	NEGATIVE	NE	TNBC	DOXORUBICIN + DOCETAXEL	CISPLATIN + VINORELBINE + RADIOTHERAPY	PACLITAXEL + BEVACIZUMAB; VINORELBINE + CAPECITABINE + BEVACIZUMAB	CISPLATIN + OLAPARIB	PRE	0	SENSITIVE (PR)	CR (CISPLATIN); SD (OLAPARIB)
PDX127	DOXORUBICIN + CYCLOPHOSPHAMIDE + DOCETAXEL; RADIOTHERAPY; CISPLATIN + OLAPARIB (CT D0810C00021 (NCT00782574)); CAPECITABINE + RADIOTHERAPY; RADIOTHERAPY; PACLITAXEL	FEMALE	BREAST	T2N0M0	NEGATIVE	NEGATIVE	NEGATIVE	NE	TNBC	DOXORUBICIN + CYCLOPHOSPHAMIDE + DOCETAXEL	RADIOTHERAPY	-	CISPLATIN + OLAPARIB	PRE	0	SENSITIVE (PR)	PR (CISPLATIN); PD (OLAPARIB)
PDX137	5-FLUOROURACIL + EPIRUBICINE + CYCLOPHOSPHAMIDE + DOCETAXEL; RADIOTHERAPY; PACLITAXEL + BEVACIZUMAB; CARBOPLATIN + INIPARIB + GEMCITABINE (NCT01045304); CAPECITABINE; PACLITAXEL; VINORELBINE; DOXORUBICIN + CYCLOPHOSPHAMIDE + METHOTREXATE + 5-FLUOROURACIL + BEVACIZUMAB; CT CBKM 120ZES02T/SOLTI-1103 (NCT01629615)	FEMALE	BREAST	T2N1M0	NEGATIVE	NEGATIVE	NEGATIVE	NE	TNBC	5-FLUOROURACIL + EPIRUBICINE + CYCLOPHOSPHAMIDE + DOCETAXEL	RADIOTHERAPY	LITAXEL + BEVACIZUI	CARBOPLATIN + INIPARIB + GEMCITABINE	PRE	0	SENSITIVE (PR)	NA

DEMOGRAPHICS			PATIENT CLINICAL INFORMATION							PATIENT'S TREATMENTS							
ID_PDX	PATIENT'S TREATMENTS LIST	GENDER	TUMOR_TYPE	pTNM	ER_status	PR_status	HER2_status	Ki67%	MOLECULAR_SUBTYPE_ST_GALLEN	PRE-PDX_NEOADJ_TREAT	PRE-PDX_ADJ_TREAT	PRE-PDX_MET_TREAT	RELEVANT PATIENT VS PDX TREATMENT	TIME-POINT OF IMPLANTATION VS RELEVANT TREATMENT	NUMBER OF TREATMENT LINES BETWEEN PDX IMPLANTATION AND RELEVANT TREATMENT	PATIENT'S BEST RESPONSE TO RELEVANT TREATMENT	PDX RESPONSE TO RELEVANT TREATMENT
PDX156	DOXORUBICIN + DOCETAXEL; RADIOTHERAPY; CT D0810C00021 (NCT00782574); CT CTKI258A2202 (NCT00958971); VINORELBINE + CAPECITABINE; GEMCITABINE + PACLITAXEL; CT PAM4743g (NCT01090960); RADIOTHERAPY; CYCLOPHOSPHAMIDE + METHOTREXATE + 5-FLUOROURACIL	FEMALE	BREAST	TXNXM1	NEGATIVE	POSITIVE	NEGATIVE	20	LUMINAL B	-	-	CT D0810C00021 (NCT00782574); CT CTKI258A2202 (NCT00958971); VINORELBINE + CAPECITABINE; GEMCITABINE + PACLITAXEL; CT PAM4743g (NCT01090960)	-	-	-	-	-
PDX173	DOCETAXEL + CARBOPLATIN + TRASTUZUMAB; RADIOTHERAPY; LETROZOLE; changed to EXEMESTANE; changed to ANASTROZOLE; TRIPTORELINE; CT MO28230 (TDM1) (NCT01702558); CT NALA (CAPECITABINE + NERATINIB) (NCT01808573); TRASTUZUMAB + VINORELBINE; TRASTUZUMAB + PACLITAXEL; CT DS-8201-A-U201 (TDM1) (NCT03248492); CT TULIP (SYD985) (NCT03262935)	FEMALE	BREAST	TXNXM1	POSITIVE	POSITIVE	POSITIVE	20	HER2	-	-	-	DOCETAXEL + CARBOPLATIN + TRASTUZUMAB	PRE	0	SENSITIVE (PR)	CR (CISPLATIN)
PDX179	CAPECITABINE; CISPLATIN; OLAPARIB (CT D0810C00042 (NCT01078662)); 5-FLUOROURACIL + BEVACIZUMAB; RADIOTHERAPY; IRINOTECAN	FEMALE	BREAST	T1N0M0	NEGATIVE	NEGATIVE	NEGATIVE	NE	TNBC	-	CAPECITABINE	CISPLATIN	OLAPARIB	PRE	0	RESISTANT (PD)	PD (OLAPARIB)
PDX168	FOLFIRINOX; GEMCITABINE + ABRAXANE; CISPLATIN + GEMCITABINE; CAPECITABINE; CT PETRAD9720C00001 (NCT04644068)	MALE	PANCREAS	TXNXM1	-	-	-	-	-	-	-	FOLFIRINOX; GEMCITABINE + ABRAXANE; CISPLATIN + GEMCITABINE; CAPECITABINE; CT PETRAD9720C00001 (NCT04644068)	CT PETRA D9720C00001 (NCT04644068) (AZD5305 40mg QD)	ON TREATMENT	0	RESISTANT (PD)	PD (AZD5305)
PDX196	CARBOPLATIN + PACLITAXEL; CARBOPLATIN + BEVACIZUMAB; PACLITAXEL; CARBOPLATIN + DOXORUBICIN; OLAPARIB (CT D0810C00042 (NCT01078662))	FEMALE	OVARY	-	-	-	-	-	HGSOC	CARBOPLATIN + PACLITAXEL	CARBOPLATIN + PACLITAXEL	CARBOPLATIN + PACLITAXEL; CARBOPLATIN + BEVACIZUMAB; PACLITAXEL; CARBOPLATIN + DOXORUBICIN; OLAPARIB (NCT01078662)	OLAPARIB	POST	0	SENSITIVE (PR)	PR (OLAPARIB)
PDX197	CT TCD11419 (NCT01204125); 5-FLUOROURACIL + EPIRUBICINE + CYCLOPHOSPHAMIDE; RADIOTHERAPY; TAMOXIFEN	FEMALE	BREAST	T2N1M0	NEGATIVE	NEGATIVE	NEGATIVE	NE	TNBC	CT TCD11419 (NCT01204125)	-	-	-	-	-	-	-
PDX221	5-FLUOROURACIL + DOXORUBICIN + CYCLOPHOSPHAMIDE + PACLITAXEL; CISPLATIN; TAMOXIFEN; CT ABI-007-MBC-001 (NCT01881230); CT PM1183-B-003-11 (NCT01525589); RADIOTHERAPY	FEMALE	BREAST	T2N0M0	POSITIVE	NEGATIVE	NEGATIVE	90	LUMINAL B	5-FLUOROURACIL + DOXORUBICIN + CYCLOPHOSPHAMIDE + PACLITAXEL	-	-	CISPLATIN	PRE	0	RESISTANT* (2 years until metastatic relapse)	PD (CISPLATIN)
PDX230	DOXORUBICIN + CYCLOPHOSPHAMIDE + METHOTREXATE + 5-FLUOROURACIL + PACLITAXEL; RADIOTHERAPY; TAMOXIFEN	FEMALE	BREAST	T3N1M0	POSITIVE	NEGATIVE	NEGATIVE	60	LUMINAL B	DOXORUBICIN + CYCLOPHOSPHAMIDE + METHOTREXATE + 5-FLUOROURACIL + PACLITAXEL	-	-	-	-	-	-	-
PDX236	DOXORUBICIN + CYCLOPHOSPHAMIDE + DOCETAXEL; RADIOTHERAPY; PACLITAXEL + GEMCITABINE; CAPECITABINE; CT 15-102-14 (NCT02915744); CT PM1183-B-003-11 (NCT01525589); CISPLATIN	FEMALE	BREAST	T3N1M0	NEGATIVE	NEGATIVE	NEGATIVE	90	TNBC	DOXORUBICIN + CYCLOPHOSPHAMIDE + DOCETAXEL	RADIOTHERAPY	PACLITAXEL + GEMCITABINE; CAPECITABINE; CT 15-102-14 (NCT02915744)	CISPLATIN	PRE	1	RESISTANT (PD)	PD (CISPLATIN)

DEMOGRAPHICS			PATIENT CLINICAL INFORMATION							PATIENT'S TREATMENTS							
ID_PDX	PATIENT'S TREATMENTS LIST	GENDER	TUMOR_TYPE	pTNM	ER_status	PR_status	HER2_status	Ki67%	MOLECULAR_SUBTYPE_ST_GALLEN	PRE-PDX_NEOADJ_TREAT	PRE-PDX_ADJ_TREAT	PRE-PDX_MET_TREAT	RELEVANT PATIENT VS PDX TREATMENT	TIME-POINT OF IMPLANTATION VS RELEVANT TREATMENT	NUMBER OF TREATMENT LINES BETWEEN PDX IMPLANTATION AND RELEVANT TREATMENT	PATIENT'S BEST RESPONSE TO RELEVANT TREATMENT	PDX RESPONSE TO RELEVANT TREATMENT
PDX252	EPIRUBICIN + DOCETAXEL; RADIOTHERAPY; GEMCITABINE + CARBOPLATIN; CT PM1183-B-003-11 (NCT01525589); VINORELBINE + CAPECITABINE; RADIOTHERAPY	FEMALE	BREAST	T3N1M0	NEGATIVE	NEGATIVE	NEGATIVE	30	TNBC	EPIRUBICIN + DOCETAXEL	RADIOTHERAPY	GEMCITABINE + CARBOPLATIN; CT PM1183-B-003-11 (NCT01525589)	GEMCITABINE + CARBOPLATIN	POST	2	SENSITIVE (PR)	PR (CISPLATIN)
PDX270	CYCLOPHOSPHAMIDE	FEMALE	BREAST	T2N0M0	NEGATIVE	NEGATIVE	NEGATIVE	70	TNBC	-	-	-	-	-	-	-	-
PDX274	DOXORUBICIN + CYCLOPHOSPHAMIDE + DOCETAXEL; CARBOPLATIN + GEMCITABINE; ERIBULIN; DOXORUBICIN; CT PM1183-B-003-11 (NCT01525589)	FEMALE	BREAST	T2N0M0	NEGATIVE	NEGATIVE	NEGATIVE	NE	TNBC	DOXORUBICIN + CYCLOPHOSPHAMIDE + DOCETAXEL	IOPLATIN + GEMCITA	ERIBULIN; DOXORUBICIN	LURBINECTEDIN (NCT01525589)	PRE	0	RESISTANT (PD)	PD (LURBINECTEDIN)
PDX280	CARBOPLATIN + PACLITAXEL; CARBOPLATIN + PACLITAXEL; DOXORUBICIN; PACLITAXEL + BEVACIZUMAB; CT D0810C00021 (NCT00782574); CARBOPLATIN + DOXORUBICIN; GEMCITABINE; PACLITAXEL	FEMALE	OVARY	-	-	-	-	-	HGSOC	-	CARBOPLATIN + PACLITAXEL	CARBOPLATIN + PACLITAXEL; DOXORUBICIN; PACLITAXEL + BEVACIZUMAB; CT D0810C00021 (NCT00782574); RADIOTHERAPY; CARBOPLATIN + DOXORUBICIN; GEMCITABINE; PACLITAXEL	CT D0810C00021 (NCT00782574) (CISPLATIN + OLAPARIB-> OLAPARIB)	POST	0	SENSITIVE (PR)	CR (CISPLATIN); PD (OLAPARIB)
PDX288	PACLITAXEL + CARBOPLATIN + DOXORUBICIN + CYCLOPHOSPHAMIDE; CT OBU-SW-H-02 (NCT02061085); CT DEBIO 1347-101 (NCT01946297); CAPECITABINE + GEMCITABINE; VINORELBINE; CISPLATIN	FEMALE	BREAST	T1N0M0	NEGATIVE	NEGATIVE	NEGATIVE	NE	TNBC	PACLITAXEL + CARBOPLATIN + DOXORUBICIN + CYCLOPHOSPHAMIDE	-	CT OBU-SW-H-02 (NCT02061085)	CISPLATIN	PRE	4	RESISTANT (PD)	PD (CISPLATIN)
PDX291	DOXORUBICIN + CYCLOPHOSPHAMIDE + DOCETAXEL; CYCLOPHOSPHAMIDE + METHOTREXATE + 5-FLUOROURACIL; RADIOTHERAPY; PACLITAXEL + BEVACIZUMAB; CT PCD4989g (NCT01375842)	FEMALE	BREAST	T2N1M0	NEGATIVE	NEGATIVE	NEGATIVE	NE	TNBC	DOXORUBICIN + CYCLOPHOSPHAMIDE + DOCETAXEL	CYCLOPHOSPHAMIDE + METHOTREXATE + 5-FLUOROURACIL	RADIOTHERAPY; PACLITAXEL + BEVACIZUMAB; CT PCD4989g (NCT01375842)	-	-	-	-	-
PDX302	EPIRUBICIN + CYCLOPHOSPHAMIDE + METHOTREXATE + 5-FLUOROURACIL; CISPLATIN + GEMCITABINE; RADIOTHERAPY; CAPECITABINE; CT PCD4989g (NCT01375842); CISPLATIN + GEMCITABINE; CYCLOPHOSHAMIDE + METHOTREXATE; CISPLATIN + GEMCITABINE + PEMBROLIZUMAB; CYCLOPHOSPHAMIDE + METHOTREXATE + 5-FLUOROURACIL; DOXORUBICIN; PACLITAXEL + BEVACIZUMAB; ERIBULINE	FEMALE	BREAST	T4N3M0	NEGATIVE	NEGATIVE	NEGATIVE	60	TNBC	EPIRUBICIN + CYCLOPHOSPHAMIDE + METHOTREXATE + 5-FLUOROURACIL	CISPLATIN + GEMCITABINE; RADIOTHERAPY	CAPECITABINE	CISPLATIN + GEMCITABINE	PRE	1	SENSITIVE (PR)	CR (CISPLATIN)
PDX332	EPIRUBICIN + CYCLOPHOSPHAMIDE + PACLITAXEL; PACLITAXEL; DOXORUBICIN	FEMALE	BREAST	T2N0M0	NEGATIVE	NEGATIVE	NEGATIVE	20	TNBC	EPIRUBICIN + CYCLOPHOSPHAMIDE + PACLITAXEL	PACLITAXEL	DOXORUBICIN	-	-	-	-	-
PDX339	CARBOPLATIN + PACLITAXEL + DOXORUBICIN + CYCLOPHOSPHAMIDE; RADIOTHERAPY; CAPECITABINE + GEMCITABINE	FEMALE	BREAST	T3N1M0	NEGATIVE	NEGATIVE	NEGATIVE	90	TNBC	CARBOPLATIN + PACLITAXEL + DOXORUBICIN + CYCLOPHOSPHAMIDE	RADIOTHERAPY	-	CARBOPLATIN + PACLITAXEL + DOXORUBICIN + CYCLOPHOSPHAMIDE	POST	0	RESISTANT (PR, NON-pCR)	PD (CISPLATIN)
PDX341	DOXORUBICIN + CYCLOPHOSPHAMIDE + DOCETAXEL; RADIOTHERAPY; CARBOPLATIN; CT PM1183-B-003-11 (NCT01525589); ERIBULINE; PACLITAXEL	FEMALE	BREAST	T2N1M0	NEGATIVE	NEGATIVE	NEGATIVE	60	TNBC	DOXORUBICIN + CYCLOPHOSPHAMIDE + DOCETAXEL	RADIOTHERAPY	CARBOPLATIN	CARBOPLATIN	POST	0	RESISTANT (PD)	PD (CISPLATIN)
PDX350	PACLITAXEL + ADRIAMYCIN; CAPECITABINE + VINORELBINE; ERIBULINE; CISPLATIN + GEMCITABINE; EXEMESTANE + DECAPEPTYL; CT POSEIDON (GDC0032 + TAMOXIFEN) (NCT02285179); FULVESTRANT + PALBOCICLIB; CYCLOPHOSPHAMIDE + METHOTREXATE + FLUOROURACIL; DOCETAXEL + GEMCITABINE	FEMALE	BREAST	TXNXM1	POSITIVE	POSITIVE	NEGATIVE	-	LUMINAL	-	-	PACLITAXEL + ADRIAMYCIN; CAPECITABINE + VINORELBINE	CISPLATIN + GEMCITABINE	PRE	1	SENSITIVE (SD for more than 6 months, in treatment with Cisplatin + Gemcitabine)	PR (CISPLATIN)
PDX377	CT NEOERIBULINE (ERIBULINE) (NCT01669252); DOXORUBICIN + CYCLOPHOSPHAMIDE + METHOTREXATE + 5-FLUOROURACIL; RADIOTHERAPY	FEMALE	BREAST	T1N0M0	NEGATIVE	NEGATIVE	NEGATIVE	70	TNBC	CT NEOERIBULINE (ERIBULINE) (NCT01669252)	-	-	-	-	-	-	-

DEMOGRAPHICS			PATIENT CLINICAL INFORMATION							PATIENT'S TREATMENTS							
ID_PDX	PATIENT'S TREATMENTS LIST	GENDER	TUMOR_TYPE	pTNM	ER_status	PR_status	HER2_status	Ki67%	MOLECULAR_SUBTYPE_ST_GALLEN	PRE-PDX_NEOADJ_TREAT	PRE-PDX_ADJ_TREAT	PRE-PDX_MET_TREAT	RELEVANT PATIENT VS PDX TREATMENT	TIME-POINT OF IMPLANTATION VS RELEVANT TREATMENT	NUMBER OF TREATMENT LINES BETWEEN PDX IMPLANTATION AND RELEVANT TREATMENT	PATIENT'S BEST RESPONSE TO RELEVANT TREATMENT	PDX RESPONSE TO RELEVANT TREATMENT
PDX384	ADRIAMYCIN + CYCLOPHOSPHAMIDE + DOCETAXEL; CT BRAVO (CAPECITABINE) (NCT01905592); ERIBULINE; CT VIOLETTE (OLAPARIB) (NCT03330847); CT GO30103 (TIRAGOLUMAB + ATEZOLIZUMAB) (NCT02794571); CT J1F-MC-JZFA (LY3405105) (NCT03770494); CARBOPLATIN; DOXORUBICIN + CYCLOPHOSPHAMIDE	FEMALE	BREAST	T2N1M0	NEGATIVE	NEGATIVE	NEGATIVE	35	TNBC	ADRIAMYCIN + CYCLOPHOSPHAMIDE + DOCETAXEL	-	-	OLAPARIB	PRE	2	SENSITIVE (SD for 13 months)	SD (OLAPARIB)
PDX397	CARBOPLATIN + PACLITAXEL; CARBOPLATIN + DOXORUBICIN; CT ATOM D6500C00001 (AZD0156 + OLAPARIB) (NCT02588105); PACLITAXEL	FEMALE	OVARY	TXNXM1	-	-	-	-	-	-	-	CARBOPLATIN + PACLITAXEL; CARBOPLATIN + DOXORUBICIN	AZD0156 + OLAPARIB	PRE	0	RESISTANT (PD)	PD (OLAPARIB)
PDX405	NA	NA	NA	NA	NA	NA	NA	NA	NA	NA	NA	NA	NA	NA	NA	NA	NA
PDX418	PACLITAXEL + GEMCITABINE; CT EMBRACA (TALAZOPARIB) (NCT01945775); CARBOPLATIN + GEMCITABINE; CAPECITABINE; ERIBULINE; DOXORUBICIN; DOCETAXEL; CT 1280.18 (ABEMACICLIB + XENTUZUMAB) (NCT03099174)	FEMALE	BREAST	T4N2M1	POSITIVE	NEGATIVE	NEGATIVE	60	LUMINAL B	-	-	PACLITAXEL + GEMCITABINE; CT EMBRACA (TALAZOPARIB) (NCT01945775); CARBOPLATIN + GEMCITABINE; CAPECITABINE; ERIBULINE; DOXORUBICIN; DOCETAXEL	TALAZOPARIB	POST	4	RESISTANT (PD)	PD (OLAPARIB)
PDX427	ADRIAMYCIN + CYCLOPHOSPHAMIDE + PACLITAXEL; TAMOXIFEN; DOCETAXEL + BEVACIZUMAB; CAPECITABINE + BEVACIZUMAB; CT MK3475-119 (ERIBULINE) (NCT02555657); CT CPDR001X2101 (PDR001) (NCT02404441); CARBOPLATIN (changed to CISPLATIN) + GEMCITABINE; CT IMMU-132-01 (SACITUZUMAB GOVITECAN) (NCT01631552); DOXORUBICIN; NAB-PACLITAXEL; CYCLOPHOSPHAMIDE + METHOTREXATE; VINORELBINE; IRINOTECAN; ETOPOSIDE; EC MASTERKEY-318 (T-VEC + PEMBROLIZUMAB) (NCT02509507)	FEMALE	BREAST	T2N1M0	POSITIVE	NEGATIVE	NEGATIVE	60	LUMINAL B	ADRIAMYCIN + CYCLOPHOSPHAMIDE + PACLITAXEL	TAMOXIFEN	DOCETAXEL + BEVACIZUMAB; CAPECITABINE + BEVACIZUMAB; CT MK3475-119 (ERIBULINE) (NCT02555657); CT CPDR001X2101 (PDR001) (NCT02404441)	CARBOPLATIN (changed to CISPLATIN) + GEMCITABINE	PRE	0	RESISTANT (PD)	PD (CISPLATIN)
PDX432	CT NEOERIBULINE (ERIBULINE) (NCT01669252); DOCETAXEL + ADRIAMYCIN + CYCLOPHOSPHAMIDE; CAPECITABINE + VINORELBINE; CARBOPLATIN + GEMCITABINE; DOXORUBICIN; PACLITAXEL; CT ASCENT (NCT02574455); CARBOPLATIN + PACLITAXEL + ETOPOSIDE	FEMALE	BREAST	T2N0M0	NEGATIVE	NEGATIVE	NEGATIVE	80	TNBC	CT NEOERIBULINE (ERIBULINE) (NCT01669252)	DOCETAXEL + ADRIAMYCIN + CYCLOPHOSPHAMIDE	CAPECITABINE + VINORELBINE; CARBOPLATIN + GEMCITABINE	CARBOPLATIN + GEMCITABINE	POST	0	SENSITIVE (PR)	PD (CISPLATIN)
PDX440	ADRIAMYCIN + CYCLOPHOSPHAMIDE + PACLITAXEL; CAPECITABINE	FEMALE	BREAST	T4N1M0	NEGATIVE	NEGATIVE	NEGATIVE	40	TNBC	ADRIAMYCIN + CYCLOPHOSPHAMIDE + PACLITAXEL	CAPECITABINE	-	-	-	-	-	-
PDX445	CARBOPLATIN + PACLITAXEL; CARBOPLATIN + PACLITAXEL; CARBOPLATIN + DOXORUBICIN; CARBOPLATIN + DOXORUBICIN; CT ATOM D6500C00001 (AZD0156 + OLAPARIB) (NCT02588105)	FEMALE	OVARY	TXNXM0	-	-	-	-	-	-	CARBOPLATIN + PACLITAXEL	CARBOPLATIN + PACLITAXEL; CARBOPLATIN + DOXORUBICIN; CARBOPLATIN + DOXORUBICIN	AZD0156 + OLAPARIB	PRE	0	RESISTANT (PD)	PD (OLAPARIB)
PDX453	EPIRUBICIN + CYCLOPHOSPHAMIDE + PACLITAXEL; CAPECITABINE + BEVACIZUMAB; ERIBULINE; CARBOPLATIN + GEMCITABINE; CT PDR001X2102 (PDR001 + LCL161) (NCT02890069); DOXORUBICIN + CISPLATIN + FLUOROURACIL + FOLINIC ACID; CARBOPLATIN	FEMALE	BREAST	T3N1M0	NEGATIVE	NEGATIVE	NEGATIVE	90	TNBC	EPIRUBICIN + CYCLOPHOSPHAMIDE + PACLITAXEL	-	CAPECITABINE + BEVACIZUMAB; ERIBULINE; CARBOPLATIN + GEMCITABINE	CARBOPLATIN + GEMCITABINE	POST	0	RESISTANT (PD)	PD (CISPLATIN)

DEMOGRAPHICS			PATIENT CLINICAL INFORMATION							PATIENT'S TREATMENTS							
ID_PDX	PATIENT'S TREATMENTS LIST	GENDER	TUMOR_TYPE	pTNM	ER_status	PR_status	HER2_status	Ki67%	MOLECULAR_SUBTYPE_ST_GALLEN	PRE-PDX_NEOADJ_TREAT	PRE-PDX_ADJ_TREAT	PRE-PDX_MET_TREAT	RELEVANT PATIENT VS PDX TREATMENT	TIME-POINT OF IMPLANTATION VS RELEVANT TREATMENT	NUMBER OF TREATMENT LINES BETWEEN PDX IMPLANTATION AND RELEVANT TREATMENT	PATIENT'S BEST RESPONSE TO RELEVANT TREATMENT	PDX RESPONSE TO RELEVANT TREATMENT
PDX457	EPIRUBICINE + PACLITAXEL + CYCLOPHOSPHAMIDE; DOCETAXEL + BEVACIZUMAB; CARBOPLATIN + GEMCITABINE	FEMALE	BREAST	T2N1M0	POSITIVE (MILD)	NEGATIVE	NEGATIVE	80	TNBC	EPIRUBICINE + PACLITAXEL + CYCLOPHOSPHAMIDE	-	-	CARBOPLATIN + GEMCITABINE	PRE	1	RESISTANT (PD)	CR (CISPLATIN)
PDX467	DOXORUBICIN + CYCLOPHOSPHAMIDE + CARBOPLATIN + PACLITAXEL; CAPECITABINE; RADIOTHERAPY; CAPECITABINE + GEMCITABINE; ERIBULINE; DOCETAXEL + GEMCITABINE	FEMALE	BREAST	T4N3M0	NEGATIVE	NEGATIVE	NEGATIVE	70	TNBC	DOXORUBICIN + CYCLOPHOSPHAMIDE + CARBOPLATIN + PACLITAXEL	-	-	DOXORUBICIN + CYCLOPHOSPHAMIDE + CARBOPLATIN + PACLITAXEL	POST	0	RESISTANT (PR, NON-pCR)	PD (CISPLATIN)
PDX473	DOCETAXEL + DOXORUBICIN; MYOCET + CYCLOPHOSPHAMIDE; CT LUCY (OLAPARIB) (NCT03286842); CARBOPLATIN + GEMCITABINE; PACLITAXEL + ERIBULINE; CAPECITABINE + VINORELBINE	FEMALE	BREAST	T4N3M0	NEGATIVE	NEGATIVE	NEGATIVE	NA	TNBC	DOCETAXEL + DOXORUBICIN	-	-	OLAPARIB	PRE	1	RESISTANT (PD)	CR (OLAPARIB)
PDX474.1	LETROZOLE + PALBOCICLIB; PACLITAXEL + BEVACIZUMAB; TALAZOPARIB; CAPECITABINE changed to CARBOPLATIN + GEMCITABINE; DOCETAXEL + GEMCITABINE	FEMALE	BREAST	T4N3M1	POSITIVE	POSITIVE	NEGATIVE	80	LUMINAL B	-	-	-	TALAZOPARIB	PRE	2	SENSITIVE (SD)	PR (OLAPARIB)
PDX474.2	LETROZOLE + PALBOCICLIB; PACLITAXEL + BEVACIZUMAB; TALAZOPARIB; CAPECITABINE changed to CARBOPLATIN + GEMCITABINE; DOCETAXEL + GEMCITABINE	FEMALE	BREAST	T4N3M1	POSITIVE	POSITIVE	NEGATIVE	80	LUMINAL B	-	-	-	TALAZOPARIB	PRE	1	SENSITIVE (SD)	PR (OLAPARIB)
PDX474.7	LETROZOLE + PALBOCICLIB; PACLITAXEL + BEVACIZUMAB; TALAZOPARIB; CAPECITABINE changed to CARBOPLATIN + GEMCITABINE; DOCETAXEL + GEMCITABINE	FEMALE	BREAST	T4N3M1	POSITIVE	POSITIVE	NEGATIVE	80	LUMINAL B	-	-	LETROZOLE + PALBOCICLIB; PACLITAXEL + BEVACIZUMAB; TALAZOPARIB	TALAZOPARIB	POST	0	SENSITIVE (SD)	PD (OLAPARIB)
PDX509	ADRIAMYCIN + CYCLOPHOSPHAMIDE + PACLITAXEL; CARBOPLATIN; CT IMMU-132-01 (SACITUZUMAB GOVITECAN) (NCT01631552); CAPECITABINE	FEMALE	BREAST	T4N1M1	NEGATIVE	NEGATIVE	NEGATIVE	32	TNBC	-	-	ADRIAMYCIN + CYCLOPHOSPHAMIDE + PACLITAXEL; CARBOPLATIN	CARBOPLATIN	POST	0	RESISTANT (PD)	PD (CISPLATIN)
PDX539	DOCETAXEL + CYCLOPHOSPHAMIDE	FEMALE	BREAST	T1N0M0	NEGATIVE	NEGATIVE	NEGATIVE	90	TNBC	-	-	-	-	-	-	-	-
PDX549	CARBOPLATIN + PACLITAXEL + DOXORUBICIN + CYCLOPHOSPHAMIDE; DOCETAXEL (changed to CAPECITABINE) + BEVACIZUMAB; CT IMMU-132-05 (NCT02574455); CARBOPLATIN + GEMCITABINE	FEMALE	BREAST	T2N0M0	NEGATIVE	NEGATIVE	NEGATIVE	85	TNBC	CARBOPLATIN + PACLITAXEL + DOXORUBICIN + CYCLOPHOSPHAMIDE	-	-	CARBOPLATIN + PACLITAXEL + DOXORUBICIN + CYCLOPHOSPHAMIDE	POST	0	RESISTANT (PR, NON-pCR)	-
STG201	FEC/T (5-FU, EPIRUBICIN,CYCLOPHOSPHAMIDE, DOCETAXEL), RADIOTHERAPY, CARBOPLATIN+GEMCITABINE, CAPECITABINE	FEMALE	BREAST	NA	NEGATIVE	NA	NEGATIVE	NA	TNBC	FEC/T (5-FU, EPIRUBICIN,CYCLOPHOSPHAMIDE, DOCETAXEL)	-	-	CARBOPLATIN + GEMCITABINE	PRE	0	SENSITIVE** (treatment duration 5.3 months)	CR (CISPLATIN)
STG316	FEC/T (3 cycles), CISPLATIN (1 cycle), CARBOPLATIN AUC 6 (2 cycles)	FEMALE	BREAST	NA	NEGATIVE	NEGATIVE	NEGATIVE	NA	TNBC	FEC/T (3 cycles), CISPLATIN (1 cycle), CARBOPLATIN AUC 6 (2 cycles)	-	-	CISPLATIN; CARBOPLATIN	POST	0	RESISTANT (PD, NON-pCR)	PD

Supplementary Table 4. Characterization of PDX models of ductal carcinoma *in situ* (DCIS).

PDX						Patient			
ID	Molecular subtype	RAD51 score (%)	BRCA1 score (%)	γ-H2AX score (%)	Invasion	ID	RAD51 score (%)	BRCA1 score (%)	γ-H2AX score (%)
20-HUT-450-1	HR+	92,4	47,5	81,6	Yes	T19-04980	12	46,6	50
20-HUT-633-1	NA	90	95	97,5	NA	NA	NA	NA	NA
20-HUT-844-1	NA	64	85	92,5	NA	NA	NA	NA	NA
19-HUT-378-1	HR+	52,94118	81,3	85,71429	Yes	T19-04192	13	2,5	40
19-HUT-277-1	HR+	43,24324	24,1	54,54	Yes	T18-11629	15	60	45
20-HUT-711-1	HR+	40,4	95	87,5	Yes	T19-09180	30	16,7	30
20-HUT-631-1	HER2+	40	41,6	87,5	Yes	T19-06033	0	2	33,3
19-HUT-237-1	NA	39,28571	NE	100	NA	NA	NA	NA	NA
18-HUT-240-1	NA	37,93103	36,8	68,7	NA	NA	NA	NA	NA
19-HUT-161-1	NA	34,84848	53,3	81,6	NA	NA	NA	NA	NA
19-HUT-093-1	NA	31,25	38,9	65	NA	NA	NA	NA	NA
20-HUT-610-1	NA	27,6	63,3	90	NA	NA	NA	NA	NA
19-HUT-274-1	HER2+	25,31646	21,2	76	Yes	T19-01392	24	12,5	65
19-HUT-240-4	NA	24,63768	85	45	NA	NA	NA	NA	NA
19-HUT-303-1	HR+	22,5	62	50	No	T19-02369	35	80	34
19-HUT-238-1	TNBC	17,91045	67,5	85	Yes	T19-02185	21	19,5	98,8
19-HUT-140-1	HR+	11.7	62,5	62	No	T18-03761	4,5	4	41,6
19-HUT-124-3	TNBC	6,349206	14,9	40	No	T18-03567	5	40	52,5
18-HUT-220-1	HR+	4,054054	40	50	No	T18-04175	38	60	55
19-HUT-373-1	NA	3,88	2	98	NA	NA	NA	NA	NA
19-HUT-426-1	HR+	0,9174312	56,6	92	Yes	T18-10669	55	50	16,25
19-HUT-121-1	NA	0	0	50	NA	NA	NA	NA	NA

Supplementary Table 5. Clinical and molecular characteristics of the PDX cohort used to evaluate the AZD5305 antitumour activity alone or in combination with carboplatin or an TR inhibitor (AZD6738).

PDX	Primary/Metastatic (P/M) tumor	Cancer subtype	Patient previous treatment	HRR alteration	cDNA change	AA change	Domain	Variant effect	RAD51 (%)	BRCA1 (%)	Mechanism of Resistance to PARPi
PDX168	M	PaC	Yes	*PALB2*	c.1965dupT	p.P656fs	Ring	Frameshift	38	94	No gsLOH
PDX474.2OR2	M	ER+	Yes	*BRCA2*	c.3922G>T	p.E1308*	Non recognized domain region	Nonsense	43	65	BRCA2 reversion (c.3848_3931delTAAGTGAAAAAAATAATAAATGCCAACTGATATTACAAAATAATATTGAAATGACTACTGGCACTTTTGTTGAAGAAATTACTG)
PDX474.7	M	ER+	Yes	*BRCA2*	c.3922G>T	p.E1308*	Non recognized domain region	Nonsense	18	89	Hypomorphic BRCA2 protein
PDX230OR5	P	TNBC	Yes	*BRCA1*	c.185delAG	p.E23fs	Ring	Frameshift	11	0,5	Unknown
PDX173OR3	P	HER2+	Yes	*BRCA2*	c.9808delG	p.A3270Pfs*5	NLS	Nonsense	33	82,5	-
PDX127	M	TNBC	Yes	*BRCA1*	c.185delAG	p.E23fs	Ring	Frameshift	16,3	0	53BP1 pathway dysregulation (FAM35A homodel)
PDX341	M	TNBC	Yes	*BRCA1*	c.2404delGA	p.R762fs	Exon 11	Frameshift	16,7	29	Low SHLD1 mRNA expression
PDX196	M	OvC	Yes	*BRCA1*	c.1961delA	p.K654fs	Exon 11	Frameshift	28,3	68	-
PDX179	M	TNBC	Yes	*BRCA1*	c.185delAG	p.E23fs	Ring	Frameshift	22	7	Unknown
PDX173	P	HER2+	Yes	*BRCA2*	c.9808delG	p.A3270Pfs*5	NLS	Nonsense	0	29	-
PDX474.2	M	ER+	Yes	*BRCA2*	c.3922G>T	p.E1308*	Non recognized domain region	Nonsense	0	45	-
PDX124	M	TNBC	Yes	*BRCA1*	c.1961delA	p.K654fs	Exon 11	Frameshift	8,3	10	-
PDX230	P	TNBC	Yes	*BRCA1*	c.185delAG	p.E23fs	Ring	Frameshift	0,3	0	-

Supplementary Table 6. Molecular characteristics of tumors with acquired resistance to AZD5305 and olaparib.

ID	PDX	Treat-ment	Disease progression	Stop treatment ?	CR/PR treatment discontinuation	Day of best response	RAD51 (%)	BRCA1 (%)	γ-H2AX (%)	Exome sequencing	Targeted sequencing	RNA-sequencing	Mechanism of resistance to PARPi	53BP1 IF (+/-/heterogeneous)	Reversion mutation cDNA change	Reversion mutation AA change	VAF reversion mutation (%)	MMEJ signature (microhomology regions)	Fraction of mutations unique to resistant
1	124	Olaparib	14	No	-	10	11,6	13,8	65	Yes	No	Yes	SHLD3 mutation (c.426_432delTAAAAAC, VAF: 0.2)	+	-	-	-	-	2
2	124	Olaparib	44	No	-	39	22,5	55	90	Yes	No	No	Hypomorphic BRCA1	+	-	-	-	-	0
3	124	Olaparib	84	No	-	57	40	42,5	72,5	Yes	No	No	Reversion mutation	+	c.2037_2053delGAAGAGTAACAAGCCAA	p.K680fs	29	6 bp	1
4	124	Olaparib	84	No	-	74	17,5	50	80	Yes	No	Yes	Hypomorphic BRCA1	+	-	-	-	-	1
5	124	Olaparib	113	No	-	36	27,5	97,5	90	Yes	No	Yes	Hypomorphic BRCA1	+	-	-	-	-	3
6	124	Olaparib	113	No	-	46	16,6	50	75	Yes	No	No	Hypomorphic BRCA1	+	-	-	-	-	1
7	124	Olaparib	113	No	-	57	20	40	80	Yes	No	No	Hypomorphic BRCA1	+	-	-	-	-	0
8	124	Olaparib	119	No	-	80	20	12,5	50	Yes	No	Yes	Unknown	+	-	-	-	-	1
9	124	Olaparib	122	No	-	46	35	27,5	92,5	No	Yes	No	Hypomorphic BRCA1	+	-	-	-	-	
10	230	Olaparib	70	Yes	36	25	26,7	0	75	Yes	No	Yes	Unknown	+	-	-	-	-	3
11	230	Olaparib	77	Yes	36	25	10	0	70	Yes	No	No	Unknown	+	-	-	-	-	4
12	230	Olaparib	77	Yes	36	28	20	1	37,5	Yes	No	No	Unknown	+	-	-	-	-	4
13	230	Olaparib	98	Yes	36	22	NA*	NA*	NA*	No	No	No	Unknown	NA*	-	-	-	-	-
14	230	Olaparib	126	Yes	36	36	11,25	7,5	92,5	No	No	No	Unknown	+	-	-	-	-	-
15	230	Olaparib	264	Yes	127	40	13,3	0	45	Yes	No	Yes	Unknown	+	-	-	-	-	2
16	341	Olaparib	26	No	-	16	50	52,5	27,5	No	No	No	Hypomorphic BRCA1	NA*	-	-	-	-	-
17	341	Olaparib	30	No	-	19	62,5	42,5	40	No	No	No	Unknown	+	-	-	-	-	-
18	341	Olaparib	69	No	-	32	30	20	82,5	No	No	No	Unknown	+	-	-	-	-	-
19	341	Olaparib	79	No	-	16	42,5	45	95	No	No	No	Hypomorphic BRCA1	+	-	-	-	-	-
20	341	Olaparib	90	No	-	40	30	90	80	No	No	No	Hypomorphic BRCA1	+	-	-	-	-	-
21	341	Olaparib	98	No	-	24	50	80	100	Yes	No	Yes	Hypomorphic BRCA1	+	-	-	-	-	0
22	341	Olaparib	98	No	-	38	60	45	85	Yes	No	Yes	Hypomorphic BRCA1	+	-	-	-	-	3
23	341	Olaparib	101	No	-	24	22,5	30	47,5	No	No	No	Unknown	+	-	-	-	-	-
24	341	Olaparib	116	No	-	38	55	50	90	No	No	No	Hypomorphic BRCA1	+	-	-	-	-	-
25	341	Olaparib	119	No	-	44	45	70	95	Yes	No	Yes	Hypomorphic BRCA1	+	-	-	-	-	3
26	474.2	Olaparib	50	No	-	28	51,2	100	85	Yes	Yes	Yes	Reversion mutation	Not done	c.3848_3931delTAAGTGAAAAAAATAATAAATGCCAACTGATATTACAAAATAATATTGAAATGACTACTGGCACTTTTGTTGAAGAAATTACTG	p.V1283_T1310del	40	4 bp	3
27	474.2	Olaparib	78	No	-	32	67,5	77,5	60	Yes	No	Yes	Reversion mutation	Not done	c.3922G>C	p.E1308Q	41	-	3

ID	PDX	Treat-ment	Disease progression	Stop treatment ?	CR/PR treatment discontinuation	Day of best response	RAD51 (%)	BRCA1 (%)	y-H2AX (%)	Exome sequencing	Targeted sequencing	RNA-sequencing	Mechanism of resistance to PARPi	53BP1 IF (+/-/heterogeneous)	Reversion mutation cDNA change	Reversion mutation AA change	VAF reversion mutation (%)	MMEJ signature (microhomology regions)	Fraction of mutations unique to resistant
28	474.2	Olaparib	85	No	-	32	93,7	90	97,5	Yes	No	No	Reversion mutation	Not done	c.3750_4157del	p.E1250_S1385del	64	2 bp	14
29	474.2	Olaparib	92	No	-	28	55	75	95	Yes	Yes	No	Reversion mutation	Not done	c.3908_3952delGCACTTTTGTTGAAGAAATTACTGAAAATTACAAGAGAAATACTG	p.G1303_T1317del	17	5 bp	4
30	474.2	Olaparib	113	No	-	28	50	80	97,5	Yes	No	No	Unknown	Not done	-	-	-	-	3
31	124	AZD5305	136	No	-	25	22,5	23,3	55	No	Yes	No	Hypomorphic BRCA1	+	-	-	-	-	
32	124	AZD5305	274	No	-	44	45	4	70	No	Yes	No	Suspected 53BP1 pathway	-	-	-	-	-	
33	179	AZD5305	83	No	-	36	62,5	0	45	Yes	No	Yes	Suspected ABCB1 upregulation	+	-	-	-	-	1
34	179	AZD5305	93	No	-	32	40	2	42	No	Yes	Yes	Suspected PARP1 downregulation	+	-	-	-	-	
35	179	AZD5305	114	No	-	68	57,5	0	55	Yes	No	Yes	Suspected ABCB1 upregulation	+	-	-	-	-	2
36	341	AZD5305	130	No	-	32	95	72,5	77,5	Yes	No	No	Hypomorphic BRCA1	+	-	-	-	-	1
37	341	AZD5305	140	No	-	48	95	92,5	100	Yes	No	No	Hypomorphic BRCA1	+	-	-	-	-	4
38	341	AZD5305	165	No	-	54	52,5	57,5	90	Yes	No	No	Hypomorphic BRCA1	+	-	-	-	-	0
39	474.2	AZD5305	78	No	-	22	65	92,5	60	Yes	No	No	Unknown	Not done	-	-	-	-	4

Supplementary Table 7. Mechanisms of resistance to PARPi evaluated inthe cohort of PDX models.

Mechanism of PARPi resistance	Molecular alteration	Publication
Target modulation	Loss of PARP1	Pettitt et al., 2013; PLoS One; Pettitt et al., 2018; Nat. Commun.
Pump efflux	*ABCB1* upregulation	Vaidyanathan et al., 2016; Br. J. Cancer
PARylation	Loss of PARG	Gogola et al., 2018; Cancer Cell
End resection dysregulation	Loss of TP53BP1 (in *BRCA1*-mutated)	Cao et al., 2009; Mol. Cell; Bouwman et al., 2010; Nat. Struct. Mol. Biol.; Bunting et al., 2010; Cell
End resection dysregulation	Loss of RIF1 (in *BRCA1*-mutated)	Di Virgilio et al., 2013; Science; Feng et al., 2013; J. Biol. Chem.
End resection dysregulation	Loss of REV7 (in *BRCA1*-mutated)	Xu et al., 2015; Nature
End resection dysregulation	Loss of SHLD complex (in *BRCA1*-mutated)	Dev et al., 2018; Nat- Cell Biol.
End resection dysregulation	Loss of CST complex (in *BRCA1*-mutated)	Barazas et al., 2018; Cell Rep.
End resection dysregulation	Loss of HELB (in *BRCA1*-mutated)	Tkáč et al., 2016; Mol. Cell
End resection dysregulation	Loss of DYNLL1 (in *BRCA1*-mutated)	He et al., 2018; Nature
End resection dysregulation	Loss of ATMIN (in *BRCA1*-mutated)	He et al., 2018; Nature
End resection dysregulation	Loss of ERCC6L2 (in *BRCA1*-mutated)	Francica et al., 2020; Cell Rep.
End resection dysregulation	TIRR overexpression (in *BRCA1*-mutated)	Drané et al., 2017; Nature
End resection dysregulation	TRIP13 overexpression (in *BRCA1*-mutated)	Clairmont et al., 2020; Nat. Cell Biol.
Replication fork protection	Loss of MRE11	Schlacher et al., 2011; Cell; Ying, Hamdy & Helleday etal., 2012; Cancer Res.; Waks et al., 2020; Ann. Oncol.
Replication fork protection	Loss of CHD4	Ray Chaudhuri et al., 2016; Nature; Guillemette et al., 2015; Genes Dev.
Replication fork protection	Loss of MUS81	Schlacher, Wu & Jasin et al., 2012; Cancer Cell; Ray Chaudhuri et al., 2016; Nature; Lemançon et al., 2017; Nat. Commun.
Replication fork protection	Loss of SMARCL1	Taglialatela et al., 2017; Mol. Cell; Kolinjivadi et al., 2017; Mol. Cell
Replication fork protection	Loss of PAXIP1	Ray Chaudhuri et al., 2016; Nature
Replication fork protection	Loss of RADX (in *BRCA2*-mutated)	Dungrawala et al., 2017; Mol. Cell
Replication fork protection	Loss of EZH2 (in *BRCA2*-mutated)	Rondinelli et al., 2017; Nat. Cell Biol.
Replication fork protection	Loss of EXO1	Lemançon et al., 2017; Nat. Commun.
Replication fork protection	Loss of SLFN11	Zoppoli et al., 2012; Proc. Natl Acad. Sci.
Cell cycle regulation	Loss of CDK12 (in *BRCA1*-mutated)	Bajrami et al., 2014; Cancer Res.

Supplementary Table 8. Clinical and molecular characteristics of the PDX cohort used to evaluate POLθi antitumour activity.

PDX	Cancer subtype	Primary/Metastatic (P/M) tumor	Patient previous treatment	HRR alteration	cDNA change	AA change	Domain	Variant effect	CNV	RAD51 (%)	BRCA1 (%)	HRDetect	HRD score (Myriad)	GIS	Mechanism of Resistance to PARPi	DNA sequencing	Drug (POLQi)
PDX474.7	ER+	M	Yes	*BRCA2*	c.3922G>T	p.E1308*	Non recognized domain region	Nonsense	-	18	89	NA	NA	NA	Unknown	Panel	AZ'8649
PDX583.2	M	ER+	Yes	*BRCA2*	c.8954-5A>G	-		Splicing	-	17	45	NA	NA	NA	Unknown	Exome	AZ'1576
PDX127	TNBC	M	No	*BRCA1*	c.185delAG	p.E23fs	Ring	Frameshift	-	16,3	0	0,999983359	NA	87	53BP1 pathway dysregulation (FAM35A homodel)	Exome	AZ'8649
PDX196	OvC	M	Yes	*BRCA1*	c.1961delA	p.K654fs	Exon 11	Frameshift	-	28,3	68	0,99967619	NA	72	-	Exome	AZ'8649
PDX179	TNBC	M	Yes	*BRCA1*	c.185delAG	p.E23fs	Ring	Frameshift	-	22,3	7	NA	NA	NA	Unknown	Exome	AZ'8649
BB3RC31/PDX481	ER+	M	Yes	*BRCA2*	c.7976+1G>C	-	Intronic variant	Splicing	-	0	78	NA	NA	NA	-	Panel	AZ'8649
PDX124	TNBC	M	Yes	*BRCA1*	c.1961delA	p.K654fs	Exon 11	Frameshift	-	8,3	10	NA	NA	NA	-	Exome	AZ'1576

Supplementary Table 9. Clinical and molecular characteristics of the PDX cohort used to evaluate DNA-PKi antitumour activity.

PDX	Cancer subtype	Primary/Metastatic (P/M) tumor	Patient previous treatment	HRR alteration	cDNA change	AA change	Domain	Variant effect	CNV	BRCA1 promoter hypermethylation	RAD51 (%)	BRCA1 (%)	HRDetect	HRD score (Myriad)	GIS	Mechanism of Resistance to PARPi
PDX274	TNBC	M	Yes	*BRCA1*	-	-	-	-	Homoloss	-	22,7	12	0,999883399	NA	76	Hypomorphic BRCA1
PDX221	TNBC	P	Yes	*BRCA1*	c.5027delT	p.L1676fs	BRCT	Frameshift	-	-	20,3	66	0,999829767	NA	83	Hypomorphic BRCA1
PDX098	TNBC	P	Yes	-	-	-	-	-	-	-	60	94	NA	NA	NA	-
PDX124OR	TNBC	M	Yes	*BRCA1*	c.1961delA	p.K654fs	Exon 11	Frameshift	-	-	16,3	10,5	NA	NA	NA	Suspected replication fork
STG316	TNBC	P	Yes	*BRCA1*	c.134+3A>C	-	Intronic variant	Splicing	-	-	36,7	26	NA	NA	NA	Hypomorphic BRCA1 and 53BP1 pathway dysregulation (53BP1 homodel)
PDX179	TNBC	M	Yes	*BRCA1*	c.185delAG	p.E23fs	Ring	Frameshift	-	-	22,3	7	NA	NA	NA	Unknown
PDX102	TNBC	P	No	-	-	-	-	-	-	-	52	82	NA	NA	NA	-
PDX332	TNBC	M	Yes	*BRCA2*	c.7796A>G	p.E2599G	DNA binding (Helical domain)	Missense	-	-	13	80	0,05659481	NA	39	HRR genetic reversion (VAF > 0.1)
PDX156	TNBC	M	Yes	-	-	-	-	-	-	-	49	68	NA	NA	NA	-
PDX094	TNBC	P	Yes	-	-	-	-	-	-	-	58	58	NA	NA	NA	-
PDX252	TNBC	M	Yes	*BRCA1*	c.5123C>A	p.A1708E	BRCT	Missense	-	-	21,5	0	0,997235532	NA	70	Unknown
PDX060	TNBC	M	Yes	-	-	-	-	-	-	-	48	47,1	NA	NA	NA	-
PDX127	TNBC	M	No	*BRCA1*	c.185delAG	p.E23fs	Ring	Frameshift	-	-	16,3	0	0,999983359	NA	87	53BP1 pathway dysregulation (FAM35A homodel)
PDX288	TNBC	M	Yes	-	-	-	-	-	-	-	50	65	0,695911274	NA	33	-
PDX270	TNBC	P	No	*BRCA1*	-	-	-	-	-	Yes	12	0	NA	NA	NA	Unknown
PDX339	TNBC	M	Yes	*BRCA1*	c.211A>G	p.R71G	Ring	Missense	-	-	21	8	0,9998763	NA	84	Unknown
PDX236	TNBC	M	Yes	*BRCA1*	c.5194-12G>A	-	Intronic variant	Splicing	-	-	27	60	0,984120074	NA	58	Hypomorphic BRCA1
PDX341	TNBC	M	Yes	*BRCA1*	c.2404delGA	p.R762fs	Exon 11	Frameshift	-	-	16,7	29	NA	NA	NA	Hypomorphic BRCA1 and 53BP1 pathway dysregulation (C20orf196 downregulation)
PDX384	TNBC	M	Yes	*BRCA1*	791-794delGT	p.S264Mfs*33	Exon 11	Frameshift	-	-	15,5	38	NA	NA	NA	-
PDX302	TNBC	M	Yes	*BRCA1*	-	-	-	-	-	Yes	0	0	0,993121792	NA	58	-
PDX124	TNBC	M	Yes	*BRCA1*	c.1961delA	p.K654fs	Exon 11	Frameshift	-	-	8,3	10	NA	NA	NA	-
PDX230	TNBC	P	Yes	*BRCA1*	c.185delAG	p.E23fs	Ring	Frameshift	-	-	0,3	0	0,999977931	NA	83	-
PDX405	TNBC	M	Yes	*BRCA2*	c.5909C>A	p. S1970*	Non recognized domain region	Nonsense	-	-	2,7	90	NA	NA	NA	-

Supplementary Table 10. Clinical and molecular characteristics of TNBC patients enrolled in the PETREMAC clinical trial. *Modified from Eikesdal et al.,*

Sample ID	Molecular subtype	HRR alteration	AA change	Domain	Study arm	RAD51 (%)	BRCA1 (%)	γ-H2AX (%)	MRI response
1	TNBC	*BRCA1*	p.K339fs	Exon 11	G	8	31	58	-100
2	TNBC	*BRCA1*-low	-	-	H	5	37	96	-48
3	TNBC	*BRCA1*	p.S784fs	Exon 11	G	NA	NA	NA	-50
4	TNBC	*BRCA1*-low	-	-	H	2	4	64	-41
5	TNBC	*BRCA1*-low	-	-	H	2	1	100	-37
6	TNBC	*BRCA2*	p.K1274N	Non recognized domain region	H	16	54	56	-30
7	TNBC	*BRCA1*	p.R1726fs	BRCT	H	1	2	78	-59
8	TNBC	*BRCA1*-low	-	-	H	4	19	65	-64
9	TNBC	*BRCA1*-low	-	-	H	1	6	82	-39
10	TNBC	WT	-	-	H	1	6	70	-54
11	TNBC	WT	-	-	H	10	62	86	-53
12	TNBC	WT	-	-	G	29	68	100	-31
13	TNBC	*BRCA1*-low	-	-	G	1	3	58	-50
14	TNBC	*BRCA1*-low	-	-	H	6	0	90	-69
15	TNBC	*BRCA2*	p.K169X	Non recognized domain region	H	4	98	100	-50
16	TNBC	*BRCA1*-low	-	-	H	6	4	96	-50
17	TNBC	*PALB2*	p.W906X	-	H	0	70	70	-61
18	TNBC	WT	-	-	H	4	63	90	-64
19	TNBC	WT	-	-	H	NA	NA	NA	-9
20	TNBC	*BRCA1*-low	-	-	H	11	11	82	-31
21	TNBC	WT	-	-	H	20	37	96	-20
22	TNBC	WT	-	-	H	20	73	98	4
23	TNBC	WT	-	-	H	64	84	92	-10
24	TNBC	WT	-	-	G	22	50	88	-3
25	TNBC	*BRCA1*	p.V233fs	Exon 11	H	0	1	82	-9
26	TNBC	WT	-	-	G	15	100	100	0
27	TNBC	WT	-	-	H	80	84	100	3
28	TNBC	WT	-	-	H	51	69	90	-21
29	TNBC	WT	-	-	H	24	50	90	-21
30	TNBC	WT	-	-	G	15	32	92	33
31	TNBC	*BRCA1*-low	-	-	G	41	49	80	22
32	TNBC	*BRCA1*-low	-	-	H	1	9	62	11

Supplementary Table 11. Clinical and molecular characteristics of non-TNBC patients enrolled in the PETREMAC clinical trial. *Modified from Yndestad et al.,*

			Wide-HRD			Strict-HRD			Biomarker scoring		
Sample ID	Treatment arm	Molecular subtype	Altered - wide	HRD Wide	HRD-W Cause	HRR mutation - Strict	HRD Strict	HRD-S Cause	γ-H2AX (%)	BRCA1 (%)	RAD51 (%)
1001	B	HR+	WT	HRP		HRR wt	HRP		100,0	97,5	73,3
1003	A	HR+	WT	HRP		HRR wt	HRP		50	90,0	48,3
1006	A	HR+	Altered	HRD	HRR-W mut	HRR mutation	HRD	Deleterious germline *BRCA1* mut	40,0	2,5	1,7
1007	F	HER2+ HR+	Altered	HRD	HRR-W mut	HRR wt	HRP		98,3	80,0	73,3
1008	E	HER2+	WT	HRP		HRR wt	HRP		62,5	95,0	56,7
1009	E	HER2+ HR+	Altered	HRD	HRR-W mut	HRR mutation	HRD	Deleterious germline *BRCA2* mut	NE	NE	NE
1010	E	HER2+ HR+	WT	HRP		HRR wt	HRP		95,0	92,5	71,7
1012	F	HER2+	WT	HRP		HRR wt	HRP		80,0	82,5	70,0
1014	A	HR+	WT	HRP		HRR wt	HRP		82,5	92,5	41,7
1015	F	HER2+	WT	HRP		HRR wt	HRP		35,0	96,4	46,3
1016	E	HER2+ HR+	WT	HRP		HRR wt	HRP		85,0	80,0	51,1
1017	A	HR+	WT	HRP		HRR wt	HRP		35,0	90,0	61,7
1018	E	HER2+	WT	HRP		HRR wt	HRP		85,0	95,0	15,9
1019	A	HR+	WT	HRP		HRR wt	HRP		40,0	50,0	37,7
1021	A	HR+	WT	HRP		HRR wt	HRP		NE	NE	NE
1022	E	HER2+ HR+	Altered	HRD	HRR-W mut	HRR wt	HRP		50,0	80,0	51,7
1024	D	HR+	WT	HRD	BRCA1-low	HRR wt	HRD	*BRCA1-low+BRCA1* LOH	55,0	2,5	8,2
1025	E	HER2+	WT	HRP		HRR wt	HRP		72,5	40,0	30,0
1028	B	HR+	WT	HRP		HRR wt	HRP		87,5	90,0	31,7
1029	A	HR+	WT	HRP		HRR wt	HRP		NE	NE	NE
1031	E	HER2+ HR+	Altered	HRD	HRR-W mut	HRR wt	HRP		35,0	50,0	55,0
1032	B	HR+	WT	HRP		HRR wt	HRP		70,0	80,0	52,0
1033	B	HR+	Altered	HRD	HRR-W mut	HRR mutation	HRD	Deleterious *BRCA1* mut + LOH	82,5	2,5	0,0
1034	A	HR+	WT	HRP		HRR wt	HRP		30,0	77,5	25,0
1035	E	HER2+	WT	HRP		HRR wt	HRP		30,0	80,0	38,3
1036	A	HR+	WT	HRP		HRR wt	HRP		NE	NE	NE
1037	A	HR+	Altered	HRD	HRR-W mut	HRR wt	HRP		42,5	85,0	45,0
1038	A	HR+	Altered	HRD	HRR-W mut	HRR wt	HRP		NE	NE	NE
1040	E	HER2+ HR+	WT	HRP		HRR wt	HRP		72,5	70,0	52,0
1041	A	HR+	WT	HRP		HRR wt	HRP		87,2	55,0	44,8
1042	A	HR+	WT	HRP		HRR wt	HRP		60,0	87,5	50,0
1043	A	HR+	WT	HRP		HRR wt	HRP		77,5	75,0	21,7
1044	A	HR+	WT	HRP		HRR wt	HRP		90,0	97,5	51,7
1045	A	HR+	WT	HRP		HRR wt	HRP		92,5	65,0	20,0
1046	A	HR+	WT	HRP		HRR wt	HRP		NE	NE	NE
1047	B	HR+	WT	HRP		HRR wt	HRP		82,5	85,0	60,0
1048	C	HR+	Altered	HRD	HRR-W mut	HRR wt	HRP		87,5	95,0	40,0

			Wide-HRD			Strict-HRD			Biomarker scoring		
Sample ID	Treatment arm	Molecular subtype	Altered - wide	HRD Wide	HRD-W Cause	HRR mutation - Strict	HRD Strict	HRD-S Cause	γ-H2AX (%)	BRCA1 (%)	RAD51 (%)
1049	A	HR+	WT	HRP		HRR wt	HRP		NE	NE	NE
1051	A	HR+	WT	HRP		HRR wt	HRP		72,5	60,0	23,3
1052	A	HR+	WT	HRP		HRR wt	HRP		47,5	80,0	30,6
1053	F	HER2+ HR+	WT	HRP		HRR wt	HRP		27,5	47,5	32,1
1054	B	HR+	WT	HRP		HRR wt	HRP		NE	NE	NE
1055	A	HR+	WT	HRP		HRR wt	HRP		NE	NE	NE
1056	A	HR+	Altered	HRD	HRR-W mut	HRR wt	HRP		65,0	47,5	45,0
1058	A	HR+	Altered	HRD	HRR-W mut	HRR wt	HRP		30,0	47,5	25,0
1059	A	HR+	WT	HRP		HRR wt	HRP		50,0	97,5	30,5
1060	A	HR+	WT	HRP		HRR wt	HRP		37,5	90,0	23,3
1061	A	HR+	Altered	HRD	HRR-W mut	HRR wt	HRP		59,0	72,7	17,8
1063	E	HER2+ HR+	WT	HRP		HRR wt	HRP		90,0	80,0	64,1
1064	A	HR+	WT	HRP		HRR wt	HRP		29,5	88,5	40,0
1065	E	HER2+ HR+	Altered	HRD	HRR-W mut	HRR wt	HRP		40,0	75,0	28,3
1066	A	HR+	WT	HRP		HRR wt	HRP		35,0	62,5	16,7
1067	F	HER2+ HR+	WT	HRP		HRR wt	HRP		50,0	40,0	38,0
1068	F	HER2+ HR+	Altered	HRD	HRR-W mut	HRR wt	HRP		60,0	65,0	41,7
1069	F	HER2+ HR+	WT	HRP		HRR wt	HRP		45,0	45,0	42,5
1070	F	HER2+	WT	HRP		HRR wt	HRP		57,5	70,0	56,7
1071	A	HR+	WT	HRP		HRR wt	HRP		27,5	47,5	51,7
1073	B	HR+	WT	HRP		HRR wt	HRP		90,0	90,0	44,4
1074	E	HER2+ HR+	WT	HRP		HRR wt	HRP		80,0	80,0	33,3
1075	A	HR+	WT	HRP		HRR wt	HRP		92,5	85,0	32,0
1076	A	HR+	WT	HRP		HRR wt	HRP		NE	NE	NE
1077	A	HR+	WT	HRP		HRR wt	HRP		92,8	60,0	45,7
1078	E	HER2+ HR+	Altered	HRD	HRR-W mut	HRR wt	HRP		30,0	65,0	43,3
1079	A	HR+	Altered	HRD	HRR-W mut	HRR mutation	HRD	Deleterious germline *BRCA2* mut	93,8	82,1	5,0
1081	A	HR+	WT	HRP		HRR wt	HRP		NE	NE	NE
1082	B	HR+	Altered	HRD	HRR-W mut	HRR wt	HRP		80,0	97,5	45,5
1083	A	HR+	WT	HRP		HRR wt	HRP		30,0	67,5	43,3
1084	A	HR+	WT	HRP		HRR wt	HRP		NE	NE	NE
1086	A	HR+	WT	HRP		HRR wt	HRP		82,5	95,0	40,0
1087	F	HER2+	Altered	HRD	HRR-W mut	HRR wt	HRP		85	92,5	66,7

Annex III: Supplementary figures

List of supplementary figures

Supplementary Figure 1. Characterization of PDX models. ..... - 259 -

Supplementary Figure 2. DNA-based biomarkers of homologous recombination deficiency (HRD) in PDXs. ..... - 260 -

Supplementary Figure 3. Biomarkers of homologous recombination deficiency (HRD) in PDXs. ..... - 261 -

Supplementary Figure 4. Relative tumour volume upon PARPi treatment over time. ..... - 262 -

Supplementary Figure 5. Characterization of PARPi-sensitive, cisplatin-resistant PDX models..... - 262 -

Supplementary Figure 6. Homologous recombination repair functionality in PDXs and correspondent PDCs. ..... - 263 -

Supplementary Figure 7. Characterization of DCIS-MIND PARPi-sensitive, cisplatin-resistant PDX models..... - 264 -

Supplementary Figure 8. Characterization of mechanisms of resistance to PARPi in PDX models. ..... - 265 -

Supplementary Figure 9. Analysis of response to AZD5305 and olaparib in PDXs. ..... - 266 -

Supplementary Figure 10. Assessment of the functional HRD status by RAD51 foci..... - 267 -

Supplementary Figure 11. Representative immunofluorescence images of two tumours after progression to olaparib or AZD5305. ..... - 268 -

Supplementary Figure 12. Schematic illustration of the position in *BRCA1* where the qPCR probes are bound. ..... - 269 -

Supplementary Figure 13. Homologous recombination repair (HRR)-independent mechanisms of acquired resistance to AZD5305 in tumours from PDX179. ..... - 269 -

Supplementary Figure 14. Analysis of the catalytic activity of PARPi in PDXs. ..... - 270 -

Supplementary Figure 15. Antitumour activity of AZD5305 in combination with DNA-damaging agents..... - 271 -

Supplementary Figure 16. Characterization of antitumour activity and progression events upon treatment with POLθi alone or in combination with AZD5305..... - 272 -

Supplementary Figure 17. Characterization of antitumour activity and progression events upon treatment with DNA-PKi alone or in combination with olaparib. ..... - 273 -

Supplementary Figure 18. Characterization of DNA-damaging agents antitumour activity as single agent or in combination with PARPi in PARPi-sensitive and -resistant homologous recombination repair (HRR)-altered PDX models. ..... - 274 -

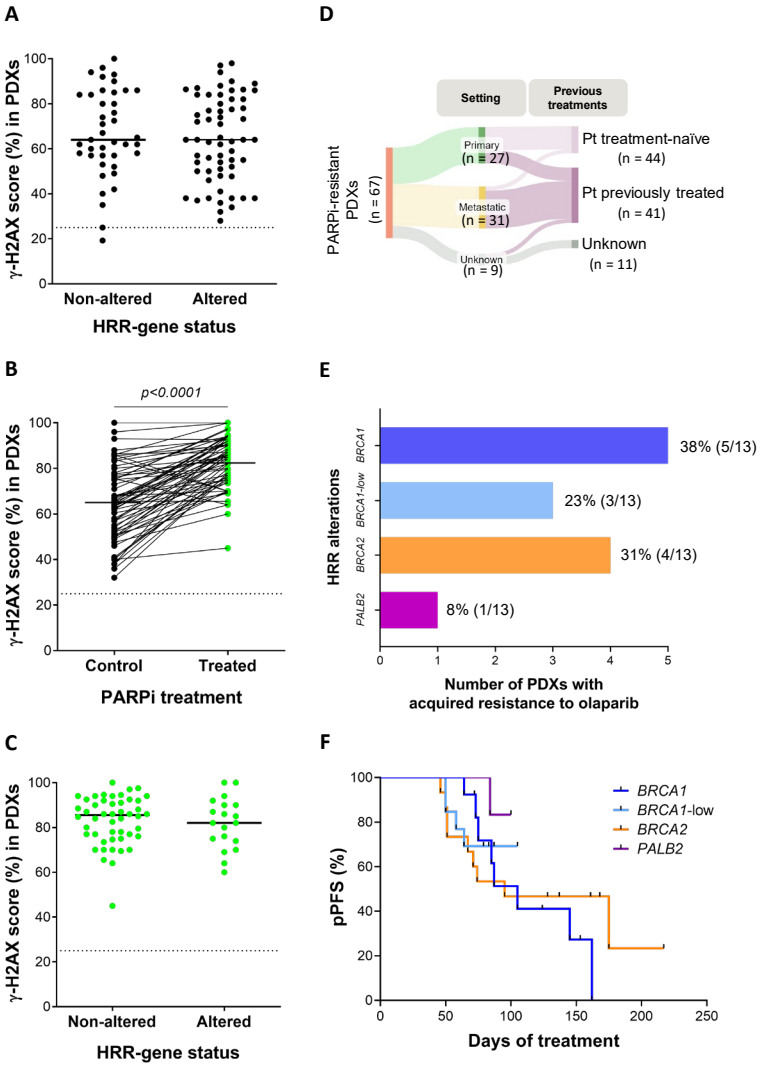
Supplementary Figure 19. Characterization of DNA-damaging agents antitumour activity as single agent or in combination with PARPi according to the affected gene domain in *BRCA1*-mutated PDX models..... - 275 -

Supplementary Figure 20. Analysis of BRCA1 nuclear foci by IF in geminin^{+} tumour cells. ..... - 277 -

Supplementary Figure 21. Analytical validation and interobserver agreement of final γ-H2AX scores..... - 277 -

Supplementary Figure 22. Example of a high-grade serous ovarian cancer (HGSOC) specimen with heterogeneous RAD51 nuclear foci distribution.... - 278 -

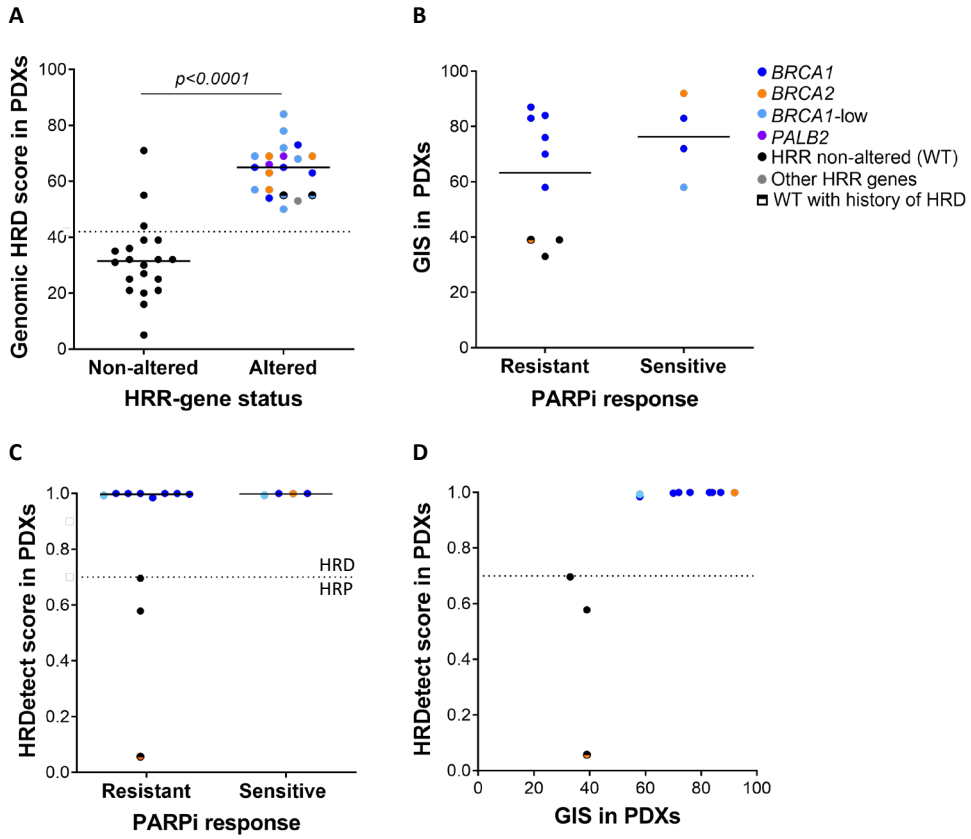
Supplementary figures



Supplementary Figure 1. Characterization of PDX models.

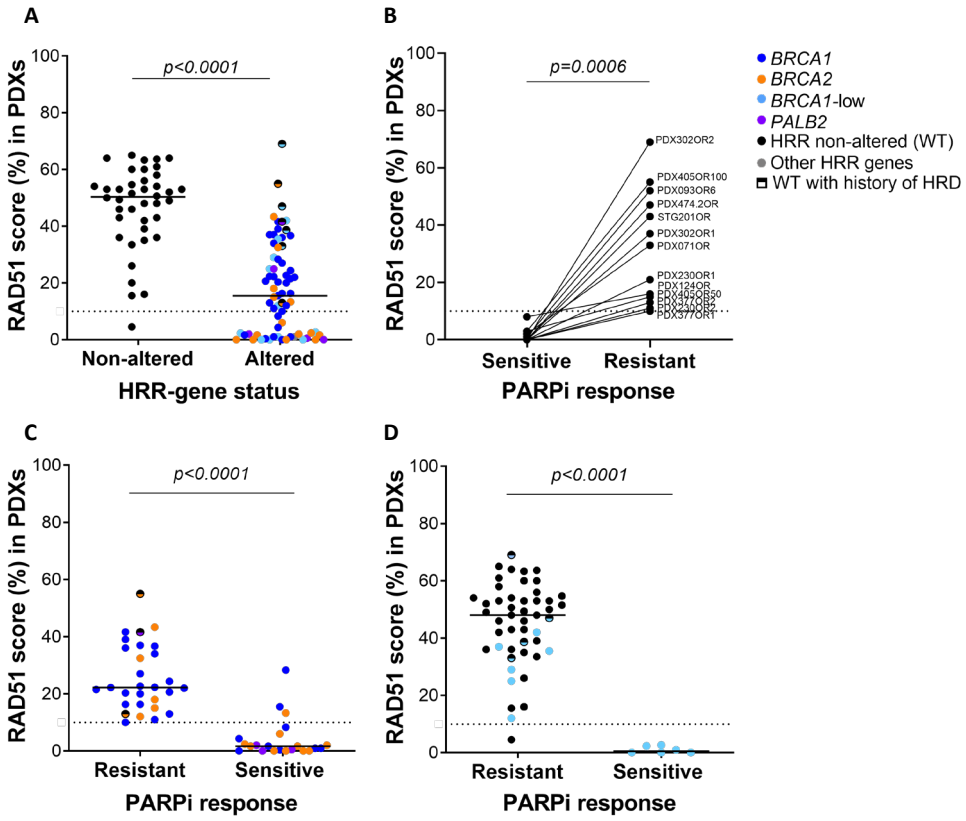
Distribution of the γ-H2AX score according to **A.** HRR-gene status in untreated tumours (n = 109), **B.** PARPi treatment in control (black) and PARPi-treated (green) tumours (n = 109) and **C.** HRR-gene status in olaparib-treated tumours (n = 109). Each dot represents the mean of at least three tumours for each PDX model. Lines represent the mean of each group. Dashed lines indicate the test cut-off (low γ-H2AX≤25%). Unpaired t-tests were applied in panels A and C and a paired t-test was applied in panel B. **D**. Sankey plot showing the setting and patients' previous treatment of PARPi-resistant PDX models (n = 67). **E.** Number of PDXs with acquired resistance to olaparib (OR) according to their HRR-gene status (n = 13). **F.** Preclinical

progression free survival (pPFS) according to the type of HRR alteration in PDX samples (n = 13). Ticks indicate that mice have either shown a disease progression of have been censored. Adapted from *Pellegrino & Herencia et al.*,[98].



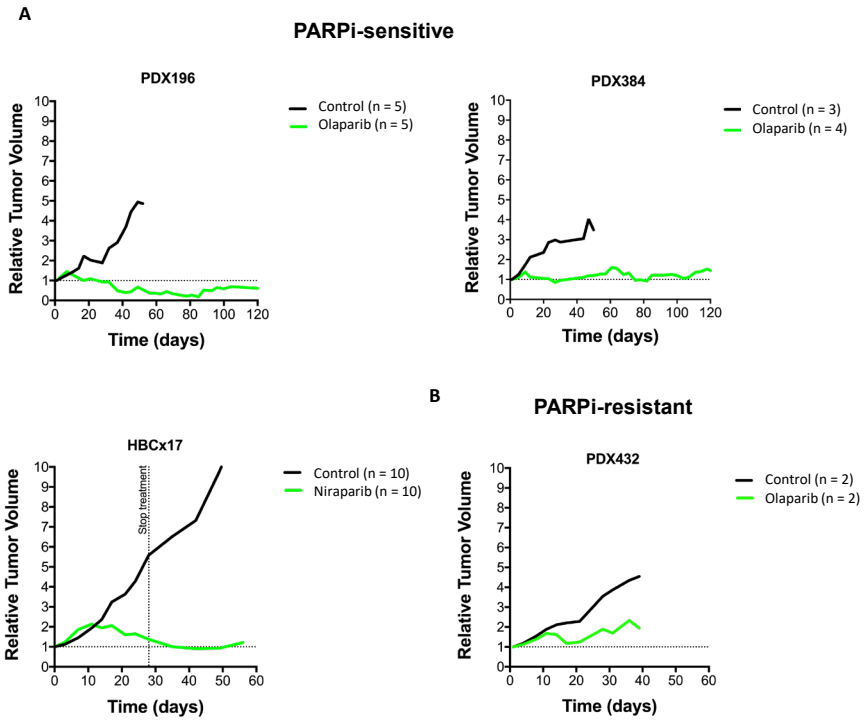
Supplementary Figure 2. DNA-based biomarkers of homologous recombination deficiency (HRD) in PDXs.

A. Distribution of genomic HRD by Myriad myChoice® according to alterations in HRR-gene status (n = 41). Dashed lines indicate the test cut-off (HRD≥42). Distribution of **B.** GIS values (n = 13) and **C.** HRDetect scores (n = 15) according to response to PARPi. Dashed lines indicate the test cut-off (HRD>0.7). Lines represent the mean of each group in panels A-C. An unpaired t-test was applied in panels A-C. **D**. Comparison of the genomic HRD tests GIS vs. HRDetect in PDX models (n = 13). Abbreviations: WT: wild-type; GIS: Genomic Instability Score. Adapted from *Pellegrino & Herencia et al.*,[98].



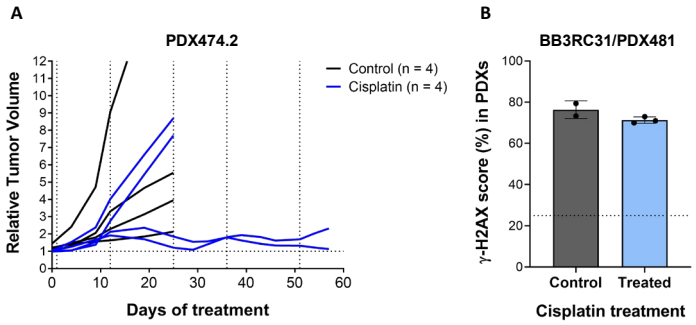
Supplementary Figure 3. Biomarkers of homologous recombination deficiency (HRD) in PDXs.

A. Distribution of the RAD51 score according to alterations in HRR genes (n = 109). **B.** Evolution of the RAD51 score in olaparib-sensitive vs. resistant paired models (n = 13). **C.** Distribution of the RAD51 score according to PARPi response in PDX harbouring mutations in *BRCA1*, *BRCA2* or *PALB2* (n = 51). **D** Distribution of the RAD51 score according to PARPi response in PDXs without mutations in these genes (n = 58). Each dot represents the mean of at least three tumours for each PDX model and lines represent the mean of each group in all panels. Dashed lines indicate the test cut-off (low RAD51≤10%). An unpaired t-test was applied in panels A, C and D. An unpaired t-test was applied in panel C. Abbreviations: WT: wild-type. Adapted from *Pellegrino & Herencia et al.*,[98].



Supplementary Figure 4. Relative tumour volume upon PARPi treatment over time.

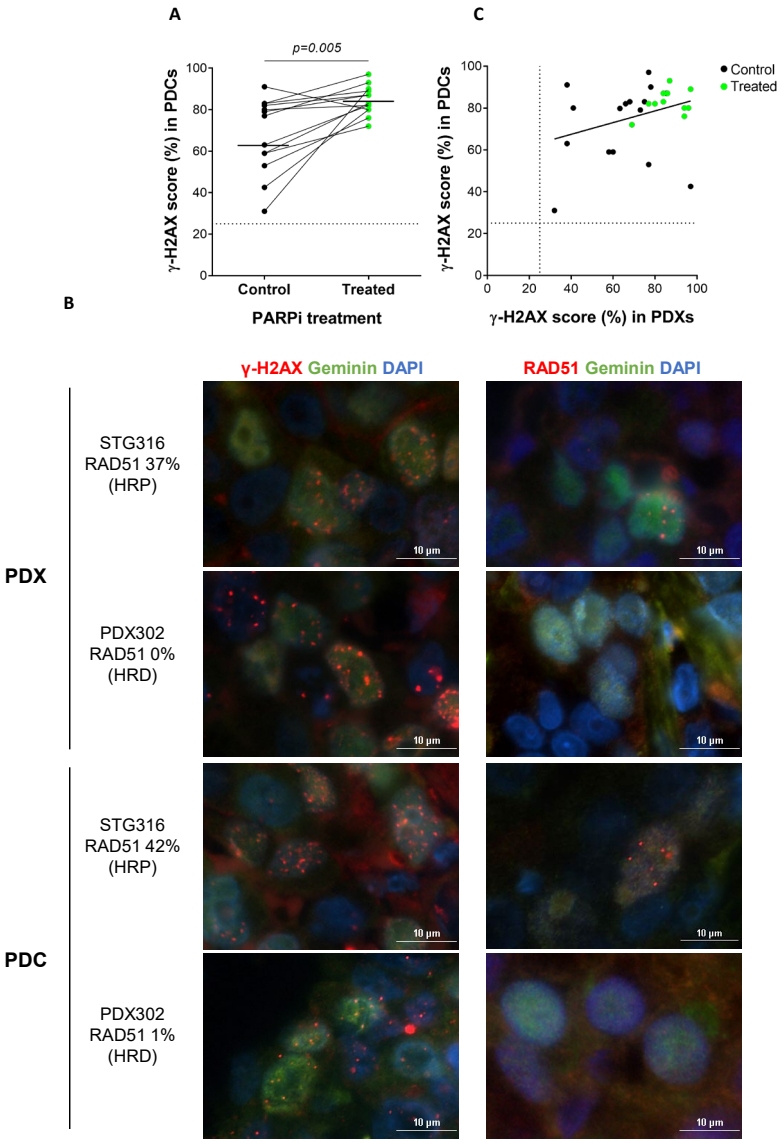
A. The PARPi-sensitive PDX196 and PDX384 treated with olaparib (100 mg/kg), and HBCx17 treated with niraparib (75 mg/kg). **B.** The PARPi-resistant PDX432 treated with olaparib (100mg/kg). Adapted from *Pellegrino & Herencia et al.*,[98].



Supplementary Figure 5. Characterization of PARPi-sensitive, cisplatin-resistant PDX models.

A. Relative tumour volume over time of individual tumours from PDX474.2 treated with cisplatin (6 mg/kg, n = 4) or left untreated (control, n = 4). Each line represents an individual tumour. Dashed lines indicate timepoints of cisplatin administration. **B.** Distribution of the γ-H2AX score according to treatment in BB3RC31/PDX481. Each dot represents the mean of at least three

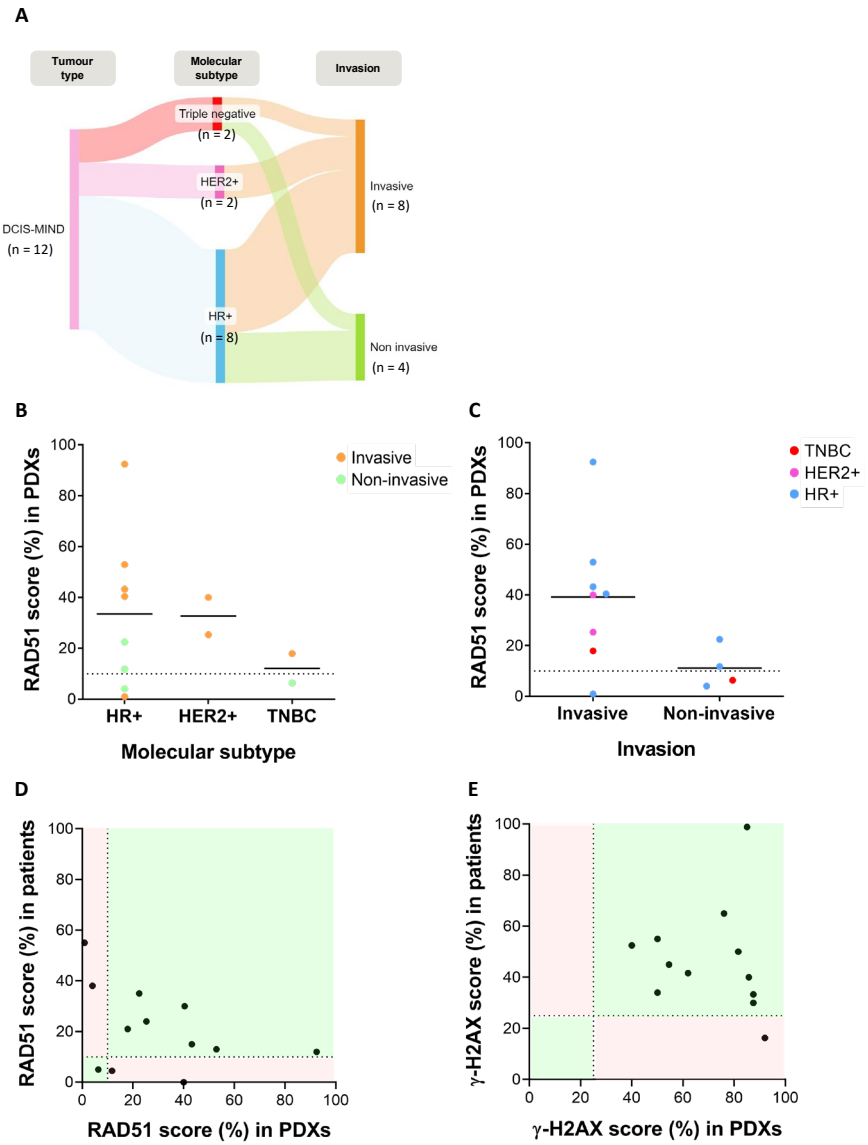
tumours for each PDX model. Lines represent the mean and SD of control or cisplatin-treated models. Dashed lines indicate the test's cut-off (low γ-H2AX≤25%). An unpaired t-test was applied in panel B.



Supplementary Figure 6. Homologous recombination repair functionality in PDXs and correspondent PDCs.

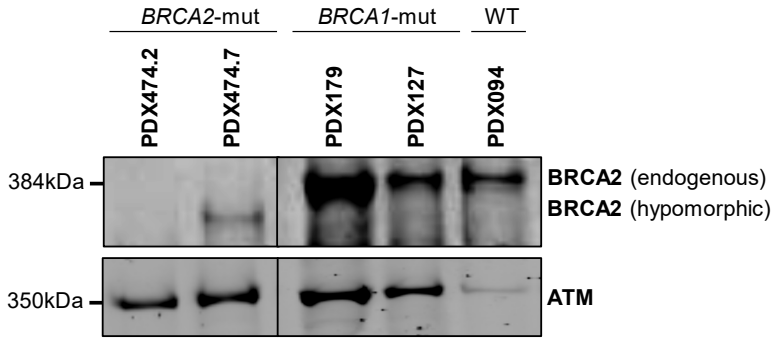
A. Distribution of the γ-H2AX score according to PARPi treatment (n = 14). Lines represent the mean of control or PARPi-treated PDCs. A paired t-test was applied in panel A. **B.** Immunofluorescence microscope images showing γ-H2AX and RAD51 nuclear foci in two

representative PDXs and correspondent PDCs of one PARPi-resistant (STG316) and one PARPi-sensitive model (PDX405). **C.** Distribution of the γ-H2AX score in PDXs and their corresponding PDCs treated with PARPi or left untreated (n = 14). Tumours treated with PARPi or left untreated are shown in green and black, respectively, in panels A and C. Each dot represents the mean of at least three tumours for each sample. Dashed line indicates the test cut-off (low γ-H2AX≤25%). A linear regression model was applied. Adapted from *Pellegrino & Herencia et al.*,[98].



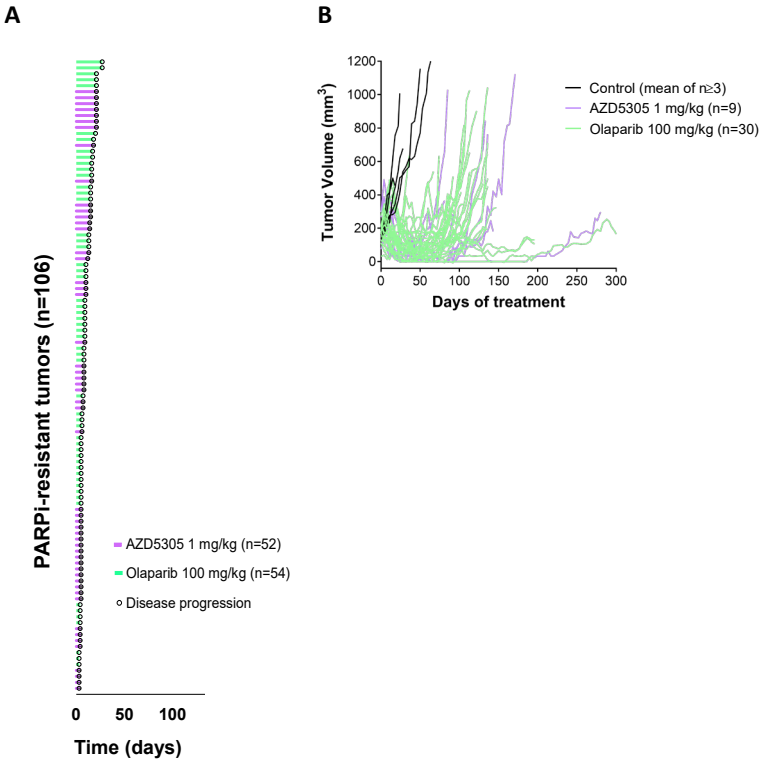
Supplementary Figure 7. Characterization of DCIS-MIND PARPi-sensitive, cisplatin-resistant PDX models.

A. Sankey plots showing PDX molecular subtypes (based on the IHC) and tumour invasion (n = 12). **B.** Distribution of the RAD51 score according to **B.** the molecular subtype (n = 12) and **C.** tumour invasion. Lines represent the mean of each group. Unpaired t-test was applied in panels B and C. Distribution of **D.** the RAD51 score and **E.** γ-H2AX score in PDXs and the corresponding patient both taken at the same timepoint (n = 12). Green and brown areas indicate HRD concordant and discordant cases according to test's cut-off, respectively. Dashed line indicates the test cut-off (low RAD51≤10% in panels B-D and low γ-H2AX<25%).



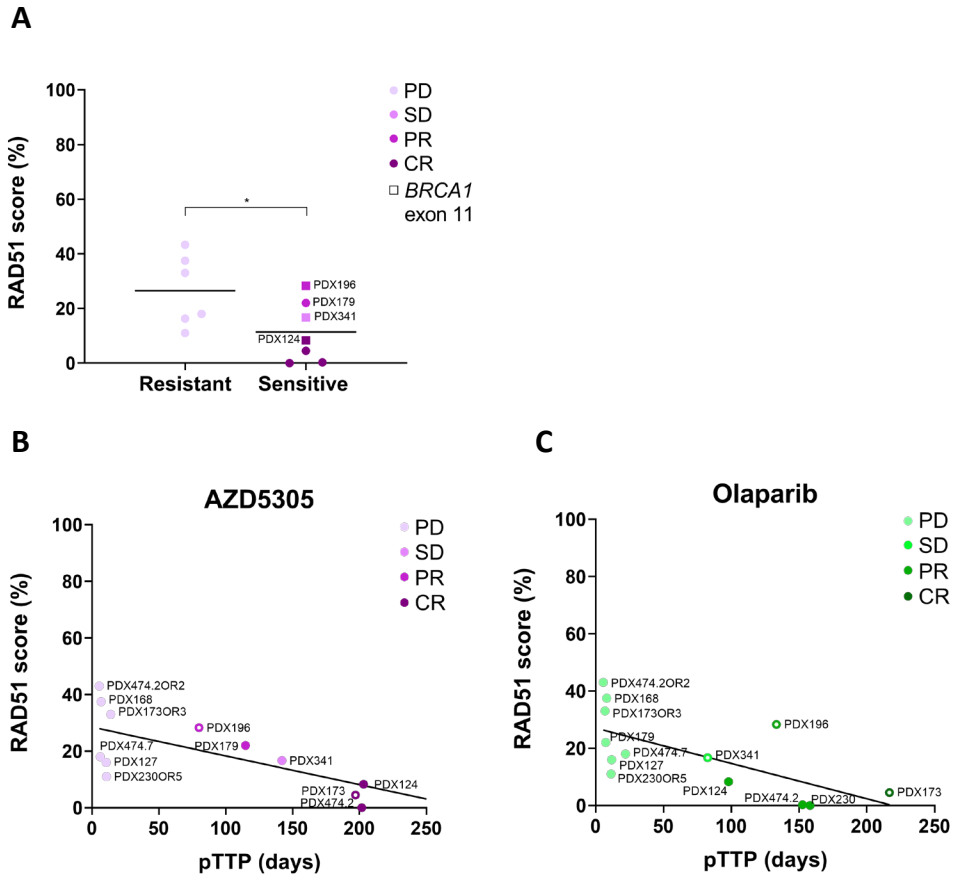
Supplementary Figure 8. Characterization of mechanisms of resistance to PARPi in PDX models.

Representative immunoblot showing endogenous and hypomorphic BRCA2 and the loading control ATM in the untreated *BRCA2*-mutated, PARPi-sensitive PDX474.2 and its resistant counterpart PDX474.7. PDX179, PDX127 (*BRCA1*-mutated) and PDX094 (*BRCA1/2*-WT) are shown as controls. Abbreviations: mut: mutated; WT: wild-type.



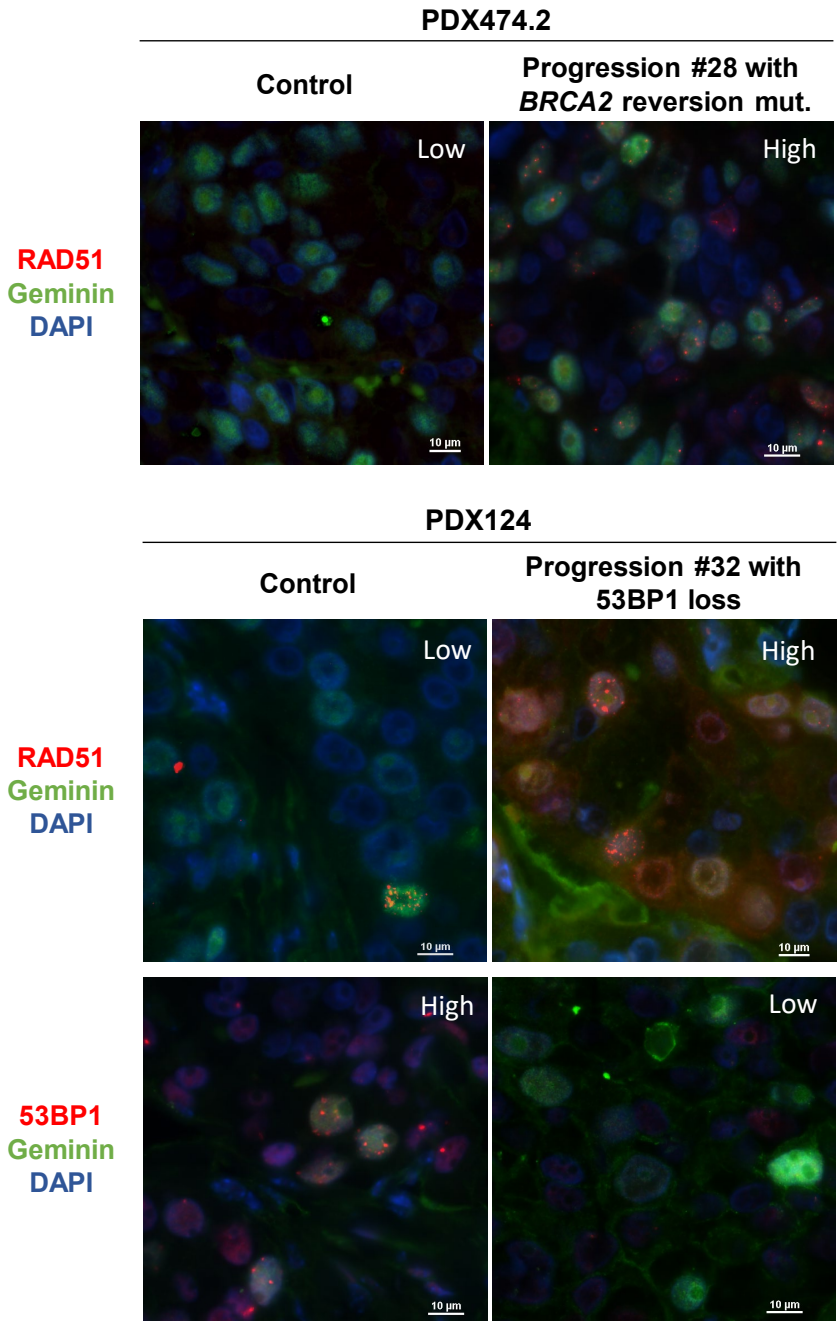
Supplementary Figure 9. Analysis of response to AZD5305 and olaparib in PDXs.

A. Swimmer plot showing the timeline of the *in vivo* experiments with individual PARPi-resistant tumours. **B.** Tumour volume of control tumours and PARPi-treated tumours with acquired resistance along time. The mean of at least three replicates per PDX was included in the control arm.



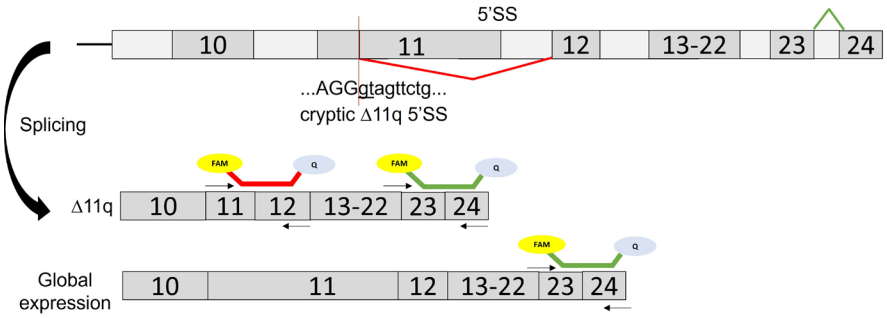
Supplementary Figure 10. Assessment of the functional HRD status by RAD51 foci.

A. Quantification by IF of the RAD51 score according to response to AZD5305 (n = 13). PDXs with a mutation in the exon 11 of *BRCA1* are indicated with squares and the name of models with intermediate RAD51 scores are shown. An unpaired t-test was performed. *, *p*-value ≤ 0.05. Correlation analysis of the RAD51 score vs. pTTP upon treatment with **B.** AZD5305 or **C.** olaparib. PDX responses according to the mRECIST criteria are shown. Open circles represent end of study without progression. Abbreviations: pTTP: preclinical time to progression. CR: complete response; PR: partial response; SD: stable disease; PD: progressive disease.



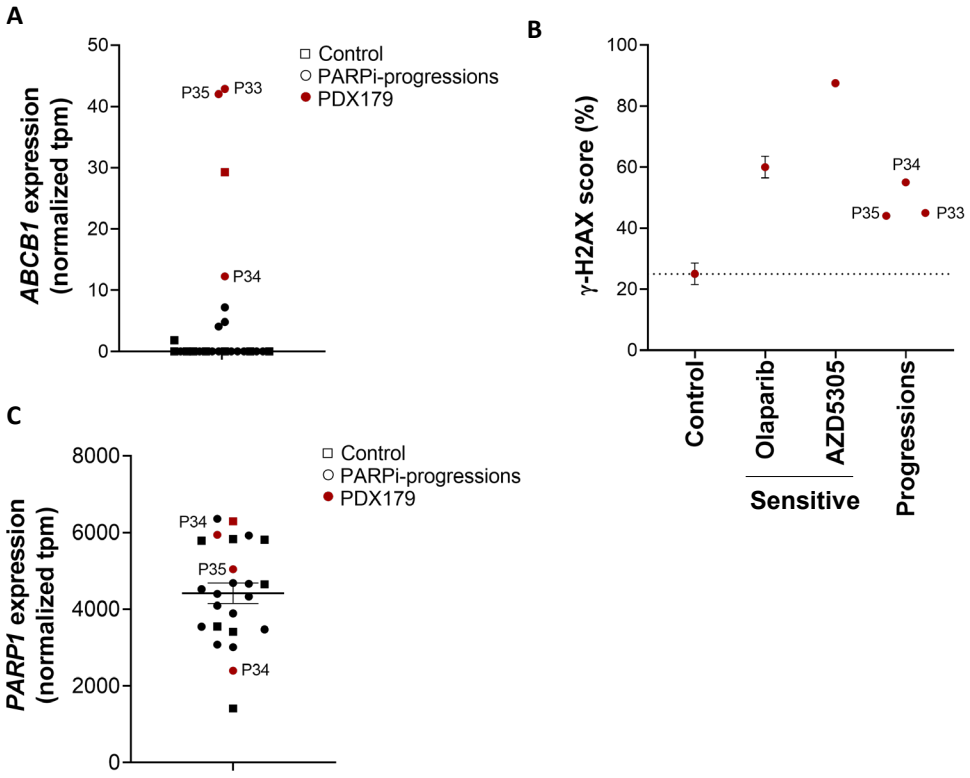
Supplementary Figure 11. Representative immunofluorescence images of two tumours after progression to olaparib or AZD5305.

PDX474.2 (progression #28) harbours a *BRCA2* reversion mutation and PDX124 (progression #32) shows 53BP1 loss. RAD51 and 53BP1 nuclear foci in geminin+ cells are shown. All pictures were taken at 600x magnification. Scale bar = 10 µm.



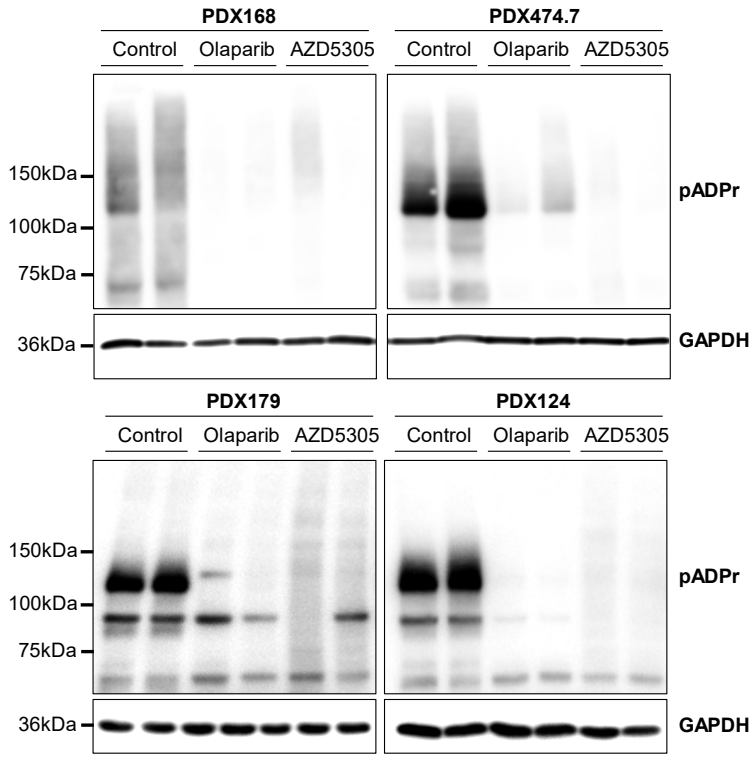
Supplementary Figure 12. Schematic illustration of the position in *BRCA1* where the qPCR probes are bound.

Custom Taqman assay targeting exon junction of cryptic 5' donor site in exon 11 and exon 12 natural 3' acceptor site is labelled in red. Taqman assay Hs01556193_m1, which spans exon 23 and 24 junction (present in both full-length and Δ11q transcripts) is labelled in green. Abbreviations: FAM: fluorochrome; Q: quencher.

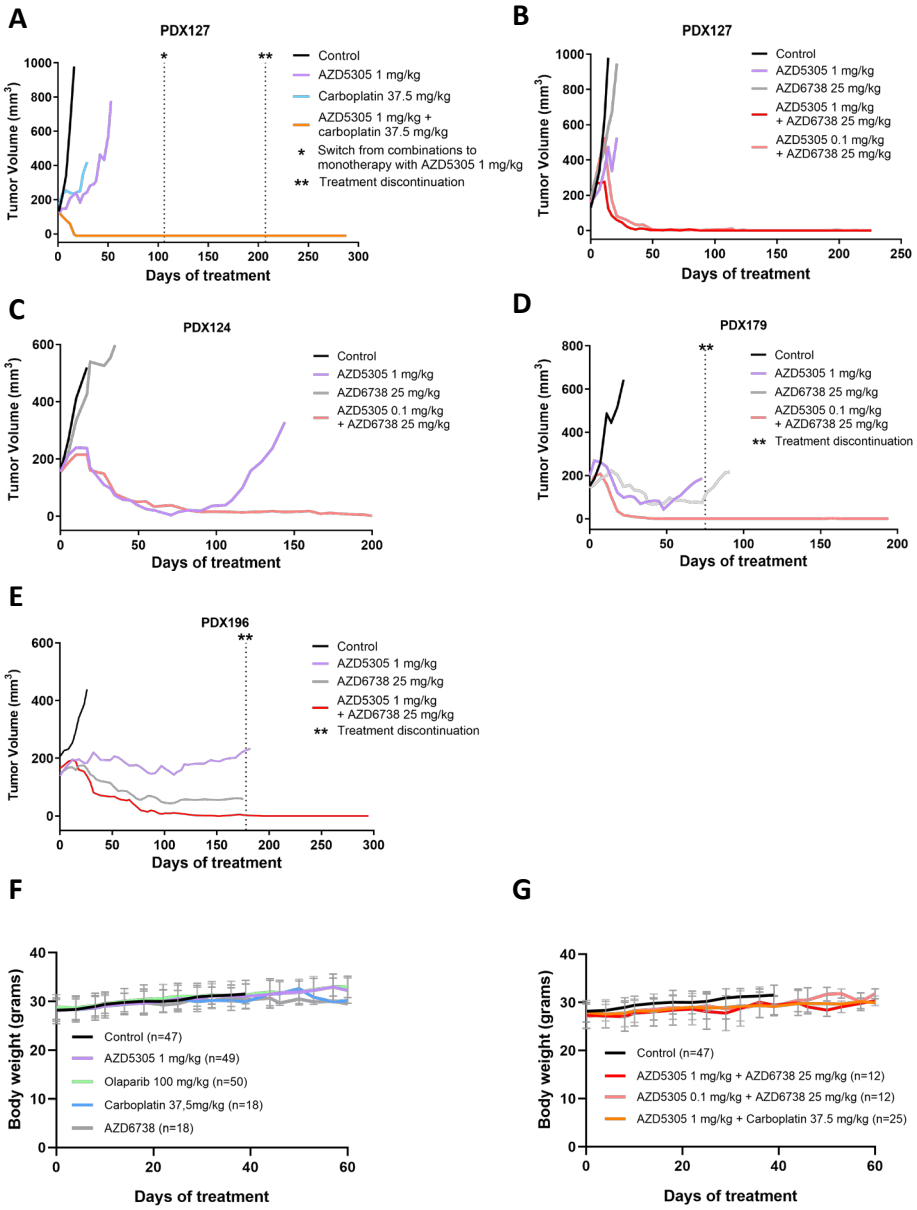


Supplementary Figure 13. Homologous recombination repair (HRR)-independent mechanisms of acquired resistance to AZD5305 in tumours from PDX179.

A. *ABCB1* expression of tumours with acquired resistance to AZD5305 and olaparib (circles) and their respective controls (squares). **B.** Distribution of the γ-H2AX score in control tumours, sensitive tumours treated with olaparib or AZD5305 and tumours with acquired resistance to AZD5305 (n = 3) of PDX179. Each dot from the control and the sensitive group represents the mean of at least two tumours. Dashed lines indicate the test cut-off (low γ-H2AX≤25%). An unpaired t-test was applied between the sensitive AZD5305-treated and the progression group. **C.** *PARP1* expression of tumours with acquired resistance to AZD5305 and olaparib (circles) and their respective controls (squares). Tumours from PDX179 are highlighted in red, and progressing tumours are labelled with their names (progressions #33, #34, #35).



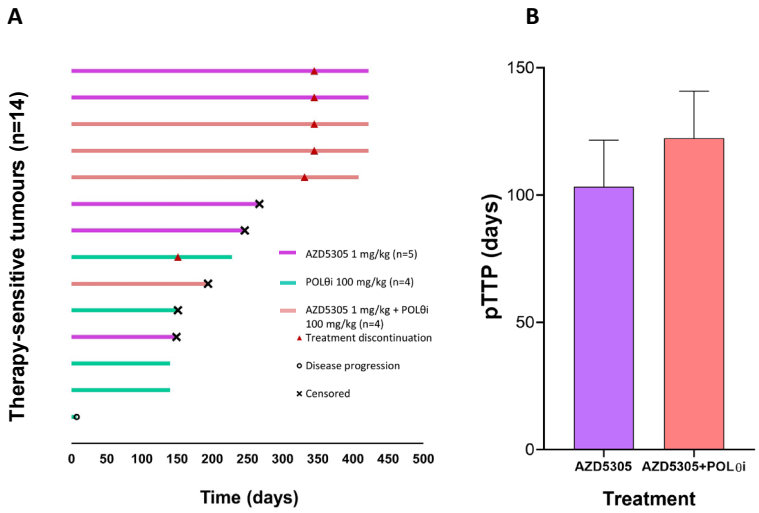
Supplementary Figure 14. Analysis of the catalytic activity of PARPi in PDXs.
Representative immunoblot showing Poly(ADP-ribose) Polymers (pPARr) and the loading control GAPDH in two representative AZD5305-resistant (PDX168 and PDX474.7) and PARPi-sensitive (PDX179 and PDX124) models untreated or treated olaparib or AZD5305. Two biological replicates per PDX and treatment are shown.



Supplementary Figure 15. Antitumour activity of AZD5305 in combination with DNA-damaging agents.

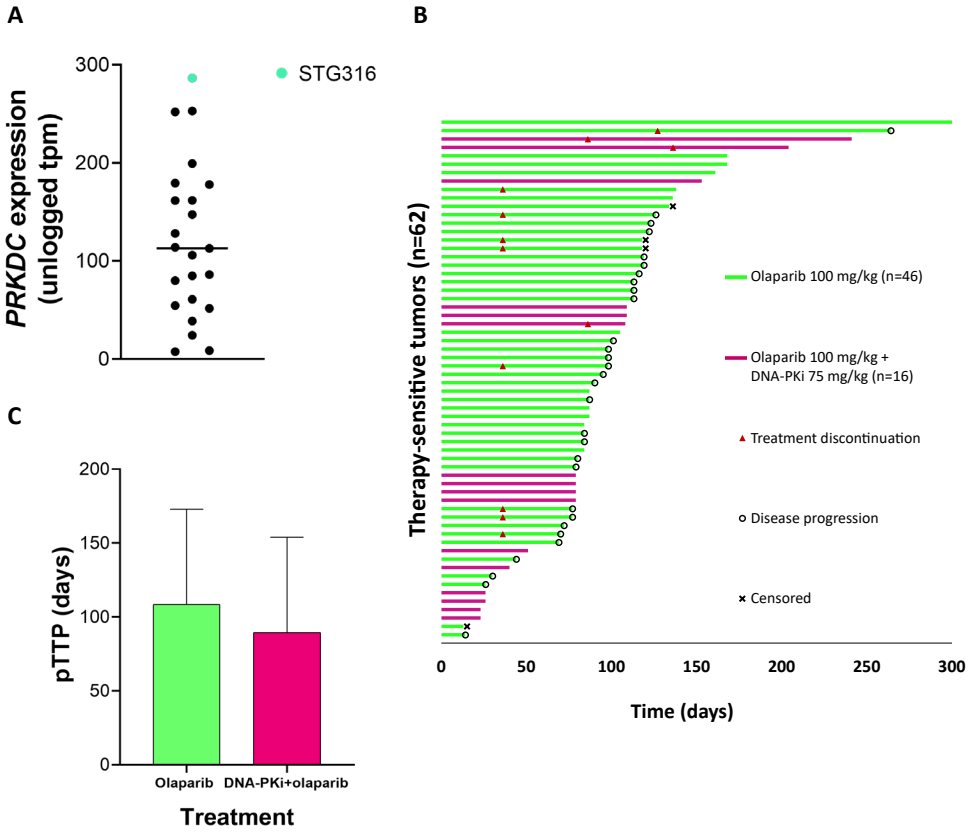
Tumour volume along time of control and tumours treated with **A.** either AZD5305 and carboplatin as single agents or in combination and **B-E**. AZD5305 and AZD6738 as single agents or in combination with the indicated doses of AZD5305 (1 mg/kg or 0.1 mg/kg). Body weight of mice untreated or treated with AZD5305, olaparib, carboplatin and AZD6738 **F.** as

single agents or **G.** in combination. For all panels, the mean of at least three individual tumours is depicted.



Supplementary Figure 16. Characterization of antitumour activity and progression events upon treatment with POLθi alone or in combination with AZD5305.

A. Swimmer plot showing the timeline of the *in vivo* experiments with individual therapy-sensitive tumours from PDX481 (n = 13). Time at which treatment discontinuation, disease progression or animal censoring occurred are labelled. **B.** Preclinical time to progression (pTTP) in tumours progressing to AZD5305 or the combination with POLθi. A Mann-Whitney two-tailed test was applied in panel C. Abbreviations: pTTP: preclinical time to progression.



Supplementary Figure 17. Characterization of antitumour activity and progression events upon treatment with DNA-PKi alone or in combination with olaparib.

A. Expression of *PRKDC* in the cohort of PDXs (n = 23). The model STG316, in which an upregulation of *PRKDC* was observed, is highlighted. **B.** Swimmer plot showing the timeline of the *in vivo* experiments with individual therapy-sensitive tumours (n = 69). Time at which treatment discontinuation, disease progression or animal censoring occurred are labelled. **C.** Preclinical time to progression (pTTP) in tumours progressing to olaparib or the combination with DNA-PKi. A Mann-Whitney two-tailed test was applied in panel C. Abbreviations: tpm: transcript per millon; pTTP: preclinical time to progression.

PDX	HRR-alteration	Gene domain	PARPi	MoR to PARPi	Platinum salts	Carbo + AZD5305	AZD6738 (ATRi)	ATRi + PARPi	AZD1775 (WEE1i)	WEE1i + Olaparib	AZD7648 (DNA-PKi)	DNA-PKi + Olaparib	POLθi	POLθi + AZD5305
HBCx6	*BRCA1*-low	-	CR		PD									
PDX230	*BRCA1*	RING	CR		PR		PD				PD	CR		
PDX124	*BRCA1*	Exon 11	CR		PR	CR	PD	CR	PD	CR	PD	PR	PD	CR
PDX474.2	*BRCA2*	NRD	CR		PD									
PDX173	*BRCA2*	NLS	CR		CR									
PDX377	*BRCA1*	Exon 11	CR		PR									
PDX071	*BRCA2*	NRD	CR		PR		PD		PD	PR	PR	CR		
PDX197	*BRCA1*-low	-	CR		CR				SD	CR				
PDX093	*PALB2*	OB3	CR		PR				PD	PR				
PDX473	*BRCA1*	BRCT	CR		PR									
PDX405	*BRCA2*	NRD	CR		PR		PD				PD	SD		
PDX179	*BRCA1*	RING	PR		PR		PR	CR	PD	SD	PD	PD	PD	CR
HBCx10	*BRCA2*	OB3	PR		PR		PD	PR	PD	CR				
STG201	*BRCA1*-low	-	PR		CR				PD	CR	PD	CR		
PDX481	*BRCA2*	Intronic	PR		PD		PD	CR					SD	CR
PDX474.1	*BRCA2*	NRD	PR		PR									
PDX302	*BRCA1*-low	-	PR		CR		PD				PD	CR		
PDX196	*BRCA1*	Exon 11	PR		PR		PR	CR	PD	PR	PD	CR	PD	PD
PDX539	*BRCA1*	BRCT	SD		PR									
HBCx17	*BRCA2*	NRD	SD		SD		PD	PD	PR	PR				
PDX384	*BRCA1*	Exon 11	SD		PR						PD	PD		
PDX341	*BRCA1*	Exon 11	SD		PD	CR	PD	PD			PD			
PDX236	*BRCA1*	BRCT	PD	Hyp BRCA1	PD		PD	PD	CR	CR	PD			
PDX339	*BRCA1*	RING	PD	Unknown	PD		PD	SD			PD	PD		
PDX270	*BRCA1*-low	-	PD	Unknown	SD		PD	PD	SD	PR	PD	SD		
PDX629	*BRCA1*	RING	PD	Unknown	PD									
PDX230OR2	*BRCA1*	RING	PD	Unknown	PD									
PDX252	*BRCA1*	BRCT	PD	Unknown	PR		PD	PD	PD	PR	PR	PR		
PDX583.2	*BRCA2*	Intronic	PD	Unknown									PD	SD
PDX332	*BRCA2*	OB3	PD	Reversion	CR		PD	PD			PD	SD		
PDX397	*BRCA1*	BRCT	PD	Hyp BRCA1	PD									
PDX280	*BRCA1*	-	PD	Unknown	CR		SD		PR	CR	PD	PD		
PDX230OR5	*BRCA1*	RING	PD	Unknown	PD	PD								
PDX418	*BRCA1*	BRCT	PD	Hyp BRCA1	PD									
STG201OR	*BRCA1*-low	-	PD	*BRCA1*-high					PD	PD				
PDX060	*BRCA2*	Intronic	PD	Unknown	PD									
STG316	*BRCA1*	RING	PD	53BP1+B1	SD		PD	SD	SD	SD	PR	PR		
PDX093OR	*PALB2*	-	PD	Reversion					PD	SD				
PDX124OR	*BRCA1*	Exon 11	PD	RAD51-i							PD	PD		
HBCx9	*BRCA1*-low	-	PD	*BRCA1*-high	PD		PD	PD	SD	PR				
PDX474.7	*BRCA2*	NRD	PD	Hyp BRCA1	PD	PD	PR	CR					PD	PD
PDX221	*BRCA1*	BRCT	PD	Hyp BRCA1	PD		PD	PD	PD	PR	PD	PD		
PDX274	*BRCA1*	-	PD	Hyp BRCA1	PD		PD	PD	PD	SD	PD	PD		
PDX127	*BRCA1*	RING	PD	53BP1 pt	PR	CR	PD	CR	PD	PD	PD	SD	PD	CR
PDX474.2OR2	*BRCA2*	NRD	PD	Unknown	PD	PD								

HRR alteration
- *BRCA1*
- *BRCA2*
- *PALB2*
- *BRCA1*-low

Gene domain

BRCA1
- RING domain
- Exon 11
- BRCT domain

BRCA2
- Intronic variant
- DNA binding (OB3)
- Nuclear localization signal
- Non recognized domain

Mechanism of resistance (MoR) to PARPi
- Hypomorphic BRCA1
- *BRCA1*-high
- HRR-gene reversions
- 53BP1 pathway
- 53BP1 pathway and hypomorphic BRCA1
- RAD51-independent
- Unknown (other RAD51-dependent)

Response to therapy (mRECIST)
- CR
- PR
- SD
- PD
- NA

Supplementary Figure 18. Characterization of DNA-damaging agents antitumour activity as single agent or in combination with PARPi in PARPi-sensitive and -resistant homologous recombination repair (HRR)-altered PDX models.

The HRR-mutation, the affected gene domain (either in *BRCA1* or *BRCA2*), mechanism of resistance to PARPi and response to therapy according to the mRECIST criteria are shown. White boxes indicate non-applicable or non-available cases. Only models in which at least one DNA-damaging agent besides PARPi has been tested are included. Abbreviations: MoR: mechanisms of resistance; carbo: carboplatin; NRD: non recognized domain; NLS: nuclear localization signal; CR: complete response; PR: partial response; SD: stable disease; PD:

progressive disease; Hyp BRCA1: hypomorphic BRCA1; 53BP1 pt: 53BP1 pathway; 53BP1+B1: 53BP1 pathway and hypomorphic BRCA1; RAD51-i: RAD51-independent.

PDX	HRR alteration	Gene domain	PARPi	Response to PARPi	MoR	Platinum salts	Carbo + AZD5305	AZD6738 (ATRi)	ATRi + PARPi	AZD1775 (WEE1i)	WEE1i + Olaparib	AZD7648 (DNA-PKi)	DNA-PKi + Olaparib	POLθi	POLθi + AZD5305
PDX230	*BRCA1*	RING	AZD5305	CR		PR		PD				PD	CR		
PDX124	*BRCA1*	Exon 11	AZD5305	CR		PR	CR	PD	CR	PD	CR	PD	PR	PD	CR
PDX377	*BRCA1*	Exon 11	AZD5305	CR		PR									
PDX473	*BRCA1*	BRCT	Olaparib	CR		PR									
PDX179	*BRCA1*	RING	Olaparib	PR		PR		PR	CR	PD	SD	PD	PD	PD	CR
PDX196	*BRCA1*	Exon 11	AZD5305	PR		PR		PR	CR	PD	PR	PD	CR	PD	PD
PDX539	*BRCA1*	BRCT	AZD5305	SD		PR									
PDX384	*BRCA1*	Exon 11	Olaparib	SD		PR						PD	PD		
PDX341	*BRCA1*	Exon 11	Olaparib	SD		PD	CR	PD	PD			PD			
PDX236	*BRCA1*	BRCT	Olaparib	PD	Hyp BRCA1	PD		PD	PD	CR	CR	PD			
PDX339	*BRCA1*	RING	Olaparib	PD	Unknown	PD		PD	SD			PD	PD		
PDX064	*BRCA1*	Exon 11	Olaparib	PD	Hyp BRCA1										
PDX641.1	*BRCA1*	BRCT	Olaparib	PD	Unknown										
PDX629	*BRCA1*	RING	Olaparib	PD	Unknown	PD									
PDX377OR1	*BRCA1*	Exon 11	Olaparib	PD	RAD51-I										
PDX230OR2	*BRCA1*	RING	Olaparib	PD	Unknown	PD									
PDX252	*BRCA1*	BRCT	Olaparib	PD	Unknown	PR		PD	PD		PR	PR	PR		
PDX230OR8	*BRCA1*	RING	Olaparib	PD	Unknown										
PDX397	*BRCA1*	BRCT	Olaparib	PD	Hyp BRCA1	PD									
PDX230OR5	*BRCA1*	RING	Olaparib	PD	Unknown	PD	PD								
HBCx11	*BRCA1*	Exon 11	Olaparib	PD	Unknown										
PDX230OR1	*BRCA1*	RING	Olaparib	PD	53BP1 pt										
PDX418	*BRCA1*	BRCT	Olaparib	PD	Hyp BRCA1	PD									
PDX377OR2	*BRCA1*	Exon 11	Olaparib	PD	RAD51-i										
STG316	*BRCA1*	RING	Olaparib	PD	53BP1+B1	SD		PD	SD	SD	SD	PR	PR		
PDX124OR	*BRCA1*	Exon 11	Olaparib	PD	RAD51-I							PD	PD		
HBCx8	*BRCA1*	RING	Olaparib	PD	Unknown										
PDX221	*BRCA1*	BRCT	Olaparib	PD	Hyp BRCA1	PD		PD	PD	PD	PR	PD	PD		
PDX127	*BRCA1*	RING	Olaparib	PD	53BP1 pt	PR	CR	PD	CR	PD	PD	PD	SD	PD	CR
HBCx28	*BRCA1*	RING	Olaparib	PD	53BP1 pt										
1	*BRCA1*	Exon 11	Olaparib	PD	53BP1 pt										
2	*BRCA1*	Exon 11	Olaparib	PD	Hyp BRCA1										
3	*BRCA1*	Exon 11	Olaparib	PD	Reversion										
4	*BRCA1*	Exon 11	Olaparib	PD	Hyp BRCA1										
5	*BRCA1*	Exon 11	Olaparib	PD	Hyp BRCA1										
6	*BRCA1*	Exon 11	Olaparib	PD	Hyp BRCA1										
7	*BRCA1*	Exon 11	Olaparib	PD	Hyp BRCA1										
8	*BRCA1*	Exon 11	Olaparib	PD	Unknown										
9	*BRCA1*	Exon 11	Olaparib	PD	Hyp BRCA1										
10	*BRCA1*	RING	Olaparib	PD	Unknown										
11	*BRCA1*	RING	Olaparib	PD	Unknown										
12	*BRCA1*	RING	Olaparib	PD	Unknown										
13	*BRCA1*	RING	Olaparib	PD	Unknown										
14	*BRCA1*	RING	Olaparib	PD	Unknown										
15	*BRCA1*	RING	Olaparib	PD	Unknown										
16	*BRCA1*	Exon 11	Olaparib	PD	Hyp BRCA1										
17	*BRCA1*	Exon 11	Olaparib	PD	Unknown										
18	*BRCA1*	Exon 11	Olaparib	PD	Unknown										
19	*BRCA1*	Exon 11	Olaparib	PD	Hyp BRCA1										
20	*BRCA1*	Exon 11	Olaparib	PD	Hyp BRCA1										
21	*BRCA1*	Exon 11	Olaparib	PD	Hyp BRCA1										
22	*BRCA1*	Exon 11	Olaparib	PD	Hyp BRCA1										
23	*BRCA1*	Exon 11	Olaparib	PD	Unknown										
24	*BRCA1*	Exon 11	Olaparib	PD	Hyp BRCA1										
25	*BRCA1*	Exon 11	Olaparib	PD	Hyp BRCA1										
31	*BRCA1*	Exon 11	Olaparib	PD	Hyp BRCA1										
32	*BRCA1*	Exon 11	Olaparib	PD	53BP1 pt										
33	*BRCA1*	RING	Olaparib	PD	Unknown										
34	*BRCA1*	RING	AZD5305	PD	Unknown										
35	*BRCA1*	RING	AZD5305	PD	Unknown										
36	*BRCA1*	Exon 11	AZD5305	PD	Hyp BRCA1										
37	*BRCA1*	Exon 11	AZD5305	PD	Hyp BRCA1										
38	*BRCA1*	Exon 11	AZD5305	PD	Hyp BRCA1										

PARPi-resistance
- Intrinsic
- Acquired

HRR alteration
- *BRCA1*

Gene domain
- RING domain
- Exon 11
- BRCT domain

PARPi
- Olaparib
- AZD5305

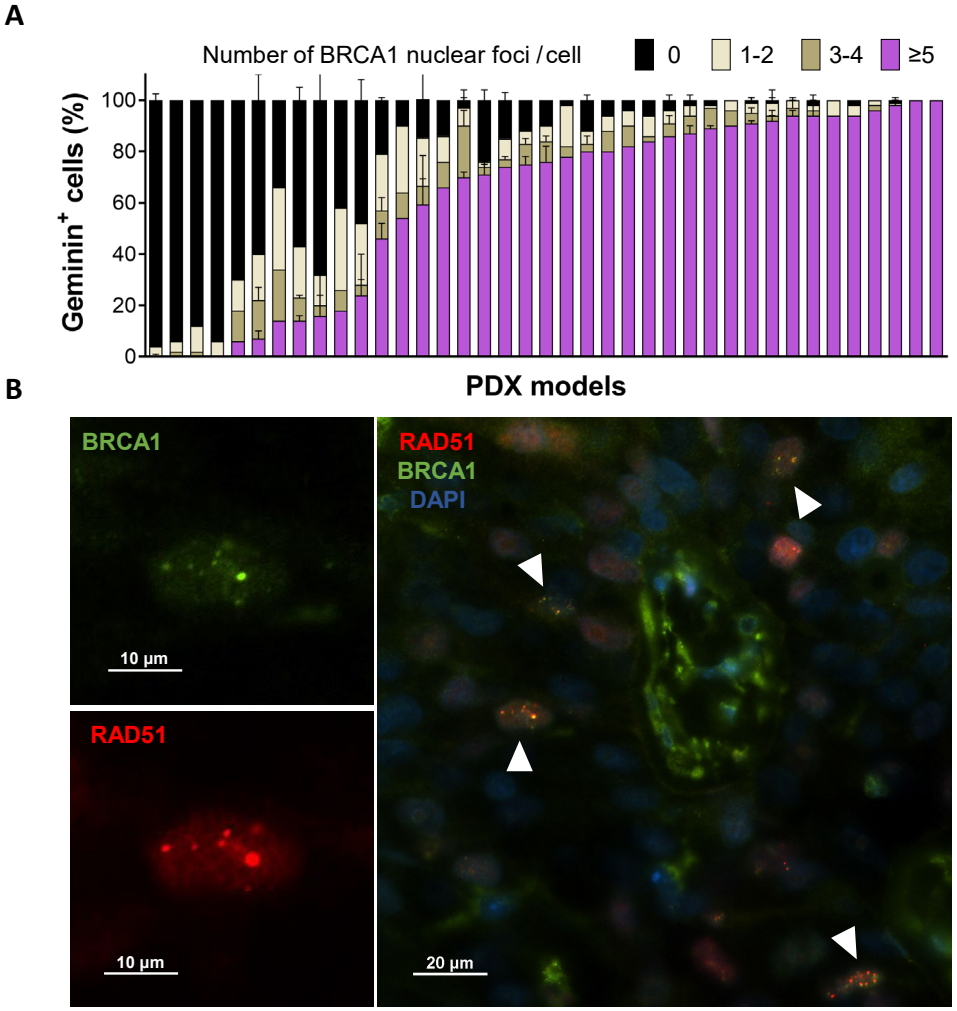
Mechanism of resistance (MoR) to PARPi
- Hypomorphic BRCA1
- 53BP1 pathway
- 3BP1 pathway and hypomorphic BRCA1
- RAD51-independent
- Unknown (other RAD51-dependent)

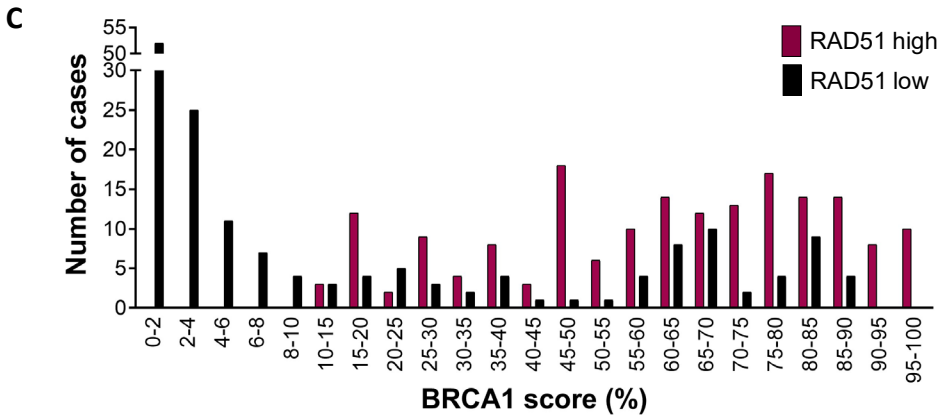
Response to therapy (mRECIST)
- CR
- PR
- SD
- PD
- NA

Supplementary Figure 19. Characterization of DNA-damaging agents antitumour activity as single agent or in combination with PARPi according to the affected gene domain in *BRCA1*-mutated PDX models.

The PARPi to which each model has progressed, the mechanism of resistance and the response to other DNA-damaging agents according to the mRECIST criteria are shown. Tumours with acquired resistance to PARPi are highlighted. Tumour IDs 1-38 correspond to

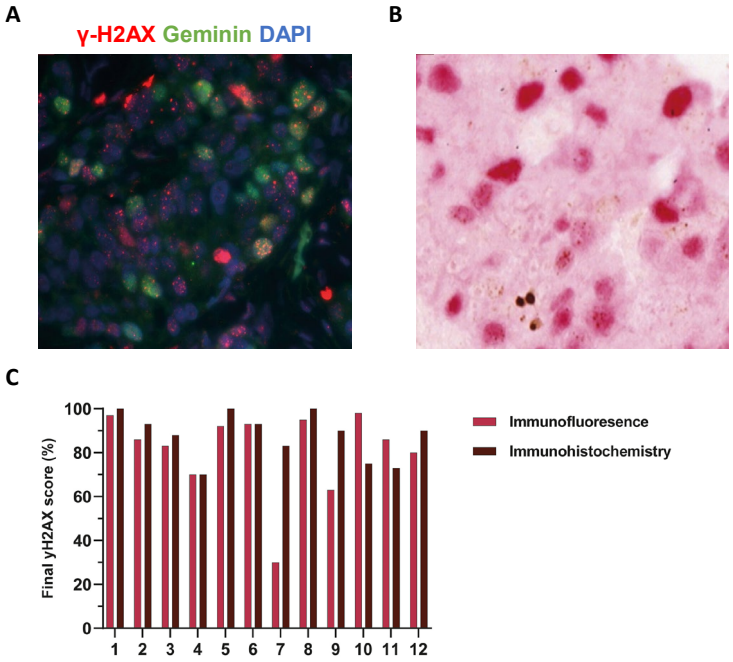
IDs from Supplementary Table 5. White boxes indicate non-available cases. All PARPi-sensitive and resistant tumours were included. Abbreviations: MoR: mechanisms of resistance; carbo: carboplatin; CR: complete response; PR: partial response; SD: stable disease; PD: progressive disease; Hyp BRCA1: hypomorphic BRCA1; 53BP1 pt: 53BP1 pathway; 53BP1+B1: 53BP1 pathway and hypomorphic BRCA1; RAD51-i: RAD51-independent.





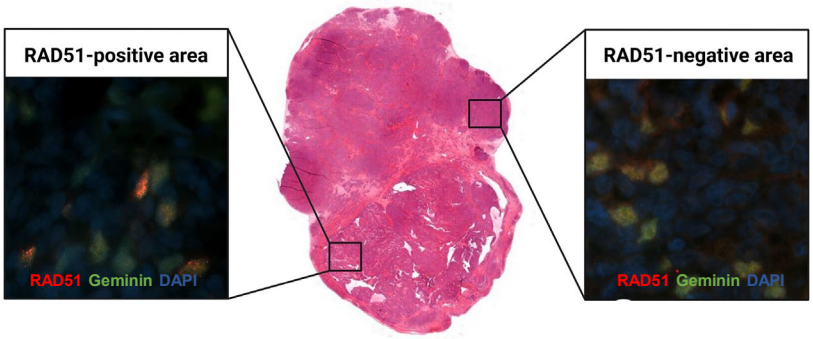
Supplementary Figure 20. Analysis of BRCA1 nuclear foci by IF in geminin+ tumour cells.

A. Distribution of the percentage of geminin^{+} cells with 0, 1-2, 3-4 or ≥5 BRCA1 foci in PDXs. **B.** Representative immunofluorescence images of BRCA1 (green) and RAD51 (red) nuclear foci from an untreated HRR-WT PDX model shown separately (scale bar = 10 μm) and merged (scale bar = 20 μm). BRCA1/RAD51-positive cells are highlighted with white arrows. **C.** Number of clinical breast cancer samples with high or low RAD51 levels according to BRCA1 score.



Supplementary Figure 21. Analytical validation and interobserver agreement of final γ-H2AX scores.

Illustration of **A.** IF and **B.** IHC-based γ-H2AX/geminin-staining of a HGSOC specimen (case ID 10). **C.** Concordance of γ-H2AX scores of HGSOC specimens in the training phase, determined by IF or IHQ staining. Adapted from *Kramer et al*[150].



Supplementary Figure 22. Example of a high-grade serous ovarian cancer (HGSOC) specimen with heterogeneous RAD51 nuclear foci distribution.
Representative hematoxylin and eosin image is shown. The boxes indicate RAD51-high and -low tumour areas with the representative IF image. This highlights that the RAD51 assay enables the identification of heterogeneity in HRD. Adapted from *Kramer et al*[150].

Annex IV: Other publications

Additional publications in which the PhD candidate has been involved during the thesis are the following:

- Hutten SJ, de Bruijn R, Lutz C, et al. A living biobank of patient-derived ductal carcinoma in situ mouse-intraductal xenografts identifies risk factors for invasive progression. Cancer Cell. 2023;41(5):986-1002.e9. doi:10.1016/j.ccell.2023.04.002.
- Blanc-Durand F, Yaniz-Galende E, Llop-Guevara A, et al. A RAD51 functional assay as a candidate test for homologous recombination deficiency in ovarian cancer [published correction appears in Gynecol Oncol. 2023 Aug;175:194]. Gynecol Oncol. 2023;171:106-113. doi:10.1016/j.ygyno.2023.01.026.
- Compadre AJ, van Biljon LN, Valentine MC, et al. RAD51 Foci as a Biomarker Predictive of Platinum Chemotherapy Response in Ovarian Cancer. Clin Cancer Res. 2023;29(13):2466-2479. doi:10.1158/1078-0432.CCR-22-3335.
- Pascual-Reguant L, Serra-Camprubí Q, Datta D, et al. Interactions between BRD4S, LOXL2, and MED1 drive cell cycle transcription in triple-negative breast cancer. EMBO Mol Med. 2023;15(12):e18459. doi:10.15252/emmm.202318459.